The topology of A'Campo deformations of singularities: an approach through the lotus.

Roberto Castellini

Université de Lille 1 SCIENCES ET TECHNOLOGIES

Laboratoire Paul Painlevé

École Doctorale Science pour l'Ingénieur, Université de Lille I

Thèse de doctorat

Discipline : Mathématiques

présentée par

Roberto Castellini

La topologie des déformations d'A'Campo des singularités: une approche par le lotus

---

Soutenue le 11 septembre 2015 devant le jury composé de :

M. Norbert A'Campo	Examinateur
M. Arnaud Bodin	Examinateur
M. Pedro González Pérez	Examinateur
M. Walter Neumann	Rapporteur
M. Adam Parusiński	Rapporteur
M. Patrick Popescu-Pampu	Directeur de Thèse
M. Mihai Tibăr	Examinateur

Laboratoire Paul Painlevé
Cité Scientifique
59655 Villeneuve d'Ascq

EDSPI
École Doctorale Science pour
l'Ingenieur,
Université de Lille I
Cité Scientifique
59655 Villeneuve d'Ascq

To my family and friends.

Success consists of going from failure to failure without loss of enthusiasm.
(Winston Churchill)

Acknowledgements

I would like to thank my advisor Patrick Popescu-Pampu for his help and understanding during all the thesis. I am grateful to him for always being present, for mathematical problems and for personal ones. Even when he was busy, he could find time to answer my questions.

I am grateful to Walter Neumann and Adam Parusiński for accepting to be reviewers. I would also like to thank Pedro González Pérez, Arnaud Bodin, Mihai Tibăr and Norbert A'Campo for accepting to be part of my jury. Moreover, I would like to thank Pedro González Pérez for the several detailed discussions about the lotus and about my general ideas. My research would not have been the same without the help of Norbert A'Campo, whose ideas have always been really inspiring. Our informal discussions have always been extremely significant. I would like to thank Mihai Tibăr and Arnaud Bodin for our informal meetings.

I would like to thank all the people working in Singularity Theory, for the useful, and also nice, moments. Special thanks to Camille Plénat, Anne Pichon, Maria Pe Pereira, and Hussein Mourtada. Many thanks also to all the other Ph.D. students, especially to Thomas, Leire, Hans, and Ferran.

I would like to thank all the members of the Laboratoire Paul Painlevé, in particular Ivo Dell'Ambrogio, David Chataur, Valerio Vassallo, Amaël Broustet and all the Ph.D. students and Post-Docs of the laboratory, especially Landry, Aygul, Najib, Pierre-Louis, Florent, and Florence. The time passed with you has been really important for my "work-life" balance. I would like to give a special thank to Antoine, with whom I shared an office for my first 3 years, and whose friendship has been really important to pass through several hard times.

I would like to thank all other Ph.D. students from the university of Lille and all the other friends I made during those four years. A special thank to Matthieu, who has always been next to me when I needed it.

At last, I would like to thank my family. I would give some special thank to some people I couldn't see much, but, thank to technology, I could talk to regularly. Eugenio, Laura, Jacopo, and Nicola, we spent together many years during our university, in Bologna, and you stayed next to me for all those years. I think I would have been really lucky if I had only one of you next to me, to listen to my doubts and to my problems. I don't think I will ever be able to thank you enough for it. And, finally, thank you Justine for having the patience and the will to stay next to me during the harder part of this work. Your presence helped me a lot during those final months.

Résumé

En théorie des singularités, il est important de mieux comprendre la topologie des déformations des paramétrisations des singularités de courbes planes réelles, en particulier celles dont les fibres génériques sont des *partages* : des immersions d'intervalles dans lesquelles toutes les intersections sont transverses. Cette topologie est encore bien mystérieuse : on ne sait décrire ni les partages, ni les singularités que l'on peut obtenir lors de telles déformations. De plus, on ne connaît que deux méthodes pour fabriquer de tels partages, dues à A'Campo et Gusein-Zade. Dans ma thèse *j'ai réussi à décrire avec précision un partage de A'Campo canonique associé à tout type topologique de singularité de courbe plane*. Dans le cas où la singularité est *irréductible*, je retrouve ainsi la description donnée par Schulze-Röbbecke en 1976. *J'ai aussi décrit les multigermes des singularités des courbes obtenues en appliquant partiellement l'algorithme de A'Campo.* Et ceci pour toutes les déformations partielles possibles. Enfin, *j'ai étudié de manière très détaillée la topologie des espaces totaux des résolutions plongées des singularités de courbes planes réelles*, en donnant une version réelle de l'approche classique via des graphes de plombage, utilisée dans le cas complexe.

Tout au long de la thèse, j'ai utilisé de manière essentielle un codage récent du type topologique de la singularité initiale, son *lotus*, introduit par Popescu-Pampu. Mon travail met ainsi en évidence le fait que dans l'étude des déformations, le lotus est un outil particulièrement bien adapté.

Abstract

In singularity theory, it is important to understand better the topology of the deformations of the parametrizations of plane curve singularities, particularly those whose fibres are *divides*: embeddings of intervals such that all intersections are transverse. This topology is still mysterious: one does not know descriptions either of the divides or of the singularities which appear in such deformations. Moreover, one knows only two algorithms whose results are divides, introduced by A'Campo and Gusein-Zade. In my thesis *I described a canonical A'Campo divide associated to every topological type of plane curve singularities*. In the case where the singularity is irreducible, I rediscovered the description given by Schulze-Röbbecke in 1976. *I've also described the multi-germs of singularities of curves obtained by partially applying A'Campo's algorithm.* And this for every possible partial deformation. In the end, *I studied in a detailed way the topology of the embedded resolution spaces of real plane curve singularities*, giving a real version of the classical approach via plumbing graphs, used in the complex case.

All along my thesis I used in an essential way a recent encoding of the topological type of the initial singularity, its *lotus*, introduced by Popescu-Pampu. Therefore my work shows that the lotus is a particularly well adapted tool for the understanding of deformations.

Contents

Introduction (Version française)

Le contexte de ma recherche

Étant donnée une singularité isolée d'hypersurface, on peut lui associer canoniquement une *déformation semi-universelle*, qui est localement la fibration triviale, hors d'une hypersurface discriminante. Les groupes de monodromie de cette fibration, qu'ils soient géométriques ou homologiques, sont des invariants fondamentaux de la singularité initiale. Ils sont encore largement inconnus.

Au début des années 1970, Arnold a proposé une stratégie pour donner une présentation dans le cas des singularités de courbes planes. Il faut commencer par une paramétrisation d'un représentant réel du type topologique donné. Après, il faut la déformer - une telle déformation de la paramétrisation est dite une *déformation δ-constante* - de telle manière que ses courbes génériques sont les immersions des segments pour lesquelles toutes les intersections sont transverses. Des immersions qui satisfont ces propriétés sont appelés des *partages*. Arnold a compris que la topologie d'un partage défini de cette manière détermine le groupe de monodromie de la singularité initiale. De cette façon, le groupe de monodromie est relié à l'étude de la topologie des déformations δ-constantes.

Plus récemment, en 1995, De Jong et Van Straten (voir [dJS98]) ont montré que les déformations δ-constantes de singularités des courbes planes (pas nécessairement réelles) sont aussi reliées aux déformations (abstraites) d'une classe de singularités normales de surfaces, les singularités *sandwichs*. Leur importance dans l'étude des singularités normales de surface en utilisant les modifications de Semple-Nash a été mise en évidence par Hironaka et Spivakovsky.

Dans un voisinage d'une *singularité ordinaire* de courbe plane, toutes les branches sont lisses et deux à deux transverses - dans le cas réel on obtient exactement les propriétés locales de la définition d'un partage. Comme cas particulier de la théorie de De Jong et Van Straten, les déformations δ-constantes avec fibres génériques ayant seulement des singularités ordinaires correspondent aux lissages de la singularité de la surface sandwich associée. Plus généralement, ils ont montré qu'à toute déformation δ-constante de la courbe est associée une déformation de la surface. Donc, une manière d'étudier les types topologiques des singularités qui peuvent être obtenues par déformation de la singularité sandwich - appelées singularités *adjacentes* - est d'étudier les type topologiques des singularités des fibres génériques de toutes les déformations δ-constantes possibles.

Pour ces différentes raisons, c'est important de mieux comprendre la topologie des déformations δ-constantes des singularités de courbes planes. Cette topologie est encore inconnue : on ne connaît même pas une description des partages ou des singularités qui

peuvent apparaître comme fibres génériques en faisant ces déformations.

On connaît seulement deux méthodes pour construire ces déformations δ-constantes et qui donnent des partages. Elles ont été obtenues par A'Campo ([A'C75]) et Sabir Gusein-Zade ([GZ74a] et [GZ74b]). La méthode de Gusein-Zade utilise les polynômes de Chebyshev, et elle est plus algébrique. Par contre, la méthode d'A'Campo est plus topologique. En fait, A'Campo a développé, sans le savoir, une idée qui avait été introduite par Angas Scott en 1892 ([AS92]).

L'avantage de la méthode d'A'Campo est que l'algorithme donne plusieurs partages différents, qui dépendent des choix faits. La question initiale de mon travail, que Popescu-Pampu m'a posée en 2011, était :

Question : *Comment peut-on caractériser les partages d'A'Campo parmi tous les partages possibles ?*

Le seul résultat en cette direction a été prouvé par Schulze-Röbbecke en 1977. Dans un Diplomarbeit, fait sous la supervision de Brieskorn (voir [SR77]), il a décrit un type particulier de partage d'A'Campo dans le cas des branches - c'est-à-dire, pour les singularités de courbes planes irréductibles - mais son travail ne contenait aucune suggestion pour une possible généralisation aux singularités ayant plusieurs branches.

Mes résultats

Dans ma thèse j'ai étudié en détail les types topologiques des partages obtenus par l'algorithme d'A'Campo - qu'on appellera dans la suite les *partages d'A'Campo*. Cet algorithme commence par la résolution plongée minimale de la singularité de courbe plane initiale et à chaque étape se compose d'une contraction d'une composante exceptionnelle et d'une translation de la courbe contractée le long d'une composante exceptionnelle. À chaque étape de translation, il faut choisir dans quel sens translater, ce qui donne plusieurs résultats finaux possibles.

Cet algorithme peut aussi être appliqué si on travaille avec une singularité complexe, mais dans ce cas on a seulement un résultat final possible. Ce résultat est tout simplement la complexification d'un des résultats réels possibles. Mais il est possible d'obtenir aussi dans le cas complexe des résultats différents en éliminant certains pas de translation - et on dit qu'on applique *l'algorithme d'A'Campo partiel*.

Les principaux résultats de ma thèse sont les suivants :

— une extension du résultat de Schulze-Röbbecke à *tout type topologique de singularité de courbes planes*. À savoir, je suis capable de décrire le partage fabriqué par l'algorithme d'A'Campo, quand on l'applique aux *singularités positives* qui sont *déformées de manière positive*.

— la description des types topologiques pour les multi-germes des singularités sur les fibres génériques des déformations partielles d'A'Campo. Ici je considère la situation complexe, sans aucune restriction sur la manière d'exécuter l'algorithme d'A'Campo partiel.

Dans les deux cas j'ai utilisé de manière essentielle un codage récent du type topologique de la singularité initiale, son *lotus*, introduit par Popescu-Pampu en 2009 (voir [PP11]).

C'est un objet géométrique qui unifie tous les codages précédents et qui permet de passer facilement de l'un à l'autre. Mes descriptions des types topologiques sont très naturelles en termes de lotus pour tous les problèmes étudiés, mais elles se traduisent mal en termes d'invariants classiques. Mon travail souligne donc le fait que, dans l'étude des déformations, les lotus sont des outils particulièrement bien adaptés.

Mes résultats en détail

Dans cette section je vais donner plus des détails au sujet des résultats de ma thèse.

L'algorithme d'A'Campo

Soit $(C, O) \hookrightarrow (S, O)$ une **singularité de courbe plane**, c'est-à-dire le germe d'une courbe réduite sur une surface analytique. Si on travaille avec des *germes analytiques complexes*, on parlera plutôt de **singularités de courbes planes complexes**. Mais notre travail concerne surtout des germes contenus dans des surfaces analytiques *réelles*. On supposera toujours que, vu dans la complexification de la surface, le germe de la courbe a toutes ses branches - c'est-à-dire, ses composantes irréductibles complexes - invariantes par conjugaison complexe. On parlera dans ce cas de **singularités de courbes planes réelles**. Les points réels de chacune de ces branches complexes sont des courbes topologiques dans un voisinage de O sur la surface topologique S.

Dans les deux cas, réel et complexe, (C, O) admet un procédé canonique de *résolution plongée minimale* : on éclate à chaque étape les points où la transformée totale de (C, O) n'est pas à croisements normaux. Quand (C, O) est réelle, on travaille seulement avec les points réels sur les différents niveaux des surfaces d'éclatement.

L'algorithme d'A'Campo exécute les étapes suivantes qui suivent le processus d'éclatement en *ordre inverse* :

1. on commence par la résolution plongée et on se concentre sur la transformée stricte de (C, O) ;
2. étant donnée une surface, on déforme la courbe produite par l'algorithme à cette étape par une *translation* en coordonnées locales qui est transverse à la courbe exceptionnelle qu'on contractera à l'étape suivant ;
3. on contracte ces composantes exceptionnelles et on se concentre sur l'image de la courbe déformée ;
4. si on est arrivé à la surface initiale S, on s'arrête ;
5. sinon, on revient à l'étape (2).

Quand on applique cet algorithme, il est important de commencer par un représentant de Milnor du couple (S, C). On suppose que S est un disque compact, de dimension réelle 2 quand on travaille avec des singularités réelles et de dimension réelle 4 quand on travaille avec des singularités complexes. En effet, quand on commence à déformer et contracter, on ne travaille plus avec des germes, mais avec des objets globaux, dont on étudie la topologie dans la préimage de la boule de Milnor de C. On va toujours supposer dans ce qui suit que S désigne un tel représentant.

La courbe obtenue par l'algorithme est une immersion propre dans le disque S de l'union disjointe de disques dans $\mathbb{R}/\mathbb{C}$. De plus, en chaque point singulier de l'image de l'immersion, les branches sont lisses et s'intersectent deux à deux transversalement : on dit qu'on n'a que des **singularités ordinaires**. Dans le cas *réel*, une telle immersion d'intervalles dans un disque compact de dimension 2 est appelée un **partage**. Pour cette raison, dans le cas *complexe* on parlera de **partages complexes** pour les immersions des disques de dimension 2 dans des boules de dimension 4.

La courbe finale obtenue par l'algorithme d'A'Campo est un partage (un partage complexe si on travaille sur $\mathbb{C}$). On dira que ces courbes sont des **partages d'A'Campo**. Un exemple de partage d'A'Campo obtenu à partir d'une singularité de courbe plane avec 3 branches est montré dans la Figure 1.

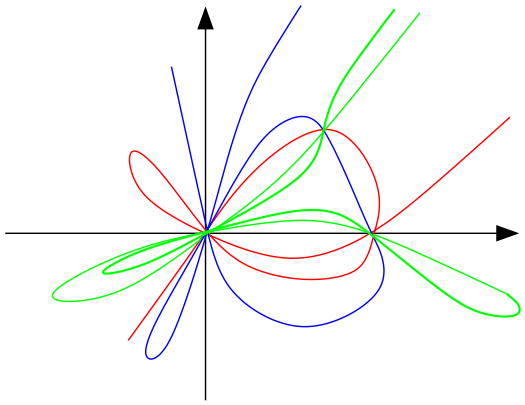

FIGURE 1 – Un exemple de partage d'A'Campo.

Les partages d'A'Campo sont les fibres génériques d'une déformation δ-constante à plusieurs paramètres, où chaque paramètre correspond à une étape de translation. Quand on travaille sur le corps $\mathbb{C}$, on n'obtient qu'un seul partage à isotopie près, car la surface discriminante dans l'espace des paramètres - qui correspond aux fibres de la déformation qui n'a pas que des singularités ordinaires - ne disconnecte pas l'espace. Mais sur $\mathbb{R}$ on obtient plusieurs composantes connexes du complémentaire du discriminant. Pour cette raison, *on obtient plusieurs types topologiques de partages d'A'Campo.*

Je me suis concentré sur le problème de décrire au moins un tel partage, pour un représentant réel bien déterminé du type topologique complexe de la singularité de courbe plane. J'ai complètement réussi dans cette direction. En effet :

J'ai défini une classe de singularités de courbes réelles planes positives *et des déformations d'A'Campo associées spécifiques, celles* positives*, et j'ai pu décrire les partages d'A'Campo associés.*

Après avoir obtenu ce résultat, j'ai appris par Ebeling que, dans le cas de *branches* cette description avait déjà été obtenue par Schulze-Röbbecke en [SR77], un Diplomarbeit fait sous la supervision de Brieskorn. Mais après sa description n'a pas été étendue, pas même sous forme de conjecture, aux germes *réductibles*. Je crois que cela est dû au fait que la structure des partages ne devient descriptible que lorsqu'on travaille avec les *lotus*, de nouveaux codages de la topologie des singularités de courbes planes introduits par Popescu-

Pampu en 2009 ([PP11]), mais qu'elle est bien plus compliqué à décrire en utilisant les codages classiques.

Positivité

Je vais expliquer maintenant la notion de *positivité* que j'ai introduite.

On suppose que (S, C) est une courbe réelle plane singulière *quelconque*. On choisit des coordonnées locales (x, y) dans (S, O). On obtient des axes de coordonnées *orientés*, marqués par les lettres x, y. On peut alors distinguer le *quadrant positif* dans leur complémentaire. Si on n'éclate que des points singuliers de la transformée totale de l'union des deux axes, on obtient à chaque étape une manière canonique d'orienter localement les deux nouveaux axes - les branches du diviseur exceptionnel des transformées strictes des axes initiaux - et de les marquer par x et y. Donc, on obtient de nouveau à chaque point un *quadrant positif* bien distingué. Si on éclate un point libre de la transformée stricte des deux axes, on choisit au début une **curvette** - une branche lisse transverse au diviseur exceptionnel. On a donc besoin d'une convention pour orienter la curvette et le diviseur exceptionnel dans un voisinage de ce point, et pour les marquer par x et y. J'ai choisi la convention suivante :

— on se concentre sur la carte de la description algébrique canonique de l'éclatement dans laquelle la courbe exceptionnelle qui contient ce point est l'axe y ;
— on l'oriente de la même manière que l'axe y ;
— après on marque la curvette par x et on l'oriente en translatant l'orientation de l'axe x de la carte.

De cette manière on peut, de manière inductive, orienter et marquer les **croix locales** - les unions de deux branches lisses transverses - contenant le germe du diviseur exceptionnel, au voisinage de tout point infiniment voisin de O qui est éclaté, pour obtenir la résolution plongée de C. Leurs analogues dans la situation complexes sont basiques pour le travail de García Barroso, González Pérez et Popescu-Pampu (voir [BPPP14]), qui appliquent la notion de lotus à l'étude des singularités de courbes planes complexes.

La convention pour les orientations et les étiquettes n'est pas nécessaire dans le cas complexe, mais elle est cruciale dans le cas réel. En effet, elle permet de définir le **quadrant positif** dans le voisinage de chaque croix. Mes définitions de positivités sont les suivantes :

Définition 0.1. Une singularité de courbe plane réelle est **positive** si la transformée stricte de chacune de ses branches passe par les quadrants positifs des points qui sont éclatés pendant le processus de résolution.

Une déformation d'A'Campo est **positive** si à chaque étape (2) de l'algorithme, on se déplace dans la direction positive de l'axe le long duquel on effectue la translation.

On peut remarquer que la définition précédente dépend des choix des curvettes aux points libres. Donc, la positivé est définie par rapport à ces choix, et ce n'est pas une propriété du couple (S, C).

Même si la singularité de la courbe plane réelle n'est pas positive par rapport à un choix de curvettes, on peut appliquer la convention précédente. Si on regarde la surface totale

de la résolution plongée minimale, on n'obtient pas seulement un diviseur exceptionnel qui est l'union des cercles qui s'intersectent transversalement en respectant le graphe dual classique de la configuration complexe associée, mais aussi les orientations locales de la transformée totale des curvettes dans le voisinage de toutes les croix.

J'ai défini l'*enrichissement* du graphe dual adapté à de telles structures supplémentaires, de telle manière que cet enrichissement permet de reconstruire le *plombage* - bien défini par rapport à un isomorphisme unique à isotopie près - de la surface totale avec le plongement des cercles, transformées strictes de curvettes et de toutes leurs orientations locales.

Plus généralement, j'ai défini une classe générale de graphes enrichis, que j'ai appelés graphes de colliers, qui permet de plomber de manière unique à isotopie près les ensembles finis de cylindres et rubans de Möbius dotés des cercles centraux et des ensembles finis de fibres, tous localement orientés dans un voisinage des points singuliers de leurs unions.

J'espère que cet outil permettra d'étudier topologiquement les courbes singulières plongées dans toute singularité de surface réelle normale.

Lotus

Avant d'énoncer le premier théorème principal de ma thèse, j'ai besoin d'expliquer aussi la notion de *lotus* (voir [BPPP14]) :

Définition 0.2. Soit (S, C) une singularité de courbe plane complexe. On considère sa résolution minimale plongée, enrichie ou non par des curvettes, comme décrit ci-dessus. Le **lotus** associé est un complexe simplicial fini de dimension 2, dont l'ensemble des sommets est en bijection avec les composantes irréductibles de la transformée totale du système de curvettes dans la surface finale. Deux sommets sont reliés par une arête si et seulement si les composantes associées sont les transformées strictes de courbes qui s'intersectent dans une surface intermédiaire du processus. Chaque fois que trois sommets sont deux à deux connectés, on recolle un triangle.

On peut montrer que le lotus est un *complexe de drapeaux*, c'est-à-dire, ses simplexes maximaux correspondent aux sous-ensembles maximaux de l'ensemble des sommets qui sont deux à deux connectés. De plus chaque triangle, un **pétale** du lotus, correspond à un point infiniment voisin O_i de O. Un de ses sommets, le **sommet principal**, correspond à la courbe exceptionnelle E_i créée par l'éclatement, et les deux autres sommets correspondent aux courbes (qui peuvent être exceptionnelles ou des curvettes) qui passent par O_i.

On considère maintenant un pétale dont tous les sommets correspondent à des courbes exceptionnelles. Soit E_i son sommet principal - avec un abus de notation on utilise pour l'étiqueter le même symbole que celui pour la composante exceptionnelle associée. Parmi les deux autres sommets, on note par E_j celui créé juste avant l'éclatement de O_i, et par E_k le plus ancien. On peut dire alors que :

— j est le **prédécesseur direct** de i et on écrit $j = p_D(i)$;
— k est le **prédécesseur indirect** de i et on écrit $k = p_I(i)$.

Le Lemme suivant est très important pour ma description des fibres génériques des déformations positives d'A'Campo (voir Théorème 0.4) :

Lemme 0.3. *L'union des segments du type* $[E_i, E_{p_D(i)}]$ *est le sous-arbre de l'*1*-squelette du lotus, qui est isomorphe au diagramme d'Enriques du processus de résolution plongée de* (S, C)*.*

On dit que $[E_i, E_{p_D(i)}]$ est un **côté direct** et $[E_i, E_{p_I(i)}]$ un **côté indirect** du lotus.

Les partages de déformations d'A'Campo positives

Je vais expliquer maintenant la relation avec les partages d'A'Campo. Je l'ai découverte expérimentalement, en considérant beaucoup d'exemples, de plus en plus compliqués. Ceci m'a fait d'abord me concentrer sur les déformations positives. Après j'ai remarqué que, lorsque deux points singuliers (pas nécessairement distincts) du partage sont connectés par des arcs, en règle générale *on a plusieurs arcs parallèles qui les joignent.* Ce comportement rendait les dessins rapidement très difficiles à réaliser (on peut voir déjà ce phénomène dans la Figure 1).

Ceci m'a conduit à coder :

— n arcs parallèles par un seul arc enrichi avec le poids n : un **multi-arc** de poids n ;
— n boucles parallèles par une seule boucle enrichie avec le poids n : une **multi-boucle** de poids n.

J'ai dessiné mes expériences avec cette convention. Et voilà la surprise : *est apparue devant mes yeux émerveillés une partie d'un lotus* ! J'ai contrôlé et j'ai vu que c'était une partie du lotus de la singularité associée. En analysant attentivement les exemples redessinés comme diagrammes avec multi-arcs et multi-boucles avec les poids associés, j'ai pu énoncer une conjecture à propos de ces poids, et après j'ai commencé à la prouver. C'était aussi difficile de développer un langage convenable, tout en traitant récursivement toutes les étapes de l'algorithme d'A'Campo, mais finalement j'ai pu prouver :

Théorème 0.4. *On considère le pétale relatif à* O_i*. Soit* $[E_i, E_j]$ *son côté direct et soit* $[E_i, E_k]$ *son côté indirect. On note par* m_i *la multiplicité en* O_i *de la transformée stricte de* C*. On associe de la manière suivante des poids aux côtés du lotus qui connectent les composantes exceptionnelles :*

— *le côté indirect* $[E_i, E_k]$ *a le poids* m_i *;*
— *si* O_i *est un point satellite, le côté direct* $[E_i, E_j]$ *a le poids* l_i*, où* $0 \leq l_i \leq m_i$ *et :*

$$l_i = \sum_{h:\ i=p_D(h)} (m_h - l_h), \quad \textit{pout tout } O_i.$$

En particulier, si O_i *est une feuille de l'arbre d'Enriques,* $l_i = 0$*.*

Alors il y a une manière de plonger le lotus dans le premier quadrant, ses côtés étant considérés comme des multi-arcs avec les poids précédents, et de rattacher une multi-boucle ayant le poids $(m_i - l_i)$ *pour tout point infiniment voisin* O_i*, telle que le partage associé est isotope au partage d'A'Campo de la déformation positive associée.*

La manière détaillée de plonger le lotus et d'attacher les multi-boucles est plus compliquée, et on ne la décrit pas dans cette introduction.

Dans la Figure 2 on peut voir le lotus et le plongement enrichi associé dans le quadrant positif, enrichi aussi avec les multi-boucles, pour la singularité qui a comme partage

d'A'Campo le partage de la Figure 1. On peut remarquer que certains côtés ont les poids 0, ce qui explique pourquoi ils disparaissent dans le partage. C'est la raison pour laquelle j'ai écrit que la première fois que j'ai vu le lotus apparaître du partage redessiné comme système de multi-arcs et multi-boucles, j'en avais vu seulement *une partie*.

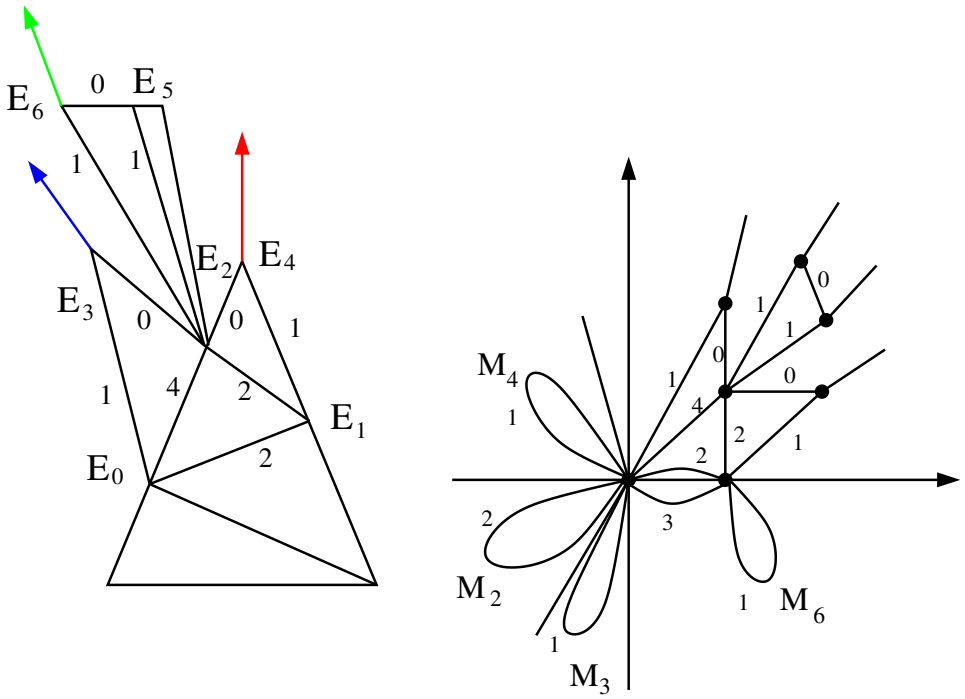

FIGURE 2 – Un lotus enrichi et le graphe du partage associé.

La topologie des déformations d'A'Campo partielles

J'ai aussi étudié un autre problème associé à l'algorithme d'A'Campo. On peut se rappeler que, dans cet algorithme, à chaque étape on translate la courbe et on contracte la composante exceptionnelle. J'ai réfléchi à la question suivante :

Quel résultat obtient-on si on ne déforme pas à chaque étape ?

La topologie réelle des fibres génériques de ces **déformations d'A'Campo partielles** est beaucoup plus compliquée que dans le cas des partages, donc je me suis concentré sur la situation *complexe*. J'ai voulu *décrire la combinatoire du multi-germe des singularités des fibres génériques*. J'ai pu résoudre complètement ce problème, en utilisant de nouveau les lotus comme outils fondamentaux.

Dans cette introduction je veux expliquer seulement ce qu'on obtient quand on saute toutes les étapes de translation, à l'exception de celle relative au point infiniment voisin O_i.

On considère un germe complexe C et un lotus $\mathcal{L}$ associé à un choix des curvettes pour son processus de résolution plongée. On peut supposer qu'on translate seulement

relativement au point O_i. Un côté du lotus est associé à ce point, connectant les sommets qui correspondent aux branches de la croix en O_i.

J'ai défini la **coupure** du lotus $\mathcal{L}$ en O_i. C'est un nouveau lotus obtenu de manière intuitive en coupant $\mathcal{L}$ le long du côté associé à O_i - avec l'exception d'une extrémité - et en lui ajoutant de nouvelles curvettes. J'ai démontré :

Théorème 0.5. *Par rapport à un système de curvettes, le lotus associé à la fibre générique de la déformation partielle d'A'Campo de (C, O) obtenue par une seule translation au point O_i est la coupure en O_i du lotus de (C, O).*

J'ai aussi démontré les deux propositions suivantes qui concernent ces déformations d'A'Campo partielles, et qui généralisent certains résultats de Gusein-Zade (voir [GZ93]) :

Proposition 0.6. *Soit C une courbe singulière complexe avec r branches. Soit μ le nombre de Milnor de C. Soit C' une fibre générique de la déformation d'A'Campo partielle de (C, O) obtenue en translatant seulement au point O_i. On a :*

— *si O_i est un* point satellite*, c'est-à-dire un point singulier du diviseur exceptionnel, alors C' a un seul point singulier, avec nombre de Milnor :*

$$\mu' = \mu - \sum_{h \in \mathcal{B}(O_i)} m^h_{p_D(i)};$$

— *si O_i est un* point libre*, c'est-à-dire un point lisse du diviseur exceptionnel, alors C' a deux points singuliers, avec nombres de Milnor :*

$$\mu' = \sum_{k : O_i \not\preceq O_k} m_k(m_k - 1) - \sum_{h \in \mathcal{B}(O_i)} m^h_{p_D(i)} - r + \#\{\mathcal{B}(O_i)\} + 1$$

et :

$$\mu'' = \sum_{k : O_i \preceq O_k} m_k(m_k - 1) - \#\{\mathcal{B}(O_i)\} + 1.$$

Ici on note par $\mathcal{B}(O_i)$ l'ensemble des branches de C dont la transformée stricte passe par O_i, par $m^h_{p_D(i)}$ la multiplicité de la branche C_h au point $O_{p_D(i)}$ et $O_i \preceq O_k$ signifie que O_k est infiniment voisin de O_i.

Proposition 0.7. *Soit (C, O) une courbe complexe plane singulière qui n'est pas une singularité ordinaire. Soit (Σ, E) la résolution minimale plongée de C. Soit $\{E_{i_j}\}_{j=1,\dots,k}$ l'ensemble des composantes exceptionnelles telles que $E^2_{i_j} = -1$ et pour tout $j = 1, \dots, k$ soit $n_j = \#\{\mathcal{B}(O_{i_j})\}$. Alors il existe une déformation d'A'Campo partielle de (C, O) qui a un point singulier avec nombre de Milnor $\mu' = min\{n_1, \dots, n_k\} - 1$.*

Perspectives

Il y a plusieurs problèmes qui continuent de manière naturelle le travail de ma thèse, et pour lesquels je pense d'avoir développé des outils adaptés à leur résolution :

1. *Trouver une méthode générale pour étudier tous les partages obtenus par la méthode d'A'Campo (et pas seulement les partages canoniques). En déduire un algorithme qui permet de comprendre si un partage donné a été obtenu en appliquant l'algorithme d'A'Campo.*

   On aurait un critère suffisant pour décider si une déformation δ-constante ne provient pas de la méthode d'A'Campo. Cet outil serait donc très précieux pour l'étude de ces déformations.

2. *Décrire le multi-germe des singularités obtenues en appliquant partiellement l'algorithme d'A'Campo des germes* réels.

   C'est l'analogue réel du deuxième problème principal résolu dans ma thèse. Les codages des types combinatoires des singularités réelles décrits dans ma thèse pourraient être la donnée de départ pour l'analyse de ce problème.

3. *Utiliser la compréhension des déformations d'A'Campo partielles pour décrire la topologie des déformations associées des singularités de surfaces sandwich.*

   La réponse à cette question permettrait de progresser dans le problème complètement ouvert de décrire les singularités qu'on pourrait obtenir en déformant une surface normale singulière donnée.

Structure de la thèse

Le Chapitre 1 présente une synthèse des résultats connus en théorie de singularités, en particulier dans le cas des courbes algébriques planes. Dans la Section 1.1 on donne les définitions fondamentales et on présente les propriétés algébriques des singularités des courbes planes. À la fin de la section, on rappelle la construction de *l'arbre de Eggers-Wall*. Dans la Section 1.2 on introduit un des plus importants outils de la théorie de singularités : l'éclatement. De plus, on introduit les deux invariants classiques qu'on peut définir à partir de l'éclatement, le *graphe dual* et l'*arbre d'Enriques*. La Section 1.3 est dédiée à l'explication des résultats concernant les fractions continues et la géométrie torique, dont on aura besoin dans la suite. Dans la Section 1.4 on définit le *lotus* d'une courbe singulière, introduit pour la premier fois par P. Popescu-Pampu dans [PP11]. Cet invariant sera utilisé extensivement dans tous les chapitres.

Dans le Chapitre 2 on se concentre sur la méthode d'A'Campo, en particulier sur des applications partielles de son algorithme. Dans la Section 2.1 on rappelle l'algorithme d'A'Campo, en l'introduisant comme algorithme topologique et comme algorithme algébrique. Dans la Section 2.2 on introduit la notion de *coupure du lotus*, et on l'utilise pour étudier en détail les partages qu'on obtient en appliquant partiellement l'algorithme d'A'Campo.

Le Chapitre 3 est dédié à l'étude des courbes analytiques réelles singulières. La combinatoire du cas réel est plus compliquée que celle du cas complexe, surtout pour le cas des courbes réductibles. Dans la Section 3.1 on décrit l'opération de *plombage* : pour la définir de la manière la plus précise possible, on introduit les concepts de *colliers* et de *bandes*. Dans la Section 3.2 on donne les définitions fondamentales sur les singularités de courbes réelles. Enfin, dans la Section 3.3 on donne quelques résultats et une construction

explicite de la *surface plongée de résolution* d'une courbe singulière réelle. On définit aussi la notion de *courbe réelle positive*.

Dans le Chapitre 4 on donne un algorithme qui permet de trouver le *partage canonique* d'une *courbe réelle positive*. La Section 4.1 est dédiée à l'étude des partages. On donne quelques résultats concernant leur structure et leurs propriétés. De plus, on introduit les *points marqués* et les *multi-boucles*. Dans la Section 4.2 on donne la définition du partage canonique, et on explique l'algorithme qui permet de le calculer.

Introduction (English version)

The context of my research

Given an isolated hypersurface singularity, one may associate canonically to it a *semi-universal deformation*, which is a locally trivial fibration outside a discriminant hypersurface. The monodromy groups of this fibration, either geometrical or homological, are fundamental invariants of the initial singularity. They are still largely mysterious.

At the beginning of the years 1970, Arnold proposed a strategy for giving a presentation in the case of singularities of plane curves. One has to start from a parametrization of a real representative of the given topological type, then one has to deform it – such a deformation of the parametrization is called a *δ-constant deformation* – in such a way that its generic curves are immersions of segments in which all the intersections are transverse. Immersions satisfying this constraint are called *divides*. Arnold realized that the topology of such a divide determines the monodromy group of the initial singularity. In this way, the monodromy group becomes related to the study of the topology of δ-constant deformations.

More recently, around 1995, De Jong and Van Straten showed that δ-constant deformations of (not necessarily real) plane curve singularities are also intimately related to the (abstract) deformations of certain normal surface singularities, the *sandwiched* ones (see [dJS98]). Their key-role in the study of normal surface singularities using Semple-Nash modifications had been emphasized before by Hironaka and Spivakovsky.

At an *ordinary singularity* of a plane curve all the branches are smooth and pairwise transversal – in the real case one obtains exactly the local constraint of the definition of divides. As a particular case of the theory of De Jong and Van Straten, the δ-constant deformations with generic fibers having only ordinary singularities correspond to the *smoothings* of the associated sandwiched surface singularity. More generally, they showed that to any δ-constant deformation of the curve corresponds a deformation of the surface. Therefore, a way to study the topological types of the singularities which may be obtained by deforming sandwiched surface singularities – the so-called *adjacent* ones – is to understand the topological types of the singularities of the generic fibers of all possible δ-constant deformations.

For these various reasons, it is important to understand better the topology of δ-constant deformations of plane curve singularities. This topology is still mysterious: one does not know descriptions either of the divides or of the singularities which may appear on the generic fibers while doing such deformations.

There are only two known methods to construct δ-constant deformations which give divides. They were obtained by Norbert A'Campo ([A'C75]) and Sabir Gusein-Zade

([GZ74a] and [GZ74b]). Gusein-Zade's method uses Chebyshev polynomials, and is mostly algebraical, while A'Campo's method is more topological. In fact, A'Campo developed, without knowing it, an idea which was first introduced by Angas Scott in 1892 (see [AS92]).

The advantage of A'Campo's method is that it gives an algorithm with several choices, which allows to construct many different divides. The starting question of my work, asked to me by Popescu-Pampu in 2011, was:

Question: *How to characterize A'Campo divides among all possible divides?*

The only result in this direction had been proved by Schulze-Röbbecke in 1977. In a Diplomarbeit done under the supervision of Brieskorn (see [SR77]), he described a particular A'Campo divide in the case of *branches* – that is, irreducible plane curve singularities – but his work contained no hint about a possible generalization for singularities with several branches.

My results in brief

In my thesis I studied carefully the topological types of the divides obtained by A'Campo's algorithm – to be called in the sequel *A'Campo divides*. This algorithm starts from the minimal embedded resolution of the initial plane curve singularity and does at each step either a contraction of an exceptional component or a translation of the contracted curve along an exceptional component. At each translation step, one has to choose in which sense to do that translation, which is the reason one gets many possible outcomes.

This algorithm may be also applied if one works with a complex singularity, but there is then only one possible outcome of it. And this outcome is simply the complexification of any one of the real outcomes. But one obtains even in this complex situation many outcomes by eliminating certain translation steps – we say then that we execute a *partial A'Campo algorithm*.

The main results of my thesis are:

— an extension of Schulze-Röbbecke's result *to all topological types of plane curve singularities*. Namely, I am able to describe the divide produced by A'Campo's algorithm when one applies it to *positive singularities* which one *deforms in a positive way*.

— *the description of the topological types of the multigerms of singularities on the generic fibers of partial A'Campo deformations*. Here I treat the complex situation, without restrictions on the way we perform the partial A'Campo algorithm.

In both cases I used in an essential way a recent encoding of the topological types of the initial singularity, its *lotus*, introduced by Popescu-Pampu in 2009 (see [PP11]). It is a geometrical object which unifies all the previous encodings and which allows to pass easily between them. My descriptions of topological types are very natural for both problems when one uses loti, but translate awkwardly in terms of classical invariants. My work emphasizes therefore the fact that in the study of deformations, loti are particularly well-adapted tools.

Details about my results

In this section I give more details about the results of my thesis.

A'Campo's algorithm

Let $(C, O) \hookrightarrow (S, O)$ be a **plane curve singularity**, that is, a germ of reduced curve on a smooth analytic surface. If we work with *complex analytic germs*, we will speak about **complex plane curve singularities**. But our work concerns mainly germs contained in *real* analytic surfaces. We will always assume that, seen in the complexification of the surface, the germ of curve has all its branches – that is, its complex irreducible components – invariant under complex conjugation. We will speak in this case about **real plane curve singularities**. The real points of each one of its complex branches form therefore topological curves in the neighborhood of O on the topological surface S.

In both cases (C, O) admits a canonical process of **minimal embedded resolution**: one blows-up at each step the points where the total transform of (C, O) has not normal crossings. When (C, O) is real, we work only with the real points of the various levels of blown-up surfaces.

A'Campo's algorithm performs the next steps which follow the process of blowing-ups *in the reverse order*:

1. start from the final surface of the embedded resolution process and look at the strict transform of (C, O) on it;
2. on a given surface, deform the curve produced by the algorithm at that step by a *translation* in local coordinates which is transversal to the exceptional curves to be contracted at next step;
3. contract those exceptional curves and look at the image of the deformed curve;
4. if one arrived on the surface S, then STOP;
5. otherwise, go to step (2).

When one is performing this algorithm, it is important to start from a Milnor representative of the pair (S, C). That is, S is assumed to be a compact disk, which is of real dimension 2 when we work with real singularities and of real dimension 4 when we work with complex singularities. Indeed, when we start deforming and contracting, we don't work anymore with germs, but with global objects, whose topology we study in the preimage of such a Milnor ball for C. In the sequel we will assume that S denotes always such a representative.

The curve produced by the algorithm is a proper immersion in the disk S of a disjoint union of disks in $\mathbb{R}/\mathbb{C}$. Moreover at each singular point of the image of this immersion, the branches are smooth and intersect pairwise transversally: one says that one has only **ordinary singularities**. In the *real* case, such an immersion of intervals in a 2-dimensional compact disk is called a **divide**. For this reason, in the *complex* case we will speak about **complex divides** for such immersions of 2-dimensional disks in 4-dimensional balls.

The final curve built by A'Campo's algorithm is a divide (a complex one if we work over $\mathbb{C}$). We will call such curves **A'Campo divides**. An example of A'Campo divide obtained from a real plane curve singularity with 3 branches in shown in Figure 3.

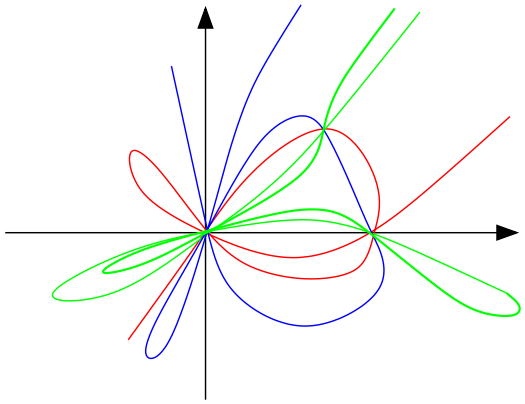

Figure 3 – An example of A'Campo divide.

The A'Campo divides are the generic fibers of a δ-constant deformation with many parameters, each parameter corresponding to a step of translation. When we work over $\mathbb{C}$, one gets only one divide up to isotopy, as the discriminant hypersurface in the space of parameters – corresponding to the fibers of the deformation which do not have only ordinary singularities – does not disconnect this space. But over $\mathbb{R}$ one gets many connected components of the complement of the discriminant. For this reason *one gets many topological types of A'Campo divides.*

I concentrated on the problem of describing at least one such divide, for a well-chosen real representative of a complex topological type of plane curve singularity. I had complete success in this direction. Indeed:

I defined a class of positive real plane curve singularities *and special A'Campo deformations of them, the* positive ones *and I could describe the associated A'Campo divides.*

After obtaining this result, I learnt from Ebeling that, in the case of *branches*, this description had already been obtained by Schulze-Röbbecke in [SR77], a Diplomarbeit done under the supervision of Brieskorn. But, since then, there were not even conjectures about the situation for *reducible* germs. I believe that this is due to the fact that the structure of the divide becomes descriptible when one works with *loti*, new encodings of the topology of plane curve singularities introduced by Popescu-Pampu [PP11] in 2009, but it is much more complicated to describe in terms of classical encodings.

Positivity

Let me explain now the notions of *positivity* which I introduced.

Assume first that (S, C) is *any* real plane curve singularity. Choose local coordinates (x, y) on (S, O). One gets *oriented* coordinate axes labeled by the letters x, y. This

distinguishes a *positive quadrant* in their complement. If one blows-up only singular points of the total transform of the union of the two axes, one gets at each step a canonical way to orient locally the two new axes – the branches of the exceptional divisor or the strict transforms of the initial axes – and to label them by x and y. Therefore, one gets again at each such point a distinguished *positive quadrant*. At a smooth point of the total transform of the two axes one chooses first a **curvetta** – a smooth branch transversal to the exceptional divisor. Then one needs a convention in order to orient the curvetta and the exceptional divisor in the neighborhood of that point, and to label them by x and y. I chose the following one:

Convention
— Look at the chart of the canonical algebraic description of the blow-up in which the exceptional curve containing that point is the y-axis.
— Orient it as that axis.
— Then label the curvetta by x and orient it by translating the orientation of the x-axis of that chart.

In this way one may recursively define oriented and labeled local **crosses** – unions of two transverse smooth branches – containing the germ of the exceptional divisor, in the neighborhood of all the points infinitely near O which are blown-up in order to get the embedded resolution of C. Their analogs in the complex situation are basic for the work of García Barroso, González Pérez and Popescu-Pampu (see [BPPP14]), which applies the notion of lotus to the study of complex plane curve singularities.

The convention for fixing orientations and labelings is not needed in the complex situation, but is crucial in the real situation. Indeed, it allows to define a **positive quadrant** in the neighborhood of each cross. Here are my definitions of positivity:

Definition 0.1. A real plane curve singularity is **positive** if the strict transforms of all its branches pass through all the positive quadrants of the points which are blown up in the resolution process. An A'Campo deformation is **positive** if at each step (2) of the algorithm, one moves in the positive direction of the axis along which is done the translation.

Note that the previous definition depends on the choices of curvettas at smooth points. Therefore, positivity is relative to this choice, it is not only a property of the pair (S, C).

Now, even if a real plane curve singularity is not positive with respect to some choice of curvettas, one may apply the previous convention. If one looks at the total surface of the minimal embedded resolution, one gets not only an exceptional divisor which is a union of circles intersecting transversally according to the classical dual graph of the complexified configuration, but also local orientations of the total transform of the curvettas in the neighborhood of all the crosses.

I defined an *enrichment* of the dual graph adapted to such supplementary structures, in such a way that this enrichment allows to reconstruct by *plumbing* – up to an isomorphism which is unique up to isotopy – the total surface with the embedding of circles, strict transforms of curvettas and all their local orientations.

More generally, I defined a general class of such enriched graphs, which I called graphs of necklaces, which allow to plumb in a unique way up to isotopies finite sets of cylinders

and Möbius bands endowed with core circles and finite sets of fibers, all of them locally oriented near the singular points of their unions.

I hope that this tool will allow to study topologically the curve singularities drawn on arbitrary real normal surface singularities.

Loti

Before stating the first main theorem of my thesis, I need to explain also the notion of *lotus* (see [BPPP14]):

Definition 0.2. Let us consider a complex plane curve singularity (S, C) and its minimal embedded resolution process. Enrich it with curvettas as explained before. The associated **lotus** is a finite 2-dimensional simplicial complex whose set of vertices is in bijection with the irreducible components of the total transform of the system of curvettas in the final surface. Two vertices are joined by an edge if and only if the corresponding components are strict transforms of curves which intersected on some intermediate surface of the process. Each time three vertices are pairwise connected, one glues a triangle.

One may show that the lotus is a *flag complex*, that is, its maximal simplices correspond to the maximal subsets of the vertex set which are pairwise connected. Moreover, each triangle – a **petal** of the lotus – corresponds to an infinitely near point O_i of O to be blown-up. One of its vertices – the **top vertex** – corresponds to the exceptional curve E_i created by this blow-up, the two other vertices corresponding to the curves (either exceptional or curvettas) which pass through O_i.

Assume now that we look at a triangle all of whose vertices correspond to exceptional curves. Let E_i be its top vertex – by abuse of notations, we use the associated component of the exceptional divisor to label it. Among the two other vertices, denote by E_j the one created just before blowing up O_i, and by E_k the oldest one. One says then that:

— j is the **direct predecessor** of i and we write $j = p_D(i)$;

— k is the **indirect predecessor** of i and we write $k = p_I(i)$.

The following basic fact is very important for my description of the generic fibers of positive A'Campo deformations (see Theorem 0.4 below):

Lemma 0.3. *The union of the segments of the form* $[E_i, E_{p_D(i)}]$ *is a subtree of the* 1*-skeleton of the lotus, which is isomorphic to the Enriques diagram of the embedded resolution process of* (S, C)*.*

I say that $[E_i, E_{p_D(i)}]$ is a **direct edge** and $[E_i, E_{p_I(i)}]$ an **indirect edge** of the lotus.

The divides of positive A'Campo deformations

Let me explain now the relation of loti with A'Campo divides. I discovered it starting from an experimental basis built during a long practice with examples, which were more and more complicated. This made me first concentrate on the positive deformations. Then I noticed that, when two singular points – not necessarily distinct – of the divide were

connected by an arc, then as a general rule *one had many parallel arcs between them.* This made the drawings rapidly very awkward to be done (see already this phenomenon in Figure 3).

This led me to encode:

— n such parallel arcs by a single arc endowed with the weight n: a **multiarc** of weight n;

— n parallel loops by a single loop endowed with the weight n: a **multiloop** of weight n.

I redrew my experiments with this convention. And here came the surprise: *popped up to my amazed eyes part of a lotus*! I checked and I saw that it was part of the lotus of the associated singularity. Looking carefully again at my examples redrawn as diagrams with multiarcs and multiloops with the associated weights, I could build a conjecture about those weights, then start to prove it. It was still difficult to develop a convenient language, as well as to deal recursively with all the steps of A'Campo's algorithm, but finally I could prove:

Theorem 0.4. *Let us consider the petal relative to O_i. Let $[E_i, E_j]$ be its direct edge and $[E_i, E_k]$ be its indirect edge. Denote by m_i the multiplicity at O_i of the strict transform of C. Associate in the following way weights to the edges of the lotus which join exceptional components:*

— *the indirect edge $[E_i, E_k]$ has weight m_i;*

— *if O_i is a satellite point, the direct edge $[E_i, E_j]$ has weight l_i, $0 \leq l_i \leq m_i$ and:*

$$l_i = \sum_{h:\ i=p_D(h)} (m_h - l_h), \quad \textit{for any } O_i.$$

— *if O_i is a free point, the direct edge $[E_i, E_j]$ has weight m_i.*

In particular, if O_i is a leaf of the Enriques tree, then $l_i = 0$.

Then there is a way to embed the lotus in the first quadrant, its edges being seen as multi-arcs with the previous weights, and to attach a multi-loop with weight $(m_i - l_i)$ for each infinitely near point O_i, such that the associated divide is isotopic to the A'Campo divide of the associated positive deformation.

The detailed way of embedding the lotus and of attaching the multiloops is more complicated, and we don't describe it in this introduction.

In Figure 4 one can see the lotus and the associated weighted embedding in the positive quadrant, enriched with multiloops, for the singularity which has the A'Campo divide represented in Figure 3. Note that some edges have weight 0, which explains why they disappear in the divide. This is the reason I wrote that the first time I saw the lotus popping up from the divide redrawn as a system of multiarcs and multiloops, I saw only *part of it.*

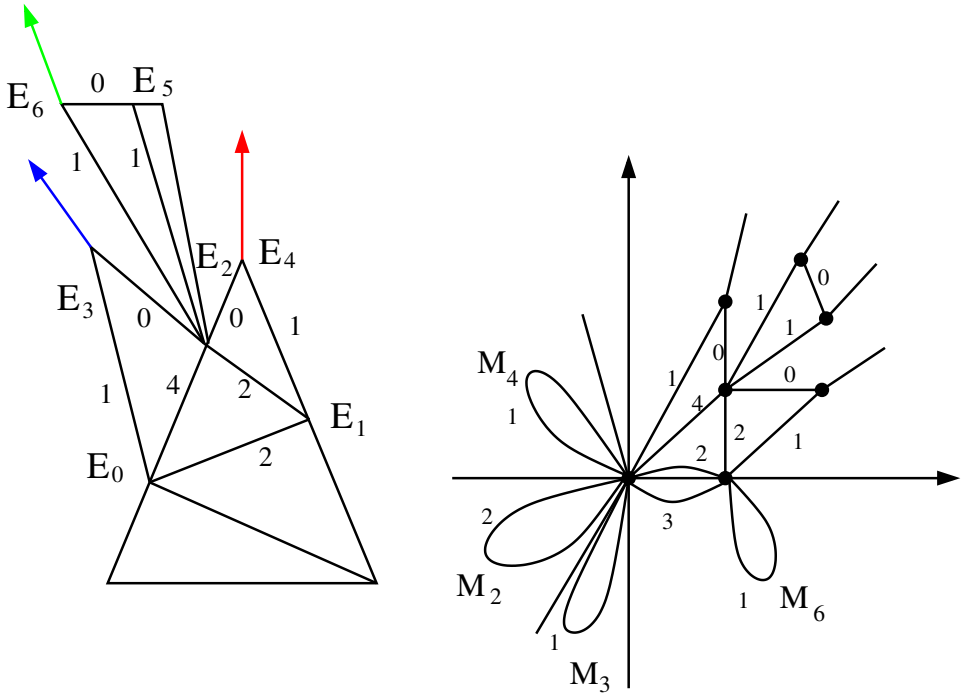

Figure 4 – An enriched lotus and the graph of the associated divide.

The topology of partial A'Campo deformations

I also studied another problem related with A'Campo's algorithm. Recall that in this algorithm, at every step either we deform the curve or we contract it. I thought about the question:

What happens if we don't deform at each step?

The real topology of the generic fibers of such a **partial A'Campo deformation** is much more complicated than in the case of divides, therefore I concentrated first on the *complex* situation. I wanted *to describe the combinatorics of the multigerm of singularities of the generic fibers.* I could completely solve this problem, again using the loti as fundamental tools.

In this introduction I want to explain only what happens when one skips all the translation steps with the exception of the one done near the infinitely near point O_i.

Let us consider a complex germ C and a lotus $\mathfrak{L}$ associated to a choice of curvettas for its process of embedded resolution. Assume that we perform only a translation near the point O_i. To this point is associated an edge in the lotus, connecting the vertices which correspond to the branches of the cross at O_i.

I define the **cut** of the lotus $\mathfrak{L}$ at O_i. It is a new lotus obtained intuitively by cutting $\mathfrak{L}$ open along the edge associated to O_i – except at one extremity – and by adding new curvettas to it. I proved:

Theorem 0.5. *With respect to natural systems of curvettas, the lotus associated to the*

generic fiber of the partial A'Campo deformation of (C, O) obtained by translating only at O_i is the cut at O_i of the lotus of (C, O).

I also proved the two following propositions concerning such partial A'Campo deformations, generalizing results of Gusein-Zade (see [GZ93]):

Proposition 0.6. *Let C be a complex curve singularity with r branches. Let μ be the Milnor number of C. Let C' be a general fiber of the partial A'Campo deformation of (C, O) obtained by translating only at O_i. Then:*

— *if O_i is a* satellite point*, that is, a singular point of the exceptional divisor, then C' has only one singular point, with Milnor number:*

$$\mu' = \mu - \sum_{h \in \mathcal{B}(O_i)} m^h_{p_D(i)};$$

— *if O_i is a* free point*, that is, a smooth point of the exceptional divisor, then C' has two singular points, with Milnor numbers:*

$$\mu' = \sum_{k : O_i \not\preceq O_k} m_k(m_k - 1) - \sum_{h \in \mathcal{B}(O_i)} m^h_{p_D(i)} - r + \#\{\mathcal{B}(O_i)\} + 1$$

and:

$$\mu'' = \sum_{k : O_i \preceq O_k} m_k(m_k - 1) - \#\{\mathcal{B}(O_i)\} + 1.$$

Here $\mathcal{B}(O_i)$ denotes the set of branches of C whose strict transforms pass through O_i, $m^h_{p_D(i)}$ denotes the multiplicity of the branch C_h at the point $O_{p_D(i)}$ and $O_i \preceq O_k$ means that O_k is infinitely near O_i.

Proposition 0.7. *Let (C, O) be a complex plane curve singularity which is not an ordinary singularity. Let (Σ, E) be the minimal embedded resolution space of C. Moreover, let $\{E_{i_j}\}_{j=1,\dots,k}$ be the set of exceptional components such that $E^2_{i_j} = -1$ and for all $j = 1, \dots, k$ let $n_j = \#\{\mathcal{B}(O_{i_j})\}$. Then there exists a partial A'Campo deformation of (C, O) which has a singular point with Milnor number $\mu' = min\{n_1, \dots, n_k\} - 1$.*

Perspectives

There are several problems which continue in a natural way the work of my thesis, and for which I believe I developed tools and an experience adapted to their resolution:

1. *Find a general method for studying all the divides obtained by A'Campo's method (not only the canonical ones). Deduce an algorithm which allows to understand if a given divide was obtained by applying A'Campo's algorithm.*

   This would provide a sufficient criterion to decide that a δ-constant deformation does not come from A'Campo's method. This tool would therefore be very precious for the subsequent study of those deformations.

2. *Describe the multi-germ of singularities obtained by applying partially the A'Campo algorithm to* real *germs.*

   It is the real analog of the second main problem solved in my thesis. The encodings of the combinatorial types of real singularities described in my thesis could be the starting data of the analysis of the problem.

3. *Use the understanding of the partial A'Campo deformations in order to describe the topology of the corresponding deformations of the sandwiched surface singularities associated to them.*

   This would allow to progress in the largely open problem of the description of the singularities which may be obtained by deforming a given normal surface singularity.

Structure of the thesis

Chapter 1 provides a survey of known results on singularity theory, in particular on algebraic plane curves. In Section 1.1 we state the fundamental definitions and we present the algebraic properties of plane curve singularities. At the end of the section, we recall the construction of the *Eggers tree*. In Section 1.2 we introduce one of the most important tool in singularity theory: the blow-up. Moreover, we introduce the two classical invariants definable by blow-ups, the *dual graph* and the Enriques' tree. Section 1.3 is dedicated to the explanation of results about continued fractions and toric geometry needed in the sequel. In Section 1.4 we define the *lotus* of a curve singularity, introduced for the first time by P. Popescu-Pampu in [PP11]. This invariant will be extensively used in all the chapters.

In Chapter 2 we focus on A'Campo's method, in particular on partial applications of the algorithm. In Section 2.1 we recall A'Campo's algorithm, introducing it both as a topological algorithm, and an algebraical one. In Section 2.2 we introduce the notion of the *cut of the lotus*, and we use this notion to study in detail the resulting divides of a partial application of A'Campo's algorithm.

Chapter 3 is dedicated to the study of real analytic curve singularities. The combinatorics of the real case is more complicated than the complex one, mostly in dealing with reducible curves. In Section 3.1 we describe the operation of *plumbing*: to define it as precisely as possible, we introduce the concepts of *necklaces* and *bands*. In Section 3.2 we give the fundamental definitions about real curve singularities. Finally, in Section 3.3 we state some results and an explicit construction of the *embedded resolution surface* of a real curve singularity. We also define the notion of *real positive curve*.

In Chapter 4 we give an algorithm to find the *canonical divide* of a *real positive curve*. Section 4.1 is dedicated to the study of divides. We give then some results about their structures and their properties. Moreover, we introduce *marked points* and *multi-loops*. In Section 4.2 we give the definition of canonical divide, and we explain the algorithm to compute it.

Chapter 1

Complex curve singularities

Chapter overview

The main motivation to this chapter is to state the definitions and theorems about complex plane curve singularities needed in the thesis.

In Section 1.1 we consider the classical definitions of the *complex curve singularities* (Definition 1.1.1). In Section 1.1.2 we recall the fundamental *Newton-Puiseux* Theorem (Theorem 1.1.9). We define then the *Puiseux characteristic* and the *Puiseux exponents* (Definition 1.1.11). The importance of the Puiseux characteristic is that it is, as we will see in Definition 1.1.15, a complete invariant for a branch. In the case of a curve singularity having several irreducible components, we also need to consider the *contact order* (see Definition 1.1.13). We end this section by introducing the Eggers-Wall tree (Section 1.1.3), first introduced by Eggers in his Ph.D. Thesis (see [Egg83]). We are going to use the slightly different construction (see Definition 1.1.18) given by C.T.C Wall, see [Wal03] or [Wal04]. The advantage of this invariant is that it is defined only by the knowledge of the algebraic properties of the curves relative to a smooth branch.

Section 1.2 is dedicated to the study of the operation of *blow-up* (see Definition 1.2.1). In Section 1.2.1 we introduce the terminology we are going to use in all this work. The terminology is slightly different from the standard one, because we will need, in the following chapters, to be able to follow in detail what happens at every step of the *resolution process*. In Section 1.2.2 we introduce the first invariant extracted from the resolution process, the *Enriques tree* (Definition 1.2.11), whose vertices are in bijection with the *infinitely near points* (Definition 1.2.5) appeared during the resolution process. The type of its edges, straight or curvilinear, gives information about the properties of the infinitely near points, that can be either *satellite points*, or *free points* (Definition 1.2.8). Moreover, for each infinitely near point O_i it also gives information about its *direct and indirect predecessor* (Definitions 1.2.5 and 1.2.9). In the final part, Section 1.2.3, we talk about two other invariants of curve singularities, the multiplicity sequence, which is defined for branches, (Definition 1.2.14) and the dual graph (Definition 1.2.21). Proposition 1.2.19 gives an effective way to compute the *multiplicity* m_i associated to each *infinitely near point* O_i. It is then possible to enrich the Enriques tree by the data of multiplicities. We end this section by stating (and partially proving) Theorem 1.2.25. The statement is that all the invariants introduced in Section 1.1 and Section 1.2 are equivalent. We say then

that two curves have the same *topological type* if they have isomorphic Eggers-Wall trees, isomorphic dual graphs or isomorphic Enriques trees.

In Section 1.3 we consider two different notions, namely, continued fractions and toric surfaces, that we will see to be really important in Section 1.4. The first one, explained in Section 1.3.1, is the *continued fractions* (Definition 1.3.2), which are a special way of writing real numbers. A branch having only one Puiseux pair has naturally associated a rational number λ: Proposition 1.3.8 gives the consequences of this fact, showing how the multiplicity sequence depends on the continued fraction associated to λ. Moreover, we can define, by Klein's geometric interpretation of a continued fraction, the *characteristic points* (see Definition 1.3.9). Those points are fundamental to understand the blow-up sequence of a branch having only one Puiseux pair. Section 1.3.2 is dedicated to some basic definitions and results about *toric geometry*. The 2-dimensional toric varieties we are interested in are built starting from binomial equations $x^a = y^b$, where a and b are co-prime. It is then natural to use toric techniques to study in detail curve singularities, in particular branches having only one Puiseux pair. Moreover, as we can see in Example 1.3.27, the blow-up surface of a branch is also a toric variety, if we suppose that the branch has only one Puiseux pair.

The final section of this chapter, Section 1.4, is about the *lotus*. This is a new invariant of plane curve singularities, introduced by Popescu-Pampu in 2009 (see [PP11]), which has the property of containing the other three invariants, the Eggers-Wall tree, the Enriques tree, and the dual graph. The idea is really simple. The dual graph is the graph usually computed at the end of the resolution process. If we look at the action on the dual graph of a blow-up of the satellite point $O_i = E_j \cap E_k$, we see that it consists in adding a vertex E_i on the edge $[E_j E_k]$. Instead of adding a vertex on the edge, we substitute the edge, which is a 1-simplex, with a *petal*, i.e., a 2-simplex having vertices E_i, E_j, and E_k (see Definition 1.4.5). The *lotus* is obtained as the union of all the petals. Proposition 1.4.10 explains the isomorphism between the boundary of the lotus and the dual graph. In the original construction (see [PP11] and [BPPP14]) the Enriques tree was considered inside the lotus as an additional structure. I remarked that this additional structure isn't necessary. In fact, if O_i is a satellite point, the two vertices E_j and E_k have a different behaviour: one is associated to the *direct predecessor*, and the other one to the *indirect predecessor* (see Definition 1.4.13). In this way, it is possible to embed the Enriques graph in the sub-tree of the lotus such that its edges are the direct edges (Proposition 1.4.14). Section 1.4.2 is dedicated to the equivalence between the lotus and the Eggers-Wall tree. At the end of the Section we compute the toric morphism associated to a resolution (see Proposition 1.4.30). We finish this Section (and the Chapter) by the definition of the *multi-lotus*, associated to a *multi-germ* (Definition 1.4.31). Multi-germs will be important in Chapter 2.

1.1 Basic notions defined through series

1.1.1 Milnor numbers and intersection numbers

In the sequel, (Σ, p) denotes a germ of smooth complex analytic surface, $\mathcal{O}_{\Sigma,p}$ its local ring of germs of holomorphic functions and $\mathfrak{m}_{\Sigma,p} \subset \mathcal{O}_{\Sigma,p}$ its maximal ideal of germs of functions vanishing at p. If $f \in \mathfrak{m}_{\Sigma,p}$, we denote by $V(f)$ its divisor.

Definition 1.1.1. A **curve singularity** in (Σ, p) is a germ $(C, p) \hookrightarrow (\Sigma, p)$ of a reduced complex analytic curve. If C is irreducible, then we say that (C, p) is a **branch**.

If $f \in \mathcal{O}_{\Sigma,p}$ is such that $V(f) = C$, we say that $f = 0$ is a **local equation** of C and f is a **defining function** of C.

Definition 1.1.2. Let (C, p) be a curve singularity such that (C, p) is not smooth. Then p is a **singular point** of C.

Let us consider local holomorphic coordinates (x, y) on (Σ, p). The point p gets identified with $O = (0, 0) \in \mathbb{C}^2$. Let $f \in \mathbb{C}\{x, y\}$ be a defining function of curve singularity C at O. The **Milnor number** of C at O is defined by (see [Mil68]):

$$\mu(C, O) = dim_{\mathbb{C}} \frac{\mathbb{C}\{x, y\}}{(\frac{\partial f}{\partial x}, \frac{\partial f}{\partial y})}.$$

Remark 1.1.3. The Milnor number vanishes if and only if the germ C is smooth at p.

Let $f \in \mathbb{C}\{x, y\}$ be reduced. A **parametrization** of C is a couple of functions $(\Phi_1(t), \Phi_2(t)) \in \mathbb{C}\{t\}$ such that $f(\Phi_1(t), \Phi_2(t)) = 0$.

A parametrization is **good** if the map $t \mapsto (\Phi_1(t), \Phi_2(t))$ is injective for $|t| < \epsilon$, if $\epsilon > 0$ is small enough.

Let $h \in \mathbb{C}\{x\}$ such that $h = x^m \sum_{i=0}^{\infty} a_i x^i$, $a_0 \neq 0$, $m \geq 0$. Then $v_x(h) = m$ is the **x-order** of h at O.

Remark 1.1.4. $v_x(\sum_{j \in \mathbb{N}} a_j x^j) := \min\{j \in \mathbb{N} |\ a_j \neq 0\}$.

Definition 1.1.5. Let C and C' be two germs at $O \in \mathbb{C}^2$ and let f and g be defining functions for them. Then the **intersection number** $i(C, C') \in \mathbb{N}$ is defined in the following way:

$$i(C, C') = dim_{\mathbb{C}} \frac{\mathbb{C}\{x, y\}}{(f, g)}.$$

The intersection number $i(C, C')$ is also denoted $C.C'$.

The following properties of intersection numbers are classical:

Proposition 1.1.6. *Let C and C' be two germs at O without common branches. Let f be a defining function of C and let $(x, y) = (\Phi_1(t), \Phi_2(t))$ be a good parametrization of C'. Then:*

$$i(C, C') = v_t(f(\Phi_1(t), \Phi_2(t))).$$

Moreover:

— *if C and C' are smooth and transverse at O, then $i(C, C') = 1$;*
— *$i(C, C') = i(C', C)$;*
— *if $C = C_1 \cup C_2$, $C' = C'_1 \cup C'_2$, then*

$$i(C, C') = i(C_1, C'_1) + i(C_1, C'_2) + i(C_2, C'_1) + i(C_2, C'_2).$$

A proof can be found in [Wal04, Lemma 1.2.1].

1.1.2 The Newton-Puiseux Theorem

Definition 1.1.7. Let $f = \sum_{r,s=0}^{\infty} a_{r,s} x^r y^s \in \mathbb{C}\{x, y\}$. Its **support** is defined by:

$$S(f) := \{(r, s) \in \mathbb{N}^2 \mid a_{r,s} \neq 0\}.$$

The **Newton diagram** $\tilde{\mathcal{N}}(f)$ of f is defined as the convex hull of:

$$\bigcup_{(r,s)\in S(f)} ((r, s) + \mathbb{R}^2_{\geq 0}).$$

The **Newton polygon** $\mathcal{N}(f)$ of f is the union of the compact edges of $\partial\tilde{\mathcal{N}}(f)$.

Remark 1.1.8. Let $(C, p) \hookrightarrow (\Sigma, p)$ be a curve singularity, $C = V(f)$. A choice of a **cross** on Σ at p is the choice of a pair (L', L) of smooth curves intersecting transversally at p. The Newton polygon $\mathcal{N}(f)$ depends only on the cross $(L', L) = (V(y), V(x))$ defined by (x, y) and on the curve singularity (C, p).

In the case of a smooth point of a curve we know, by the Implicit Function Theorem, that there exists a local parametrization. The following Theorem gives an answer to the same problem in the case of a singular point.

Theorem 1.1.9. *[Newton-Puiseux] Let C be a branch at O and let (x, y) be a coordinate system at O. Moreover, let us assume that the y axis is not a branch of C. Then there exists a parametrization $(\Phi_1(t), \Phi_2(t))$ of C such that:*

$$\begin{cases} \Phi_1(t) = t^m \\ \Phi_2(t) = \sum_{r=1}^{\infty} a_r t^r \end{cases} \tag{1.1}$$

where $m = i(C, L)$ and $L = V(x)$.

Proof. The proof is classical and is based on the construction of the Newton polygon. See [Wal04, Theorem 2.1.1].

□

Corollary 1.1.10. *Let C be a branch at O of multiplicity $m \in \mathbb{N}^*$ and (x, y) a system of coordinates such that $x = 0$ is not tangent to C. Then there exists a good parametrization such that:*

$$\begin{cases} x = t^m \\ y = \sum_{r=m}^{\infty} a_r t^r \end{cases} \tag{1.2}$$

Definition 1.1.11. The **Puiseux characteristic** of a branch C of multiplicity $m \in \mathbb{N}^*$ is the sequence of numbers:

$$(\beta_0; \beta_1, \ldots, \beta_g)$$

where $\beta_0 = m$, $e_0 = m$ and $\beta_1, \ldots, \beta_g$ are defined in the following inductive way:

— for every $i \geq 1$, $\beta_i = min\{k|\ a_k \neq 0, e_{i-1} \nmid k\}$, $e_i = gcd(e_{i-1}, \beta_i)$;

— the algorithm stops with $e_g = 1$.

The integers $(\beta_i)_{0 \leq i \leq g}$ are called the **Puiseux characteristic numbers**. Following [Wal04], we call the rational numbers $\alpha_i = \frac{\beta_i}{m}$ the **Puiseux exponents**.

Two branches C and C' are **combinatorially equivalent** (or **topologically equivalent**) if and only if they have the same Puiseux characteristic.

Remark 1.1.12. Note that one has:

$$1 = e_g \mid e_{g-1} \mid \cdots \mid e_0 = m,$$

all the divisibilities being strict.

Let C be a branch having a good Newton-Puiseux parametrization. In particular, $x = t^m$. Let then x_m be such that $x_m^m = x$. By the substitution $t = x_m$ we obtain a series $y = \sum_{r=m}^{\infty} a_r x_m^r$. Moreover, we have m different choices for x_m, which are the m different roots of $t^m - x = 0$. For each choice of the root x_m we obtain a **pro-branch** of the branch C.

A pro-branch is defined in a sector of the form $|\arg(x) - \alpha| < \epsilon$, where $\epsilon > 0$ is small enough. The terminology of pro-branch has been introduced in [Wal04, Section 4.1]. The set of pro-branches of a branch C is denoted by $\mathbf{pro}(\mathbf{C})$.

Let γ_i and γ_i' be pro-branches of C_i and C_i' such that they are defined on the same sector. Consider the equations of the pro-branches:

$$y = \sum_{s \in \mathbb{Q}^+}^{\infty} a_s x^s, \quad y = \sum_{s \in \mathbb{Q}^+}^{\infty} a_s' x^s.$$

Definition 1.1.13. The **exponent of contact of two pro-branches** γ and γ' is

$$\mathcal{O}(\gamma, \gamma') := min\{s|\ a_s \neq a_s'\}.$$

The **exponent of contact of two branches** C and C' is

$$\mathcal{O}(C, C') = min\{\mathcal{O}(\gamma, \gamma')|\ \gamma \in pro(C), \gamma' \in pro(C')\}.$$

Proposition 1.1.14 allows to compute intersections between branches by using the data given by the exponents of contact.

Proposition 1.1.14.

$$i(C, C') = \sum_{\gamma \in pro(B), \gamma' \in pro(B')} \mathcal{O}(\gamma, \gamma').$$

A proof can be found in [Wal04, Proposition 4.1.5].

Definition 1.1.15. Let $C = C_1 \cup \cdots \cup C_r$ and $C' = C_1' \cup \cdots \cup C_r'$ be curve singularities at O such that

— C_i and C'_i have the same Puiseux characteristic for all $i = 1, \dots, r$;
— $\mathcal{O}(C_i, C_j) = \mathcal{O}(C'_i, C'_j)$ for all $1 \leq i < j \leq r$.
Then C and C' are **combinatorially equivalent** (or **topologically equivalent**).

Definition 1.1.16. Let C_1 and C_2 be branches of C such that:
— C_1 has Puiseux characteristic $(m; \beta_1, \dots, \beta_r, \beta_{r+1}, \dots, \beta_{r+k})$;
— C_2 has Puiseux characteristic $(m'; \beta'_1, \dots, \beta'_r)$;
— $\beta_i/m = \beta'_i/m'$ for all $i = 1, \dots, r$;
— $\mathcal{O}(C_1, C_2) > \beta'_r/m'$.
Then C_2 is a **truncation** of C_1.

1.1.3 The Eggers-Wall tree

We now want to define the *Eggers-Wall tree*, an invariant coding classes of topologically equivalent germs. We take the idea of the construction from [Wal04, Section 4.2].

We have seen that a single branch C is characterized topologically by its Puiseux characteristic $(m; \beta_1, \dots, \beta_g)$. We consider a tree $\Gamma_{EW}(C)$ homeomorphic to the compact segment $[0, \infty]$ and two inverse homeomorphisms

$$\nu_C : \Gamma_{EW}(C) \to [0, \infty], \quad \pi_C : [0, \infty] \to \Gamma_{EW}(C).$$

such that $v_C \circ \pi_C : [0, \infty] \to [0, \infty]$ is the identity.

We consider then on $\Gamma_{EW}(C)$ marked points $A_k := \pi_C(\beta_k/m)$, and points $A_0 = \pi_C(0)$ and $A_C = \pi_C(\infty)$. Such points in $\Gamma_{EW}(C)$ correspond to the Puiseux exponents of the curve. Moreover, let $p \in (A_i, A_{i+1}]$. We define $h_C : \Gamma_{EW}(C) \to [0, \infty]$ as $h_C(p) = m/e_i$. In particular $h_C(0) = 1$ and $h_C(A_C) = m$.

Let us consider now a germ C having several branches $C_1, \dots, C_r$. Let $o_{ij} = \mathcal{O}(C_i, C_j)$. We define then $\Gamma_{EW}(C_i \cup C_j)$ by:

$$\Gamma_{EW}(C_i \cup C_j) = \frac{\Gamma_{EW}(C_i) \cup \Gamma_{EW}(C_j)}{\pi_{C_i}[0, o_{ij}] \simeq \pi_{C_j}[0, o_{ij}]},$$

the two segments being identified by $\pi_{C_i} \circ id_{[0,o_{ij}]} \circ \nu_{C_j}$. The two functions ν_{C_i}, ν_{C_j} glue into $\nu_{C_i \cup C_j} : \Gamma_{EW}(C_i \cup C_j) \to [0, \infty]$. Moreover, $h_{C_i}|_{\pi_{C_i}[0,o_{ij}]} = h_{C_j}|_{\pi_{C_j}[0,o_{ij}]}$ and so they glue also into a function $h_{C_i \cup C_j} : \Gamma_{EW}(C_i \cup C_j) \to \mathbb{N}^*$.

It is now possible to compute inductively this tree by adding the different branches and then obtaining the tree $\Gamma_{EW}(C)$. We consider it as a **rooted tree** with root A_0, the point obtained by identifying all the points $A_0 \in \Gamma_{EW}(C_i)$.

Remark 1.1.17. One has that $h_C(A_0) = 1$ and $h_C(A_{C_i}) = m_i$.

Definition 1.1.18. Let C be a curve singularity. The **Eggers-Wall tree** of C is the rooted tree constructed before, endowed with the two functions $h_C : \Gamma_{EW}(C) \to [0, \infty]$ and $\nu_C : \Gamma_{EW}(C) \to [0, \infty]$.

An example of Eggers-Wall tree is shown in Figure 1.4.

1.2 Blow-up and singularity invariants

1.2.1 Notations for blow-up sequences

Definition 1.2.1. Let $\Sigma^{(0)} = \mathbb{C}^2$ and let $\Sigma^{(1)}$ be the surface defined by:

$$\Sigma^{(1)} = \{(x,\ y;\ \nu : \eta) \in \mathbb{C}^2 \times P^1(\mathbb{C}) |\ x\eta = y\nu\}.$$

The **blow up** of $\mathbb{C}^2$ of **centre** O is the morphism $\pi_1 = \Phi_1 : \Sigma^{(1)} \to \mathbb{C}^2$, restriction to $\Sigma^{(1)}$ of the first projection $\mathbb{C}^2 \times P^1(\mathbb{C}) \to \mathbb{C}^2$. It satisfies the following properties:

1. $(\Phi_1)^{-1}(O) = E_0^{(1)} = E^{(1)}$ is a smooth rational curve,
2. $\Phi_1(\Sigma^{(1)} - E^{(1)}) \to \mathbb{C}^2 - \{O\}$ is an algebraic isomorphism,
3. $\Sigma^{(1)}$ is smooth,
4. Φ_1 is proper.

The subspace $E^{(1)}$ is the **exceptional locus** of Φ_1.

Let us study more in detail the manifold $\Sigma^{(1)}$. The space $P^1(\mathbb{C})$ has two affine coordinate charts, U_1 and U_2. In the first chart we consider $\eta \neq 0$ and in the latter $\nu \neq 0$. We take respectively coordinates $u_1 = \frac{\nu}{\eta}$ and $v_2 = \frac{\eta}{\nu}$. On U_1 the equation $x\eta = y\nu$ becomes $x = yu_1$, and we can consider v_1 to be the lift of y to U_1. In this way we obtain a coordinate system (u_1, v_1) on U_1. The restriction of the morphism Φ_1 to U_1 is described by:

$$\begin{cases} x = u_1 v_1 \\ y = v_1 \end{cases} \tag{1.3}$$

In the same way, we obtain for U_2 a coordinate system (u_2, v_2), for which Φ_1 is described by:

$$\begin{cases} x = u_2 \\ y = u_2 v_2 \end{cases} \tag{1.4}$$

Moreover, the change of coordinates on $U_1 \cap U_2$ is given by:

$$\begin{cases} u_2 = u_1 v_1 \\ v_2 = \frac{1}{u_1} \end{cases} \tag{1.5}$$

More generally, one may blow up any point of a smooth surface, by using the previous description in local coordinates. One may show that the resulting morphism is independent of the choice of local coordinates ([Wal04, Lemma 3.2.1]).

Let us explain now the notations used throughout this thesis for the morphisms obtained as finite compositions of points blow-ups and for their exceptional loci.

Assume inductively that for some $i \in \mathbb{N}^*$ we have defined a map

$$\pi_i : \Sigma^{(i)} \to \mathbb{C}^2$$

such that:

1. $E^{(i)} = \pi_i^{-1}(O)$;

2. $\pi_i : \Sigma^{(i)} - E^{(i)} \to \mathbb{C}^2 - \{O\}$ is an analytical isomorphism;
3. $\Sigma^{(i)}$ is smooth;
4. π_i is proper.

We call $E^{(i)} \hookrightarrow \Sigma^{(i)}$ the **exceptional locus** of π_i. Consider the **blow up**:

$$\Phi_{i+1} : \Sigma^{(i+1)} \to \Sigma^{(i)}$$

of $\Sigma^{(i)}$ with finite set of centres $\{O_j \mid j \in J(i)\} \subset E^{(i)}$, where $J(i)$ is a set of indices depending on i. Denote $\Phi_{i+1}^{-1}(O_j) = E_j^{(i+1)}$. We define the map $\pi_{i+1} : \Sigma^{(i+1)} \to \mathbb{C}^2$ as:

$$\pi_{i+1} = \pi_i \circ \Phi_{i+1}.$$

Let $C \subset \mathbb{C}^2$ be a curve singularity, $O \in C$. Then $\bar{C}^{(i)} = \pi_i^{-1}(C)$ is the **total transform** of C in $\Sigma^{(i)}$. Let $C^{(i)}$ be the closure in $\Sigma^{(i)}$ of $\bar{C}^{(i)} - E^{(i)}$. Then $C^{(i)}$ is the **strict transform** of C in $\Sigma^{(i)}$.

Let $E_j^{(i)}$ be an irreducible component of $E^{(i)} \subset \Sigma^{(i)}$. Then $E_j^{(i+1)}$ is the strict transform of $E_j^{(i)} \subset \Sigma^{(i+1)}$ by the morphism Φ_{i+1}.

Definition 1.2.2. Let C be a curve singularity and let $\Sigma^{(N)}$ be a surface such that $C^{(N)}$ is smooth and transverse to $E^{(N)}$, that is, such that *the total transform* $\bar{C}^{(N)}$ is a normal crossing divisor. The map

$$\pi_N : (\Sigma^{(N)}, E^{(N)}) \to (\mathbb{C}^2, O)$$

is then called an **embedded resolution** of C.

Theorem 1.2.3 (M. Noether)**.** *Let C be a curve singularity at O. Then there exists an embedded resolution π_N of C, obtained recursively by blowing-up on every surface $\Sigma^{(j)}$ all the points O_i such that $\bar{C}^{(j)}$ does not have normal crossings at O_i.*

*Moreover, one gets in this way the **minimal embedded resolution**, in the sense in which every other embedded resolution factors through it.*

For a proof, see [Wal04, Theorem 3.3.1].

1.2.2 Infinitely near points and Enriques diagrams

Remark 1.2.4. We keep the notations of the previous subsection.

Definition 1.2.5. Let $O_i \in \Sigma^{(k)}$ be a point. We consider the map $\Phi_{k+1} : \Sigma^{(k+1)} \to \Sigma^{(k)}$, and a point $O_j \in \Phi_{k+1}^{-1}(O_i)$. We say that O_i is the **direct predecessor** of O_j and we write $p_D(O_j) = O_i$. We set by convention $p_D(O) = O$. A point O_i is an **infinitely near point** of O.

For every $i \in \{0, \ldots, N-1\}$ let $\mathcal{P}^{(i)}$ be the set of infinitely near points on the surface $\Sigma^{(i)}$. For every i, we can define the **direct predecessor function** $p_D : \mathcal{P}^{(i)} \to \mathcal{P}^{(i-1)}$. Moreover, we can consider the iterations $p_D^r : \mathcal{P}^{(k+r)} \to \mathcal{P}^{(k)}$.

Definition 1.2.6. The set of points $\mathcal{P} := \cup_{i=0}^{N-1}\mathcal{P}^{(i)}$ is a **constellation** of points. In particular, $\mathcal{P}^{(0)} = \{O\}$.

Let C be a curve singularity. Its **associated constellation** is the set of infinitely near points of the minimal embedded resolution.

Remark 1.2.7. A constellation of points can be defined *independently* from the curve singularity C as the sequence of sets of points that are centres of blow up on each surface $\Sigma^{(i)}$.

Let $O_i \in \Sigma^{(k_1)}$ and $O_j \in \Sigma^{(k_2)}$, $k_1 < k_2$. We say that $O_i \preceq O_j$ if $\Phi_{k_1+1} \circ \cdots \circ \Phi_{k_2}(O_j) = O_i$, i.e., if there exists $r \geq 0$ such that $p_D^r(O_j) = O_i$. In this case, we say that O_i is a **predecessor** of O_j. Moreover, $p_D(O) = O$, so that O is the only point which is stable under p_D.

The couple $(\mathcal{P}, \preceq)$ is a partially ordered set, therefore we can consider its associated **Hasse diagram**. In our case, it is a tree. It is a combinatorial invariant of curve singularities, but it is not sufficiently rich to encode the full combinatorial type. We can consider an enrichment of the Hasse diagram, the **Enriques tree**, giving us all topological information about the blowing up sequence. Before defining it, let us introduce more terminology about infinitely near points.

Definition 1.2.8. Let $O_i \in \mathcal{P}^{(j)} \subset \Sigma^{(j)}$.
— O_i is a **satellite point** if $O_i = E_{k_1}^{(j)} \cap E_{k_2}^{(j)}$ for $k_1 \neq k_2$;
— O_i is a **free point** if O_i is a smooth point of $E^{(j)}$.

Let O_i be a satellite point. If $E_{k_1}^{(j)}$ is the exceptional component obtained by the blow up of centre $O_{k_1}^{(j-1)} \in \Sigma^{(j-1)}$, then $p_D(O_i) = O_{k_1}$. By definition there exists another component $E_{k_2}^{(j)}$ such that $O_i \in E_{k_2}^{(j)}$. Such component has been obtained by blow up of a surface $\Sigma^{(j-r)}$ with centre $O_{k_2}^{(j-r)}$.

Definition 1.2.9. There exists a function $p_I : \mathcal{P} \to \mathcal{P} \cup \{\emptyset\}$ such that:
— if $O_i^{(j)}$ is a free point, then $p_I(O_i^{(j)}) = \emptyset$;
— if $O_i^{(j)}$ is a satellite point, $O_i^{(j)} \in E_{k_1}^{(j)} \cap E_{k_2}^{(j)}$ with $p_D(O_i^{(j)}) = O_{k_1}^{(j-1)}$, then:

$$p_I(O_i^{(j)}) = O_{k_2}^{(j-r)}.$$

The point $p_I(O_i^{(j)})$ is the **indirect predecessor** of $O_i^{(j)}$.

We define the set of **proximity points** of O_i as $\mathcal{P}(O_i) = \mathcal{P}_D(O_i) \cup \mathcal{P}_I(O_i)$, where:
— $\mathcal{P}_D(O_i) = \{O_j \in \mathcal{P} \mid \ O_i = p_D(O_j)\}$;
— $\mathcal{P}_I(O_i) = \{O_k \in \mathcal{P} \mid \ O_i = p_I(O_k)\}$.
If $\mathcal{P}(O_i) = \emptyset$, then O_i is a **leaf** of $\mathcal{P}$.

Remark 1.2.10. Let $O_i = E_j \cap E_k$, $k < j$. In the following we will sometimes write $j = p_D(i)$ and $k = p_I(i)$ to indicate $O_j = p_D(O_i)$ and $O_k = p_I(O_i)$.

Let us come back to the Hasse diagram. It has been defined using only the information given by the direct predecessor. The Enriques diagram is an enrichment of the Hasse diagram which uses also the information about the indirect predecessor. We will see that in this way we obtain an invariant which encodes the topological type of a curve singularity.

Definition 1.2.11. Let C be a curve singularity and let $\mathcal{P}$ be the associated constellation. The **Enriques tree** $\mathcal{E}(C)$ is the graph obtained in the following way:

1. the vertices are the points $O_i \in \mathcal{P}$;
2. if O_i is a free point, then O_i is joined to $p_D(O_i)$ by a curvilinear line;
3. if O_i is a satellite point, then O_i is joined to $p_D(O_i)$ by a segment;
4. the union of two consecutive segments is a straight line if the two starting points O_i and $p_D(O_i)$ have the same indirect predecessor;
5. the union of two consecutive segments is a broken line if O_i and $p_D(O_i)$ don't have the same indirect predecessor;
6. if a branch $C_l \subset C$ is transverse to a component E_i, we indicate it by an arrowhead attached to the vertex O_i.

The details of this construction can be found in [CA00]. It has been initially defined in [EC15].

Example 1.2.12. The Enriques tree for the singularity $C = C_1 \cup C_2 \cup C_3 \cup C_4$, where:

1. $C_1 : \ y = x^{13/8}$;
2. $C_2 : \ y = x^{3/2} - x^{7/4}$;
3. $C_3 : \ y = 2x^{3/2} + x^{5/3}$;
4. $C_4 : \ y = -x^{3/2} - x^{11/6}$;

is shown in Figure 1.1. To compute the tree we use the method of [BPPP14], which will be explained in Proposition 1.4.14.

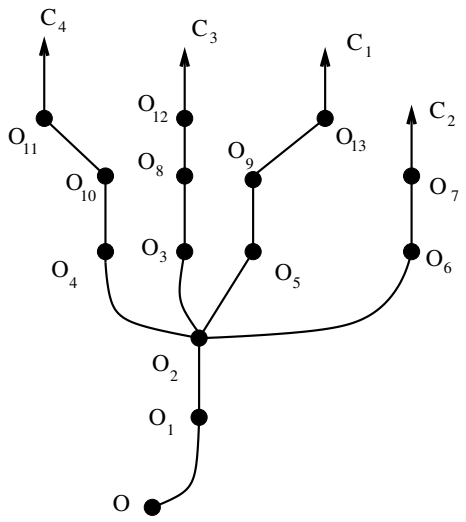

Figure 1.1 – An Enriques diagram.

1.2.3 Multiplicities and dual graph

Remark 1.2.13. Let C be a branch. Then one may index the associated infinitely near points by $(O_0, O_1, \ldots, O_N)$, where $O_0 = O$, and $O_i = p_D^{j-i}(O_j)$ for every $i, j = 0, \ldots, N$, $i < j$. Moreover, $E_{i-1}^{(i)} = \Phi_i^{-1}(O_{i-1})$.

Definition 1.2.14. Let C be a *curve singularity* and $O_i \in \Sigma^{(j)}$. We say that $m_i = m_{O_i}(C^{(j)})$ is the **multiplicity** of C at the point O_i.

Let C be a *branch*. The indices being chosen as in the previous remark, the sequence of numbers $\{m_0, m_1, \ldots, m_N\}$ is the **multiplicity sequence** of C.

Remark 1.2.15. In the case of a curve singularity $C = C_1 \cup \cdots \cup C_r$ we have one multiplicity sequence for each branch C_i.

The multiplicity at a point O_i for the curve singularity C is the sum of the multiplicities at O_i of all the branches of C.

Lemma 1.2.16. *Let C be a curve singularity and $O_i \in \Sigma^{(j-1)}$. The multiplicity*

$$m_i = m_{O_i}(C^{(j-1)})$$

is equal to the intersection number of the strict transform $C^{(j)}$ of C in $\Sigma^{(j)}$ with the exceptional component $E_i^{(j)}$.

The following Proposition (see [Wal04, Theorem 3.5.5]) allows to compute the multiplicity sequence of a branch starting from its Puiseux characteristic.

Proposition 1.2.17. *Let C be a branch, $(m; \beta_1, \ldots, \beta_g)$ its Puiseux characteristic. The blow up of centre O gives a new branch C' such that:*

1. *if $\beta_1 > 2m$, then the Puiseux characteristic is $(m; \beta_1 - m, \ldots, \beta_g - m)$;*
2. *if $\beta_1 < 2m$ and $(\beta_1 - m) \nmid m$, then the Puiseux characteristic is $(\beta_1 - m; m, \beta_2 - (\beta_1 - m), \ldots, \beta_g - (\beta_1 - m))$;*
3. *if $\beta_1 < 2m$ and $(\beta_1 - m) \mid m$, then the Puiseux characteristic is $(\beta_1 - m; \beta_2 - (\beta_1 - m), \ldots, \beta_g - (\beta_1 - m))$.*

We can apply inductively Proposition 1.2.17 to the curve $C^{(j)} \subset \Sigma^{(j)}$, until we obtain a curve $C^{(N)}$ having Puiseux characteristic $(1; 1)$. This proposition can be used to prove the existence of a minimal embedded resolution for a branch (see [Wal04, Theorem 3.5.5]).

Theorem 1.2.18. *Let C and C' be two branches. Then C and C' are topologically equivalent if and only if they have the same multiplicity sequence.*

Proof. Let us only prove the non-trivial implication. We will use an argument taken from [Wal04, Theorem 3.5.6].

Let $\{m_0, m_1, \ldots, m_N\}$ be a multiplicity sequence. Then we have that $(m_N; \beta_N) = (1, 1)$.

Let us consider the two multiplicities m_0 and m_1, $m_1 > 1$. The algorithm will be the same for any couple of multiplicities m_i and m_{i+1}.

Let us consider the sequence $(m_1; \beta_1, \ldots, \beta_g)$.

1. If $m_0 = m_1$, the new Puiseux characteristic is $(m_0; \beta_1 + m_1, \ldots, \beta_g + m_1)$.
2. If $m_1 \nmid m_0$, the new Puiseux characteristic is $(m_0; \beta_1 + m_1, \ldots, \beta_g + m_1)$.
3. If $m_1 \mid m_0$ and $m_1 \neq m_0$, then $(m_0; m_0 + m_1, \beta_1 + m_1, \ldots, \beta_g + m_1)$ is the new characteristic of Puiseux.

Then we have an algorithm which allows us to compute the Puiseux characteristic from the multiplicity sequence.

□

Proposition 1.2.19. *Let C be a curve singularity and $O_i \in \mathcal{P}$. Then:*

$$m_i = c_i + \sum_{h:\ O_h \in \mathcal{P}(O_i)} m_h, \tag{1.6}$$

where $\mathcal{P}(O_i)$ is the set of proximity points of O_i and c_i is the number of irreducible components of C that are transversal to E_i.

Corollary 1.2.20. *Let C be a branch. Let O_i be a point and*

$$\mathcal{P}(O_i) = \{O_{i+1}, O_{i+2}, \ldots, O_{i+h-1}, O_{i+h}\},\ h \geq 1.$$

Then the multiplicity sequence is such that:

$$m_i = m_{i+1} + m_{i+2} + \cdots + m_{i+h-1} + m_{i+h}$$

and moreover $m_{i+1} = \cdots = m_{i+h-1}$.

A proof of the two statements can be found in [Wal04, Proposition 3.5.1].

We can then enrich the Enriques diagram with the corresponding multiplicities, using Equation 1.6. In Figure 1.2 we can see the result of the computation for the curve of Example 1.2.12.

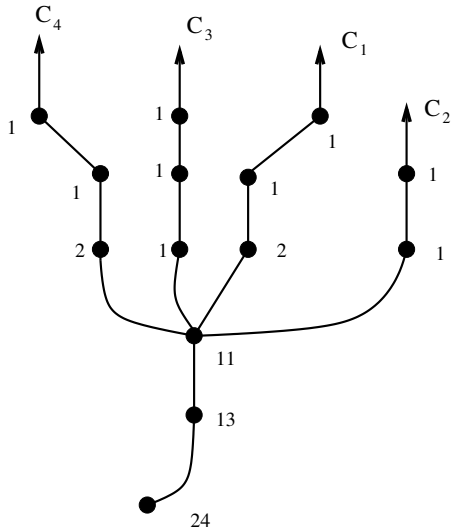

Figure 1.2 – The multiplicities of a curve singularity.

Definition 1.2.21. Let C be a curve singularity and let $(\Sigma^{(N)}, E^{(N)})$ be its minimal embedded resolution space. The **dual graph** $\gamma(C)$ of C is a graph such that:

1. the vertices are in bijective correspondence with the irreducible components of the total transform $\bar{C}^{(N)}$;

2. two vertices are adjacent if and only if the associated irreducible components intersect;
3. a branch of C transversal to a component E_i is represented by an arrowhead attached to the vertex E_i;
4. to each vertex E_i we attach the intersection number $E_i.E_i$ of the associated irreducible component E_i.

Remark 1.2.22. The dual graph $\gamma(C)$ is a tree.

Using the fact that each time we blow up a point of a component $E_i^{(j)}$ its self intersection drops by 1, one gets:

Proposition 1.2.23. *Let $E_i^{(N)} \subset \Sigma^{(N)}$ be an exceptional component. Then:*

$$(E_i^{(N)})^2 = -1 - \#\mathcal{P}(O_i).$$

Example 1.2.24. The dual graph of the singularity of Example 1.2.12 is shown in Figure 1.3.

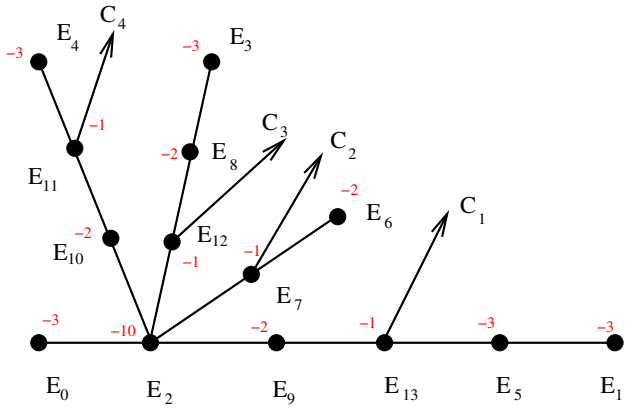

Figure 1.3 – A weighted dual graph.

The following classical theorem states that the various enriched trees associated to a curve singularity encode its topological type:

Theorem 1.2.25. *The following statements are equivalent:*

1. *C and C' have the same topological type;*
2. *C and C' have isomorphic Eggers-Wall trees;*
3. *C and C' have isomorphic dual graphs;*
4. *C and C' have isomorphic Enriques trees.*

Proof. The proof that the first three statements are equivalent can be found in [Wal04, Proposition 4.3.8]. We want now to prove the equivalence between 1 and 4.

Let C and C' have the same combinatorial type. Then they have isomorphic minimal resolution space, and the construction of the minimal resolution space is encoded by the Enriques tree.

Assume conversely that $\mathcal{E}(C)$ and $\mathcal{E}(C')$ are isomorphic trees. Then the spaces $\Sigma^{(0)} = \mathbb{C}^2$ and $(\Sigma^{(0)})' = \mathbb{C}^2$ are isomorphic. We blow up the surface with centre O, giving two analytically isomorphic surfaces $\Sigma^{(1)}$ and $(\Sigma^{(1)})'$.

Let us suppose that $\Sigma^{(j)}$ and $(\Sigma^{(j)})'$ are two isomorphic surfaces. The Enriques trees give information on how to choose the centres of the blow ups of the two surfaces, thus $\Sigma^{(j+1)}$ and $(\Sigma^{(j+1)})'$ are still isomorphic.

By induction we have an isomorphism between the two resolution spaces $\Sigma^{(N)}$ and $(\Sigma^{(N)})'$, and C and C' have the same *topological type*.

□

We have now the following problem: given one of the three invariants (the Eggers-Wall tree, the dual graph, and the Enriques tree), how can one compute the others?

The Enriques tree gives information about the steps needed to obtain the resolution space, but without showing the final result. The dual graph gives information about the final resolution space, but without showing how it was actually obtained. And the Eggers-Wall tree gives information about the algebraic properties of the curve, but no direct information about the resolution space.

In Section 1.4 we will show a recent invariant, the *lotus*, that has been introduced by Popescu-Pampu ([PP11]) to give an easy way to compute the previous invariants of singularities just by the knowledge of one of them.

Example 1.2.26. Let $C = \cup_1^7 C_i$, whose branches have the following Puiseux characteristics:
- C_1 : $(12; 18, 44, 45)$;
- C_2 : $(2; 3)$;
- C_3 : $(3; 5)$;
- C_4 : $(5; 8)$;
- C_5 : $(1; 1)$;
- C_6 : $(1; 1)$;
- C_7 : $(4; 6, 7)$.

and whose exponents of contact $o_{ij} = \mathcal{O}(C_i, C_j)$ are:

$$(o)_{ij} = \begin{pmatrix} 0 & 3/2 & 3/2 & 3/2 & 1 & 1 & 7/4 \\ 3/2 & 0 & 3/2 & 3/2 & 1 & 1 & 3/2 \\ 3/2 & 3/2 & 0 & 5/3 & 1 & 1 & 3/2 \\ 3/2 & 3/2 & 5/3 & 0 & 1 & 1 & 3/2 \\ 1 & 1 & 1 & 1 & 0 & 1 & 1 \\ 1 & 1 & 1 & 1 & 1 & 0 & 1 \\ 7/4 & 3/2 & 3/2 & 3/2 & 1 & 1 & 0 \end{pmatrix}$$

Then the Eggers-Wall tree of C, its Enriques tree and its dual graph are represented from left to right in Figure 1.4.

The germs C_5 and C_6 are transversal to the exceptional component E_0, so that their minimal resolution space is $\Sigma^{(0)}$. Moreover, on the component E_2 we have a blow up having as center a satellite point $P_3 = E_2 \cap E_1$ and a free point P_4.

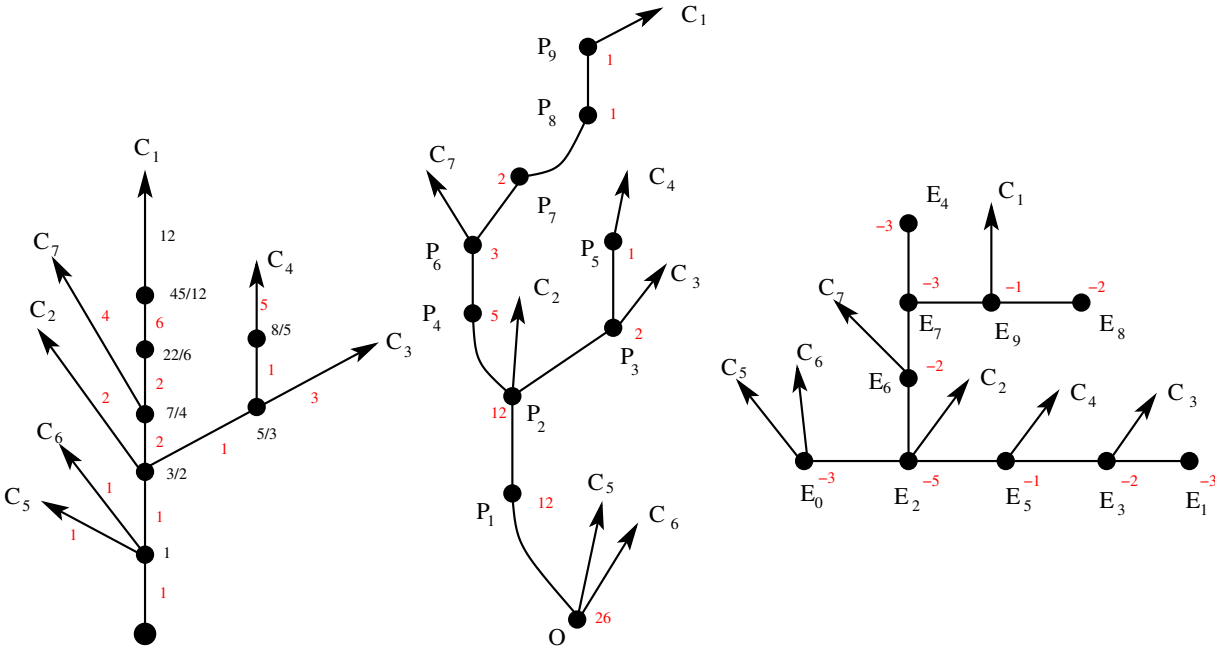

Figure 1.4 – The three kinds of trees.

1.3 Continued fractions and toric geometry.

1.3.1 Continued fractions

Let (p, q) be a pair of natural numbers. Then there exists a unique pair $(a_0, r_1) \in \mathbb{N}^2$ such that $r_1 < q$, and:

$$p = a_0 \cdot q + r_1.$$

Remark 1.3.1. One has that $p < q$ if and only if $a_0 = 0$.

We can then write:

$$\frac{p}{q} = a_0 + \frac{r_1}{q} = a_0 + \frac{1}{\frac{q}{r_1}}.$$

We can apply the same argument to the pair (q, r_1) and find new natural numbers a_1 and r_2. Then repeat. This algorithm is nothing else than the *Euclidean algorithm*, introduced by Euclid in his *Elements* to find the greatest common divisor of a pair of natural numbers. Therefore, we are analysing the results for each step of this algorithm for a couple of coprime numbers. Let us concentrate on the sequence of numbers a_i.

Definition 1.3.2. Let $(a_0, a_1, \ldots, a_n)$ be a sequence of natural numbers such that $a_i \geq 1$ for $i \geq 1$. The associated **continued fraction** is:

$$[a_0, \ldots, a_n] := a_0 + \cfrac{1}{a_1 + \cfrac{1}{\cdots + \cfrac{1}{a_n}}}.$$

This shows that every non-negative rational number may be expressed as a finite continued fraction. This expression is almost unique, as explained in Lemma 1.3.3:

Lemma 1.3.3. *The only possible equalities between continued fractions are:*

$$[a_0, \dots, a_n, 1] = [a_0, \dots, a_n + 1].$$

Remark 1.3.4. Every rational number can be expressed as a finite continued fraction if in Definition 1.3.2 we allow also negative values of a_0.

The previous constructions can be summarized in the following proposition:

Proposition 1.3.5. *Let $(p, q) \in \mathbb{N} \times \mathbb{N}^*$ be a pair of coprime integers. Let $a_0, \dots, a_n$ be the sequence of values obtained by the Euclidean algorithm applied the to the pair (p, q). Then:*

$$\frac{p}{q} = [a_0, \dots, a_n].$$

Definition 1.3.6. Let $\frac{p}{q} = [a_0, \dots, a_n]$. We define p_k and q_k, $0 \leq k \leq n$ as the two coprime natural numbers such that:

$$\frac{p_k}{q_k} = [a_0, \dots, a_k].$$

Proposition 1.3.7.

$$\frac{p_0}{q_0} < \frac{p_2}{q_2} \cdots \leq \frac{p}{q} \leq \cdots < \frac{p_3}{q_3} < \frac{p_1}{q_1}.$$

Proof. See [Kar13, Proposition 1.18]. □

Proposition 1.3.8. *Let C be a branch having Puiseux characteristic $(m; \beta)$, such that $\frac{\beta}{m} = [a_0, \dots, a_n]$. Then in the associated multiplicity sequence $\{m_i\}_{i=1}^k$ there are exactly a_h elements m_i such that $m_i = r_h$, $\forall h \in \{0, \dots, n\}$, $m_0 = r_0 = m$.*

Proof. This result is a consequence of Proposition 1.2.17. In fact, if $\beta = a_0 \cdot m + r_1$, if we blow up $a_0 - 1$ times we obtain a new Puiseux pair $(m; m + r_1)$. By construction, $m + r_1 < 2m$. The blow-up of this Puiseux pair gives a pair $(r_1; m)$. We can then apply the same algorithm to the pair $(r_1; m)$.

□

Continued fractions have a geometric interpretation, introduced by Klein [Kle96]. Let us explain it.

We associate to $p/q = [a_0, \dots, a_n]$ the point $(q, p) \in \mathbb{R}^2$ and the line passing through the origin and the point (q, p). If $gcd(q, p) = 1$, the only integer points of the line are the points (kq, kp), $k \in \mathbb{Z}$.

The equation of the line is $qy = px$. It sub-divides the first quadrant into two parts. Call them $\sigma_1 = \{(x, y) |\ x \geq 0,\ y \geq 0,\ qy \leq px\}$ and $\sigma_2 = \{(x, y) |\ x \geq 0,\ y \geq 0,\ qy \geq px\}$. We can consider the convex hulls R_1 and R_2 of all integer points in $\sigma_1 - \{0, 0\}$ and $\sigma_2 - \{0, 0\}$. Then R_1 and R_2 are unions of a finite numbers of segments, whose endpoints are integer points. An example of this construction can be seen in Figure 1.5.

Definition 1.3.9. Let $A := (q, p)$. Let $(A'_0, A'_1, \ldots, A)$ and $(A''_0, A''_1, \ldots, A)$ be respectively the sequences of integer points of R_1 and R_2. We call such points the **characteristic points** of (q, p).

Proposition 1.3.10. *Let $p/q = [a_0, \ldots, a_n]$. Then the points A'_i and A''_i have respectively coordinates (p'_i, q'_i) and (p''_i, q''_i), such that:*

$$p'_i/q'_i = \{[a_0, \ldots, a_{2j-1}, a'_{2j}],\ 1 \leq a'_{2j} \leq a_{2j},\ j = 0, \ldots, n\},\ i = a_0 + a_2 + \cdots + a_{2j-2} + a'_{2j},$$

$$p''_i/q''_i = \{[a_0, \ldots, a_{2j}, a'_{2j+1}],\ 1 \leq a'_{2j+1} \leq a_{2j+1},\ j = 0, \ldots, n\},\ i = a_1 + \cdots + a_{2j-1} + a'_{2j+1},$$

and $A'_0 = (1, 0)$, $A''_0 = (0, 1)$.

For a proof, see [PP07].

Example 1.3.11. We consider the continued fraction:

$$\frac{8}{5} = [1, 1, 1, 2].$$

Then we have:

$$\frac{1}{1} = [1],\quad \frac{2}{1} = [1, 1],\quad \frac{3}{2} = [1, 1, 1].$$

Moreover, $1 < \frac{3}{2} < \frac{8}{5}$ and $2 > \frac{8}{5}$. We consider then the points:

$$A'_0 = (1, 0),\ A'_1 = (1, 1),\ A'_2 = (2, 3),\ A'_3 = (5, 8);$$

$$A''_0 = (0, 1),\ A''_1 = (1, 2),\ A''_2 = (3, 5),\ A''_3 = (5, 8).$$

The complete construction of Klein can be seen in Figure 1.5.

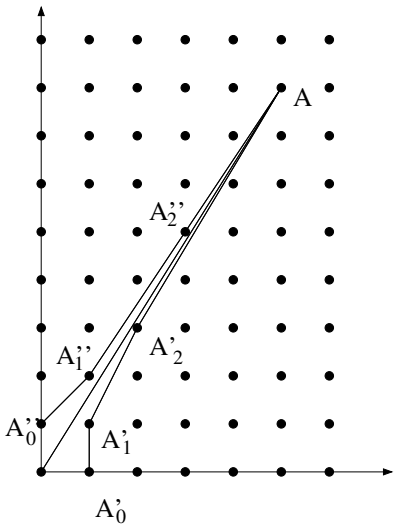

Figure 1.5 – Klein's construction.

1.3.2 Toric geometry

In this section we will state some important facts about toric varieties. The majority of the definitions and of the terminology has been inspired by [Ful93], which is also recommended for further understandings.

Definition 1.3.12. Let $\mathbb{K}$ a characteristic 0 field. A **toric variety** X of dimension n is a normal algebraic variety that contains a torus $T = (\mathbb{K}^*)^n$ as dense open subset, together with an action $T \times X \to X$ extending the natural action $T \times T \to T$ of T on itself by translation.

Definition 1.3.13. Let $N \cong \mathbb{Z}^n$ be a lattice of rank $n \in \mathbb{N}^*$ and $N_{\mathbb{R}} := N \otimes_{\mathbb{Z}} \mathbb{R}$ the associated real vector space. A **strongly convex rational polyhedral cone** $\sigma \subset N_{\mathbb{R}}$ is a convex cone such that:

— the origin is the apex;
— it is generated by a finite set of elements of N;
— if $v \in \sigma$, then $-v \notin \sigma$.

In the following we will write simply *cone* instead of *strongly convex rational polyhedral cone.*

Example 1.3.14. In Figure 1.6 we can see an example of a cone in $\mathbb{R}^2$, where $N = \mathbb{Z}^2$, generated by the two vectors $(1, 1)$ and $(3, 1)$.

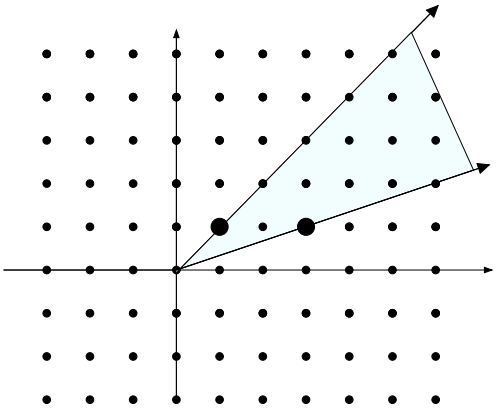

Figure 1.6 – A cone in $\mathbb{R}^2$.

Definition 1.3.15. Let $M = Hom(N, \mathbb{Z})$ be the **dual lattice**, $M_{\mathbb{R}} = M \otimes_{\mathbb{Z}} \mathbb{R}$. The **dual cone** $\check{\sigma} \subset M$ is the set:

$$\check{\sigma} = \{u \in M_{\mathbb{R}} \mid \langle u, v \rangle \geq 0 \ \forall v \in \sigma\}.$$

Proposition 1.3.16 (Gordan's Lemma)**.** *The commutative semi-group*

$$S_\sigma := \check{\sigma} \cap M$$

is finitely generated.

For a proof, see [Ful93, Section 1.2].

Let $\mathbb{K}[S_\sigma]$ be the associated semi-group ring. As a $\mathbb{K}$-vector space it has a *canonical basis*, denoted $\{\chi^{\mathbf{u}}\}_{\mathbf{u}\in\mathbf{S}_\sigma}$ and the multiplication is given by $\chi^u\chi^{u'} = \chi^{u+u'}$. Moreover, $\chi^0 = 1$.

Definition 1.3.17. Let σ be a cone. The **affine toric variety** U_σ is defined by:

$$U_\sigma = Spec(\mathbb{K}[S_\sigma]).$$

Definition 1.3.18. Let $(e_1, \ldots, e_n)$ be a basis of N and $(e_1^*, \ldots, e_n^*)$ be the dual basis of M. We denote:

$$X_i = \chi^{e_i^*} \in \mathbb{K}[M].$$

Proposition 1.3.19. *One has:*

$$\mathbb{K}[M] = \mathbb{K}[X_1, \ldots, X_n, X_1^{-1}, \ldots, X_n^{-1}]$$

the ring of Laurent polynomials in the n variables $X_1, \ldots, X_n$. Moreover,

$$U_{\{0\}} = Spec(\mathbb{K}[M]) \simeq (\mathbb{K}^*)^n$$

is an affine algebraic torus.

Proof. The proof, along with all the details of this constructions, can be found in [Ful93, Section 1.3]. □

Definition 1.3.20. Let $\mathbb{K}$ be a characteristic 0 field. We define:

$$T_{N,\mathbb{K}} := Spec(\mathbb{K}[M]).$$

We will write simply T_N if $\mathbb{K}$ is understood from the context.

Theorem 1.3.21. *Assume that $u_1, \ldots, u_r$ generate the semi-group S_σ. Then:*

$$\mathbb{K}[S_\sigma] = \mathbb{K}[Y_1, \ldots, Y_r]/I,$$

where I is the ideal generated by the binomials $Y_1^{a_1} \ldots Y_r^{a_r} - Y_1^{b_1} \ldots Y_r^{b_r}$, where $a_i, b_i \geq 0$ vary along the integers which describe the relations with non negative coefficients with the generators u_i:

$$a_1u_1 + \cdots + a_ru_r = b_1u_1 + \cdots + b_ru_r.$$

This fundamental theorem is stated in [Ful93] as an Exercise, Section 1.3.

Proposition 1.3.22. *Let σ be a cone in $N_\mathbb{R}$, $t \in T_N$ and $x \in U_\sigma$. The point t may be seen as a morphism $(M, +) \to (\mathbb{K}^*, \cdot)$ of groups, while the point x as a morphism $(S_\sigma, +) \to (\mathbb{K}, \cdot)$ of semi-groups. Then the map:*

$$T_N \times U_\sigma \to U_\sigma$$

is described dually as the morphism of algebras:

$$\mathbb{K}[S_\sigma] \to \mathbb{K}[M \oplus S_\sigma],$$

induced by the following morphism of semigroups:

$$s \mapsto (s, s).$$

Lemma 1.3.23. *For each cone σ we consider the affine toric variety U_σ. Moreover, given σ and σ', $\sigma \cap \sigma'$ is a cone and $U_{\sigma\cap\sigma'}$ is an open subvariety of U_σ and $U_{\sigma'}$.*

Definition 1.3.24. A **fan** $\Delta \subset N$ is a finite set of cones $\sigma \subset N_{\mathbb{R}}$ such that:
— a face of a cone in Δ is a cone in Δ;
— if σ and σ' are two cones in Δ, then $\sigma \cap \sigma'$ is a cone in Δ.

Proposition 1.3.25. *Let Δ be a fan. Given two cones σ and σ' in Δ, $U_{\sigma\cap\sigma'}$ is a principal open subvariety of both U_σ and $U_{\sigma'}$. Moreover, if we glue U_σ to $U_{\sigma'}$ along $U_{\sigma\cap\sigma'}$, we get a separated variety.*

Definition 1.3.26. Let Δ be a fan. The **toric variety** $X(\Delta)$ is the variety constructed by gluing in the previous way all the affine toric varieties U_σ, when σ varies among the cones in Δ.

Example 1.3.27. Let us consider two cones σ and σ' in $N_R = \mathbb{Z}^2 \otimes \mathbb{R}$, generated respectively by $(1,0),(1,1)$ and by $(1,1),(0,1)$. We notice that $(1,1) = (1,0) + (0,1)$. Denote by Δ the fan formed by σ, σ' and their faces. Then $U_\sigma = Spec(\mathbb{C}[Y, XY^{-1}])$ and $U_{\sigma'} = Spec(\mathbb{C}[X, X^{-1}Y])$, thus both U_σ and $U_{\sigma'}$ are isomorphic to $\mathbb{C}^2$.

We have then two charts, isomorphic to $\mathbb{C}^2$ and generated respectively by (U_1, V_1), (U_2, V_2). The morphisms of change of charts are defined by:

$$\begin{cases} U_1 = U_2 V_2 \\ V_1 = V_2^{-1} \end{cases} \tag{1.7}$$

$$\begin{cases} U_2 = U_1 V_1 \\ V_2 = V_1^{-1} \end{cases} \tag{1.8}$$

Comparing this with the description done in Subsection 1.2.1, we obtain that the toric variety $X(\Delta)$ is the blow-up of $\mathbb{C}^2$ with centre O.

Proposition 1.3.28. *An affine toric variety U_σ is isomorphic to $\mathbb{K}^n$ if and only if σ is generated by a basis for N. Moreover, a toric variety is* smooth *if and only if all the cones of its fan are generated by vectors which may be extended to a basis of N.*

Proposition 1.3.29. *Let $N = \mathbb{Z}^2$ and $v \in \mathbb{N}^2$, being oriented by the basis $(1,0),(0,1)$. Let σ and σ' be the cones generated respectively by $\{(1,0), v\}$ and $\{v, (0,1)\}$. Then there exists a minimal set $\{v_0, \ldots, v_{i-1}, v_i, v_{i+1}, \ldots, v_n\}$ such that:*
— *$v_0 = (1,0)$;*
— *$v_n = (0,1)$*
— *$v_i = v$*
— *$(v_k, v_{k+1})_{k\in 0,\ldots,n-1}$ is a direct basis for N.*

Definition 1.3.30. Let $v = (q,p)$ and let $p/q = [a_0, \ldots, a_j]$. An **approximate vector** v_h of p/q is a vector having coordinates (q_h, p_h), where (q_h, p_h) is a *characteristic point* of $[a_0, \ldots, a_j]$ (see Definition 1.3.9).

Proposition 1.3.31. *The vectors of Proposition 1.3.29 are exactly the approximate vectors of v, listed according to increasing slopes.*

Example 1.3.32. Let $v = (5, 7)$, $7/5 = [1, 2, 2]$. The approximate vectors have coordinates:
- $[1] = 1/1$;
- $[1, 1] = [2] = 2/1$;
- $[1, 2] = 3/2$;
- $[1, 2, 1] = [1, 3] = 4/3$;
- $[1, 2, 2] = 7/5$.

Moreover, $1 < 4/3 < 7/5 < 3/2 < 2$. Then we take vectors $v_0 = (1, 0)$, $v_1 = (1, 1)$, $v_2 = (3, 4)$, $v_3 = (5, 7)$, $v_4 = (2, 3)$, $v_5 = (1, 2)$ and $v_6 = (0, 1)$. An illustration of this case can be seen in Figure 1.7.

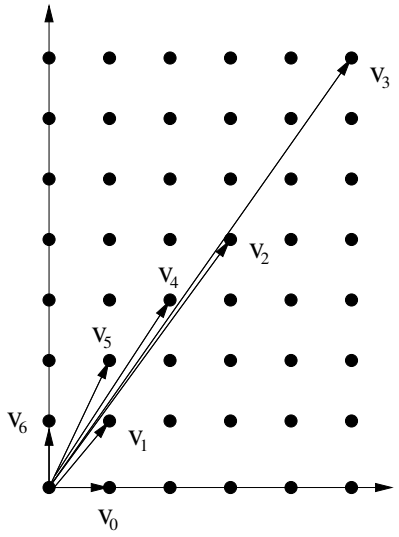

Figure 1.7

If we work with the field $\mathbb{K} = \mathbb{R} \subset \mathbb{C}$, we get the set of **real points** $X_{\mathbb{R}}(\Delta)$ of the complex toric variety $X_{\mathbb{C}}(\Delta)$. We will say that it is a **real toric variety**.

Moreover, as $(\mathbb{R}_{>0}, \cdot)$ is a semi-group, the set $X_{>0}(\Delta)$ of **positive real points** is also well defined:

$$X_{>0}(\Delta) := Hom_{sg}(\check{\sigma} \cap M, \mathbb{R}_{>0}) \subset Hom_{sg}(\check{\sigma} \cap M, \mathbb{R}) \subset Hom_{sg}(\check{\sigma} \cap M, \mathbb{C}).$$

As $\mathbb{R}^*$ has two connected components, $(\mathbb{R}^* = \mathbb{R}_{>0} \times \{\pm 1\})$, the two-dimensional real torus has four connected components: $(\mathbb{R}^*)^2 = \mathbb{R}_{>0} \times \{\pm 1\}^2$. Consider the map

$$sign : \mathbb{R}^* \to \mathbb{F}_2$$

which associate to each non-zero number its *sign*, seen additively:

$$sign(x) := \begin{cases} 0 & if\ x > 0, \\ 1 & if\ x < 0. \end{cases} \tag{1.9}$$

This map is a morphism of semigroups from $(\mathbb{R}^*, \cdot)$ to $(\mathbb{F}_2, +)$. By functiorality of Hom_{sg} we get a morphism

$$Hom_{sg}(\check{\sigma} \cap M, \mathbb{R}^*) \to Hom_{sg}(\check{\sigma} \cap M, \mathbb{F}_2)$$

that is a morphism of abelian groups $T_{N,\mathbb{R}} \to T_{N,\mathbb{F}_2}$.

1.4 The lotus of a curve singularity

1.4.1 The crossed constellation

This section is based on the results of [BPPP14]. The first ideas of the following construction can be found in [PP11].

Definition 1.4.1. Let Σ be a surface obtained by blowing up all points of a constellation $\mathcal{P}$ and let E be its exceptional locus.

- Let $L', L \subset \Sigma$ be two smooth branches which intersect transversally at an infinitely near point P. The couple (L', L) is called a **cross** at P.
- Any smooth branch L' at P is called a **smooth frame** at P.
- Let L' be a smooth frame at P. A **completion** of L' is a cross (L, L') at P.
- A **frame** is either a cross or a smooth frame.

Remark 1.4.2. Let (Σ, E) be a surface obtained by a sequence of blow ups of points belonging to a constellation $\mathcal{P}$. Whenever $E_i \cap E_j \neq \emptyset$, in which case this intersection is a point, a couple (E_i, E_j) indicates the cross given by the localization of E_i and E_j at $E_i \cap E_j$. If $O_h \in E_i$ is a smooth point of E, then E_i is a smooth frame at O_h.

Definition 1.4.3. Let $P \in E$ be an infinitely near point. If L_h is a smooth branch on Σ at P which is transversal to E, then it is a **curvetta** at P.

A **crossed constellation** is the data of a constellation $\mathcal{P}$ and of a cross at each point of $\mathcal{P}$, subject to the following constraints: .

1. in the initial surface $\mathbb{C}^2 \simeq \Sigma^{(0)}$ we always consider two transversal curvettas $L' = V(y)$ and $L = V(x)$;
2. if O_i is a smooth point of $E^{(j)}$, then the germ of $E^{(j)}$ is a branch of the cross at O_i;
3. if O_i is a satellite point, then the cross at O_i is the germ of $E^{(j)}$ at O_i;
4. if $O_j \preceq O_i$, then the germ at O_i of the total transform of the cross at O_j is contained in the cross at O_i.

We denote by $\check{E}^{(l)}$ the union of $E^{(l)}$ with the curvettas belonging to the crosses of points of $E^{(l)}$. The set $\mathcal{B}^{(l)}$ of curvettas contained in $\check{E}^{(l)}$ is called the **associated system of curvettas**.

Remark 1.4.4. In Section 1.2 we have defined the resolution space associated to a constellation. Now we don't consider just the blow up with centre a point O_i, but the blow-up of a point O_i relative to a cross (D', D), where D and D' are irreducible components of $\check{E}$.

In the case where this cross isn't well defined, i.e., the case of a smooth frame, we add a curvetta L_h. The surface Σ depends then on the choice of the system of curvettas $\mathcal{B}$, i.e., it doesn't depend only on the constellation, but on the choice of a crossed constellation.

Definition 1.4.5. Let $\mathcal{P}$ be a crossed constellation. If $O_i \in \mathcal{P}$ and (D, D') is the cross at O_i, the **petal associated to** O_i is the 2-simplex with vertices D, D', and E_i. We will also call it the **petal associated to** E_i, or the i**-th petal**. Its **base** is $[D, D']$. If a vertex corresponds to a curvetta L_j, then it is a **base point**.

If $O_0 = O$, then the petal associated to O (or the 0-petal) is the petal having vertices E_0, L, and L', where $[L, L']$ is the base. A vertex E_i is called a **node**.

If O_i is a satellite point we will say, with abuse of notation, that E_i is a **satellite node**.

If O_i is a free point we will say, with abuse of notation, that E_i is a **free node**.

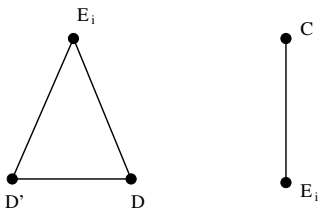

Figure 1.8 – A petal and an edge.

In Definition 1.4.5 a component D or D' can be either an irreducible component of E or a curvetta. We can then introduce the main combinatorial tool of this thesis:

Definition 1.4.6. Let $\mathcal{P}$ be a crossed constellation. The **lotus** $\mathcal{L}$ of $\mathcal{P}$ is the simplicial complex obtained from the disjoint union of all petals by affine isomorphisms which identify the vertices having the same labels.

Example 1.4.7. Let us give an example of construction of the lotus. The idea is the following:

1. if E_i, $\tilde{E}$ are irreducible components of $\check{E}$ such that $E_i \cap \tilde{E} \neq \emptyset$, then E_i and $\tilde{E}$ are two nodes, and there exists an edge $[E_i, \tilde{E}]$ contained in the boundary of the lotus. The blow-up with centre the point $O_h = E_i \cap \tilde{E}$ gives a new node E_h, and two edges $[E_i, E_h]$, $[E_h, \tilde{E}]$ contained in the boundary of the (new) lotus.
2. If $O_h \in E_i$ is a smooth point of $\check{E}$, we can't directly proceed as in the previous case. We obtain the same structure if we add a node L_h, joined only to the node E_i. Then it is the same case as the previous one.

So, we start with two smooth branches L and L', which intersect at the origin O. The blow-up is then the petal LE_0L'. Every time we blow-up a smooth point $O_h \in E_i$, we consider the completion of the frame to a cross (L_h, E_i) (see Figure 1.9).

Definition 1.4.8. Let C be a curve singularity and let Σ be a resolution surface of C. Let $\mathcal{P}$ be the crossed constellation of the infinitely near points O_i of the minimal resolution surface Σ and enriched by crosses which make it into a crossed constellation. The lotus of C is then the lotus associated to the crossed constellation $\mathcal{P}$. We will also call $\mathcal{P}$ an **associated crossed constellation** of C. If a branch $C_l \subset \Sigma$ of C is transversal to an exceptional component E_i, we will then attach an arrowhead edge, also labelled C_l, at E_i.

Remark 1.4.9. Given a curve singularity C, we can also consider crossed constellations $\mathcal{P}$ such that the associated resolution space is not the minimal resolution space. Those crossed constellation will be important in Chapter 2.

Proposition 1.4.10. *Let C be a curve singularity and let $\mathcal{P}$ be an associated crossed constellation.*

Then the edges $[E_iE_j]$ belonging to the boundary of $\mathcal{L}$, and not containing the base points of $\mathcal{L}$, together with the arrowheads C_l attached to nodes E_h, form a tree isomorphic to the dual graph of C.

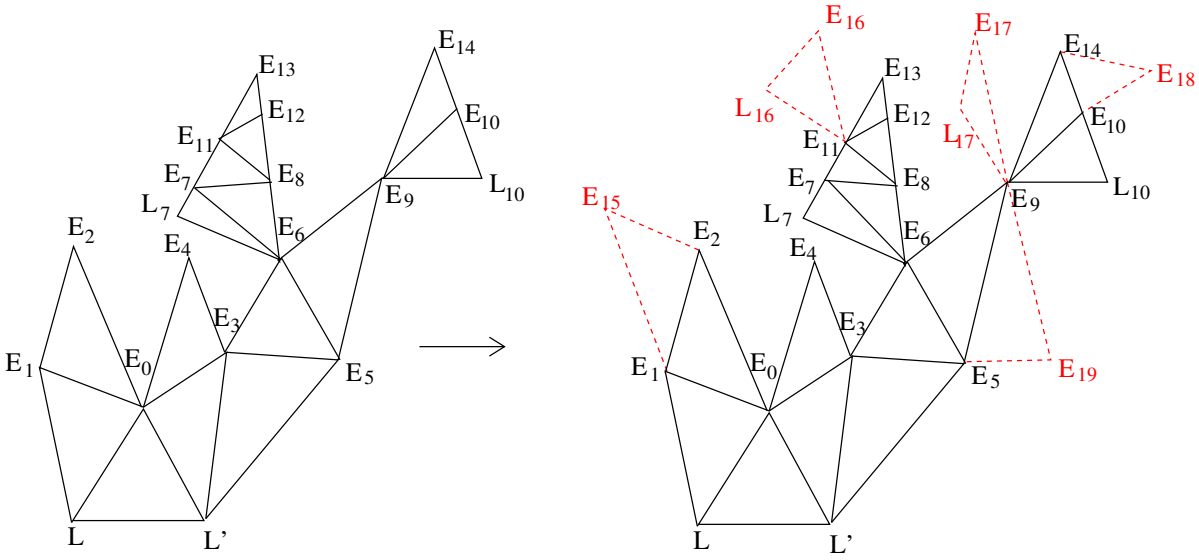

Figure 1.9 – A lotus, before and after a blow-up.

A proof can be found in [PP11] and [BPPP14].

Example 1.4.11. In Figure 1.10 we consider a lotus and, in red and in bigger size, the edges $[E_iE_j]$ belonging to the boundary of it. One may see that they form a tree, isomorphic to the dual graph of E, drawn to the right.

One may also read the weights of the dual graph in the lotus (see [PP11]):

Proposition 1.4.12. *Let E_i be a node of the lotus. Let $t_i = \#\{T \text{ petal} \mid E_i \in T\}$. Then:*

$$E_i^2 = -t_i.$$

Proof. The number t_i is equal to the number of simplices containing the node E_i, which is equal to $\#\{j \mid O_j \in E_i\} + 1 = -E_i.E_i$. □

Definition 1.4.13. Let E_i be a satellite node,whose associated petal Π_i has the basis $[E_jE_k]$, where $j = p_D(i)$, $k = p_I(i)$ (see Remark 1.2.10 and Definition 1.4.5). The edge $[E_iE_j]$ is the **i-th direct edge** and the edge $[E_iE_k]$ is the **i-th indirect edge** of Π_i.

We also say that the node E_j is the *i*-**direct node**, while the node E_k is the *i*-**indirect node**.

If E_i is a free node, then we define analogously the *i*-**th direct edge** and the *i*-**th direct node**.

The union of all the direct edges is isomorphic to the Enriques tree:

Proposition 1.4.14. *Let $\mathcal{P}$ be a crossed constellation and let $\mathcal{L}$ be the associated lotus. Then there is a canonical embedding of the Enriques tree onto the subtree of $\mathcal{L}$ given by the direct edges, such that the image of an infinitely near point O_i is the node E_i. Moreover:*

- *two points O_i and O_j are connected if and only if E_j is the i-direct node;*
- *O_i is connected by a curvilinear edge to O_j if and only if E_i is a free node and E_j is the i-direct node;*

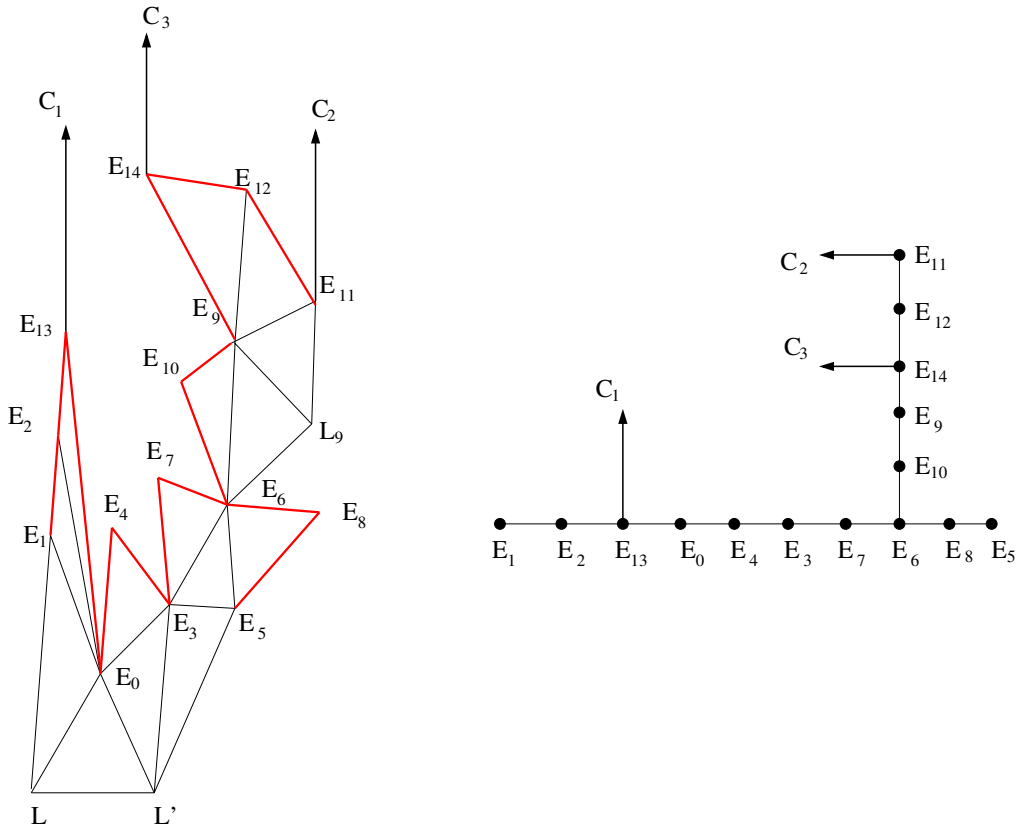

Figure 1.10 – The dual graph as boundary of the lotus.

— *O_k is the indirect predecessor of O_i if and only if E_k is the i-indirect node.*

Proof. Let $O := O_0$. If E_i and E_j are joined by a direct edge, $j < i$, then $j = p_D(i)$. In the same way, if E_i and E_k, $k < i$, are joined by an indirect edge, then $k = p_I(i)$. For every satellite point O_i we know then which point O_j is its direct predecessor and which one is its indirect predecessor.

If E_i is a node and the i-th indirect node isn't defined, then O_i is a free point. The two infinitely near points O_i and O_j are joined by a curvilinear edge.

Two points O_i and $O_{i'}$ have the same indirect predecessor if and only if E_k is both the i-indirect node and the i'-indirect node. □

Example 1.4.15. In Figure 1.11 we can see the Enriques tree for the same lotus we have studied in Example 1.4.11. In this case, the red and wider edges are the direct edges, and the blue and dashed ones are the indirect edges.

Remark 1.4.16. Let O_i be an infinitely near point and let $O_j \in \mathcal{P}(O_i)$. Then the two nodes E_i and E_j are joined by an edge of $\mathcal{L}$.

Let C be a curve singularity and $\mathcal{L}$ be an associated lotus. We can attach to each node E_i the multiplicity m_i of C at O_i. Then we can rewrite Proposition 1.2.19 in the following way:

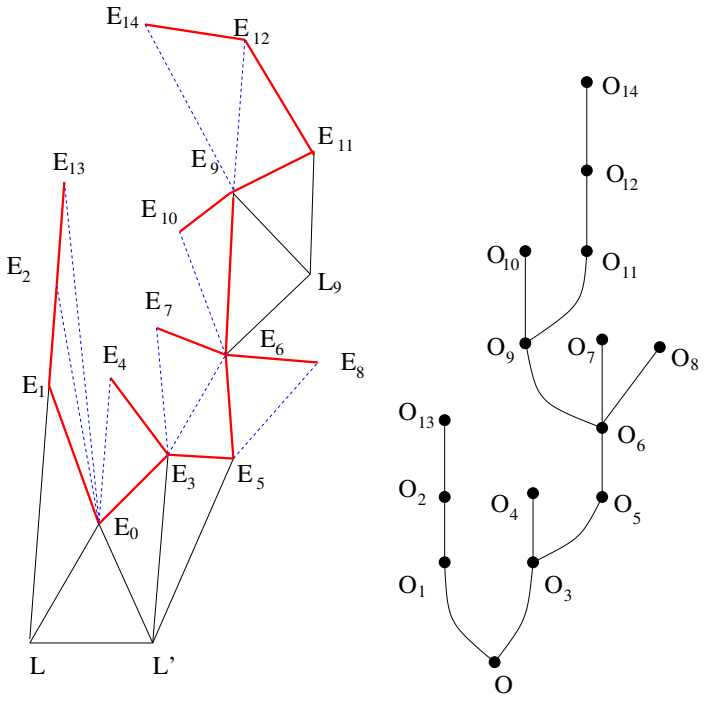

Figure 1.11 – The embedding of the Enriques tree in the lotus.

Proposition 1.4.17. *Let E_i be a node and let $\mathcal{P}(E_i) = \{h > i \mid E_h, E_i$ are joined by an edge$\}$. Moreover, let c_i be the number of arrowheads attached to E_i. Then*

$$m_i = c_i + \sum_{h \in \mathcal{P}(E_i)} m_h.$$

Proof. It is an easy application of Proposition 1.2.19, if we remark that $E_h \in \mathcal{P}(E_i)$ if and only if $O_h \in \mathcal{P}(O_i)$. An example of the situation can be seen in Figure 1.12. □

Example 1.4.18. Let us consider a germ C, having irreducible components C_1, C_2, C_3 and C_4 with Newton-Puiseux series:

— $C_1 : \ y = x^{35/25} + x^{38/25}$;
— $C_2 : \ y = 2x^{7/5}$;
— $C_3 : \ y = x^{3/2} + x^{9/4}$;
— $C_4 : \ y = x^{4/3}$.

Then the associated lotus with the attachment of all the multiplicities m_i at a node E_i computed, as explained in Proposition 1.4.17, can be seen in Figure 1.13.

1.4.2 The lotus and the Eggers-Wall tree.

Let us suppose now that we know the Eggers-Wall tree of a given curve singularity C. How do we associate a lotus to it?

We have seen in Proposition 1.3.8 that a complete topological characterization for a branch having one Puiseux pair is given by its **continued fraction expansion**.

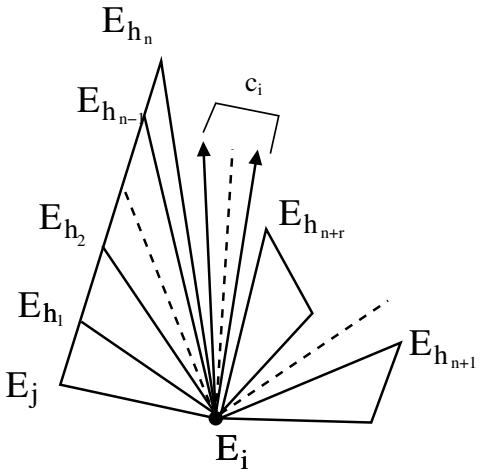

Figure 1.12 – Understanding multiplicities.

Let us consider a triangle having basis vertices L and L' and apex A. We want to associate to a continued fraction expansion $\lambda = [a_0, \ldots, a_n]$ a subdivision of such triangle. The triangle has a base (the segment LL') and two sides, $L'A$ and LA. We consider then the following decomposition: first we take a triangle T_0 with base LL', having apex on the side LA, and then we consider triangles $T_1, \ldots, T_n$ having apexes alternatively on each side, their bases being internal edges of the triangle $LL'A$ (see Figure 1.14). Those edges are called the **deviation edges**. The obtained decomposition is the **zig-zag decomposition** of the original 2-simplex.

We associate the number a_i to the triangle T_i. Let us suppose that the apex vertex of T_i belongs to the side LA. We subdivide then T_i in a_i triangles, such that the basis of each one is the internal edge of the previous one, and such that the apex always belongs to the side AL. We call this subdivision the **total decomposition** of the original triangle (see Figure 1.14).

Definition 1.4.19. Let us consider E_i and E_k, $k = p_I(i)$. Let h be such that $E_k \preceq E_h \preceq E_i$, $k = p_D(h)$. Then E_h is the **deviation node** of E_i. In a similar way, O_h is the **deviation point** of O_i.

This triangulation of the triangle ALL' is the **lotus** $\mathbf{\Delta}(\lambda)$ of the rational λ. It is well defined up to simplicial isomorphism. We will also say that it is a **triangular lotus**.

One has the following Proposition, proven in [PP11]:

Proposition 1.4.20. *Let $y^a - x^b = 0$ be a curve singularity, $(a, b) = 1$. Then the associated lotus is $\Delta(b/a)$, enriched with an arrowhead on the only node having self-intersection -1.*

Example 1.4.21. Let us consider $\lambda = \frac{19}{8} = [2, 2, 1, 2]$. The associated decomposition is represented in Figure 1.15.

Let us consider now the case of a singularity having two characteristic exponents. Let $(m; \beta_1, \beta_2)$ be its characteristic sequence. To define an analogous construction, we consider two different 2-simplices and a way to glue one to each other. In particular, we have two

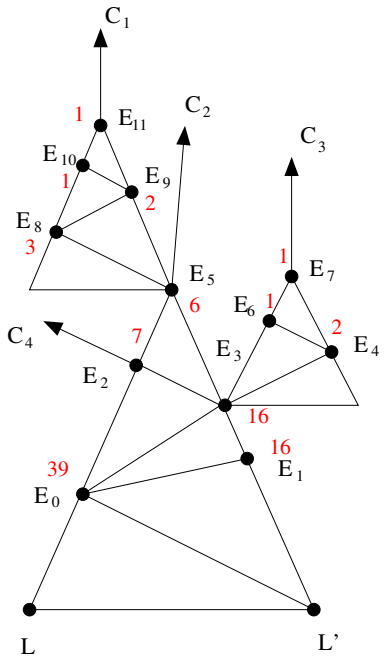

Figure 1.13 – A lotus associated to a singularity and its multiplicities.

different crosses (L, L') and (E_i, L_h), obtained by adding new curvettas, where E_i is the apex of the simplicial complex having basis L, L' and $O_h \in E_i \cap L_h$.

Therefore we have two simplicial complexes, with a common vertex E_i. To the 2-complex having basis L' and L we associate the construction for the curve having one Puiseux exponent (m, β_1). It is then sufficient to understand what we need to do for the second triangle. More generally, for an arbitrary number of Puiseux exponents, we use then the following construction, introduced in [BPPP14]:

Definition 1.4.22. Let $(\alpha_1, \alpha_2, \ldots, \alpha_k)$ be a sequence of Puiseux exponents. Its **renormalized sequence** $(\alpha'_1, \alpha'_2, \ldots, a'_k)$ is defined by:

$$\alpha'_i = e_{i-1}(\alpha_i - \alpha_{i-1}),\ i = 1, \ldots, k$$

where $\alpha_0 = 0$, $e_0 = 1$ (see Definition 1.1.11). **The lotus of** $(\alpha_\mathbf{1}, \alpha_\mathbf{2}, \ldots, \alpha_\mathbf{k})$ is the simplicial complex:

$$\Delta(\alpha_1, \ldots, \alpha_k) := \frac{\coprod_{i=1,\ldots,k}(\Delta(\alpha'_i))}{\simeq},$$

where we glue the first base vertex of $\Delta(\alpha'_{j+1})$ to the apex of $\Delta(\alpha'_j)$, $\forall\ j = 1, \ldots, k-1$.

The following Proposition is proved in [BPPP14]:

Proposition 1.4.23. *Let C be a branch and $\alpha_1, \ldots, \alpha_k$ its Puiseux exponents. Then there exists a system of curvettas $\mathfrak{B}$ such that the lotus of C with respect to $\mathfrak{B}$ is $\Delta(\alpha_1, \ldots, \alpha_n)$.*

Example 1.4.24. Let us consider the curve singularity having Puiseux characteristic

$$(12; 18, 20, 21).$$

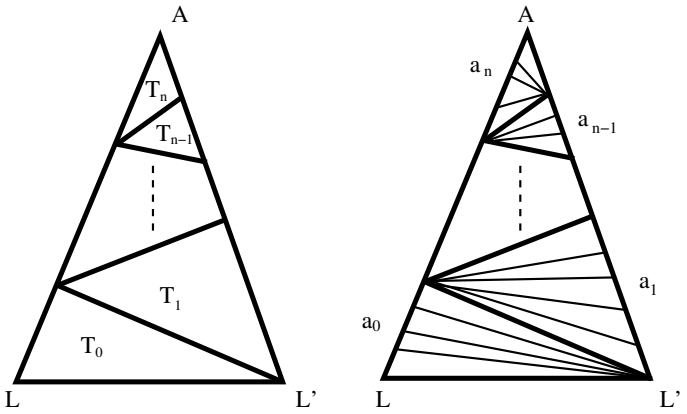

Figure 1.14 – A zig-zag decomposition and a total one.

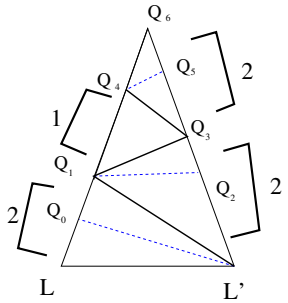

Figure 1.15 – An example of total decomposition.

Then $\alpha_1 = \frac{3}{2}$, $\alpha_2 = \frac{5}{3}$ and $\alpha_3 = \frac{7}{4}$, while $e_1 = 2$, $e_2 = 6$ and $e_3 = 12$.
We get $\alpha_1' = \frac{3}{2}$, $\alpha_2' = 6(\frac{5}{3} - \frac{3}{2}) = \frac{1}{3}$ and $\alpha_3' = 12(\frac{21}{12} - \frac{20}{12}) = \frac{1}{2}$.
The associated lotus $\Delta(\alpha_1, \alpha_2, \alpha_3)$ can then be seen in Figure 1.16.

We have seen that the Eggers-Wall tree of a reducible curve singularity is defined by gluing the Eggers-Wall trees of its irreducible components. Let then $C = C_1 \cup C_2$ be a reducible curve and let $\mathcal{L}_1$ and $\mathcal{L}_2$ be respectively the loti associated to C_1 and C_2. Moreover, we know that C_1 and C_2 share a part of the Eggers-Wall tree, the segment $[O, o_{12})$. We can associate to this segment a lotus, that will be then a sublotus $\mathcal{L}_1 \cap \mathcal{L}_2$ of both $\mathcal{L}_1$ and $\mathcal{L}_2$. The lotus of C is then the lotus $\mathcal{L}$ defined as $(\mathcal{L}_1 \coprod \mathcal{L}_2)/(\mathcal{L}_1 \cap \mathcal{L}_2)$. The intersection $\mathcal{L}_1 \cap \mathcal{L}_2$ can be computed by using the following Proposition (see [BPPP14]):

Proposition 1.4.25. *Let λ, $\mu \in \mathbb{Q}_+^*$. If $\lambda = [a_1, \ldots, a_k]$, $\mu = [b_1, \ldots, b_l]$, let $j = \max\{h \mid a_h = b_h\}$. Then*

$$\lambda \wedge \mu := \begin{cases} [a_1, \ldots, a_j], \ j = \min\{k, l\} \\ [a_1, \ldots, a_j, \min\{a_{j+1}, b_{j+1}\}], \ j+1 = \min\{k, l\} \\ [a_1, \ldots, a_j, \min\{a_{j+1}, b_{j+1}\} + 1], \quad j+1 < \min\{k, l\}; \end{cases}$$

Let $\Delta(\mu)$ and $\Delta(\lambda)$ be the associated loti. Then $\Delta(\lambda) \cap \Delta(\mu) = \Delta(\lambda \wedge \mu)$.

More details on the construction of a lotus of C starting from an Eggers-Wall tree may be found in [BPPP14].

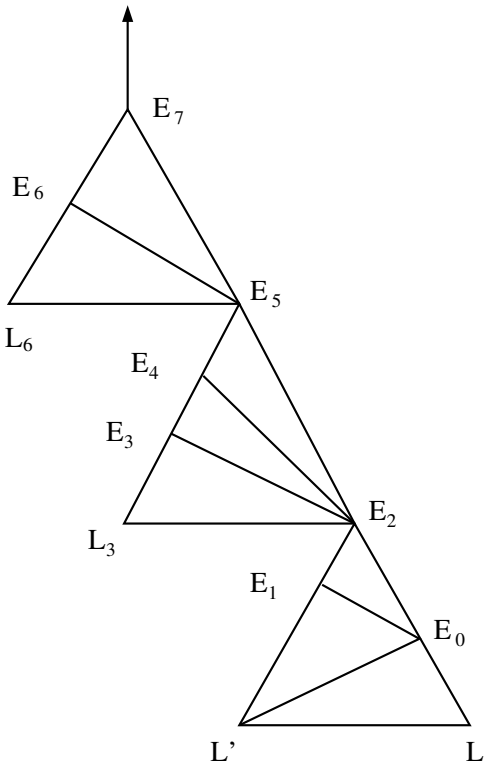

Figure 1.16 – The lotus $\Delta(\frac{3}{2}, \frac{5}{3}, \frac{7}{4})$.

The same arguments work for a germ having any number of irreducible components.

Example 1.4.26. Let us consider the reducible curve C having the Eggers-Wall tree shown in Figure 1.17.

The lotus for the four different irreducible components can be seen in Figure 1.17. The final lotus of the curve C is also shown in Figure 1.17.

We end this subsections with some definitions that we are going to use in Chapter 3 and Chapter 4.

Definition 1.4.27. We say that a lotus $\mathcal{L}$ is a **simple lotus** if the associated system of curvettas (see Definition 1.4.3) is $\mathcal{B} = \{L', L\}$.

A simple lotus is then the lotus of a curve singularity such that all of its branches have only one Puiseux pair relative to the frame (L', L).

It is possible to associate to each node of a simple lotus a vector $v \in \mathbb{N}^2$. We remember that in Section 1.3.2 we have associated the vector $(1, 0)$ to L, and the vector $(0, 1)$ to L'. The blow-up with centre $O = L \cap L'$ gives a new vector $(1, 1) = (1, 0) + (0, 1)$ associated to E_0. In general, we have the following Definition:

Definition 1.4.28. Let $\mathcal{L}$ be a simple lotus. Let E_i be a node, such that $[\tilde{E}', \tilde{E}'']$ is the basis of its petal. Let $v' \in \mathbb{N}^2$ and $v'' \in \mathbb{N}^2$ be the vectors associated to $\tilde{E}'$ and $\tilde{E}''$. The vector $v_i \in \mathbb{N}^2$ **associated to** E_i is:

$$v_i = v' + v''.$$

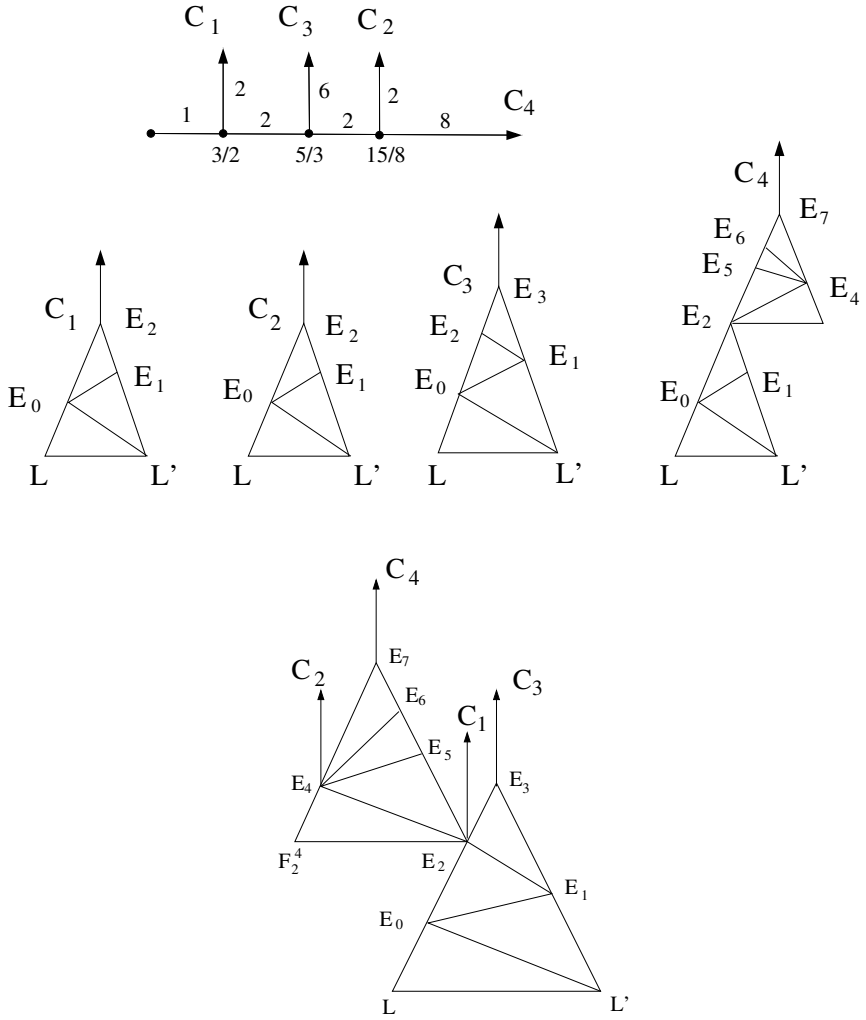

Figure 1.17 – An Eggers-Wall tree and the associated lotus.

Remark 1.4.29. By the hypothesis that $\mathcal{L}$ is a simple lotus, it is sufficient to consider the vectors associated to L and L'. Usually, we will consider $(1,0)$ and $(0,1)$ to be respectively the vectors associated to L and L'.

Proposition 1.4.30. *Let $[E_i, E_j]$ be an edge of the simple lotus. Let $v_i = (\alpha_i, \beta_i)$ and $v_j = (\alpha_j, \beta_j)$ be the vectors associated to E_i and E_j. Let us suppose that $\beta_i/\alpha_i < \beta_j/\alpha_j$, i.e., $v_i < v_j$. If $v_j = (0,1)$, we consider $v_i < v_j$ for all v_i such that $\alpha_i \neq 0$. The matrix of change of basis from the canonical basis of $\mathbb{R}^2$ to (v_i, v_j) is the following:*

$$\begin{pmatrix} \alpha_i & \alpha_j \\ \beta_i & \beta_j \end{pmatrix} \tag{1.10}$$

Then the toric morphism associate to the chart containing $E_i \cap E_j$ is given by:

$$\begin{cases} x = u^{\alpha_i} v^{\alpha_j} \\ y = u^{\beta_i} v^{\beta_j} \end{cases} \tag{1.11}$$

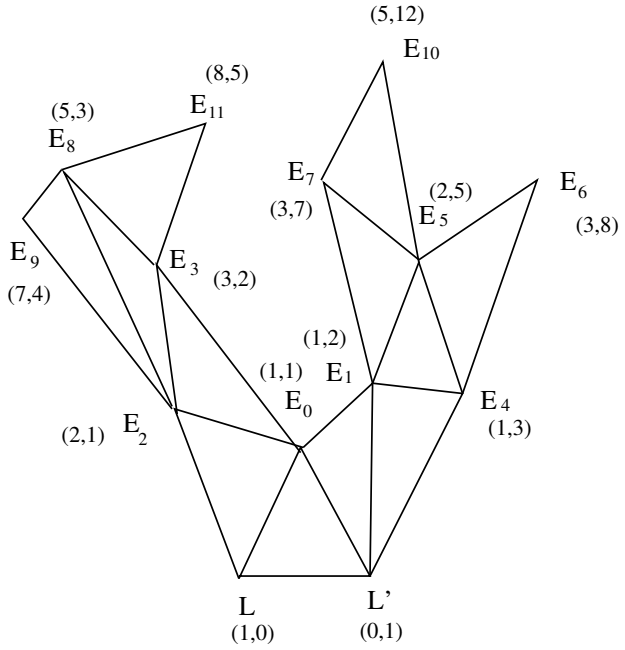

Figure 1.18 – An example of computation of the vectors associated to the nodes of a lotus.

Proof. A proof can be found in [PP01, Example, pag. 54].

□

1.4.3 An introduction to multi-loti.

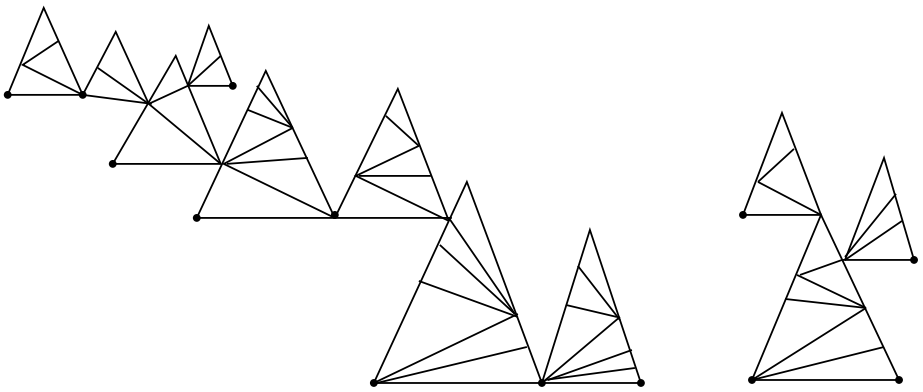

Figure 1.19 – An example of multi-lotus.

Definition 1.4.31. A **multi-singularity** is a disjoint union of curve singularities on a smooth surface Σ.

The **global constellation** of a multi-singularity is the disjoint union of the constellations of the minimal embedded resolution of each germ.

To each germ we associate a system of curvettas $\mathfrak{B}$, and then consider its lotus. In each lotus there are some special vertices, corresponding to the curvettas. When a curvetta L is a germ of a global curve in Σ, we can have several vertices labelled L within the multi-lotus, each representing a germ of the same irreducible global curve. We can consider this situation by taking the disjoint union of all the loti, and identifying the vertices corresponding to the same irreducible curve on Σ (see Figure 1.19).

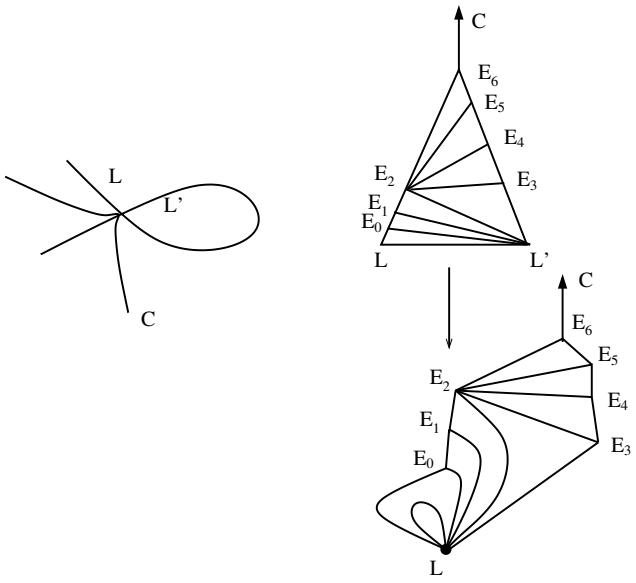

Figure 1.20 – An example of curve for Remark 1.4.33.

Definition 1.4.32. Let C be a multi-singularity in the surface Σ, $C = C^1 \coprod C^2 \coprod \dots \coprod C^r$. Let $\mathcal{L}^1, \dots \mathcal{L}^r$ be the loti corresponding to the associated systems of curvettas $\mathfrak{B}^1, \dots, \mathfrak{B}^r$. The **multi-lotus** of C is obtained by the disjoint union of the loti $\mathcal{L}^1, \dots \mathcal{L}^r$, identifying two vertices which represent germs of the same irreducible curve of Σ.

Remark 1.4.33. This construction can be done also by considering only one lotus. For example we can have locally a cross (L, L') such that L and L' are germs of the same irreducible global curve. Clearly in this situation the image of a petal is not a triangle (see Figure 1.20).

Chapter 2

A'Campo deformations of complex curve singularities

Chapter Overview

In this Chapter we want to give some results about deformations of complex curve singularities. In particular, we will partially apply the deformation algorithm introduced by A'Campo in [A'C74] and [A'C75].

Section 2.1 is dedicated to the explanation of A'Campo's original algorithm. This algorithm was applied initially to complex curves that are *completely real singularities* (Definition 2.1.1), but we will explain it for any complex curve singularity, as we will need this generality when we will study what happens when we apply it partially. The algorithm consists in a series of translations and contractions on the resolution space. The resulting curves are called *divides* (Definition 2.1.7). In Section 2.1.2 we state the same algorithm as the deformation of a parametrization of the curve singularity.

In Section 2.2 we study the case of a *partial application* of the A'Campo algorithm. We will see what happens if we don't translate the curve at every step. We prove that this case is equivalent to an operation on the multi-lotus, the *cut* (Definition 2.2.4). Several results about the cut are stated in Section 2.2.1. Theorem 2.2.9 implies that the result of a cut on a multi-lotus is again a multi-lotus. In Section 2.2.2 we show that the cut of a lotus at one node can be used to study the partial A'Campo algorithm, in the case we allow only one translation (Theorem 2.2.14). The main results of this section concern the Milnor numbers of the deformed curve singularities (see Theorem 2.2.16). The other results of the section are all consequences of this Theorem. In particular, in Corollary 2.2.18, we show that this theorem directly implies a result of Gusein-Zade (see [GZ93]). In Section 2.2.3 we apply the same method to a partial algorithm where we allow more than one translation. We prove some theorems about the Milnor numbers of the curves obtained by partially applying the deformation algorithm. In particular, we prove Proposition 2.2.31 and Proposition 2.2.32.

2.1 A'Campo's method

2.1.1 The deformation algorithm

In his articles [A'C74] and [A'C75], A'Campo introduced a method to obtain deformations of real curve singularities by a sequence of translations and contractions of the strict transforms of curves in the resolution space. A prototype of this method, formulated using global quadratic transformations of the projective plane, has been described by Angas Scott in [AS92]. A'Campo's method is instead purely local. Let us explain it.
The following is inspired by the works of Risler (see [Ris74]):

Definition 2.1.1. A germ of holomorphic function $f : (\mathbb{C}^2, O) \to (\mathbb{C}, O)$ is called **real** if $f(\mathbb{R}^2) \subset \mathbb{R}$.

A curve singularity $(C, O) \hookrightarrow (\mathbb{C}^2, O)$ is called **real** if it is invariant by conjugation. It is called a **completely real singularity** if all its complex branches are invariant by complex conjugation.

Lemma 2.1.2. *For every complex curve singularity C there exists a topologically equivalent completely real curve singularity.*

Proof. We have seen in Theorem 1.2.25 that the Eggers-Wall tree $\Gamma_{EW}(C)$ is a complete invariant of the topological type of the curve singularity C.

Let C be a branch. It is then sufficient to consider a new curve C' having the same monomials but real coefficients, instead of complex ones, to obtain a topologically equivalent real germ.

Let C be a germ, and let C_i and C_j be branches of C. We can consider then two topologically equivalent real germs C'_i and C'_j. Moreover, we can always consider real coefficients $(a')^i_l$ and $(a')^j_h$ such that $o_{ij} = o'_{ij} = min\{l \mid (a')^j_l \neq (a')^j_l\}$. By applying the same consideration to every pair of branches of C we obtain a completely real germ C' such that $\Gamma_{EW}(C')$ is isomorphic to $\Gamma_{EW}(C)$. By Theorem 1.2.25 C and C' have the same topological type. □

Let C be a completely real curve singularity. Then every infinitely near point in its resolution process is a real point. Therefore, it is possible to focus on the restriction to the real part of the resolution surface.

Let us suppose that C is a branch. The minimal embedded resolution space $\Sigma^{(N)}$ of the germ C is such that $\bar{C}^{(N)}$ has only normal crossings. The last obtained component is E_{N-1}. After contraction of this component, in $\Sigma^{(N-1)}$ the total transform $\bar{C}^{(N-1)}$ does not have any normal crossings. In fact, $O_{N-1} \in C^{(N-1)}$, where $O_{N-1} = E_{N-2} \cap E_k$, $N-2 = p_D(N-1)$ and $k = p_I(N-1)$. We consider a deformation $\tilde{C}^{(N-1)}(s_{N-1})$ of $C^{(N-1)}$ such that $\tilde{C}^{(N-1)}(s_{N-1}) \cup E_{N-2}$ has only normal crossings and such that the point $P_{N-1}(s_{N-1})$ belongs to the component E_k. One has $P_{N-1}(0) = O_{N-1}$. Such a deformation may be achieved by translating in local coordinates, therefore we speak about a **translation step** (see Figure 2.1).

We can then iterate this construction. The same construction is valid for free points as we complete the exceptional branch by a curvetta L_j, in order to get a cross.

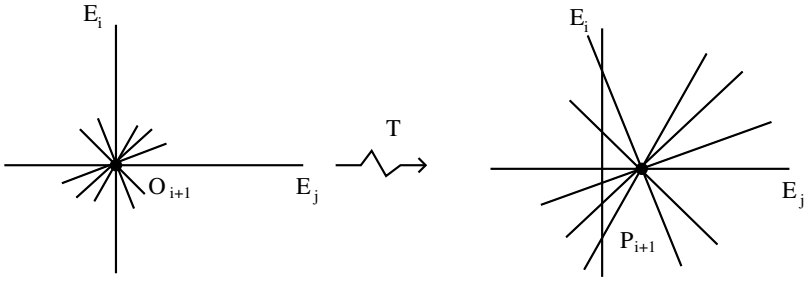

Figure 2.1 – A translation step.

Let (E_{i-1}, E_k) be a cross such that $k = p_I(i)$. We translate the curve

$$\tilde{C}^{(i)}(s_{N-1}, s_{N-2}, \ldots, s_{i+1}) \subset \Sigma^{(i)}$$

in such a way that $P_i(s_i)$ still belongs to E_k and $C^{(i)}(s_{N-1}, s_{N-2}, \ldots, s_i) \cup E_{i-1}$ has only normal crossings. Then we contract the component E_{i-1}.

In the following we will generally define the point P_i as the point obtained by translating O_i along E_k, where $k = p_I(i)$. With abuse of notation, we drop for simplicity of notation the dependency in parameters s_i and often indicate by P_i also the point $P_i(0) = O_i$.

Remark 2.1.3. The same algorithm can be done for every curve singularity C, by possibly executing several translations steps on the same surface $\Sigma^{(l)}$.

Definition 2.1.4. An **ordinary singularity** of multiplicity r is a curve singularity having the same complex topological type as $y^r - x^r = 0$.

The following proposition is elementary and left to the reader (recall that m_i was defined in Section 1.2.3, Definition 1.2.14):

Proposition 2.1.5. *Locally at P_i, $C^{(i)}(s_N, \ldots, s_i)$ is the union of m_i pairwise transversal smooth branches, i.e., it is an ordinary singularity of multiplicity m_i.*

For a proof, see [dJS98, Corollary 1.11].

Remark 2.1.6. In the following we will indicate a contraction by a straight arrow, while a translation will be indicated by a wavy arrow (see Figure 2.2).

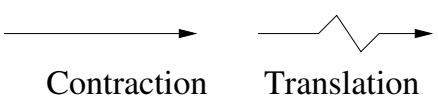

Figure 2.2 – Conventions for elementary operations.

At the end of the previous process we get a family $C^{(0)}(\underline{s})$ of deformations of C, depending on as many parameters as there are points in the constellation $\mathcal{P}$ of the minimal embedded resolution of C. As one deformed the parametrization of C, one gets in this way a δ-constant deformation of C (see [Tei80]).

Definition 2.1.7. Let D^2 be a compact disk. A **divide** in D^2 is the image of a proper immersion $\gamma : \coprod_{l\in\mathcal{I}} I_l \to D^2$, such that:

1. I_l is a compact segment and the index set $\mathcal{I}$ is finite;
2. $\gamma(I_l)$ is transversal to ∂D^2 for every l;
3. all the singular points of $\gamma(\coprod I_l)$ are **ordinary singularities**, i.e., at which all the branches are pairwise transversal.

A divide obtained as the generic fibre of $C^{(0)}(s_N, \ldots, s_0)$ in D^2, such that each s_i is a real parameter, is called an **A'Campo divide**.

An A'Campo divide deformed in such a way that all singular points are double points is a **generic A'Campo divide**.

Example 2.1.8. We consider the algorithm for the branch having Puiseux pair $(3;5)$, that is, for the $\mathbb{E}_8$ plane curve singularity. In Figure 2.3 we can see the curve obtained by contraction and translation of the components E_3 and E_2.

In Figure 2.4 we can remark that, having restricted to the real part of the resolution surface, we have different choices of translations. Such different choices give different final divides.

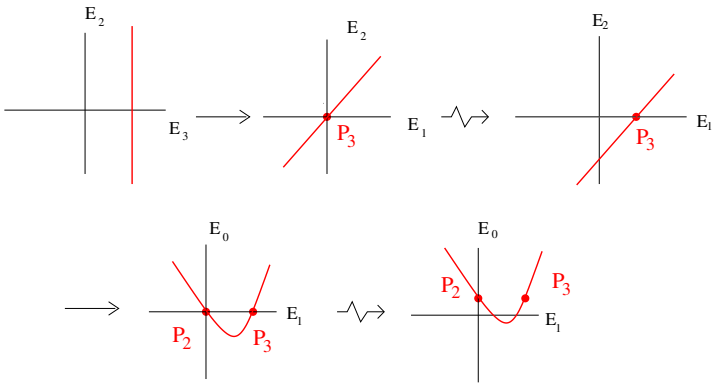

Figure 2.3 – Different translation steps.

In the end we obtain several non-isotopic generic A'Campo's divides by considering different deformations, as is shown in Figure 2.5.

Remark 2.1.9. In the sequel, the divides will be considered only up to isotopy.

The following Theorem was proved in [A'C75]:

Theorem 2.1.10 (A'Campo)**.** *Let C be a completely real curve singularity. If k is the number of double points of an associated generic A'Campo divide $\bar{C}$, r the number of irreducible components of C, then $\mu = 2k - r + 1$, where μ is the Milnor number of C.*

Definition 2.1.11. Let C be a generic A'Campo divide. A **region** R of it is a connected component of $D^2 - C$ such that $\partial R \cap \partial D^2 = \emptyset$.

Let C be a generic A'Campo divide. Let us consider for each region and for each double point an element δ_i. With abuse of notations, in the following δ_i will also denote the associated point or region.

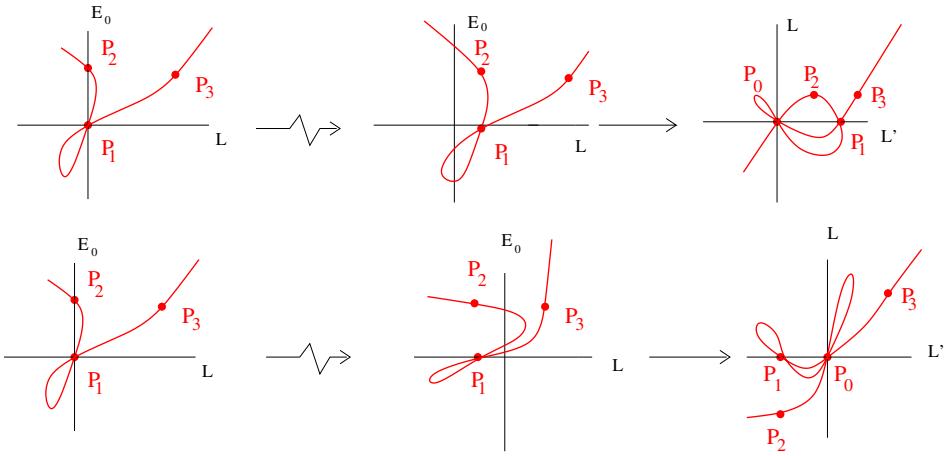

Figure 2.4 – Different translation steps.

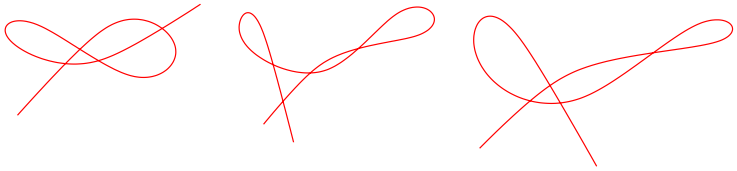

Figure 2.5 – Various generic A'Campo divides.

The **Dynkin diagram** associated to a generic A'Campo divide $\bar{C}$ is a graph with vertices δ_i defined by:

— if δ_i is a region and δ_j is a double point belonging to the boundary of the region δ_i, then δ_i and δ_j are connected by one edge;

— if δ_i and δ_j are two regions, then they are connected by as many edges as arcs of the divide contained in the intersection of their boundaries;

— otherwise δ_i and δ_j are not connected by an edge.

Theorem 2.1.12 (A'Campo)**.** *Let C be a curve singularity. For each generic A'Campo divide $\bar{C}$ the Dynkin diagram of $\bar{C}$ is the Dynkin diagram of a morsification of a defining function of C.*

Example 2.1.13. In Figure 2.6 we consider the Dynkin diagram of the three generic A'Campo divides of Example 2.1.8. The black dots denote double points, while the white ones denote regions. Moreover, we label with letters the double points, and with numbers the different regions.

Remark 2.1.14. If we want that in the Dynkin diagram any two vertices be connected by at most one edge, we need a generic A'Campo divide such that for any two regions, the intersection of their boundaries contains at most one arc of the divide. This is not always the case by applying A'Campo's method (see Figure 2.7, representing a generic A'Campo divide of a branch with Puiseux characteristic $(4; 6, 7)$).

An example of such freedom in deformation is shown in Figure 2.8, where we consider all possile deformations. In this case we consider all possible results of the A'Campo's

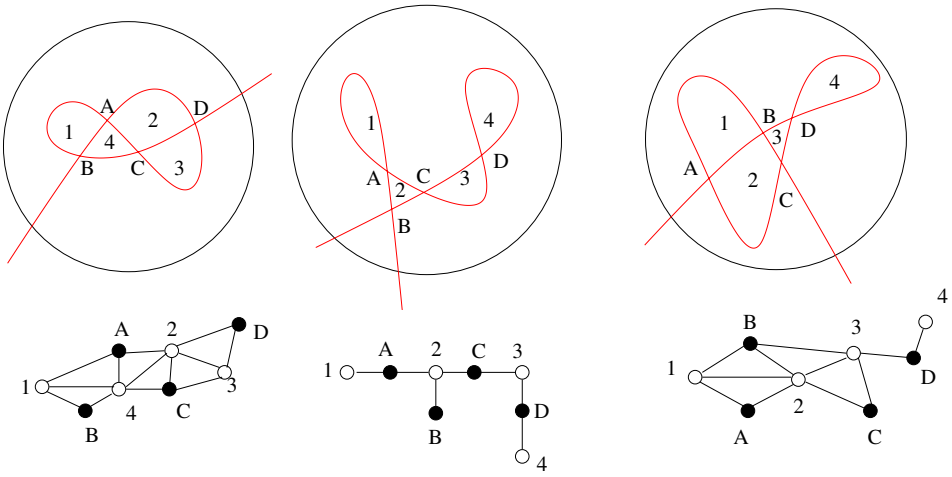

Figure 2.6 – Examples of Dynkin diagrams.

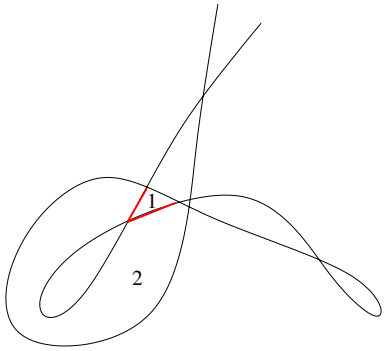

Figure 2.7 – A common boundary with two arcs.

algorithm applied to the branch having Puiseux pair $(3;5)$. The deformation is not a generic A'Campo's divide, but we can deform it more such that one gets a generic divide. We have many different ways of doing such a deformation. As it is shown in Figure 2.8, one deformation is such that two elements of the Dynkin diagram are joined by at most one edge, but there exist other deformations for which this property is not true.

In [A'C75, Section 4, Remarque 1], the author states the following:

> Let C be a generic divide and let f be a defining function of C. Then f admits at most 3 different critical values, that are the critical value $c_0 = 0$ and two critical values c_- and c_+, $c_- < c_0 < c_+$.

This Remark has been disproved in [GZ87, Assertion 1, Assertion 4].
In particular:

Theorem 2.1.15 (Gusein-Zade)**.** *Almost all non-degenerate homogeneous polynomials of degree k in n variables have no perturbations having only non-degenerate critical points with less then $d(k,n)+2$ general values. Here $d(k,n)$ is the number of integral points $(j_1,\ldots,j_n)$ for which $\sum_{i=1}^{n} j_i = k$, $0 \leq j_i \leq k-2$.*

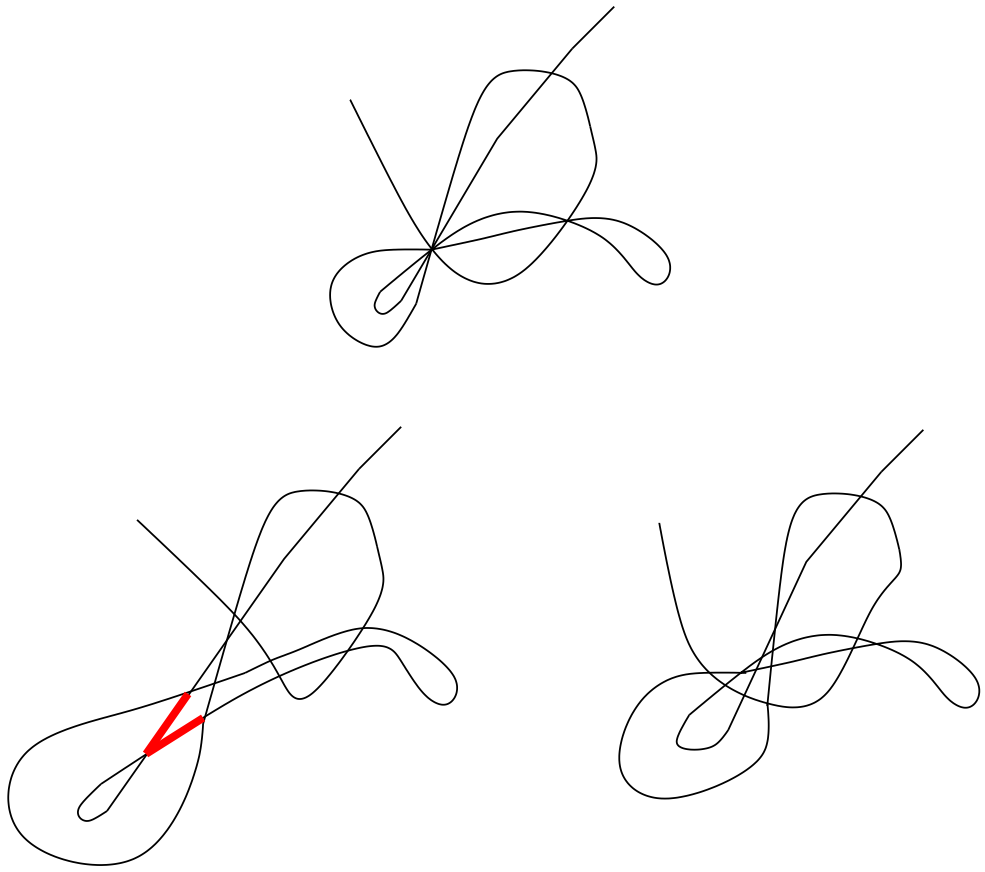

Figure 2.8 – An example of two non-isotopic deformations of a curve singularity, where one Dynkin diagram is such that two elements are joined by at most one edge.

2.1.2 Deformations of parametrizations

We will now give a different interpretation of A'Campo's method, by using parametrizations. Let C be a branch. After a convenient choice of local coordinates of $\Sigma^{(N-1)}$, the strict transform $C^{(N-1)}$ of C may be parametrized, in the surface $\Sigma^{(N-1)}$, by $(x_{N-1} = t, y_{N-1} = t)$. Let us suppose that E_j is given by the equation $x_{N-1} = 0$, where $j = p_D(N-1)$. Then a translation of $C^{(N-1)}$ is given by the deformation of parametrization $x_{N-1} = t,\ y_{N-1} = t + s_{N-1}$. The point P_{N-1} has coordinates $P_{N-1} = (0, s_{N-1})$, therefore it still belongs to the exceptional locus $E^{(N-1)}$. The curve obtained after contraction of E_{N-1} is parametrized by:

$$\begin{cases} x_{N-1} = t(t + s_{N-1}), \\ y_{N-1} = t + s_{N-1}. \end{cases}$$

Let:

$$\begin{cases} x_n = f_n(t; s_N, \ldots, s_{n+1}) \\ y_n = g_n(t; s_N, \ldots, s_{n+1}) \end{cases}$$

be the parametrization of the defined curve on the surface $\Sigma^{(n)}$, such that:

$$(0,0) = (f_n(0; s_N, \dots, s_{n+1}), g_n(0; s_N, \dots, s_{n+1})).$$

Then we proceed as in the previous step, by considering either $\tilde{f}_n = f_n + s_n$ or $\tilde{g}_n = g_n + s_n$. It is an easy remark that f_n and g_n are both real analytic.

By descending induction on n we get, even for reducible curve singularities:

Lemma 2.1.16. *Let C be a completely real curve singularity. The associated A'Campo divides may be parametrized by*

$$\begin{cases} x = f_{\underline{s}}(t) \\ y = g_{\underline{s}}(t), \end{cases}$$

where $f_{\underline{s}}(t)$, $g_{\underline{s}}(t) \in \mathbb{R}\{\{t\}\}$ and $\underline{s} := (s_{N-1}, ..., s_0)$ has all its components non-zero.

Example 2.1.17. Let us compute a deformation of parametrizations of $x^3 = y^2$. We start from:

$$\begin{cases} x_1 = t, \\ y_1 = t. \end{cases}$$

We can deform it to the parametrization:

$$\begin{cases} x_1 = t + s_1, \\ y_1 = t \end{cases}$$

By contraction we obtain

$$\begin{cases} x_0 = t + s_1, \\ y_0 = t(t + s_1) \end{cases}$$

We deform again to:

$$\begin{cases} x_0 = t + s_1, \\ y_0 = t(t + s_1) + s_0 \end{cases}$$

and after contraction we finally obtain:

$$\begin{cases} x = (t(t + s_1) + s_0)(t + s_1) \\ y = (t(t + s_1) + s_0). \end{cases}$$

If $s_1 = s_0 = 5$ the set of solutions of the parametrization is the divide in Figure 2.10, while for $s_1 = -s_0 = 0.6$ the set of solutions is the divide in Figure 2.9. Moreover, if $t = \frac{s_1 - \sqrt{s_1^2 - 4s_0}}{2}$ and $t = \frac{-s_1 + \sqrt{s_1^2 - 4s_0}}{2}$ we have $(x, y) = (0, 0)$. It is clear that we have the condition $s_1^2 - 4s_0 > 0$.

Example 2.1.18. Let us consider the singularity given by $x^3 = y^5$.

Then a deformation of parametrizations is given by:

$$\begin{cases} x(t) = (t + s_2)(t(t + s_2) + s_1) + s_0 \\ y(t) = (t(t + s_2) + s_1)((t + s_2)(t(t + s_2) + s_1) + s_0) \end{cases} \tag{2.1}$$

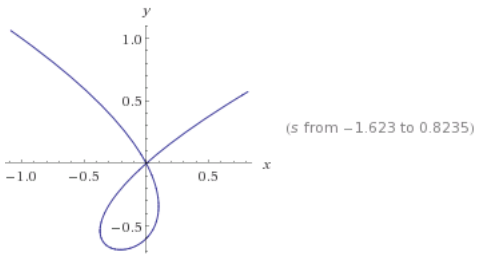

Figure 2.9

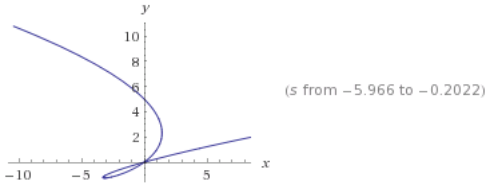

Figure 2.10

Let us suppose that s_i are chosen such that the polynomials:

$$p_2(t) = (t + s_2)(t(t + s_2) + s_1) + s_0$$

$$p_1(t) = t(t + s_2) + s_1$$

have respectively 3 and 2 real roots. Then we can write:

$$\begin{cases} x(t) = p_2(t) \\ y(t) = p_1(t)p_2(t) \end{cases} \tag{2.2}$$

There exist three points t_1, t_2, $t_3 \in \mathbb{R}$ such that $p_2(t) = 0$, which means that there are three values of t for which the solution of the system is the point $(0, 0)$. Moreover, there exist two points t_4, $t_5 \in \mathbb{R}$ such that $p_1(t_4) = p_1(t_5) = 0$. There is then a double point at $(s_0, 0)$.

It is an easy remark that the points in which the parametrization Φ is not an injective function are multiple points of the divide. Vice versa, let P_i be the local pairwise intersection of m_i smooth branches. There are m_i values $t_i^1, \ldots, t_i^{m_i}$ such that $\Phi(t_i^j) = P_i$.

Remark 2.1.19 (Explained to us by A'Campo). The operation of passing from a divide to a generic divide can be done at each singular point of the divide in an independent way. Let Φ be a parametrization given by $(x, y) = (f(t), g(t))$. We can consider a parametrization Φ^i, defined by:

$$(x, y) = (f(t) + h_i(t) \prod_{j \neq i} \prod_{k=j,\ldots,m_j} (t - t_j^k), g(t) + l_i(t) \prod_{j \neq i} \prod_{k=j,\ldots,m_j} (t - t_j^k))$$

where $h_i(t)$ and $l_i(t)$ can be chosen in such a way that they are linear functions with small coefficients, so that they don't change the topology of the divide outside a neighbourhood of the multiple point. Moreover, they don't deform the other multiple points, because we multiplied the two linear functions by a polynomial having as roots the points t_j^k.

2.2 Partial deformations

2.2.1 The cut of a lotus

Remark 2.2.1. We recall that $\mathcal{P}^{(j)}$ denotes the set of infinitely near points on the surface $\Sigma^{(j)}$, which lie on the strict transform $C^{(j)}$ of C.

Definition 2.2.2. Let $O_i \in \mathcal{P}^{(j)} \subset \Sigma^{(j)}$. We denote by $\mathcal{B}(O_i)$ the set of branches of $C^{(j)}$ which pass through O_i. Denote $\mathcal{B}(O_i) = \{C_1, \ldots, C_n\}$. Let $\mathcal{B}^{(1)}(O_i) \subset \mathcal{B}(O_i)$ be an arbitrary non-empty subset.

The multiplicity m_i associated to O_i is $m_i = m_i^1 + m_i^2 + \cdots + m_i^n$, where $\mathbf{m_i^h}$ is the multiplicity relative to the branch C_h. We define:

$$m_i^{(1)} = \sum_{h:C_h \in \mathcal{B}^{(1)}(O_i)} m_i^h.$$

Let Σ be the minimal embedded resolution surface of C. The number of branches of C which are curvettas for an exceptional component E_i on Σ is denoted by $\mathbf{c_i}$.

Remark 2.2.3. Let $\Sigma^{(j)}$ be such that $O_i \in \Sigma^{(j)}$. Let us suppose that $E_i \subset \Sigma^{(j+1)}$ is such that c_i branches of C are transverse to E_i and such that their union with $E^{(j+1)}$ has only normal crossings.

Let $i \leq l \leq N$, where $\Sigma^{(N)}$ is the minimal embedded resolution. Then there are still exactly c_i branches of C transversal to the component $E_i^{(l)} \subset \Sigma^{(l)}$.

We want now to understand the topological concepts introduced in Definition 2.2.2 via the combinatorics of the lotus.

We have seen in Proposition 1.4.14 that there exists a bijective map between the nodes E_i of the lotus and the infinitely near points O_i of the Enriques diagram. We define the **multiplicity** m_i **associated to** E_i as the multiplicity m_i associated to O_i. Moreover, we consider on the set of exceptional curves the partial order induced from the one on infinitely near points:

$$E_i \preceq E_h \Longleftrightarrow O_i \preceq O_h.$$

A branch C_j belongs to $\mathcal{B}(O_i)$ if and only if there is an arrowhead C_j attached to a node E_h such that $E_i \preceq E_h$. We can then define the set $\mathcal{B}(E_i)$ as $\mathcal{B}(E_i) := \mathcal{B}(O_i)$. In the same way, we can define $\mathcal{B}^{(1)}(E_i)$.

We now want to define an operation on the lotus, its **cut at a vertex**, **relative to a collection of arrowheads**.

Definition 2.2.4. Let $\mathcal{L}$ be a lotus.

Let $E_iE_j\tilde{E}$, where $j = p_D(i)$ and $\tilde{E}$ is a vertex of $\mathcal{L}$, be the **petal** of E_i (see Definition 1.4.5). Then $\tilde{E}$ is either a curvetta L_h or the node $E_{p_I(i)}$. Let $\mathcal{B}^{(1)}(E_i) = \{C_1, \ldots, C_k\} \subset \mathcal{B}(E_i)$.

The **cut** at E_i relative to the branches $C_1, \ldots, C_k$ is an operation on $\mathcal{L}$ such that:

1. for every petal $E_hE_{h_1}E_{h_2}$, where h is such that $E_i \prec E_h$ we consider a new petal $E_h^1E_{h_1}^1E_{h_2}^1$;

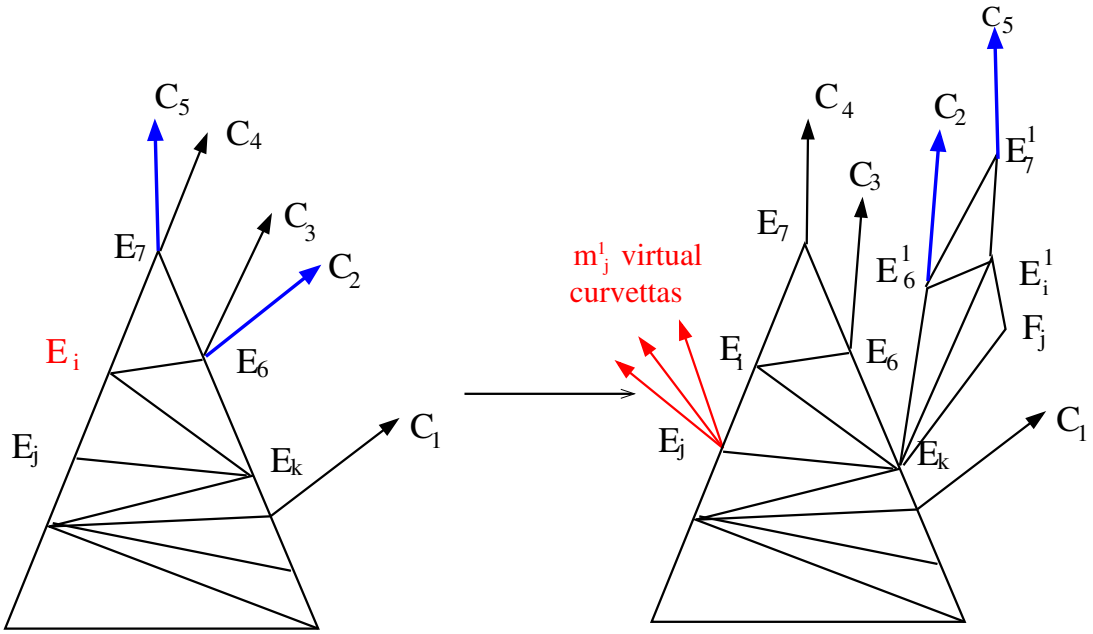

Figure 2.11 – The cut at E_i relative to the branches C_2 and C_5.

2. we define a petal having vertex E_i^1 and base $\tilde{E}$ and F_j^1;
3. we glue all such petals, respecting the labellings, and we call $\mathcal{L}^1$ the resulting lotus;
4. if an arrowhead $C_l \in \mathcal{B}^{(1)}(E_i)$ was attached to a node $E_h \in \mathcal{L}$, then it is attached to the node $E_h^1 \in \mathcal{L}^1$;
5. if an arrowhead $C_l \in \mathcal{B}(E_i) - \mathcal{B}^{(1)}(E_i)$ was attached to a node E_h before cut, it is still attached to the same node E_h after the cut;
6. we attach
$$m_j^{(1)} = \sum_{l \,:\, C_l \in \mathcal{B}^{(1)}(E_i)} m_j^l$$
curvettas at E_j. Those curvettas are called **virtual curvettas**;
7. inductively, if a vertex E_i, $E_i^2 = -1$, has no attached curvettas or virtual curvettas, we delete the associated petal.

In Figure 2.11 we can see an example of a cut at a node E_i.

Remark 2.2.5. The lotus obtained by a cut is not necessarily the lotus of a minimal embedded resolution (see Remark 1.4.9). The easiest example is the cut at an infinitely near point O_i such that $m_i = 1$. For an example, see Figure 2.14. This is why we add the condition (7) to obtain the lotus of a minimal embedded resolution.

Let us explain more concretely the construction of the previous definition. Let E_i be a node of the lotus, and let the edge $[E_j, \tilde{E}]$ be the base of its petal. It is then possible to consider this edge as the basis of a lotus, let it be $\mathcal{L}'$. More precisely, $\mathcal{L}'$ is the sublotus of $\mathcal{L}$, obtained by taking the union of all the petals associated to nodes E_h, $E_i \preceq E_h$. We can then consider a copy $\mathcal{L}^{(1)}$ of the lotus $\mathcal{L}'$, such that all nodes E_h and all curvettas L_t

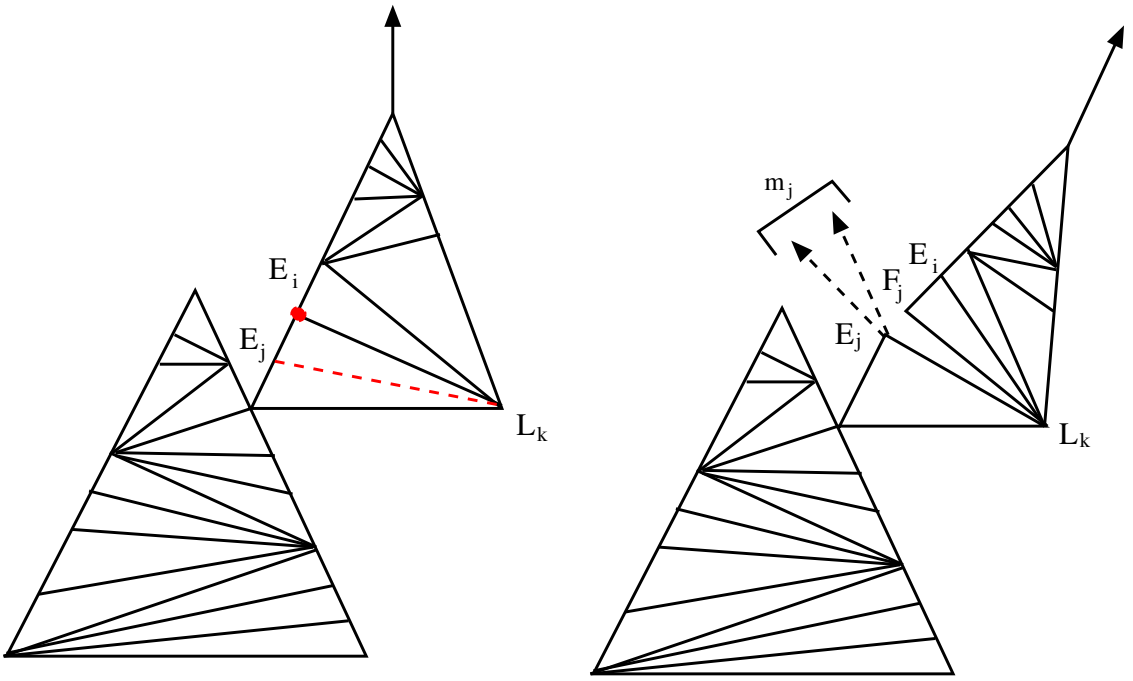

Figure 2.12 – An example of cut at a free node.

that don't belong to the basis are labelled E_h^1 and L_t^1, with the exception of the base point E_j that is labelled F_j and of $\tilde{E}$ that keeps the the same labelling. Then the lotus $\mathcal{L}^{(1)}$ is attached to $\mathcal{L}$ by identifying the vertices which have the same labels (i.e., $\tilde{E}$).

By construction, if $C_l \in \mathfrak{B}^{(1)}(E_i)$, there is an arrowhead labelled C_l attached to a node E_h, $E_i \preceq E_h$. We attach then the arrowhead C_l to the new node E_h^1. Let C_l be an arrowhead not belonging to $\mathfrak{B}^{(1)}(E_i)$. Then the arrowhead C_l is attached to the same node E_h it was attached to before the cut.

There is an invariant that we can compute on the lotus and which depends on the curvettas: the multiplicity of a certain node E_i. We will see in Proposition 2.2.10 that, in a certain sense, the multiplicity is invariant after cut.

Proposition 2.2.6. *Let E_i be a free node of the lotus. Then the cut at E_i of the branches $C_1, \ldots, C_k$ is a multi-lotus (see Definition 1.4.31).*

Proof. From the hypothesis that E_i is a free node, the i-petal is $E_iE_jL_k$, where $j = p_D(i)$ and L_k is a curvetta. After the cut we obtain a new lotus $\mathcal{L}_i^1$ having basis F_jL_k, and we add m_j^1 virtual curvettas at E_j. We can remark that the node E_i^1 is joined to the two curvettas, F_j and L_k, where L_k is a vertex of both $\mathcal{L}$ and $\mathcal{L}_i^1$. The lotus $\mathcal{L}$ is glued to $\mathcal{L}_i^1$ via the common vertex L_k. We have then obtained a multi-lotus.

□

We can see in Figure 2.12 an example of cut at the free node E_i.

Remark 2.2.7. The cut can be defined also for a finite number of sets $\mathfrak{B}^{(l)}(E_i)$, by considering a different lotus, having nodes E_h^l for all $h \succeq i$.

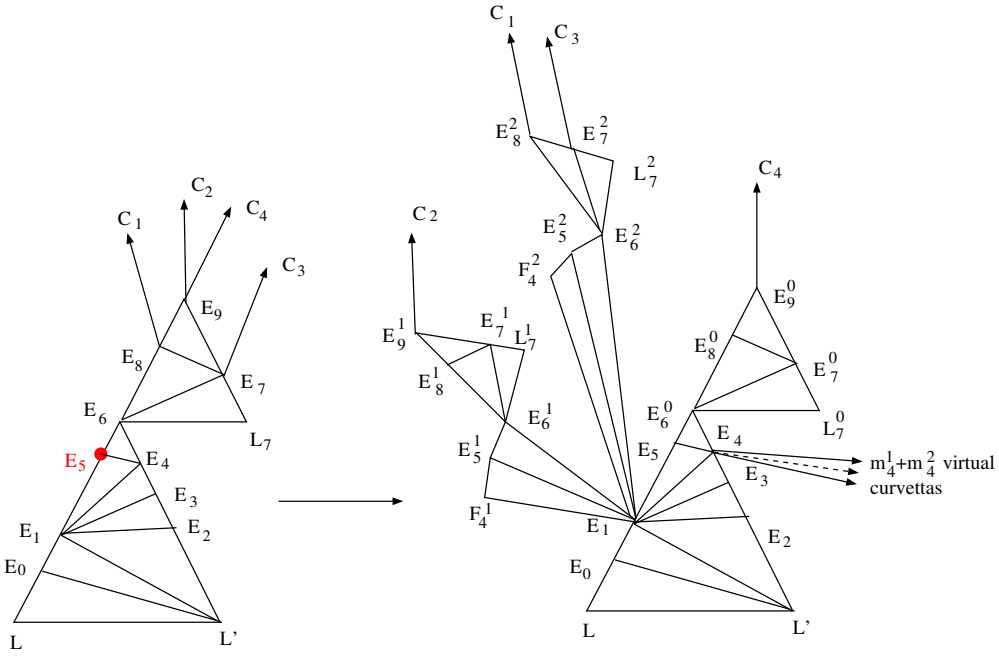

Figure 2.13 – An example of split nodes.

The definition is the same as before, we just consider a copy of the lotus $\mathcal{L}'^{(l)}$ for every l.

Definition 2.2.8. Let C be a curve singularity and let E_i be a point; let:

$$\mathcal{B}(E_i) = \mathcal{B}^{(0)}(E_i) \coprod \mathcal{B}^{(1)}(E_i) \coprod \mathcal{B}^{(2)}(E_i) \coprod \ldots \coprod \mathcal{B}^{(r)}(E_i).$$

We can then consider r different cuts at E_i of branches in $\mathcal{B}^{(l)}$, $l = 1, \ldots, r$. For every h such that $E_i \preceq O_h$ we have $r+1$ **split nodes** E_h^0, E_h^1, $\ldots$, E_h^r.

Theorem 2.2.9. *Let $\mathcal{L}$ be a multi-lotus. Then the cut of $\mathcal{B}^1(E_i)$ at E_i is a multi-lotus.*

Proof. We have seen in Proposition 2.2.6 that the cut of a lotus can give, as a result, a multi-lotus.

Moreover, a fundamental property of a multi-lotus is that every petal belongs to only one lotus. Then it possible to define the cut of a node of a multi-lotus as the cut of a particular lotus. Then again, we obtain a multi-lotus.

□

Proposition 2.2.10. *Let $\mathcal{L}'$ be the multi-lotus obtained by a cut at E_i, such that*

$$\mathcal{B}(E_i) = \mathcal{B}^{(0)}(E_i) \coprod \mathcal{B}^{(1)}(E_i) \coprod \mathcal{B}^{(2)}(E_i) \coprod \ldots \coprod \mathcal{B}^{(r)}(E_i).$$

Let m_i be the multiplicity at the node $E_i \in \mathcal{L}$. Then:

— *if $E_i \not\preceq E_h$, then the multiplicity at $E_h \in \mathcal{L}'$ is still m_h;*

— *if $E_i \preceq E_h$, then $m_h = \sum_{l=0,\ldots,r} m_h^{(l)}$,*

where $m_h^{(l)} = \sum_{C_u \in \mathcal{B}^l(E_i)} m_h^u$.

Proof. We have proved in Proposition 1.4.17 that the multiplicity m_h of a node E_h is:

$$m_h = c_h + \sum_{l:\ E_l \in \mathcal{P}(E_h)} m_l,$$

where c_h is the number of arrowheads attached to the node E_h.

Let E_h be a node, $E_h^2 = -1$. Then $\mathcal{P}(E_h) = \emptyset$. If $E_i \not\preceq E_h$, then the multiplicity at E_h is necessarily invariant, and equal to c_h. If $E_i \preceq E_h$, then we have $r+1$ split nodes $E_h^0, \ldots, E_h^r$. A node E_h^l has attached c_h^l different arrowheads. In particular, $c_h = c_h^0 + c_h^1 + \cdots + c_h^r$. It is an easy remark that $m_h = m_h^{(0)} + m_h^{(1)} + \cdots + m_h^{(r)} = c_h^0 + c_h^1 + \cdots + c_h^r = c_h$.

We can see the result by induction for every E_h such that $E_i \preceq E_h$. For every branch C_l:

$$m_h^l = c_h^l + \sum_{u: O_u \in \mathcal{P}(E_h)} m_u^l.$$

Then:

$$\sum_{l=0,\ldots,r} m_h^{(l)} = \sum_{l=0}^{r} (c_h^l + \sum_{u: O_u \in \mathcal{P}(O_h)} m_h^u) = c_h + \sum_{u: O_u \in \mathcal{P}(O_h)} \sum_{l=0}^{r} m_u^{(l)}.$$

By the induction hypothesis, we know that $\sum_{l=0}^{r} m_u^{(l)} = m_u$, $\forall E_u \in \mathcal{P}(E_h)$. Then:

$$c_h + \sum_{u: O_u \in \mathcal{P}(O_h)} \sum_{l=0}^{r} m_u^{(l)} = c_h + \sum_{u: O_u \in \mathcal{P}(O_h)} m_u = m_h.$$

Let us now consider E_j, $j = p_D(i)$. We remember that we have attached $c'_j = \sum_{l=1}^{r} m_j^l$ virtual arrowheads to E_j. Then the multiplicity associated to E_j is equal to:

$$c_j + c'_j + \sum_{u: O_u \in \mathcal{P}(O_j)} m_u = c_j + \sum_{l=1}^{r} m_j^{(l)} + \sum_{u: O_u \in \mathcal{P}(O_j)} m_u = m_j.$$

We can make the same computation for E_k, $k = p_I(i)$.

It is an easy remark that all other nodes E_h have the same multiplicity they had before the cut.

□

Remark 2.2.11. The idea of the proof is that, with the cut of the lotus, we change the information about the predecessor, and so we lose some of the multiplicities we consider in Equation 1.6. That loss is compensated by the virtual curvettas attached to the node E_j.

2.2.2 Characterization of partial deformations

Definition 2.2.12. Let us consider a point $O_i \in \Sigma^{(l)}$, $O_i \in E_j$, $j = p_D(i)$. A **translation** of a branch $C_h^{(l)}$ at O_i is a deformation with parameter $s_u \in (\mathbb{C}, 0)$ of the parametrization of the curve such that

— $P_i(s_u) \notin E_j$, for $s_u \neq 0$;
— if O_i is a free point, $P_i(s_u) \in L_j$;
— if O_i is a satellite point, then $P_i(s_u)$ is translated along $E_{p_I(i)}$.

Moreover, after translation the point $P_i(s_u)$ is a smooth point of $\tilde{E}^{(l)}$. We complete the frame $\tilde{E}^{(l)}$ by adding a curvetta $F_j(s_u)$.

The deformation of C obtained by projecting the result of the translation to $\Sigma^{(0)}$ is said to be obtained by a **partial A'Campo deformation at** O_i.

The same process can be extended to any number of branches at O_i.

Remark 2.2.13. As in Subsection 2.1.2, $P_i(s_u)$ indicates the deformation of the infinitely near point O_i. Moreover, $P_i(0) = O_i$.

Theorem 2.2.14. *Let C be a multi-germ, $C = C^1 \coprod \ldots \coprod C^n$, C^i germ at A^i, $A^i = A^j$ if and only if $i = j$. Let $\mathcal{L}$ be an associated multi-lotus. The cut of the multi-lotus $\mathcal{L}$ at E_i relative to the branches $\tilde{\mathcal{B}}(E_i) \subset \mathcal{B}(E_i)$ is the multi-lotus of the multi-germ of the generic fibre of the deformation obtained by a partial A'Campo deformation at O_i. Moreover,*

— *if E_i is a free node, then the A'Campo deformation $\check{C} = \check{C}^1 \coprod \ldots \coprod \check{C}^n \coprod \check{C}^{n+1}$, where $\check{C}^{n+1}$ is a germ at A^{n+1}, $A^{n+1} \neq A^j$ for $j = 1, \ldots, n$;*
— *if E_i is a satellite node, then there exists a germ C^j, n_j being the number of its branches, such that the A'Campo deformation $\check{C}^j$ of C^j has $n'_j > n_j$ different branches.*

Proof. Without losing generality, we can assume that C is a curve singularity. The proof is the same for multi-germs.

Let O_i be a free point and let $j = p_D(i)$. A partial deformation at O_i relative to the branches $\{C_1, \ldots, C_r\} = \tilde{\mathcal{B}}(E_i) \subset \mathcal{B}(E_i)$ is such that $P_i(s_u)$ doesn't belong any more to the exceptional locus and each branch $C_l \in \tilde{\mathcal{B}}(E_i)$ intersects the exceptional component E_j in m_j^l distinct points.

The blow down process doesn't change the topological type of the germ at $P_i(s_u)$. Moreover, the restriction of a branch C_l to a a neighbourhood of E_j is the union of m_j^l smooth branches transversal to E_j. Such branches are the virtual curvettas at E_j.

Then the deformation of the free point O_i is equivalent to the cut of the lotus at the free node E_i.

Let O_i be a satellite point, $O_i \in E_j \cap E_k$, $j = p_D(i)$, $k = p_I(i)$. A partial deformation at O_i is such that $P_i(s_u) \in E_k$ and we add a new curvetta F_j to obtain a cross at P_u. A branch $C_l \in \tilde{\mathcal{B}}(E_i)$ intersects the exceptional component E_j in m_j^l distinct points. Moreover, the restriction of C_l to a neighbourhood of E_j is the union of m_j^l smooth branches, transversal to E_j. Again, we attach m_j^l virtual curvettas at E_j for every branch C_l.

Then the deformation of the satellite point O_i is equivalent to the cut of the lotus at the satellite node E_i.

□

Definition 2.2.15. Let C be a curve singularity. A **partial A'Campo deformation**, is a deformation by A'Campo's algorithm where we consider translations only for certain points O_i and relative to certain branches belonging to $\mathcal{B}(O_i)$.

Theorem 2.2.16. *Let C be a complex curve singularity with r branches. Let μ be the Milnor number of C. Let C' be a general fiber of the partial A'Campo deformation of (C, O) obtained by translating at O_i all the branches in $\mathcal{B}(O_i)$. Then:*

— *if E_i is a* satellite node *then C' has only one singular point, with Milnor number:*

$$\mu' = \mu - \sum_{h \in \mathcal{B}(E_i)} m_j^h;$$

— *if E_i is a* free node *then C' has two singular points, with Milnor numbers:*

$$\mu' = \sum_{h : E_i \not\preceq E_h} m_h(m_h - 1) - \sum_{h \in \mathcal{B}(E_i)} m_j^h - r + \#\{\mathcal{B}(E_i)\} + 1,$$

and:

$$\mu'' = \sum_{h : E_i \preceq E_h} m_h(m_h - 1) - \#\{\mathcal{B}(E_i)\} + 1.$$

Moreover,

$$\mu' + \mu'' = \mu - \sum_{h \in \mathcal{B}(O_i)} m_j^h + 1.$$

Proof. The Milnor number associated to a curve singularity C is:

$$\mu = (\sum_{h : E_h \texttt{ node}} m_h(m_h - 1)) - r + 1,$$

where r is the number of branches (see [Wal04, Theorem 6.5.9]).

Let E_i be a satellite node and let $\mathcal{L}_i$ be the lotus obtained by cut at E_i of branches $\mathcal{B}(E_i)$. Then the multiplicity at every node E_h is preserved (see Proposition 2.2.10), and we have added $\sum_{l \in \mathcal{B}(O_i)} m_j^l$ virtual arrowheads. Moreover, we don't have any split nodes, because we deformed all branches of C. Then for a satellite node:

$$\mu' = \sum_{h : E_h \texttt{ node}} m_h(m_h - 1) - r + 1 - \sum_{l \in \mathcal{B}(O_i)} m_j^l = \mu - \sum_{l \in \mathcal{B}(O_i)} m_j^l.$$

Let E_i be a free node. A cut of $\mathcal{L}$ at E_i gives a multi-lotus. Let $\mathcal{L}'$ and $\mathcal{L}''$ be its two components, where $\mathcal{L}'$ is the lotus having basis L and L'. Such two loti are respectively the union of petals relative to points E_h such that $E_i \not\preceq E_h$ and union of petals relative to points E_h such that $E_i \preceq E_h$.

The deformation at a free point O_i is such that the point $P_i = P_i(s_{i'})$ doesn't belong any more to the exceptional component. Then if we consider a small neighbourhood of P_i, the germ in the neighbourhood isn't involved any more in the deformation process. We associate then to the point P_i a germ, whose resolution space (not necessarily minimal) is given by the component obtained by blow-up of all points O_h, $i \preceq h$. For the computation of the multiplicity, we have to consider only the multiplicities of nodes E_h such that

$E_i \preceq E_h$ and the only arrowheads are the ones such that they are attached to nodes E_h such that $E_i \preceq E_j$. The Milnor number is then clearly:

$$\mu'' = (\sum_{h:E_i \preceq E_h} m_h(m_h - 1)) - \#\{\mathcal{B}(E_i)\} + 1.$$

The germ at the origin O is described instead by all the petals associated to nodes E_h such that $E_i \not\preceq E_h$. Moreover, an arrowhead C_l such that $C_l \notin \{\mathcal{B}(O_i)\}$ is not effected by the modification, while for every arrowhead $C_l \in \{\mathcal{B}(E_i)\}$ we consider m_j^l virtual arrowheads at P_j, $j = p_D(i)$. The associated Milnor number is

$$\mu' = (\sum_{h:E_i \not\preceq E_h} m_h(m_h - 1)) - \sum_{h \in \mathcal{B}(E_i)} m_j^h - r + \#\{\mathcal{B}(E_i)\} + 1.$$

In the case of a satellite node we have seen that the new Milnor number is necessarily smaller than the original Milnor number. In this case, we can consider the sum $\mu' + \mu''$, obtaining:

$$\mu' + \mu'' = (\sum_{h:E_i \not\preceq E_h} m_h(m_h - 1)) - \sum_{h \in \mathcal{B}(E_i)} m_j^h - r +$$

$$+\#\{\mathcal{B}(E_i)\} + 1 + (\sum_{h:E_i \preceq E_h} m_h(m_h - 1)) - \#\{\mathcal{B}(E_i)\} + 1 - \sum_{h \in \mathcal{B}(E_i)} m_j^h =$$

$$= (\sum_{h:E_h \text{ node}} m_h(m_h - 1) - r + 2 - \sum_{h \in \mathcal{B}(E_i)} m_j^h = \mu + 1 - \sum_{h \in \mathcal{B}(E_i)} m_j^h.$$

□

Corollary 2.2.17. *Let C be a curve singularity, m_i be the multiplicity of a satellite node E_i such that $E_i^2 \neq -1$. Then there exists a partial A'Campo deformation C' of C such that $\mu' = \mu - m_i$.*

Proof. It is a straightforward application of Theorem 2.2.16, when considering a cut at E_{i+1} of all arrowheads in $\mathcal{B}(E_i)$. □

Corollary 2.2.18 (Gusein-Zade)**.** *Let C be a curve singularity. Denote by $\Sigma^{(N)}$ its minimal embedded resolution surface. Let us suppose that there exists an exceptional component $E_i^N \subset \Sigma^{(N)}$ such that:*

— *E_i^2 is a (-1)-curve;*

— *$m_i = 1$, that is, there is only one branch of C whose strict transform intersects E_i.*

Let μ be the Milnor number of C. Then there exists a partial A'Campo deformation such that its generic fibre has Milnor number $\mu - 1$.

Proof. The argument is the same as the one used by Gusein-Zade in [GZ93].

Let us consider a cut at E_i. Then by Theorem 2.2.16:

$$\mu' = \mu - \sum_{h \in \mathcal{B}(E_i)} m_j^h.$$

By the hypothesis $E_i^2 = -1$ and $m_i = 1$ we have that $\mathcal{B}(E_i) = C$ and $m_j = 1$. Then $\mu' = \mu - 1$. □

A proof of the same result for branches having only one Puiseux pair has been obtained in [Bod07][Theorem 6], by using the properties of the Newton polygon.

Example 2.2.19. Let us consider the curve singularity C having Puiseux pair $(24;55)$. Then $\mu = 1242$ is its Milnor number. We consider a partial deformation at the point O_8, i.e., we cut the lotus at the node E_8. After deformation, the virtual curvetta C' has Puiseux pair $(7;16)$. Moreover, $i(C,C') = 16/7$, while the curve C has Puiseux pair $(17;39)$ (see Figure 2.14).

As proved in Corollary 2.2.18, the associated Milnor number is $1241 = \mu - 1$.

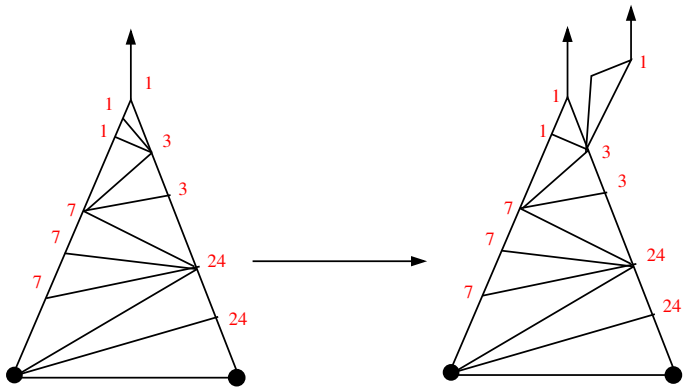

Figure 2.14 – An example of curve singularity for Corollary 2.2.18.

We can also remark that the resulting lotus is not the lotus of the minimal embedded resolution of the new curve C'.

Theorem 2.2.20. *Let (C,O) be a complex plane curve singularity which is not an ordinary singularity. Let (Σ,E) be the minimal embedded resolution space of C. Moreover, let $\{E_{i_j}\}_{j=1,\dots,k}$ be the set of exceptional components such that $E_{i_j}^2 = -1$ and for all $j = 1,\dots,k$ let $n_j = \#\{\mathcal{B}(O_{i_j})\}$. Then there exists a partial A'Campo deformation of (C,O) which has a singular point with Milnor number $\mu' = \mu - min\{n_1,\dots,n_k\}$.*

Proof. Let us consider that $c_{N_1} = n_1$, i.e., there are n_1 arrowheads attached to E_{N_1}. Let us cut the lotus at E_{N_1}. Then we don't change any member of the multiplicity sequence, and we add n_1 curvettas. The Milnor number relative to the germ obtained by such a cut is then $\mu' = \mu - n_1$.

□

2.2.3 Sequences of partial deformations

Definition 2.2.21. Let $\mathcal{L}$ be a lotus associated to a curve singularity C. A cut at two nodes E_i and E_j, $E_j \prec E_i$ is a lotus $\mathcal{L}'$ given by a cut at E_j of the lotus obtained by a cut at E_i, each time relative to **specifics sets of branches** of C.

If we consider also a cut at two nodes E_i and E_j such that $E_i \not\prec E_j$ and $E_j \not\prec E_i$, then the order of the cuts is not important.

Remark 2.2.22. Moreover, if we cut at n points $E_{i_1} \prec E_{i_2} \prec \cdots \prec E_{i_n}$, then the cut is defined inductively, starting by the cut at E_{i_n}.

A cut can be done at the same node, but relative to different branches.

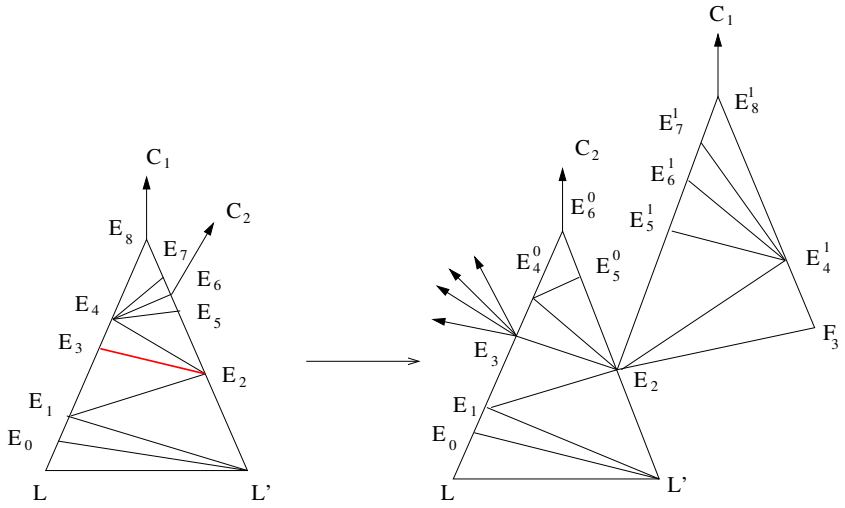

Figure 2.15 – The cut at E_4 relative to the branch C_1.

Example 2.2.23. In Figure 2.15 we can see the case of the cut at the point O_4 relative to the branch C_1, while the cut is not relative to the branch C_2.

Example 2.2.24. In Figure 2.16 we can see the case of two cuts at E_6 and E_3 of the curve singularity having Puiseux pair $(31; 71)$. We add respectively 4 and 9 virtual arrowheads at E_5 and E_2, where 4 and 9 are the multiplicities of E_5 and E_2.

Proposition 2.2.25. *Let E_i be a satellite node, $k = p_I(i)$ and $j = p_D(k)$. Then we can consider a cut at E_i and a cut at E_j. Moreover, in such a way we obtain the multi-lotus of a multi-germ $C = C^1 \coprod C^2$.*

Proof. Let us consider a cut of the lotus at E_i. Then in the new lotus E_i is a free node. A cut at E_j involves virtual arrowheads, if and only if it involves also the original arrowheads. Then a cut at E_j implies a further cut at E_i. As it have been shown in Proposition 2.2.6, a cut at a free point gives a multi-lotus. □

Example 2.2.26. In Figure 2.17 we can see the example of a cut at E_2 and at E_1.

The first germ is $y^5 - x^{18} = 0$. After the first deformation we obtain a germ having the same topological type as $(y^2 - x^{10})(y^5 - x^8) = 0$. After the second one we have three different germs, one having the same topological type as $y^5 - x^8 = 0$, the second one having the same topological type as $y^5 - x^5 = 0$ and the third one having the same topological type as $x^8 - y^8 = 0$.

Proposition 2.2.27. *Let C be a curve singularity, m_1 and m_2 be multiplicities at two points E_{i_1} and E_{i_2}, $i_1 > i_2$. Let $E_k = p_I(E_{i_1})$, $E_k = p_D(E_{j'})$, where $E_{j'}$ is the deviation node of E_{i_1} (see Definition 1.4.19). We assume that $E_{i_2} \neq E_{j'}$. Then there exists a partial A'Campo deformation of C whose generic fibre has only one singular point, with $\mu' = \mu - (m_1 + m_2)$.*

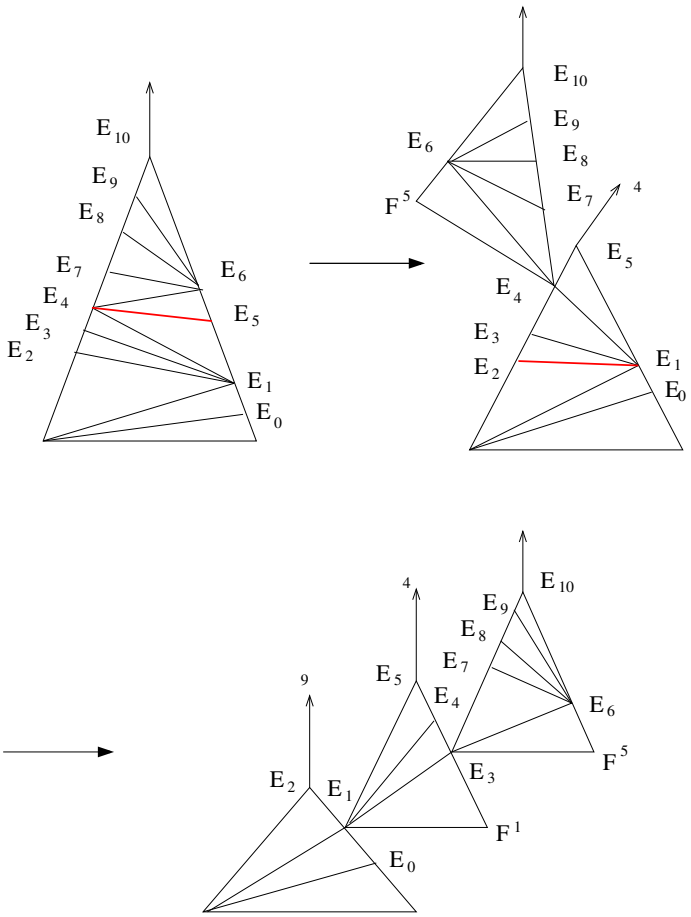

Figure 2.16 – The cut of $y^{31} - x^{71} = 0$ at E_6 and E_3.

Proof. It is a double application of Theorem 2.2.16. □

Corollary 2.2.28. *Let $\mathcal{L}$ be a lotus and let us consider n cuts at the nodes E_{i_n}, $E_{i_{n-1}}$, $\ldots$, E_{i_1}, $i_1 < i_2 < \cdots < i_n$. Denote by $\mathcal{L}'$ the resulting multi-lotus.*

Then $\mathcal{L}'$ is a lotus if and only if:

1. *for every $l = 1, \ldots, n$ there exists an exceptional component j_l such that $j_l = p_I(i_l)$;*
2. *for every $l = 1, \ldots, n$, $h < l$, we have that E_{i_h} is not the deviation point of E_{i_l}.*

Proof. It is an application of Proposition 2.2.27 to every pair of points E_{i_l} and $E_{i_{l'}}$. □

Theorem 2.2.29. *Let C be a curve singularity and let $\Sigma^{(N)}$ be the minimal embedded resolution of C. Let us suppose that there exist either an exceptional components E_i such that:*

— *E_i is a (-1)-curve;*
— *$m_i = 1$;*
— *$m_j = 1$, $j = p_D^2(i)$.*

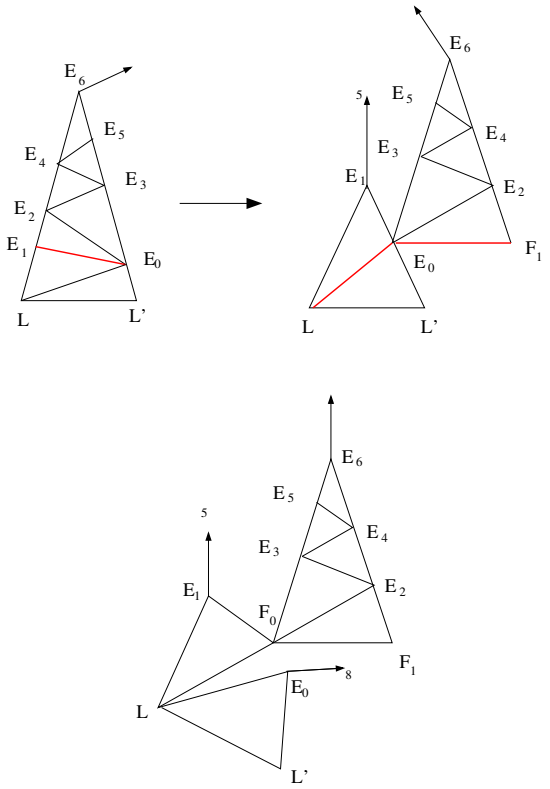

Figure 2.17

or a node E_l such that $m_l = 2$. Then there exists a deformation of the parametrization of C whose generic fibre has only one singular point with $\mu' = \mu - 2$.

Proof. Let E_i be the exceptional component such that $m_i = 1$ and respecting all the other hypotheses. Then we can consider two consecutive cuts at E_i and $E_{p_D(i)}$. After the first cut, the Milnor number is $\mu - 1$. By the hypothesis that $m_{p_D^2(i)} = 1$, the second cut also gives a Milnor number $(\mu - 1) - 1$.

If there exists a node E_l such that $m_l = 2$, it is sufficient to consider a cut at $E_{p_D(l)}$. □

Corollary 2.2.30. *Let C be a branch. Then there exists a deformation of the parametrization of C whose generic fibre has only one singular point with $\mu' = \mu - 2$.*

Proof. The proof follows from Theorem 2.2.29, as we notice that a multiplicity sequence, having only two nodes E_l such that $m_l = 1$, contains a node E_h such that $m_h = 2$.

□

The particular case of Corollary 2.2.30 for a branch having only one Puiseux pair has been proven in [Wal10][Theorem 4], by using the properties of the Newton polygon, following Bodin's method introduced in [Bod07].

Proposition 2.2.31. *Let C be a branch and let E_N be the unique (-1)-curve. Let $i = p_I(N)$, m_i the multiplicity associated to E_i. Then there exists a deformation of the*

parametrization of C whose generic fibre has only one singular point with:

$$\mu' = \mu - l, \quad l = 1, \dots, m_i.$$

Proof. By hypothesis, there are exactly m_i exceptional components E_h such that $m_h = 1$. Let them be E_N, E_{N-1}, ..., E_{i+1}. The cut at E_{i+1} gives a deformation with Milnor number $\mu' = \mu - m_i$.

Let us notice that E_{i+1} is the deviation point of E_h, $i + 2 \leq h \leq N$. If we consider $l < m_i$ cut at nodes E_N,E_{N-1},...,E_{i+2}, we obtain that $\mathcal{L}'$ is still connected (by Lemma 2.2.28) and the associated Milnor number is $\mu' = \mu - l$.

□

Proposition 2.2.32. *Let C be a curve singularity, and let m_i be the multiplicity of a certain node E_i. Then there exists a partial deformation C' of C such that:*

$$\mu' = m_i(m_i - 1) - m_i + 1 = (m_i - 1)^2.$$

Proof. We can consider a deformation at every point $\{E_h\}_{h=E,\dots,n}$ of all arrowheads. By doing that, we find $n + 1$ points P_h that are the local pairwise transversal intersection of m_h smooth branches, that is, ordinary singular points of multiplicity m_h. Then the Milnor number associated to the local singularity at P_h is $m_h(m_h-1)-m_h+1 = m_h^2-2m_h+1 = (m_h - 1)^2$. □

Remark 2.2.33. Let C be a curve singularity and let C' be a curve singularity associated to a certain cut $\mathcal{L}'$ of $\mathcal{L}$. Let L be the link associated to C and let L' be the link associated to C'. We can define a partial order $\simeq$ on the sets $\{L \mid L \text{ is an algebraic link } \}$ by:

$L' \simeq L$ if and only if L' is the link associated to a cut $\mathcal{L}'$ of $\mathcal{L}$.

It would be interesting to better understand this partial order.

Chapter 3

Real resolution spaces

Chapter Overview

In this chapter we want to study in detail the real resolution spaces. They are the real parts of the complex resolution spaces we have defined in Chapter 1. We will see that the combinatorics is far richer than in the complex case.

Section 3.1 is dedicated to define the structures we need in order to properly introduce real resolution spaces of curve singularities. In Section 3.1.1 we introduce the notions of *necklaces*, of *beads* (Definition 3.1.1) and of *bands* (Definition 3.1.3). We will see that we can consider them as vertices of a particular kind of graph, the *graph of necklaces* (Definition 3.1.4). We also introduce the *parity* of a band (Definition 3.1.6). In Section 3.1.2 we give some results about the topological properties of those spaces. Corollary 3.1.17 gives a necessary and sufficient condition for a space obtained by the *plumbing of bands* (Definition 3.1.11) to have connected boundary.

In Section 3.2 we define real singularities. We give the real equivalent of the definitions we have seen in Chapter 1 for complex curve singularities. The most important definition is Definition 3.2.12, where we introduce the notion of *combinatorial equivalence* in the case of real curve singularities. Section 3.2.2 is dedicated to some results about the combinatorics of real curves singularities, contained in a disk $D \subset \mathbb{R}^2$.

In Section 3.3 we use the notions defined in the two previous sections to understand real resolution surfaces. In Section 3.3.1 we see that we can speak in a natural way of local orientations on a real resolution surface in the case of blow-up of satellite points. In the case of blow-up of a smooth point, we will define a canonical way to choose a chart and local orientations, in such a way that the whole construction is easier to follow. Moreover, we define another invariant for exceptional components, the *orientability* (Definition 3.3.11). At the end of the section, we translate this construction in the language of graphs of necklaces. In the final part of this Chapter, Section 3.3.2, we define an invariant for real curve singularities, the *real lotus*. The idea is based on the lotus, that we have introduced in Section 1.4. More precisely, the real lotus of a real curve singularity C is built from the union of four copies of the lotus associated to the complexification of C, one for each connected component of $(\mathbb{R}^*)^2$. This idea has been inspired by the paper of Parusiński and Koike ([KP10]), in which the authors define an invariant for real curve singularities by its algebraic properties, *the real tree model*. We introduce moreover the concept of *positive*

curve singularity (Definition 3.3.30), a notion that will be extensively used in Chapter 4. In Theorem 3.3.35 we prove that the real lotus is particularly simple in the case of a positive curve singularity.

3.1 General construction

3.1.1 Graphs of necklaces

In this section we introduce a notion of *plumbing* adapted to our study of plane curve singularities. In the complex case, once a graph of plumbing is fixed, the associated plumbing operation is defined unambiguously, up to isomorphism (see [Neu81] or [PP07]). This is due to the fact that complex curves and surfaces have canonical orientations. As this is not true in the real case, we have to start from curves which are endowed with local orientations in the regions which have to be identified by plumbing.

Definition 3.1.1. A **necklace** is a pair $(E, \{\theta^i, i \in I\})$ where E is a circle and $\{\theta^i, i \in I\}$ is a finite set of points of E, called the **beads**. Moreover, there is given a choice of local orientation of E in the neighbourhood of each bead, and each arc of $E - \{\theta^i, i \in I\}$ is a **sector** of the necklace, decorated by a weight in $\mathbb{F}_2$, called its **local parity**. Two beads θ^i and θ^j are **consecutive beads** (or **neighbours**) if they are the endpoints of the closure of a sector.

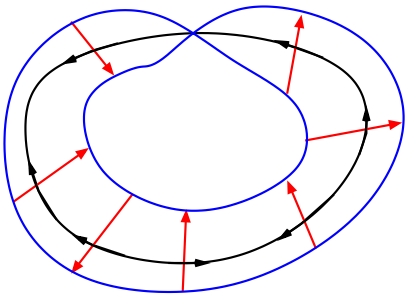

Figure 3.1 – A band with the associated fibres.

Remark 3.1.2. The beads $\theta^1, \ldots, \theta^n \in E$ have a *dihedral order*. They are not canonically cyclically ordered, because we don't have a canonical global orientation for E. In general we will consider that the beads are labelled in such a way that, for each point θ^i, the neighbouring beads are θ^{i-1} and θ^{i+1}, $i \in \mathbb{Z}/\mathbb{Z}_n$.

Definition 3.1.3. A **band** is a triple $(\mathcal{T}, E, \{T^i\})$ where:

1. $\mathcal{T}$ is either a compact cylinder or a compact Möbius band;
2. E is a necklace, and $\{\theta^i, i \in I\}$ are its beads;
3. $\{T^i : i \in I\}$ is a finite set of **fibres** of a structure of fibre bundle of $\mathcal{T}$ over S^1, such that E is a section of the fibre bundle and such that $\theta^i = T^i \cap E$. Moreover, each T^i is endowed with an orientation. Each T^i will be called a **fibre**.

Let us suppose that each sector has endpoints θ^i, θ^{i+1}. The **local parity** $p^{i,i+1} \in \mathbb{F}_2$ of the sector $[\theta^i, \theta^{i+1}]$ is such that:

— $p^{i,i+1} = 0$ if the transport by continuity of T^i on T^{i+1} preserves the orientation;

— $p^{i,i+1} = 1$ if it does not.

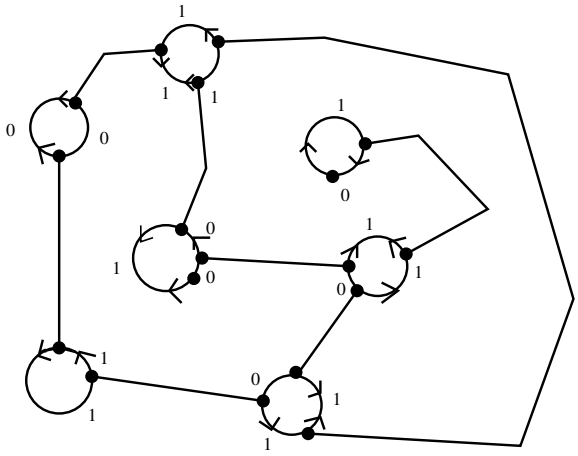

Figure 3.2 – An example of graph of necklaces.

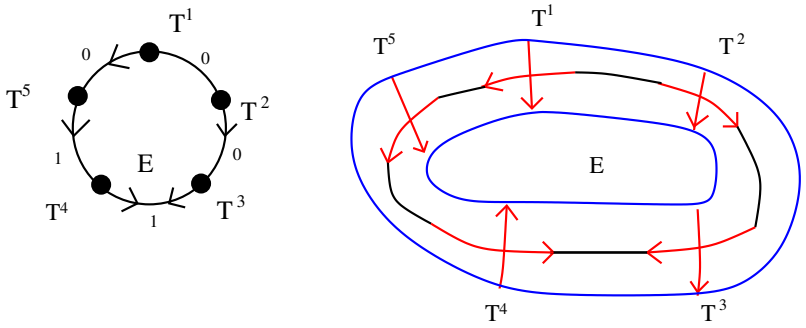

Figure 3.3 – An example of graph of necklaces for an annulus.

Definition 3.1.4. A **graph of necklaces** is a graph obtained in the following way:

— start with a disjoint union of necklaces;

— join pairwise some beads by arcs.

Such arcs, which are not parts of the necklace, are called the **connecting arcs** of the graph of necklaces.

The **directing graph** of the graph of necklaces is obtained by contracting each necklace to a point.

For an example, see Figure 3.2.

Remark 3.1.5. In the following, we won't consider the cases of two different necklaces joined to each other by more than one arc, or arcs joining two different beads on the same necklace. We won't spend either too much time in the detailed construction, because it is easy to define and it is not needed in what follows.

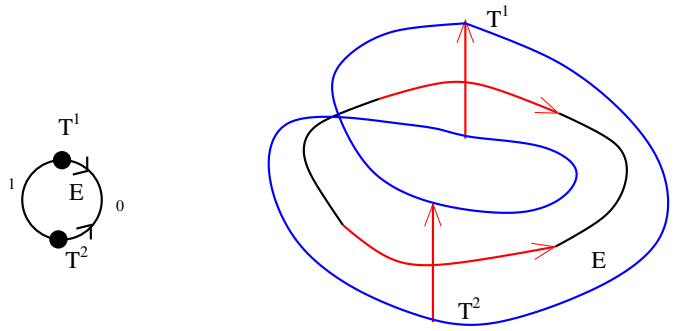

Figure 3.4 – An example of graph of necklaces for a Möbius strip.

In particular, in the rest of this work we will be interested in surfaces that are embedded resolution spaces of curve singularities. The surface shown in Figure 3.7 cannot be obtained as a sequence of blow ups of points, because the dual graph of a curve singularity is always a tree.

A little more analysis is needed for the surface shown in Figure 3.6. This surface can be obtained as a sequence of blow ups of points, but the coordinates are not compatible with the ones of a real resolution space. The property it doesn't respect is a subtle property of the plumbing of the local orientations to a global one, as we will see in Section 3.3.1.

Definition 3.1.6. Let $\mathcal{T}_i$ be a band, $\theta_i^1, \ldots, \theta_i^n$ its beads. We define its **parity** p_i as:

$$p_i = \sum_{j=1,\ldots,n} p_i^{j,j+1}.$$

Proposition 3.1.7. *If $p_i = 1$ then $\mathcal{T}_i$ is a Möbius strip. If $p_i = 0$, $\mathcal{T}_i$ is an annulus.*

Proof. Turn once around the necklace of the band, from the bead θ^k back. There are two possible outcomes: either after a full tour the orientation of T^k is the same, or it is the opposite one. In the first case we clearly have an annulus, and in the second one a Möbius strip. It is easy to convince oneself that this condition is given by the parity of the number p_i. □

Example 3.1.8. In Figure 3.3 we see an example of a necklace having 5 beads. Moreover, we can notice that $p_i = \sum_j p_i^j = 0$, and so $\mathcal{T}_i$ is an annulus.

Example 3.1.9. An example of a necklace having only two beads is shown in Figure 3.4.

Remark 3.1.10. Let E_i be a necklace having only one bead. The value of p_i associated to the only sector determines if $\mathcal{T}_i$ is either a Möbius strip or an annulus.

Definition 3.1.11. Let be given a graph of necklaces Γ. Its **associated plumbed surface** is obtained in the following way.

Consider a band $\mathcal{T}_i$ with necklace E_i for each necklace E_i of Γ. Let us consider a connecting arc between two beads θ_i^h and θ_j^k, the first one belonging to the necklace E_i and the second one belonging to the necklace E_j. Let T_i^h and T_j^k be the two associated fibres. The *plumbing* of E_i and E_j via θ_i^h and θ_j^k is such that:

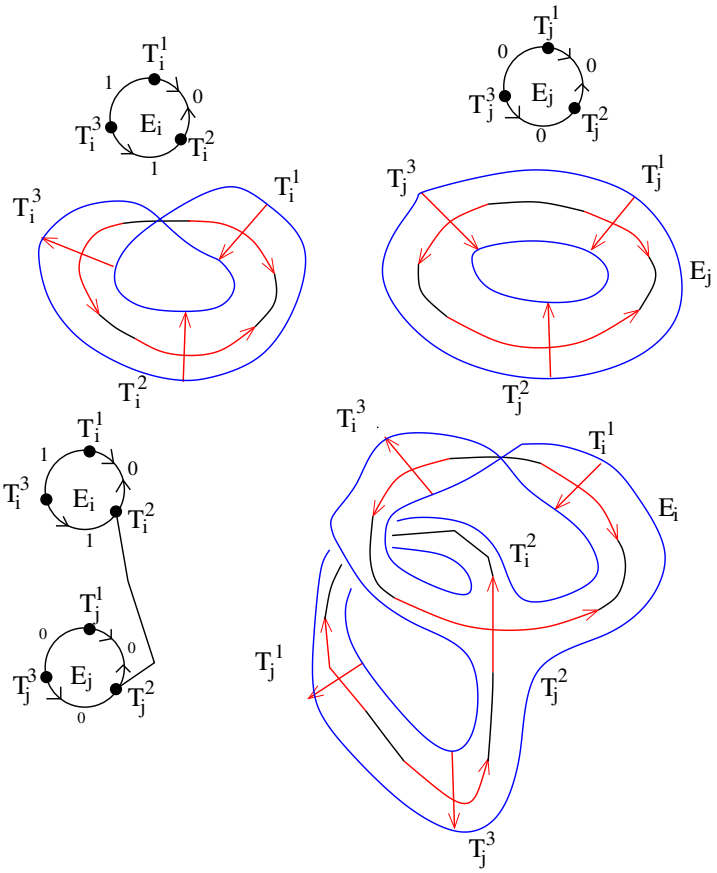

Figure 3.5 – An example of plumbing.

1. in a neighbourhood of T_i^h, E_i is identified with T_j^k respecting the orientations of E_i and T_j^k;
2. in a neighbourhood of T_j^k, E_j is identified with T_i^h respecting the orientations of E_j and T_i^h;
3. there is a local identification of the tubular neighbourhood of T_i^h with the tubular neighbourhood of T_j^k.

Remark 3.1.12. When the difference is clear from the context, we will use the notation E_i for both the topological space and the necklace.

In Figure 3.5 we can see an example of plumbing, in this case of the two beads T_i^2 and T_j^2. It is an important remark that the plumbing is compatible with all the orientations.

Example 3.1.13. An example of a plumbed surface associated to a graph of necklaces can be seen in Figure 3.6. We patch 5 different bands, in particular two annuli and three Möbius strips.

Example 3.1.14. A directing graph isn't necessarily a tree, as it is shown in Figure 3.7. In this case we consider the copy of 5 different Möbius strips, such that they have all the same local orientations.

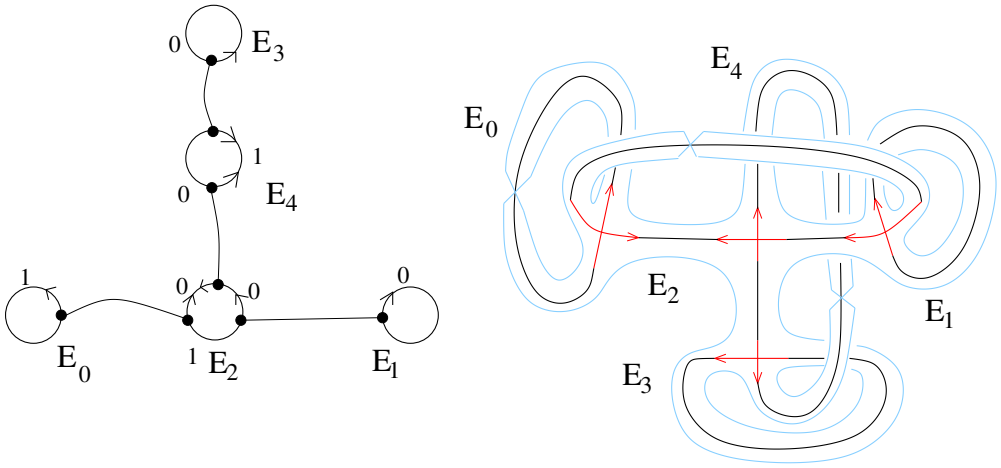

Figure 3.6 – A graph of necklaces and the associated plumbed surface.

We explained how to associate a surface endowed with locally oriented curves to any graph of necklaces. Let us introduce a special name for this kind of curves embedded in smooth real surfaces:

Definition 3.1.15. A **locally oriented curve-configuration** in a smooth real surface is a connected union with normal crossings of embedded circles and germs of arcs at smooth points of the union of the circles, such that in the neighbourhood of each singular point of the union of circles and arcs the two germs of curves are oriented.

3.1.2 Properties of the plumbed surfaces

We define the **intersection matrix** $I = (s_{ij}) \in M_n(\mathbb{F}_2)$ associated to a graph of necklaces Γ in the following way:

— $s_{ii} = p_i$, where p_i is the parity of the vertex E_i;
— $s_{ij} = 1$ if E_i and E_j are connected by an arc;
— $s_{ij} = 0$ otherwise.

Theorem 3.1.16. *Let Γ be a graph of necklaces, Γ a tree. Let I be the intersection matrix. Then $\tilde{H}_0(\partial\Sigma;\mathbb{F}_2) = n - rank(I)$, where $\tilde{H}$ is the reduced homology having coefficients in $\mathbb{F}_2$.*

Proof. Let us consider the long exact sequence of relative homology

$$\begin{array}{ccccccccc} 0 & \to & \tilde{H}_2(\partial\Sigma) & \to & \tilde{H}_2(\Sigma) & \to & \tilde{H}_2(\Sigma,\partial\Sigma) & \to & \\ & \to & \tilde{H}_1(\partial\Sigma) & \to & \tilde{H}_1(\Sigma) & \to & \tilde{H}_1(\Sigma,\partial\Sigma) & \to & \\ & \to & \tilde{H}_0(\partial\Sigma) & \to & \tilde{H}_0(\Sigma) & \to & \tilde{H}_0(\Sigma,\partial\Sigma) & \to & 0 \end{array}$$

Then $\tilde{H}_1(\Sigma) = \mathbb{F}_2^n$, where n denotes the number of vertices of the graph. Being Σ connected, $\tilde{H}_0(\Sigma) = 0$.

By Poincaré duality $\tilde{H}_1(\Sigma,\partial\Sigma) = \tilde{H}^1(\Sigma)$. Then $\psi : \tilde{H}_1(\Sigma) \to \tilde{H}^1(\Sigma)$ is represented by the intersection matrix and $dim(Im(\psi)) = rank(I)$. Let φ be the morphism $\varphi : \tilde{H}^1(\Sigma) \to \tilde{H}_0(\partial\Sigma)$. Then

$$dim(\ker(\varphi)) = dim(Im(\psi)) = rank(I), \quad \dim(Im(\varphi)) = n - rank(I).$$

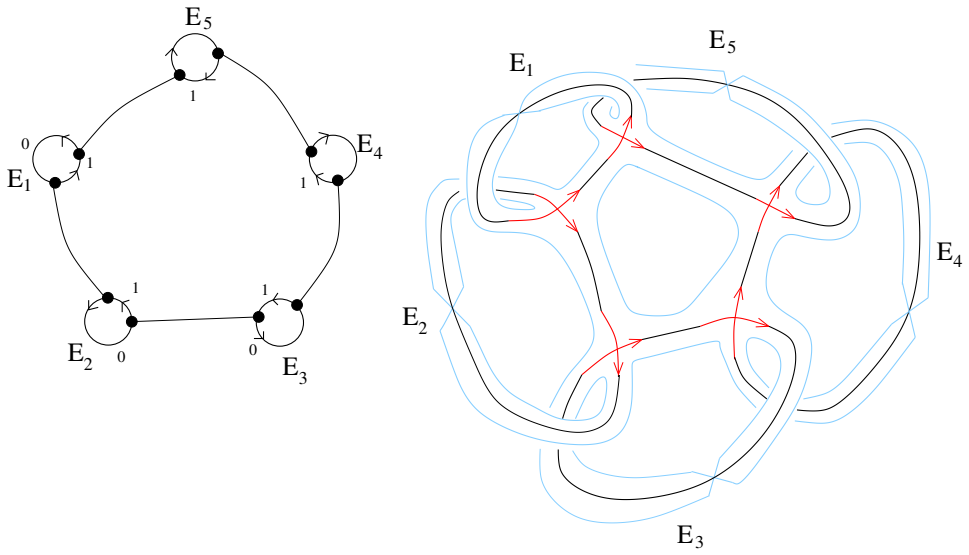

Figure 3.7 – A surface whose directing graph is not a tree.

□

Corollary 3.1.17. *$det(I) = 1$ if and only if $\partial\Sigma$ is connected.*

3.2 Real singularities

3.2.1 Combinatorial equivalence

Definition 3.2.1. A **real curve singularity** C in a neighbourhood of $O = (0,0) \in \mathbb{R}^2$ is the vanishing locus of $f = f_1 \cdots f_r$ where $f_i, ..., f_r \in \mathbb{R}\{x, y\}$ are irreducible, pairwise coprime, and such that the vanishing locus of each f_i is not reduced to the point O in some neighbourhood of O. Such a function f is called a **defining function** of C.

Remark 3.2.2. $f = (x^3 + y^5)(x^2 + y^3)(x^2 + y^2)$ is not a defining function of C. The three factors are all irreducible, but the vanishing locus $\{(x, y) \in \mathbb{R}^2 |\ x^2 + y^2 = 0\}$ contains only the origin. We notice that in a neighbourhood of the origin the polynomial is always positive.

Proposition 3.2.3. *If f_i is irreducible as an element of $\mathbb{R}\{x, y\}$, then f_i is also irreducible as an element of $\mathbb{C}\{x, y\}$ if and only if f changes signs in arbitrarily small neighbourhoods of the origin.*

A proof can be found in [Ris74]. The definition of a real germ has also been inspired by this paper.

Example 3.2.4. The polynomial $f = x^2 + y^2$ is not irreducible in $\mathbb{C}\{x, y\}$,

$$f = (x + iy)(x - iy).$$

Definition 3.2.5. Let C be a real curve singularity. A point $p \in C$ is a **singular point** if $df(p) = (0, 0)$, where f is a defining function of C.

Lemma 3.2.6. *Let C be a real curve singularity. Then $C-\{O\}$ is smooth in a sufficiently small neighbourhood of O, i.e., a singular point is **isolated**.*

Let $O_1^{(1)},\dots,O_k^{(1)}$ be points belonging to $\mathcal{P}^{(1)}\subset E^{(1)}$. By blow up of all the points we obtain a new surface $\Sigma^{(2)}$ and an exceptional locus $E^{(2)}$ such that $E^{(2)}=\Phi_1^{-1}(E^{(1)})$. We define $E_i^{(2)}=\Phi_1^{-1}(O_i^{(1)})$, $E_i^{(1)}\simeq\mathbb{P}^1(\mathbb{R})$. A curve $E_i^{(2)}$ is an **exceptional component**.

Remark 3.2.7. In the first blow-up exceptional locus and exceptional component coincide, $E^{(1)}\equiv E_0^{(1)}$. If C is a branch, then $E_i^{(i+1)}$ is the only component having self-intersection -1.

In general, let us suppose that $\Sigma^{(i)}$ is a surface obtained by blow-ups above O, $E^{(i)}$ its exceptional locus. Let $\pi_i:\Sigma^{(i)}\to D$ be defined by $\pi_i=\Phi_0\circ\Phi_1\cdots\circ\Phi_i$. Consider a set of points $\{O_j^i\}$ such that they belong to $E^{(i)}$. Then by blow up of all such points, we obtain a new surface $\Sigma^{(i+1)}$ and an exceptional locus $E^{(i+1)}$. Moreover, $\Phi_{i+1}:\Sigma^{(i+1)}\to\Sigma^{(i)}$ is its blow up.

All this construction is the real part of the construction we have done for complex surfaces in Chapter 1. We will then keep the same notations as in Chapter 1, but at every step we will only consider the real points.

Definition 3.2.8. Let (C,O) be a real curve singularity defined in a disk D. A **resolution** of C is a map $\pi:(\Sigma,E)\to(D,O)$, Σ a smooth surface, that satisfies the following properties:

1. π is analytic and proper.
2. $\pi^{-1}(C)$ has only normal crossings.

The pair (Σ,E) is a **resolution surface** for C.

Remark 3.2.9. The surface $\Sigma-E$ is oriented in a natural way by the pull-back of the orientation of $\mathbb{R}^2-\{0\}$.

Theorem 3.2.10. *Let $(C,O)\subset D$ be a real curve singularity. Then there exists a resolution π of C.*

Definition 3.2.11. Let (C,O) be a real curve singularity and let $\{\Sigma^{(i)},E^{(i)}\}_{i=0,\dots,n}$ be the maximal sequence of surfaces obtained by blow up of all points $O_j\in\Sigma^{(i)}$ such that $C^{(i)}$ is not transversal to O_j. Then:
— $(\Sigma^{(n)},E^{(n)})$ is the **minimal resolution surface** of C,
— $\{\Sigma^{(i)},E^{(i)},C^{(i)}\}_{i=0,\dots,n}$ is the associated **blow-up chain**.

Definition 3.2.12. Let C and C' be two real curve singularities such that they have **homeomorphic oriented blow-up chains**, that is:

1. for every i there exists a homeomorphism

$$h_i:(\Sigma^{(i)},E^{(i)},C^{(i)})\to((\Sigma')^{(i)},(E')^i,(C')^i)$$

such that it preserves the orientation on

$$\Sigma^{(i)}-E^{(i)}\simeq(\Sigma')^{(i)}-(E')^i;$$

2. there exists a homeomorphism
$$h : (\mathbb{R}^2, O) \to (\mathbb{R}^2, O)$$
sending each coordinate axis onto itself, preserving its orientation, and such that $C' = h(C)$;
3. the following diagram is commutative
$$\begin{array}{ccccc} (\Sigma^{(n)}, E^{(n)}, C^{(n)}) & \xrightarrow{\Phi_n} & \dots & \xrightarrow{\Phi_0} & (\mathbb{R}^2, O, C) \\ \downarrow h_n & & \downarrow h_i & & \downarrow h \\ ((\Sigma')^{(n)}, (E')^{(n)}, (C')^{(n)}) & \xrightarrow{\Phi_n} & \dots & \xrightarrow{\Phi_0} & (\mathbb{R}^2, O, C') \end{array}$$

Then C and C' are **combinatorially equivalent**.

Remark 3.2.13. In the previous Definition, the homeomorphism $h : (\mathbb{R}^2, O) \to (\mathbb{R}^2, O)$ preserves the orientation of $\mathbb{R}^2$.

3.2.2 Combinatorics of real curves

Definition 3.2.14. Let D be a disk and let $C_i \subset D$ be a real branch of a curve. Then $C_i - \{O\} = C_i^A \cup C_i^B$, are called **half-branches** of C_i.

We can consider the same construction for the x and the y axis. They are naturally oriented, so we can mark as X_+ and X_- the two intersection of the x axis with ∂D, where X_+ corresponds to the positive part of the axis. We can do the same for the y axis and obtain two intersection points Y_+ and Y_-.

Remark 3.2.15. We suppose that a real germ C is not oriented. This is why we don't speak about a positive half-branch and a negative one, but only about two different half-branches.

Definition 3.2.16. A word in $C_1, \dots, C_r, X_+, Y_+, X_-, Y_-$ such that:
— each letter C_i appears exactly twice;
— X_+, Y_+, X_-, Y_- appear each once, necessarily in this order;
— the first letter is X_+;
is the **characteristic order** $\mathcal{O}(C)$.

Let $C = C_1 \cup C_2 \cdots \cup C_r$ be a real germ. The **characteristic order of** C is the order of the intersection points of branches C_i with the boundary of the disk.

Example 3.2.17. The configuration of curves in Figure 3.8 has characteristic order
$$(X_+C_2C_4Y_+C_1C_5C_3X_-C_5C_3C_2Y_-C_1C_4).$$

Remark 3.2.18. Let us consider the two irreducible curves $C : \ y = x^{5/3}$ and $C' : \ y = -x^{5/3}$. C and C' have different characteristic orders
$$X_+CY_+X_-CY_-, \quad X_+Y_+CX_-Y_-C.$$

The curve singularities C and C' are combinatorially equivalent as complex germ, but not as real ones. A representation of this situation can be seen in Figure 3.9.

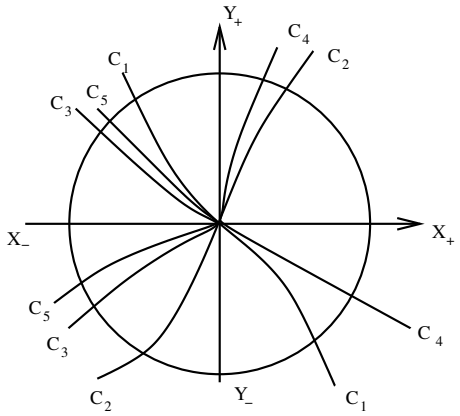

Figure 3.8 – A characteristic order.

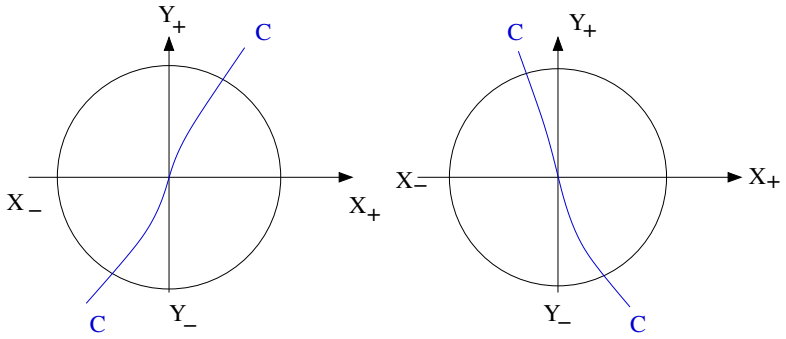

Figure 3.9 – Two branches with the same Puiseux characteristic, but with different characteristic orders.

Remark 3.2.19. The characteristic order is a manner to encode the way the branches meet at the only intersection point. When all the branches are smooth, the possible configurations have been studied by É. Ghys in [Ghy13].

The characteristic order is a way to encode the natural *dihedral order* on the half-branches of the union of C and of the coordinate axis, where:

Definition 3.2.20. A **dihedral order** on a finite set with at least three elements is a structure of combinatorial graph on it whose associated topological space is a circle. That is, each element has exactly two neighbours and, by starting at an arbitrary point, jumping to one of the neighbours and continuing to jump from neighbour to neighbour, one passes through all the elements of the set. One may represent a dihedral order on a given set by writing the sequence of elements obtained in this way.

Proposition 3.2.21. *Let C_1 and C_2 be real branches defined in a disk. Then on the boundary of the disk one has the dihedral order:*

— *$C_1C_1C_2C_2$ if and only if $C_1.C_2$ is even;*

— *$C_1C_2C_1C_2$ if and only if $C_1.C_2$ is odd.*

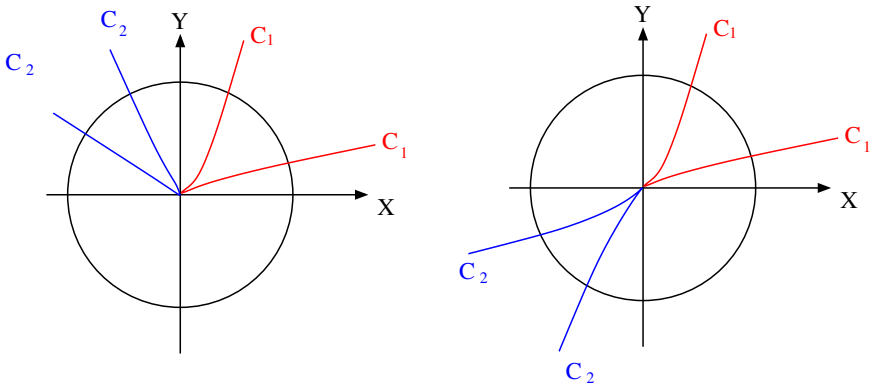

Figure 3.10 – Two different branches having the same pairwise dihedral orders.

Proof. The intersection number $C_1.C_2$ is the number of intersection points of deformations of C_1 and C_2 as complex curves. Let us consider then real deformations. Complex solutions are couples of conjugated points, so that the numbers of real and complex intersection points have the same parity.

Then let us consider the curve C_1. It divides the disk in two parts, and so it does with the disk boundary. Let $\tilde{C_1}$ be an arc on the boundary such that its endpoints are the intersection points of C_1 with the boundary of the disk. Then by Jordan's theorem, the set $C_1 \cup \tilde{C_1}$ is homeomorphic to a disk.

Let us suppose that $C_2 \in \tilde{C}$ and that $C_1.C_2$ is even. Then a point of intersection of C_2 with the boundary of the disk belongs to $\tilde{C_1}$. In fact, let suppose $\bar{C_1}$ and $\bar{C_2}$ are small real deformations of C_1 and C_2. Then $\bar{C_1}$ an $\bar{C_2}$ have even real intersections. Moreover, we can suppose, being the deformations small, that it doesn't change the dihedral order on the disk boundary. It is an easy remark then that on the disk boundary there is a dihedral order $C_1C_2C_2C_1$.

The same argument shows that if $C_1.C_2$ is odd then the dihedral order on the disk boundary is $C_1C_2C_1C_2$.

Let us suppose now that C_1 and C_2 are real curves such that the dihedral order on the boundary of the disk is $C_1C_1C_2C_2$. Let us consider the disk having boundary $C_1 \cup \tilde{C_1}$. Let us suppose that the two points of intersection of C_2 with the boundary of the disk don't belong to $\tilde{C_1}$. Then C_2 intersects C_1 an even number of time and the statement follows. □

Let us consider now n branches $C_1, \ldots, C_n$ defined in a disk and all $n(n-1)/2$ complex intersection numbers $C_i.C_j$. Therefore we know the associated dihedral order for every pair of branches.

Remark 3.2.22. It is possible to consider the x and y axes as branches, and consider $C.\{y = 0\}$ and $C.\{x = 0\}$.

The knowledge of the intersection numbers is not sufficient to understand the combinatorics of the curve. Let us suppose that we have two curves C_1, C_2 such that:

$$C_1.C_2 = 0,\ C_1.\{x = 0\} = 0,\ C_1.\{y = 0\} = 0,$$

$$C_2.\{x=0\}=0,\ C_2.\{y=0\}=0.$$

Then $X_+C_1C_1Y_+C_2C_2X_-Y_-$ and $X_+C_1C_1Y_+X_-C_2C_2Y_-$ are two characteristic orders satisfying the intersection conditions (see Figure 3.10).

3.3 Real resolution spaces

3.3.1 Surfaces and orientations

Let C a real curve singularity in a neighbourhood of $O \in \mathbb{R}^2$, $\mathbb{R}^2$ endowed with two oriented axes x, y and with the canonical orientation. We also define the **quadrants** as the canonical quadrants in $\mathbb{R}^2$.

Let $\Sigma^{(1)}$ be the surface obtained by blow up of the point $O \in \mathbb{R}^2$. The surface $\Sigma^{(1)}$ is a Möbius strip, as shown in Figure 3.11. It is important to remember that in the real case $\Sigma^{(1)} - E^{(1)}$ is oriented. The boundary is connected and oriented, and the map $\Sigma^{(1)} - E^{(1)} \to \mathbb{R}^2 - \{O\}$ is an analytical isomorphism. We can then naturally define the images of the quadrants on $\Sigma^{(1)}$. In the previous section, we have constructed some real surfaces by plumbing annuli and Möbius strips. We have seen that a fundamental property of the plumbing was that the components were locally oriented. We will now see that, in the case of real resolution surfaces, one may define canonical such orientations.

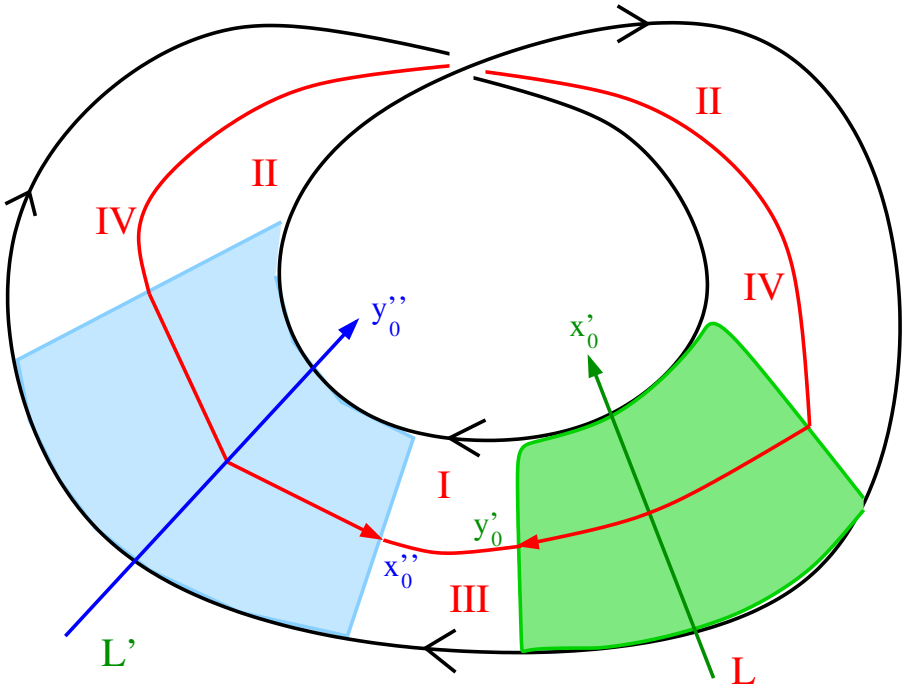

Figure 3.11 – The surface $\Sigma^{(1)}$.

We can notice that in this case the orientations are naturally given by the orientation of $\Sigma^{(1)} - E^{(1)}$. There are two different charts:

$$\begin{cases} x = x'_0 \\ y = x'_0 y'_0 \end{cases} \qquad \begin{cases} x = x''_0 y''_0 \\ y = y''_0 \end{cases} \tag{3.1}$$

Then we have two different local orientations on the exceptional components E_0. In fact, the image of the first quadrant is connected, and has as part of the boundary the $x-$axis and the $y-$axis.

We can remark that the image of the $x-$axis is present only in one of the charts. In particular, the x-axis is given by the equation $y = 0$. Then the x-axis in the new coordinates is given by $y'_0 = 0$. The other local coordinate on the chart is $x'_0 = 0$. Moreover, the component E_0 gives a coordinate axis in the chart, which is then $x'_0 = 0$, so that E_0 represents the y-axis in the local chart (x'_0, y'_0).

We can make the same remarks for the second chart. The y-axis is given by $x = 0$. In the new chart, it has coordinates $x''_0 = 0$. Moreover, the component E_0 represents a coordinate axis in the chart, which is then $y''_0 = 0$, so that E_0 represents the x-axis in the local chart. The points belonging to the first quadrant in the original disk have positive coordinates in both charts. The two local orientations of E_0, given by x'_0 and y'_0, are then one opposite to the other.

We can now recursively define the coordinate axis on every chart obtained by blow-up of points $O_i^{(l)} \in E \cup L \cup L'$.

Example 3.3.1. In Figure 3.12 we can see an example of a resolution space, with the data of the image of the quadrants.

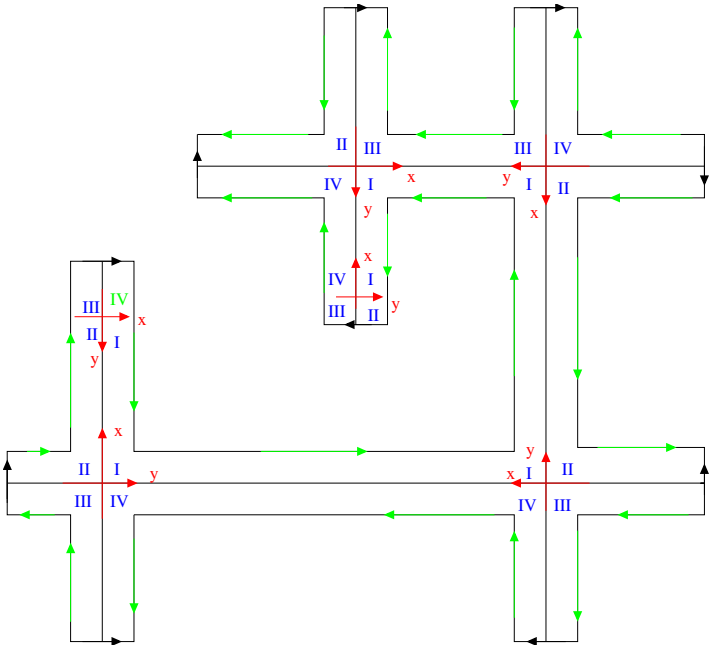

Figure 3.12 – An example of resolution space, enriched with local orientations and the images of quadrants.

Let us consider the blow up of a free point on the surface $\Sigma^{(1)}$. We can remark that $\Sigma^{(1)}$ is a Möbius strip, $E_0^{(1)}$ is homeomorphic to $\mathbb{RP}^1$ and moreover we can consider the images of the $x-$axis and of the $y-$axis. Their orientation determines the orientation on the boundary of the Möbius strip. We can see it in Figure 3.11. Moreover we have two different charts.

Remark 3.3.2. The translation of the x axis in the chart $(x, y) = (x_1, x_1y_1)$ gives a curvetta $(L')^1$.

We have now local systems of coordinates at the intersection points of E_0 with the x and y axis. By construction, those two different local orientations of the Möbius strip aren't globally compatible. So, when we blow up a free point on E_0 we need to do a canonical choice of a local chart, and also we need to have a canonical local choice of the orientations of the x and y-axis. We canonically choose the chart (x_1, y_1). We will then define a new coordinate system of a free point as a system of coordinate such that the origin is the point $(0, a)$ and the x-axis is translated in a parallel way in the chart. We can see this situation in Figure 3.13.

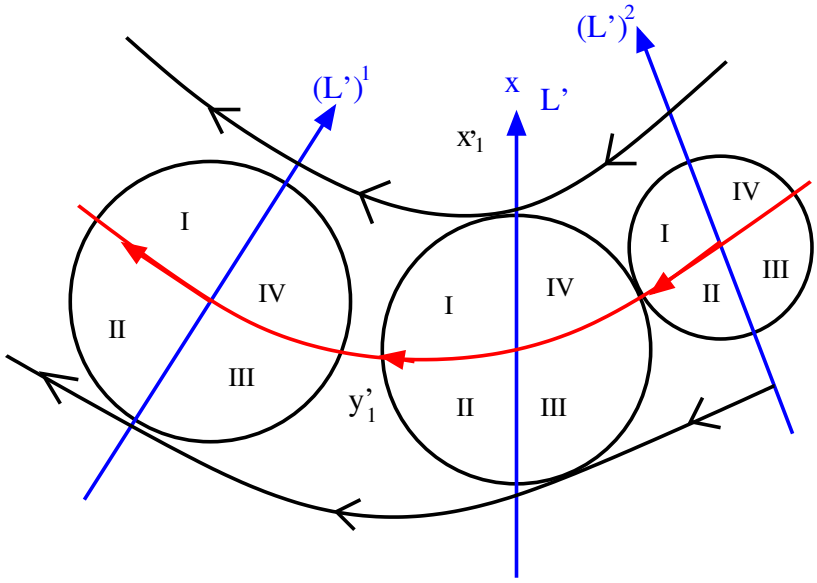

Figure 3.13 – Local coordinates for a smooth point.

Let us consider a $\mathbb{R}^2$ with the usual coordinate systems. We have seen that after blow up with centre the origin, on the resolution surface $\Sigma^{(1)}$ we can still define canonically quadrants. In general, if we consider a blow up $\Phi_{i+1} : \Sigma^{(i+1)} \to \Sigma^{(i)}$ such that the centres are only satellite points of $\check{E}^{(i)}$, we see at every cross a permutation of the quadrants in $\mathbb{R}^2$. We say that the quadrants of $\mathbb{R}^2$, are the **0-th level quadrants**.

At every cross, we can consider the *permutation* of the quadrants. We have seen in Proposition 1.4.30 that for every cross (E_i, E_j) we have a canonical way of ordering the cross, and that, by considering the two vectors $v_i \in \mathbb{N}^2$ and $v_j \in \mathbb{N}^2$, we consider the toric morphism (v_i^T, v_j^T), if E_i is the y-axis, and v_j is the x-one. Moreover, the vectors associated to L and L' are respectively $(1, 0)$ and $(0, 1)$. We can consider then the matrix

$A_{ij} \in M_2(\mathbb{N})$ associated to the cross (E_i, E_j). We can consider the reduction modulo 2 of the coefficients of the matrix. With abuse of notation, we will still call it $A_{ij} \in M_2(\mathbb{F}_2)$. As we will see also in Section 4.2.2, we can consider a function $sign(x) : \mathbb{R}^* \to \mathbb{F}_2$ such that:

$$\begin{cases} sign(x) = 0 & if\ x > 0 \\ sign(x) = 1 & if\ x < 0. \end{cases} \tag{3.2}$$

In this way, it is natural to associate:

1. the vector $(0, 0)$ to the first quadrant;
2. the vector $(1, 0)$ to the second quadrant;
3. the vector $(1, 1)$ to the third quadrant;
4. the vector $(0, 1)$ to the fourth quadrant.

Let us consider the multiplication of $A_{ij} \cdot v$, where $v \in \mathbb{F}^2$. Then the image of the points of the quadrant in $\mathbb{R}^2$ associated to v in the chart (E_i, E_j) are contained in the quadrant of (E_i, E_j) associated to $A_{ij} \cdot v$.

Remark 3.3.3. We obtain as matrices A_{ij} all the matrices of the group $GL_2(\mathbb{F}_2)$. This group is non-commutative and has 6 elements, which means that it is isomorphic to S_3.

Let us now consider the blow up at a centre a smooth point $O_i \in \check{E}_h \subset \Sigma^{(j)}$. Then locally the localization of $\check{E}_h$ is a smooth frame, so that in a neighbourhood of O_i there are points belonging to only two 0-quadrants. To complete the coordinate system, we add a curvetta L_i, so that the new coordinate system is (L_i, E_h). Moreover, we can consider the quadrants of this coordinate system. We will say that they are 1**-st level quadrants**. Then in the neighbourhood of every singular point of $\check{E}^{(j+1)} \subset \Sigma^{(j+1)}$, either there are 0-th level quadrants, or there are 1-st level quadrants. Recursively, we can speak about 2-nd, 3-rd, ..., i-th quadrants.

In general, let us suppose that $O_j \in E_h$ is a smooth point of $\check{E}$. In a neighbourhood of O_j the points are images of two i-th level quadrants. By completion of $E_h|_{O_j}$ to a cross, we introduce the $(i + 1)$-th level quadrants.

Definition 3.3.4. Let O_i be an infinitely near point. We can consider a new system of oriented coordinates (x_i, y_i) in a neighbourhood of O_i. In the local system of coordinates we can define new quadrants, that we call **local quadrants** at O_i.

Remark 3.3.5. Let $O_i \in E_h$ be a smooth point of $\check{E}$. Then we add a curvetta L_i, so that (L_i, E_h) is a local system of coordinates. We call the quadrants of the chart whose axis are L_i and E_h the local quadrants. For every point $O_h \preceq O_i$, the image of a local quadrant at O_i is contained in a local quadrant at O_h. We will call it the **associated local quadrant**.

Remark 3.3.6. Let $O_i^{(l)}$ be a smooth point of $\check{E}^{(l)}$. Then in its neighbourhood there are two quadrants of the j-th coordinate system, and four quadrant of the $(j + 1)$-th coordinate system. Then each couple of quadrants of the $(j + 1)$-th coordinate system is a subset of a quadrant of the j-th coordinate system. By the chosen convention, the first and fourth quadrant form the first couple, while the second and third quadrant form the second one.

Let us recall now the notion of log-discrepancy of an exceptional component E_i. We will see below that its parity has a real topological interpretation (see Proposition 3.3.10).

Definition 3.3.7. Let (Σ, O) be a germ of a smooth surface, and let $\pi_{E_i} : (\Sigma', E) \to (\Sigma, O)$ be a morphism such that E_i appears among the components of E. Let ω be a non-zero holomorphic 2-form on (Σ, O).

The **log-discrepancy** $\lambda(E_i)$ of E_i is defined as:

$$\lambda(E_i) = 1 + ord_{E_i}(\pi_{E_i}^*(\omega)).$$

The log-discrepancy of a branch C is $\lambda(C) = 1$.

Proposition 3.3.8. *Let O_i be an infinitely near point of O. Then:*

1. $\lambda(E_0) = 2$;
2. $\lambda(E_i) = \lambda(E_j) + \lambda(E_k)$, *if O_i satellite, $O_i = E_j \cap E_j$;*
3. $\lambda(E_i) = \lambda(E_j) + 1$, *if $O_i \in E_j$ is a free point.*

Proof. Let us consider the blow-up π_O with centre the origin:

$$\begin{cases} x = u \\ y = uv \end{cases} \tag{3.3}$$

In the local chart, E_0 has coordinates $u = 0$. Moreover:

$$\pi_O^*\omega = u\ du \wedge dv,$$

which implies $\lambda(E_0) = 1 + ord_{E_0}(\pi_O^*(\omega)) = 2$.

Let $O_i = E_j \cap E_k$ be a satellite point. Let us suppose that in the local chart (u, v), E_j is defined by $u = 0$, while E_k is defined by $v = 0$. Moreover, let:

$$\pi_{E_j}^*\omega = \Theta(u, v)\ u^{\lambda(E_j)-1}v^{\lambda(E_k)-1}du \wedge dv,$$

where $\Theta(u, v)$ is a unity. We can consider the blow up π_{O_i} with centre O_i:

$$\begin{cases} u = \tilde{u} \\ v = \tilde{u}\tilde{v} \end{cases}$$

Then:

$$(\pi_{E_j} \circ \pi_{O_i})^*\omega = \Theta(\tilde{u}, \tilde{u}\tilde{v})\ \tilde{u}^{\lambda(E_j)-1}(\tilde{u}\tilde{v})^{\lambda(E_k)-1}\tilde{v}\ d\tilde{u} \wedge d\tilde{v} =$$
$$= \Theta(\tilde{u}, \tilde{u}\tilde{v})\ \tilde{u}^{\lambda(E_j)+\lambda(E_k)-1}\tilde{v}^{\lambda(E_k)-1}d\tilde{u} \wedge d\tilde{v} =$$

which implies $\lambda(E_i) = \lambda(E_j) + \lambda(E_k)$.

Let us now suppose that $O_i \in E_j$ is a free point. Let us suppose that, in local coordinates (u, v), E_j has equation $u = 0$. Then:

$$\pi_{E_j}^*\omega = \Theta(u, v)\ u^{\lambda(E_j)-1}du \wedge dv,$$

where $\Theta(u, v)$ is a unity. We can consider the blow up π_{O_i} with centre O_i, to obtain:

$$(\pi_{E_j} \circ \pi_{O_i})^*\omega = \Theta(\tilde{u}, \tilde{u}\tilde{v})\tilde{u}^{\lambda(E_j)-1}\tilde{u}\ d\tilde{u} \wedge \tilde{v} =$$

$$= \Theta(\tilde{u}, \tilde{u}\tilde{v})\ \tilde{u}^{(\lambda(E_j)+1)-1}d\tilde{u} \wedge d\tilde{v}.$$

Therefore, $\lambda(E_i) = \lambda(E_j) + 1$.

□

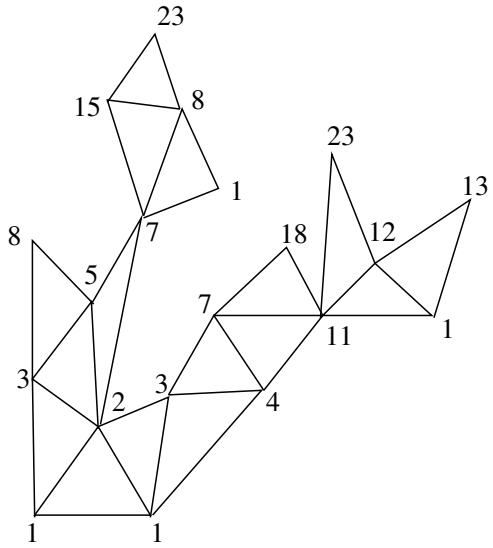

Figure 3.14 – Log-discrepancy computed via the lotus.

Let us consider the lotus $\mathcal{L}$ associated to a resolution $\pi : (\Sigma, E) \to (\mathbb{C}^2, O)$. Let E_i be a node of the lotus, E_i' and E_i'' the vertices of its basis. From the previous Proposition, one sees that one has always :

$$\lambda(E_i) = \lambda(E_i') + \lambda(E_i'').$$

This way of computing the log-discrepancies on the lotus has been described in [BPPP14]. We can see an example in Figure 3.14.

Definition 3.3.9. Let (Σ, O) be a germ of a smooth surface, and let $\pi_{E_i} : (\Sigma', E) \to (\Sigma, O)$ be a a morphism such that E_i appears among the components of E. Then E_i is **orientable** if the lift to $(\Sigma'_{\mathbb{R}}, E_{\mathbb{R}})$ of the orientation of $(\Sigma_{\mathbb{R}}, O)$ canonically orients every arc of E_i having as endpoints 2 singular points of $E_{\mathbb{R}}$, as the boundary of each one of its sides (see Figure 3.15). In the following we will only need the notion of orientable, and not the associated orientation.

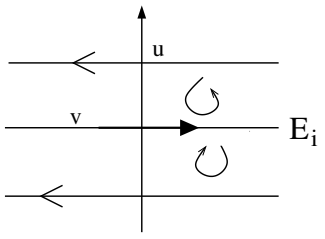

Figure 3.15 – An orientable component.

Proposition 3.3.10 (P. Popescu-Pampu)**.** *An exceptional component E_i is orientable if and only if $\lambda(E_i)$ is even.*

Proof. Let us consider a neighbourhood of a point of E_i which is smooth on E. Let us suppose that E_i is defined by $u = 0$. The local expression of $\pi^*_{E_j}\omega$ is:

$$\pi^*_{E_j}\omega = \Theta(u, v)u^{\lambda(E_i)-1}du \wedge dv.$$

The exceptional component E_i is orientable if and only if the sign of $\Theta(u, v)u^{\lambda(E_i)-1}$ changes for $u > 0$ and $u < 0$ (see Figure 3.15). This happens if and only if $\lambda(E_i) - 1$ is odd, that is, if and only if $\lambda(E_i)$ is even. □

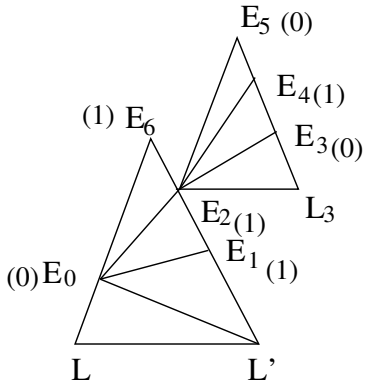

Figure 3.16 – A lotus enriched with the orientabilities w_i.

Definition 3.3.11. We define the **orientability** $w_i \in \mathbb{F}_2$ of an exceptional component E_i as the reduction modulo 2 of the log-discrepancy:
— $w_i = 0$ if λ_i is even;
— $w_i = 1$ if λ_i is odd.

Let us now consider a graph of necklaces, such as we have defined in the previous section. We want now to use this construction to effectively define the graph of necklaces for the real resolution spaces.

We will see in the next section how to enrich the lotus in such a way that it becomes an invariant for real singularities and how to use this information to explicitly construct the resolution space.

Proposition 3.3.12. *Let us consider a resolution surface Σ and a point O_k. Then:*
— *If $O_i \in E_j$ is a free point, then $p_i = 1$, $w_i = w_j + 1$. Moreover, if p'_j is the parity of E_j after the blow up of O_i, $p'_j = p_j + 1$.*
— *If $O_i \in E_j \cap E_k$, then $p_i = 1$, $w_i = w_j + w_k$. Moreover, $p'_j = p_j + 1$, $p'_k = p_k + 1$.*

Proof. A proof of the assertions concerning the parity can be found in [KK99]. The statement about the orientability w_i is proven in Proposition 3.3.8

□

Definition 3.3.13. Let Γ be a the directing tree of a graph of necklaces, assumed to be a tree, enriched with the orientability w_i.

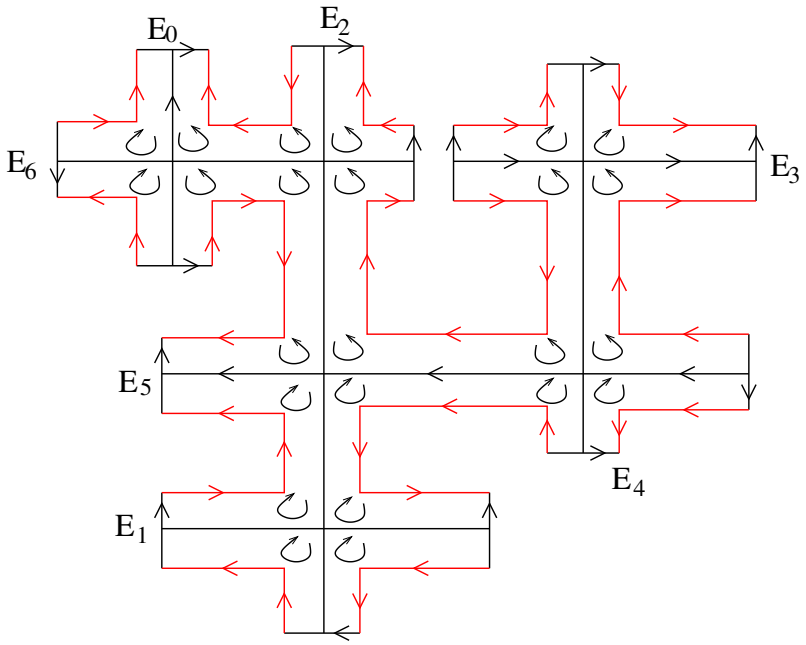

Figure 3.17 – The resolution surface associated to the lotus of Figure 3.16

A **free addition** of a vertex E_{n+1} to $\Gamma = \{E_1, \ldots, E_n\}$ is an addition of a vertex E_{n+1} adjacent to a vertex E_k.

A **satellite addition** of a vertex E_{n+1} to $\Gamma = \{E_1, \ldots, E_n\}$ is the addition of a vertex E_{n+1} such that we delete the edge between two vertices E_i and E_j and E_{n+1} is adjacent to both E_i and E_j.

Addition or subtraction of vertices respecting these properties and the conditions of Proposition 3.1.7 are called **elementary tree movements**.

Proposition 3.3.14. *Let Γ and Γ' be directing trees of necklaces such that it is possible to pass from Γ to Γ' by a sequence of elementary tree movements, or their inverses. Then* $\det(I) = \det(I')$.

We remember that we are considering the matrices to be reduced modulo 2.

Proof. Adding a free vertex gives a new matrix I' such that

$$\det(I') = \det \begin{pmatrix} a_{11} & \cdots & a_{1,n} & 0 \\ a_{21} & \cdots & a_{2,n} & 0 \\ \vdots & \vdots & \vdots & \vdots \\ a_{n,1} & \cdots & a_{n,n}+1 & 1 \\ 0 & \ldots & 1 & 1 \end{pmatrix} =$$

$$= \det \begin{pmatrix} a_{11} & \cdots & a_{1,n} & 0 \\ a_{12} & \cdots & a_{2,n} & 0 \\ \vdots & \vdots & \vdots & \vdots \\ a_{n,1} & \cdots & a_{n,n} & 0 \\ 0 & \cdots & 0 & 1 \end{pmatrix} = \det(I).$$

Adding a satellite vertex gives a new matrix such I' such that

$$\det(I') = \det \begin{pmatrix} a_{11} & \cdots & a_{1,n-1} & a_{1,n} & 0 \\ a_{12} & \cdots & a_{2,n-1} & a_{2,n} & 0 \\ \vdots & \vdots & \vdots & \vdots & \\ a_{n-1,1} & \cdots & a_{n-1,n-1}+1 & a_{n,n-1}+1 & 1 \\ a_{n,1} & \cdots & a_{n-1,n}+1 & a_{n,n}+1 & 1 \\ 0 & \cdots & 1 & 1 & 1 \end{pmatrix} =$$

$$= \det \begin{pmatrix} a_{11} & \cdots & a_{1,n-1} & a_{1,n} & 0 \\ a_{12} & \cdots & a_{2,n-1} & a_{2,n} & 0 \\ \vdots & \vdots & \vdots & \vdots & \\ a_{n-1,1} & \cdots & a_{n-1,n-1} & a_{n,n-1} & 0 \\ a_{n,1} & \cdots & a_{n-1,n} & a_{n,n} & 0 \\ 0 & \cdots & 0 & 0 & 1 \end{pmatrix} = \det(I).$$

□

Definition 3.3.15. Let Σ be a surface. A **blow down** operation is the contraction of a component E_i such that:

1. $p_i = 1$;
2. E_i intersects at most 2 exceptional components E_j and E_k;
3. $w_i = w_j + w_k$, or $w_i = w_j + 1$ if E_i is transversal to only one exceptional component.

Moreover, after contraction of E_i, the two transversal components E_j and E_k change their parity.

Proposition 3.3.16. *Let Σ be a locally oriented circle configuration such that it is possible to blow down at every step an exceptional component. Moreover, let us suppose that the last exceptional component we contract is E_i, such that $w_i = 0$. Then the surface is a real resolution of the disk.*

Proof. The first surface obtained by blowing up a disk is an oriented Möbius strip. Then all other components are obtained by blow up of points.

□

Remark 3.3.17. Given a surface there are in general different ways of blowing it down. An easy example is given by the surface given in Figure 3.18.

We can contract the exceptional components in two different orders. At least two different resolutions are compatible with that surfaces, and they are the result of two different blow-up sequences. In particular, the one on the left is obtained by blowing up a free point on E_0 and later two satellite points $E_0 \cap E_1$ and $E_1 \cap E_2$, while the one on the right is obtained by blowing up two free points on E_0 and another free point on E_2.

We end this section by analysing the properties of the graph of necklaces associated to a real resolution surface.

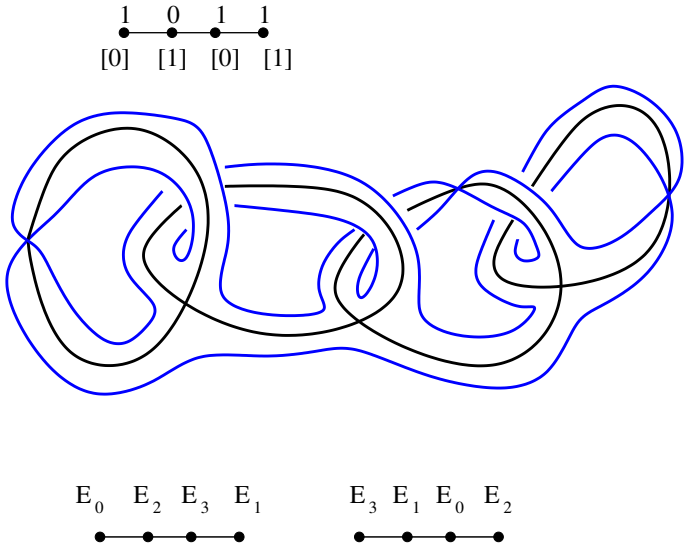

Figure 3.18 – A surface having different blow-down sequences.

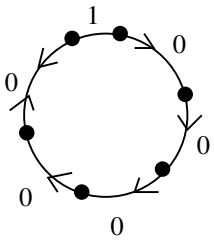

Figure 3.19 – A necklace of an exceptional component of a resolution surface.

Lemma 3.3.18. *Let E_i be a necklace with $n+1$ beads θ^1, θ^2, …, θ^n, θ^{n+1}, such that $E_i \in \Gamma$, Γ graph of necklaces associated to a resolution space Σ. Let us suppose that θ^i and θ^{i+1} are consecutive beads, for all $i = 1, \dots, n$, and that θ^{n+1} and θ^1 are also consecutive beads. Then:*

- *for $i = 1, \dots, n$, the local orientation at θ^n is oriented toward θ^{i+1};*
- *the arc $[\theta^i, \theta^{i+1}]$ has local parity 0;*
- *if we consider the triple $(\theta^n, \theta^{n+1}, \theta^1)$, the local orientation at θ^{n+1} is oriented toward θ^n;*
- *the parity p_i depends only on the local parity of the arc $[\theta^{n+1}, \theta^1]$.*

Proof. The exceptional component E_i is obtained by blow-up of $O_i = E_j \cap E_k$. Then we have seen that in the two charts centred at $E_i \cap E_j$ and $E_i \cap E_k$ the local orientations of E_i are opposite. Without loss of generality, we can associate to the exceptional component E_k the bead θ^{n+1}, and to the exceptional component E_j a bead $\theta^{j'}$, $j' \in \{1, 2, \dots, n\}$.

Let us now consider the blow-up of $n-1$ smooth points $O_h \in E_i$. Let (E_j, E_i) be the chart such that $x = 0$ is the exceptional component E_i. Then each exceptional component E_h belongs to the chart (E_j, E_i), and it is such that, in local coordinates, E_i is the y-axis. To each one of those E_h we associate a bead $\theta^{h'}$. By the choice of the orientations,the local orientation at $\theta^{h'}$ is directed toward $\theta^{h'+1}$. Moreover, the orientation of the fibres T^i

are such that they are the translation, on the local chart, of the orientation of the fibre $T^{j'}$. Then the local parity $p_{h'} = 0$, for all $h' = 1, \ldots, n$. Then the parity p_i depends only on the local parity of the arc $[\theta^{n+1}, \theta^1]$.

□

We can now see why Figure 3.6 is not a real resolution surface. In fact, if we look at the necklace E_4, we see that the two beads are such that they have opposite orientations, but the arc containing the two local positive orientations has parity 1.

3.3.2 The real lotus

Definition 3.3.19. Let C be a real plane curve singularity and let $\mathcal{L}$ be the lotus associated to its complexification. The **canonical orientation of the lotus** is such that:

1. the edge $[L', L]$ is oriented from L' to L;
2. the edge $[L_h, E_i]$ is oriented from L_h to E_i;
3. let us consider the i-petal, and let us suppose that its base $[E_{i_1}, E_{i_2}]$ is oriented from E_{i_1} to E_{i_2}. Then the edge $[E_{i_1}, E_i]$ is oriented from E_{i_1} to E_i, while the edge $[E_i, E_{i_2}]$ is oriented from E_i to E_{i_2} (see Figure 3.20);
4. The interior of the petal is oriented such that the orientation induced on its boundary is opposite to the one of its base.

We will say that a lotus, endowed with its canonical orientation, is an **oriented lotus**.

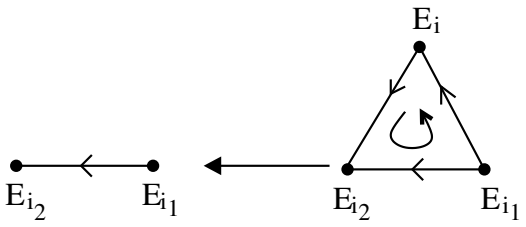

Figure 3.20 – An oriented petal.

We define the **canonical embedding** of the lotus $\mathcal{L}$ in $\mathbb{R}^2$ as the unique embedding, up to isotopy, which preserves the orientations of each petal of $\mathcal{L}$. We leave to the reader the easy proof of the fact that the previous definition of canonical embedding of the lotus is well-defined.

An example of the canonical embedding is shown in Figure 3.21.

Proposition 3.3.20. *Let $\mathfrak{L}$ be a triangular lotus. Let:*
- *C_1 be attached to the (-1) node E_n;*
- *C_2 and C_3 be attached to nodes E_{n_2}, E_{n_3}, such that $E_{n_1}, E_{n_2} \in$ the segment $[L', E_n]$, and $n_1 < n_2$;*
- *C_4 and C_5 be attached to nodes E_{n_4}, E_{n_5}, such that $E_{n_4}, E_{n_5} \in$ the segment $[L, E_n]$, and $n_4 < n_5$.*

Moreover, let us suppose that a half-branch of C_j, $j = 1, \ldots, 5$ belongs to the first quadrant in $\mathbb{R}^2$. Then in the first quadrant there is a dihedral order $L', C_2, C_3, C_1, C_5, C_4$.

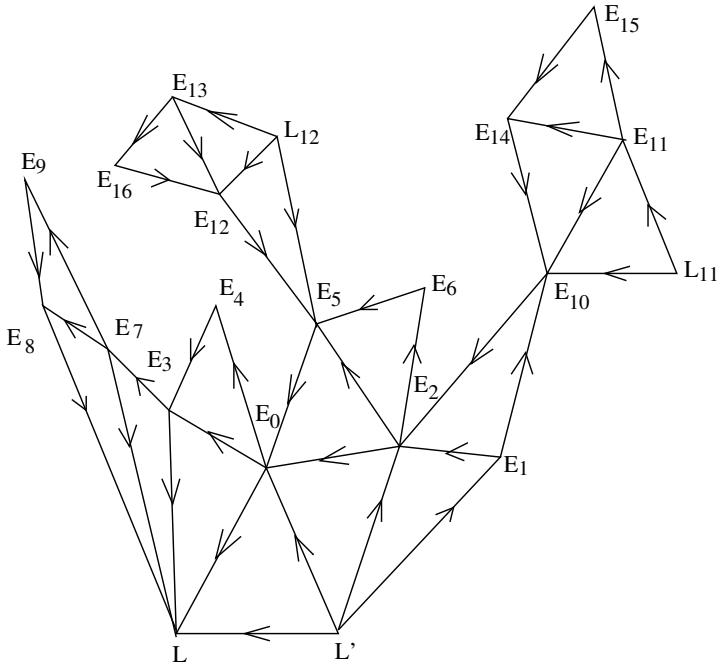

Figure 3.21 – An oriented lotus, canonically embedded in the plane.

Proof. We have seen in Proposition 1.4.20 that there is a bijection between the triangular loti and the rational numbers λ. Moreover, the structure of the triangulation is given by the continued fraction of λ.

Let λ_i be the rational number associated to the lotus. Let A_j, $j = 0, \ldots, n$ be the characteristic points of λ (see Definition 1.3.9). Moreover, there is a bijection between the sequence of characteristic points $(A'_1, \ldots, A)$ and the nodes belonging to the line $[L', E_n]$, where $A'_0 = L'$, $\ldots$, $A = E_n$ and such that if A_i, A_j, $i < j$ are associated to nodes E_{n_i}, E_{n_j}, then $n_i < n_j$.

In the same way, there is a bijection between the sequence of characteristic points $(A''_0, A''_1, \ldots, A)$ and the nodes belonging to the line $[L, E_n]$, where $A''_0 = L$, $\ldots$, $A = E_n$ and such that if A_i, A_j, $i < j$ are associated to nodes E_{n_i}, E_{n_j}, then $n_i < n_j$.

Moreover, in Proposition 1.3.7 we have proved that:

— if λ' is the number associated to a characteristic point A', and if λ'' is the number associated to a characteristic point A'', then $\lambda'' < \lambda'$;

— if λ'_1 and λ'_2 are the numbers associated to characteristic points A'_{n_1}, A'_{n_2}, such that $n_1 < n_2$, then $\lambda'_1 > \lambda'_2$;

— if λ''_1 and λ''_2 are the numbers associated to characteristic points A''_{n_1}, A''_{n_2}, such that $n_1 < n_2$, then $\lambda'_1 < \lambda'_2$;

— if λ', λ, λ'' are the numbers associated to A'_i, A_n, A''_j, then $\lambda'' < \lambda < \lambda'$.

Now, we remember that if a branch C_i is attached to a node E_j, then it has equation $y = x^{\lambda_j}$. Moreover, if $C_{i'}$ is another curve, $C_{i'}$ attached to a node $E_{j'}$, and if $\lambda_j < \lambda_{j'}$, then we have an order on the first quadrant $L', C_{j'}, C_j, L$.

The Proposition then follows from all those remarks. □

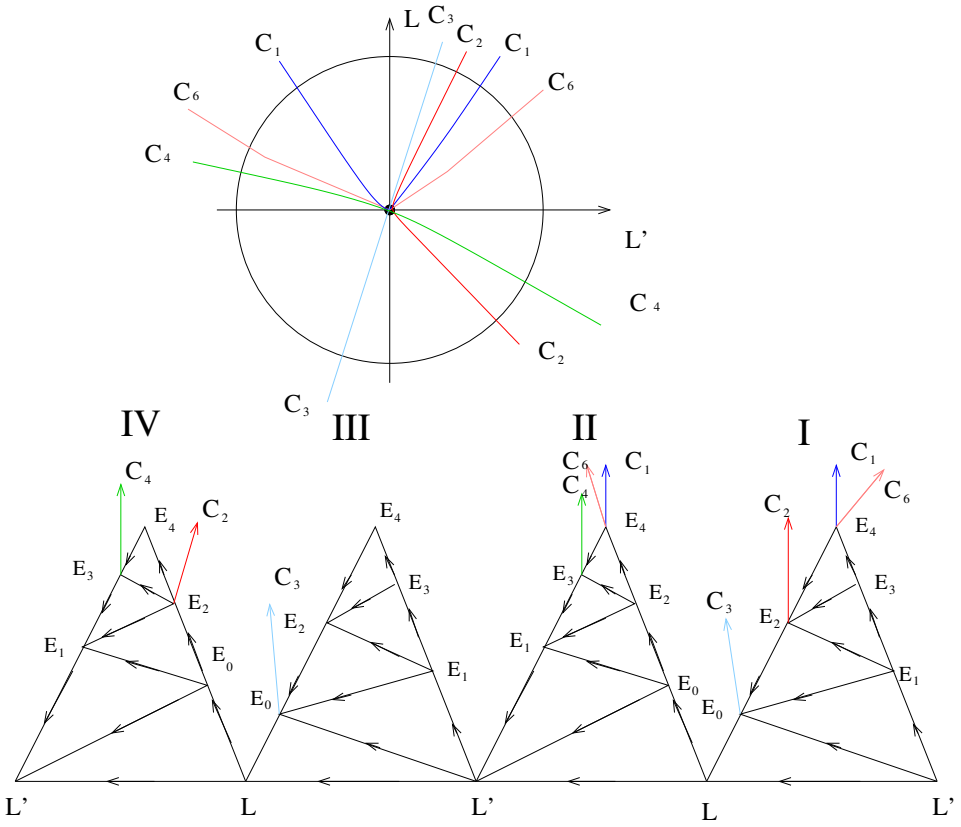

Figure 3.22 – An example of real simple lotus of a curve singularity having 6 branches.

Let now consider four copies of the simple lotus. We consider one of them oriented in the way we stated in the previous paragraph. We embed the second one in such a way that the two vertices L of the two different loti are identified. Moreover, we orient the base from L to L' and we propagate this orientation as in the previous case. We can remark that the orientations of the internal petals are compatible with the orientation of the plane.

We can now enrich it with the data of irreducible curves. We remember that to any configuration of real curves we can associate its characteristic order. The real lotus has an orientation that is compatible with the orientation of the disk, and L' and L represent respectively the x and the y axis.

Let C_i be a branch such that C_i is transversal to E_j. We want to attach the two

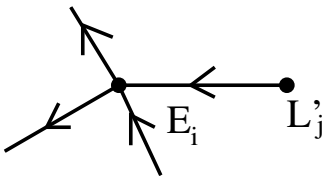

Figure 3.23 – The real completion of a smooth frame to a cross.

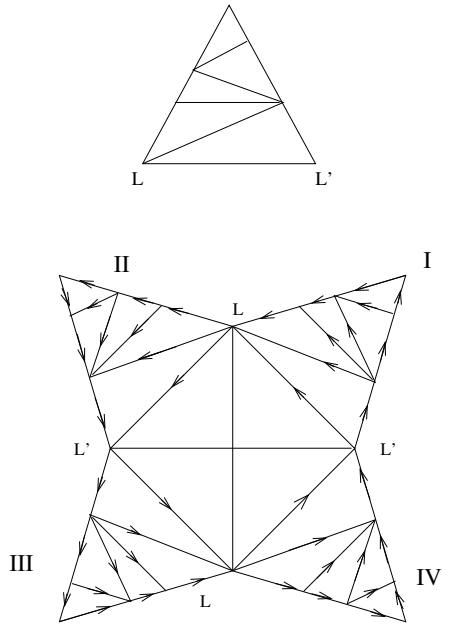

Figure 3.24 – The real lotus.

half-branches C_i^A and C_i^B to two different nodes E_j. With abuse of notation, we will call both of them C_i.

We can then associate to every one of the four loti one of the quadrants of the disk. Then the orientation on the lateral edges gives an orientation compatible with the orientation of ∂D. We will use the convention shown in Figure 3.24.

Now we know that a half-branch (or a half-curvetta) is contained in a quadrant. Then we consider it as attached to the node E_j in the lotus corresponding to that quadrant. If more than one half-branch is attached to the same node, we will see that we can order them via the local orientation of the node and the characteristic order of C. First we need some definitions.

Definition 3.3.21. Let C be a real curve singularity such that a lotus of its complexification is a simple lotus. Let us consider two copies $\mathcal{L}_1$, $\mathcal{L}_3$ of the oriented embedded lotus, and two mirror images of it, $\mathcal{L}_2$ and $\mathcal{L}_4$. Then the **real lotus** is such that:

1. for $i = 1, 3$, we identify $L \in \mathcal{L}_i$ with $L \in \mathcal{L}_{i+1}$;
2. we identify $L' \in \mathcal{L}_2$ with $L' \in \mathcal{L}_3$, and $L' \in \mathcal{L}_4$ with $L' \in \mathcal{L}_1$;
3. the order of curves and curvettas is induced by the order of the germs in the plane.

We say that the lotus $\mathcal{L}_i$ is the lotus associated to the i-th quadrant.

Remark 3.3.22. Let $\mathcal{L}'$ be an oriented simple lotus. The boundary of the associated real lotus $\mathcal{L}$ is oriented and homeomorphic to a circle.

Definition 3.3.23. Let C be a real curve singularities, such that $\mathcal{L}$ is an associated simple lotus. The **lotus order** is the order of the half-branches on the oriented boundary of the real lotus.

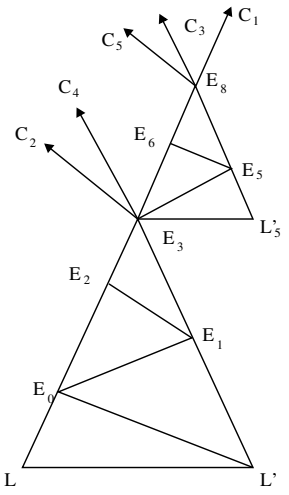

Figure 3.25 – The lotus for the complexification of the curve singularity of Example 3.3.27

Proposition 3.3.24. *Let C be a real curve singularity, and let $\mathcal{L}$ be the associated real lotus. Then the characteristic order of C and the lotus order coincide.*

Proof. If two half-branches are attached to different nodes E_i and E_j the order is correct because of Proposition 3.3.20.

If two half-branches belongs to the same quadrant and are attached to the same node E_i, then they are ordered via the local ordering at E_i.

□

Example 3.3.25. The curve C shown in Figure 3.22 has canonical order

$$(X_+, C_6, C_1, C_2, C_3, Y_+, C_1, C_6, C_4, X_- C_3, Y_-, C_2, C_4).$$

We need to understand what happens in the case of blow up of additional free points, such that they don't belong to components L and L'. The construction for the simple lotus is well defined because on the resolution space we can well define the images of the four quadrants. We need then a tool for defining it in the more general case.

In the new system of coordinates, if $O_i \in E_h$ is a smooth point, then we add a curvetta L_i, and we obtain a frame (L_i, E_h). The orientation is then compatible to the one associated to the previous lotus.

We remark that we are considering the $(i+1)$-th quadrants. Moreover, each time we blow-up a free point, a couple of $(i+1)$-th quadrants is included in a i-th quadrant. By the choice of the coordinates, the two couples are given by the first and fourth quadrant, and by the second and third one. By induction, we can define a real lotus for any real curve singularity.

Remark 3.3.26. In general, we can take as new axis any smooth curve transversal to the strict transform and to E. We have chosen to take as element of the new frame the transversal obtained by the change of coordinates in the toric space.

Example 3.3.27. Let us consider the following real germs:

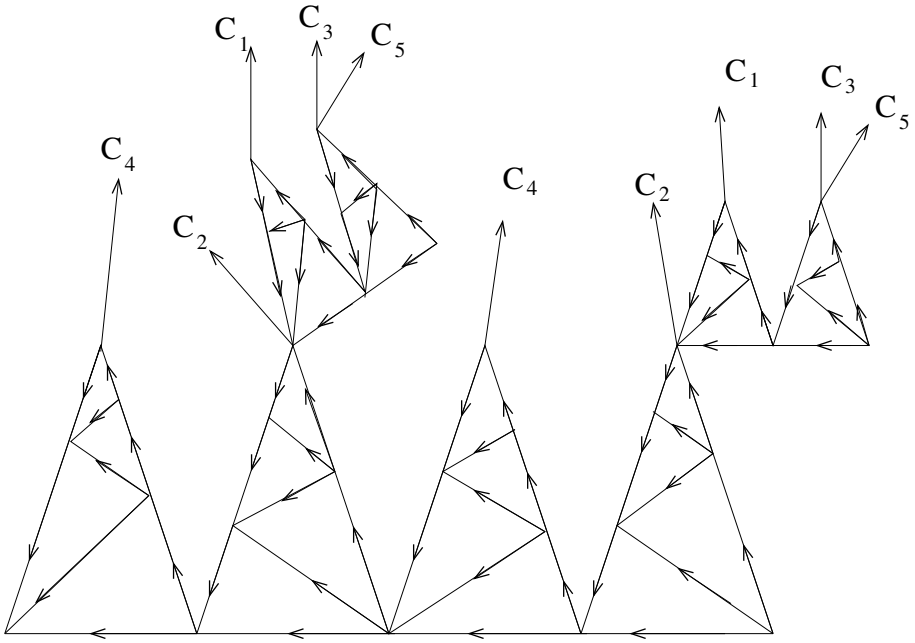

Figure 3.26 – The real lotus for the curve singularity of Example 3.3.27

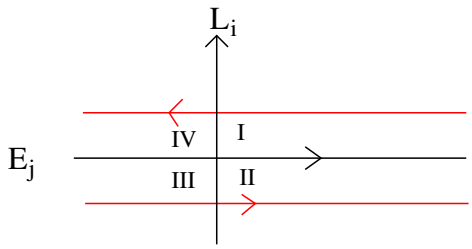

Figure 3.27 – The coordinates for a non-oriented component.

— $C_1 : \ y = x^{5/3} + x^{11/6}$
— $C_2 : \ y = 2x^{5/3}$
— $C_3 : \ y = x^{5/3} - x^{11/6}$
— $C_4 : \ y = -x^{5/3}$
— $C_5 : \ y = x^{5/3} - 2x^{11/6}$

The associated complex lotus can be seen in Figure 3.25 and the real lotus in Figure 3.26.

Let us now suppose that C is a branch, $(m; \beta_1, \ldots, \beta_{n+1})$, $n \geq 1$, its Puiseux characteristic. There are then n different system of coordinates, one for each lotus of the decomposition of the lotus $\mathcal{L}$ in simple loti. For each simple lotus we can consider the real lotus, well defined in the local coordinates. We want now to give a rule for patching together the different real loti.

Let us suppose that E_j is a non-oriented component, and $O_i \in E_j$ is a smooth point of $\check{E}$. We can see this situation in Figure 3.27. In the local coordinates (u, v), where $v = 0$ is L_i and $u = 0$ corresponds to E_j, we have four local quadrants. Moreover, if $u > 0$ we have

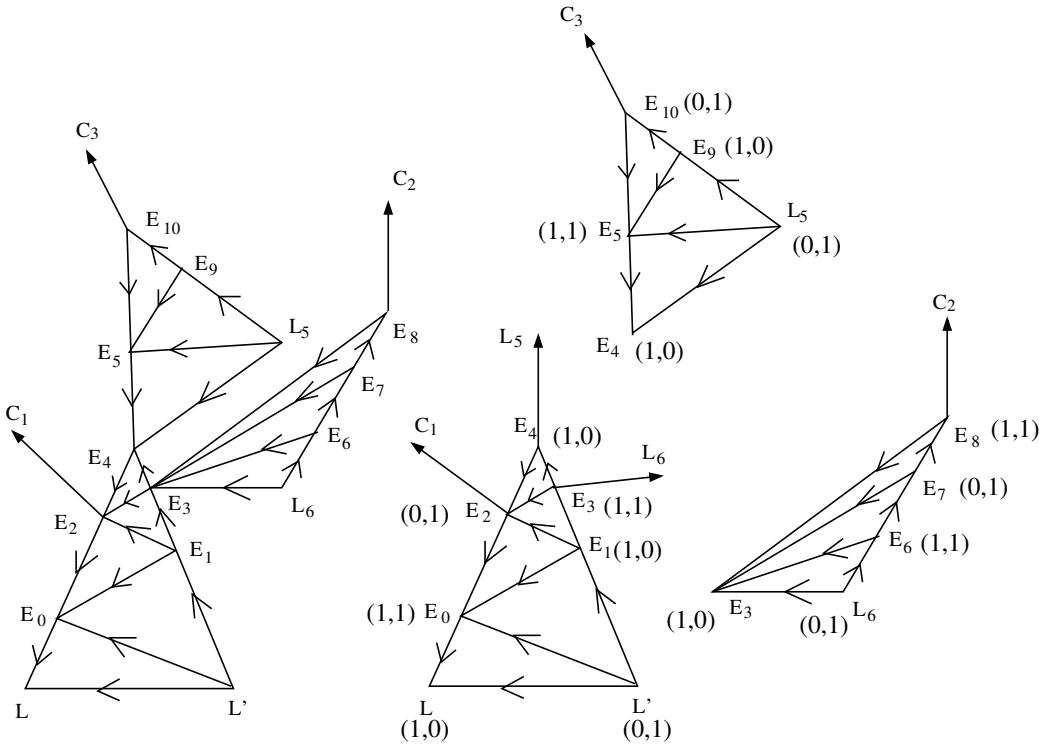

Figure 3.28 – The lotus of Example 3.3.28 and its decomposition.

the first and fourth quadrant, while if $u < 0$ we have the second and third one. The chart is endowed with its orientation, but it also has the global orientation of the complement of the exceptional divisor in the surface. We can then consider the lotus associated to one quadrant alone. It has basis (L_i, E_j). We know now to which lotus it has to be attached, i.e., the lotus associated to the quadrant in which it is contained. Moreover, we attach it in such a way that the orientation of each petal is preserved. We attach the lotus of the second quadrant of the petal by respecting the orientations of the petals, and by respecting the orientation on the boundary of the lotus, which is isomorphic to the orientation of the surface.

The case of an oriented component is exactly the same, it is only important to be more careful about the orientations.

Example 3.3.28. Let us consider a real curve singularity such that the lotus of its complexification is the lotus shown in Figure 3.28. In the same Figure, we also show the decomposition of the lotus in simple loti.

Let us now focus on the simple lotus having basis L and L'. We can notice that there are attached the branch C_1 and two curvettas L_5 and L_6 respectively to the nodes E_2, E_3 and E_4. To understand the local situation at a neighbourhood of the branch and of the curvettas, we need to study the matrices $A_{2,4}$, $A_{3,1}$ and $A_{4,3}$. They are:

$$A_{2,4} = \begin{pmatrix} 0 & 1 \\ 1 & 0 \end{pmatrix} A_{3,1} = \begin{pmatrix} 1 & 1 \\ 1 & 0 \end{pmatrix} A_{4,3} = \begin{pmatrix} 1 & 1 \\ 0 & 1 \end{pmatrix} \tag{3.4}$$

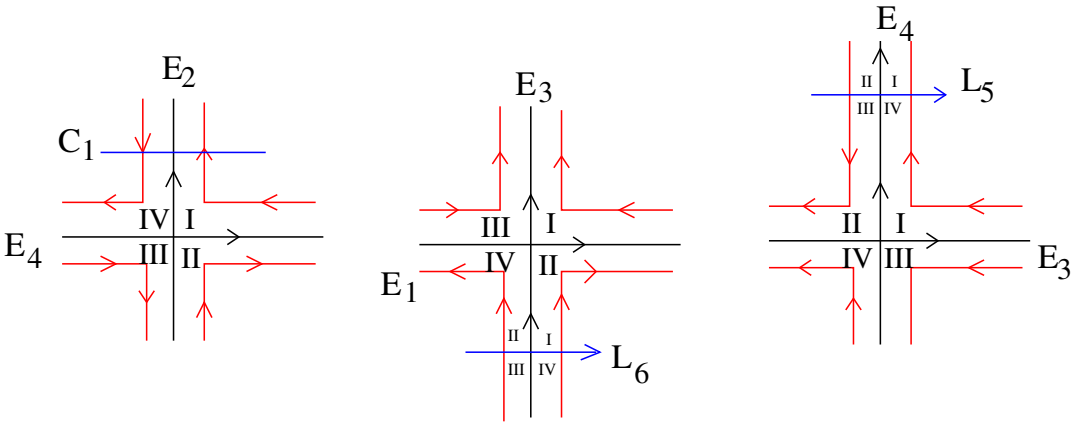

Figure 3.29 – The local coordinates of the resolution space of the curve singularity of Example 3.3.28.

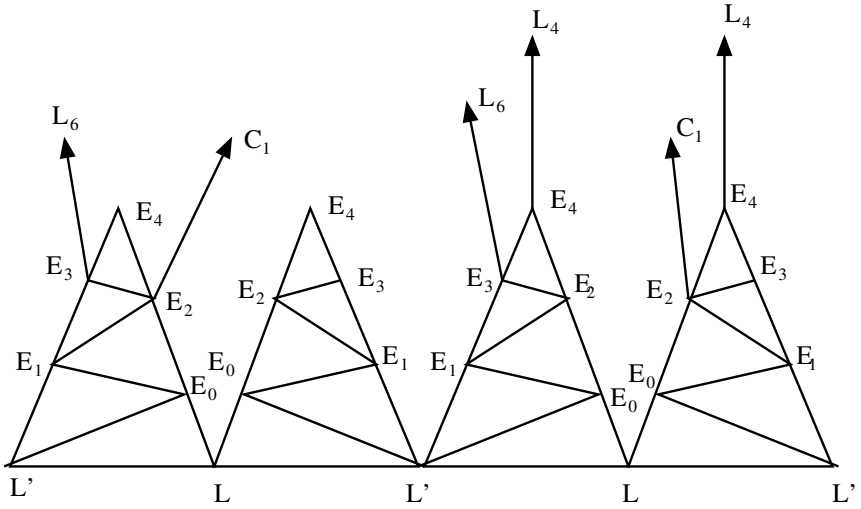

Figure 3.30 – The real lotus.

Then their inverses are:

$$B_{2,4} = \begin{pmatrix} 0 & 1 \\ 1 & 0 \end{pmatrix} B_{3,1} = \begin{pmatrix} 0 & 1 \\ 1 & 1 \end{pmatrix} B_{4,3} = \begin{pmatrix} 1 & 1 \\ 0 & 1 \end{pmatrix} \tag{3.5}$$

Locally, we have the three different situations shown in Figure 3.29. We can easily compute that the only oriented components of the simple lotus are E_0 and E_3. As we have seen, by knowing the orientation in the neighbourhood of the first quadrant, which is canonical, we can compute the orientation in the neighbourhood of every satellite point $E_i \cap E_j$. The real lotus of this simple lotus is then shown in Figure 3.30. We can now compute the two cases for the two different sets of 1-st coordinates. For the simple lotus having basis L_5, E_4, we obtain that the associated matrix and the inverse matrix of the

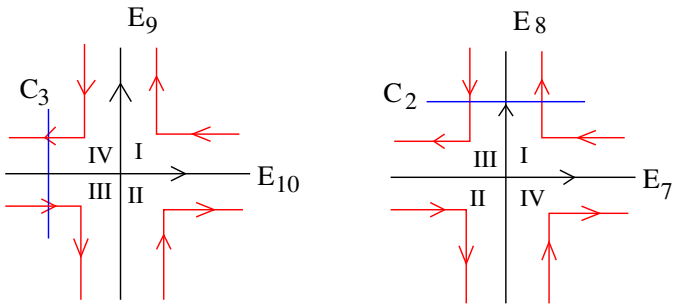

Figure 3.31 – The 1-st level coordinates.

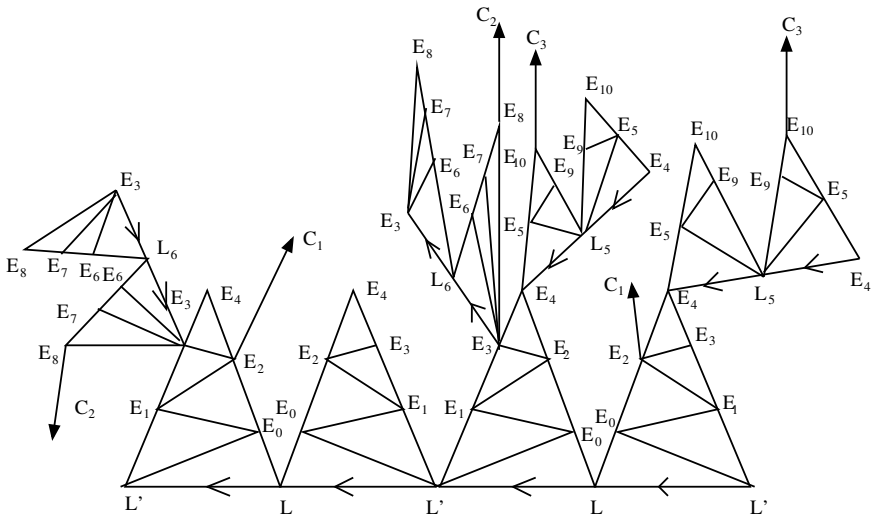

Figure 3.32 – The real lotus of the curve singularity of Example 3.3.28

chart (E_9, E_{10}) are:

$$A_{10,9} = \begin{pmatrix} 0 & 1 \\ 1 & 0 \end{pmatrix} = B_{10,9}. \tag{3.6}$$

Instead, for the simple lotus having basis L_3, E_6, we obtain that the associated matrix and the inverse matrix of the chart (E_7, E_8) are:

$$A_{8,7} = \begin{pmatrix} 1 & 0 \\ 1 & 1 \end{pmatrix} = B_{8,7} \tag{3.7}$$

The two local situations are then shown in Figure 3.31. The consequent real lotus is shown in Figure 3.32.

Theorem 3.3.29. *Two real germs C and C' have the same combinatorial type relative to a fixed crossed constellation if and only if the associated real loti are isomorphic.*

Proof. If two real germs C and C' have the same combinatorial type relative to a fixed crossed constellation, then for every i their resolution surfaces $\Sigma^{(i)}$ and $\Sigma'^{(i)}$ are homeomorphic. Then the associated real loti are necessarily isomorphic.

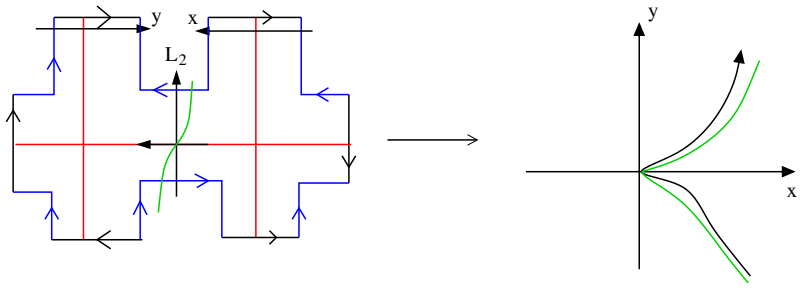

Figure 3.33 – A non-positive branch.

Let us suppose that two real germs C and C' have the same real loti. Then the complexification of C and C' have the same topological type. Moreover, the real lotus gives information on the i-th quadrants to whom the strict transforms $C^{(l)}$ and $C'^{(l)}$ belong. If the real loti are isomorphic, then the resolution surfaces $\Sigma^{(l)}$ and $\Sigma'^{(l)}$ are necessarily isomorphic, which implies that C and C' have the same combinatorial type relative to a fixed crossed constellation.

□

Definition 3.3.30. Let C be a branch and let $\mathcal{P}$ be the associated crossed constellation. For every free point O_{i_j}, $j = 1,\dots, n$, we consider a new system of coordinates. We say that C is a **positive branch** if:

— for every i, $C^{(i)}$ has a half-branch contained in the local first quadrant;

— the first quadrant of the $(j+1)$-th coordinate system is contained in the first quadrant of the j-th coordinate system, for $j = 0,\dots, n$.

Let C be a real curve singularity. The curve C is a **positive curve singularity** if and only if all its branches are positive branches.

Example 3.3.31. The curve $y^3 = -x^5$ is not a positive curve.

Another example is shown in Figure 3.33. In this case, the branch doesn't pass in the first quadrant in the local coordinates defined for the blow-up of a free point.

Proposition 3.3.32. *Let C be a complex curve singularity. Then there exists at least one real positive germ whose complexification has the same topological type as C.*

Proof. We have seen that the sequence of infinitely near points of the embedded resolution process of C is an invariant of singularity, and that we can naturally speak of positive part in the case of a real resolution surface. It is then sufficient to take all smooth points in the resolution to belong to the positive part, and consider, for each branch, a half-branch belonging to the positive part.

□

We will now see that the real lotus can be simplified in the case of a *positive germ*.

Lemma 3.3.33. *Let C be a positive branch. Then the real lotus of C is determined by the lotus of the complexification of C.*

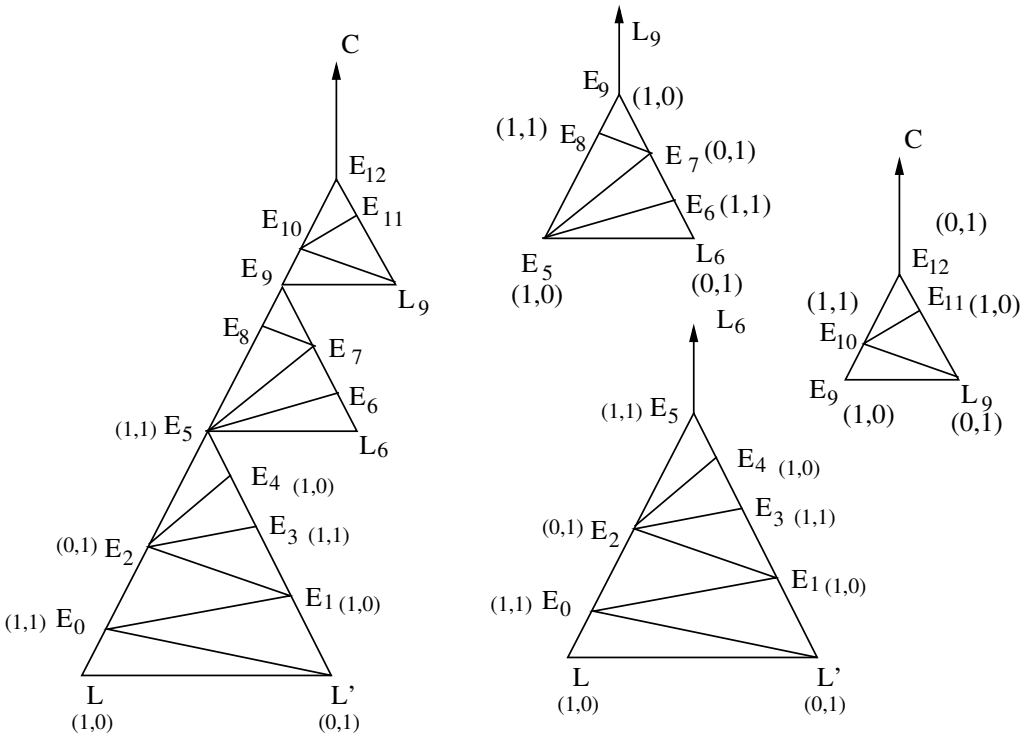

Figure 3.34 – The lotus of a positive branch.

Proof. Let us consider the lotus $\mathcal{L}$ of the complefixication of C. We can endow it with the orientation from L' to L, and from L_h to E_i, for every curvetta L_h. From the hypothesis that C is a positive germ, we have that the strict transform $C^{(l)}$ has a half-branch belonging to the local first quadrant. Moreover, all curvettas L_h intersect the local first quadrant. Then the oriented lotus $\mathcal{L}$ is isomorphic to the the subset of the real lotus corresponding to the first quadrant. For every node, we know the relative position of all other quadrants relative to the first one. Then we can compute the position of the second half-branch of $C^{(l)} \subset \Sigma^{(l)}$, $\forall\ l = 1, \ldots, N$.

□

Example 3.3.34. Let C be a positive germ having Puiseux characteristic $(70; 110, 114, 117)$. The lotus of the complexification is shown in Figure 3.34. We have that the matrix associated to the chart (E_5, E_4) is:

$$A_{5,4} = \begin{pmatrix} 1 & 1 \\ 1 & 0 \end{pmatrix} \tag{3.8}$$

By hypothesis, the curvetta L_9 has a half-branch belonging to the first quadrant. From the fact that E_5 is the y axis in the chart (E_4, E_5), and that L_6 it is transverse to E_5, we have that the second half branch passes through the second local quadrant. This implies that the position of L_6 in $\mathbb{R}^2$ is given by $A_{5,4} \cdot (1, 0)^T = (1, 1)^T$, so that it belongs to the third quadrant.

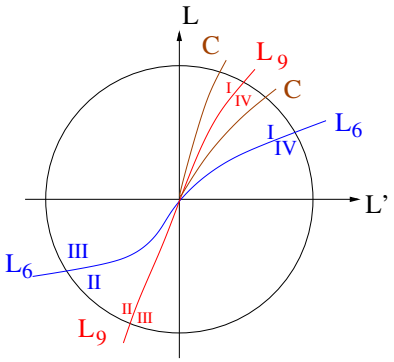

Figure 3.35 – The image in the plane of the curve $C : y = x^{110/70} + x^{114/70} + x^{117/70}$ and of its associated curvettas.

We can compute, respectively in the 1-st and 2-nd coordinates, the images of the second half-branches of L_9 and C. We obtain:

$$A_{9,7} = \begin{pmatrix} 1 & 0 \\ 0 & 1 \end{pmatrix}, \quad A_{12,11} = \begin{pmatrix} 0 & 1 \\ 1 & 0 \end{pmatrix} \tag{3.9}$$

Then the images second half-branches of L_9 and C belong respectively to $A_{9,7} \cdot (1,0)^T = (1,0)^T$ and $A_{12,11} \cdot (1,0)^T = (0,1)^T$, that is, the second quadrant of the 1-st coordinates and the fourth quadrant of the 2-nd coordinates.

We remember that the component E_5, so that the disk intersects in order the fourth, first, third and second quadrant of the first-coordinates. Therefore the union of L, L', L_6, L_9, C is (as it is shown in Figure 3.35):

$$(L',\ L_6,\ C,\ L_9,\ C,\ L,\ L',\ L_6,\ L_9,\ L).$$

Theorem 3.3.35. *Let C be a positive curve singularity. Then the real lotus of C is determined by the lotus of the complexification of C, enriched with a local ordering of the arrowheads and curvettas attached to the same node E_i.*

Proof. We have proved in Lemma 3.3.33 that the theorem is true for a branch. Moreover, we have seen in Section 1.4 that the lotus of a curve singularities is given by the identification of the loti of its singular branches. Then if there exists no node E_i such that there is only one arrowhead or curvetta attached, then the construction is already well defined.

We need only to understand the case of two arrowheads attached to a same node. From the fact that we can always consider simple loti, the same happens if one of the two arrowheads is a curvetta L_h. Let us then consider two different arrowheads C_1 and C_2, attached to the same node E_i. The images of the associated branches in the first quadrant have naturally an order, given by L', C_1, C_2, L. We remember that the lotus has been oriented, and that this orientation is compatible with the orientation of the first quadrant on $\mathbb{R}^2$. It is then sufficient to orient the two arrowheads in the same way as the two branches C_1 and C_2 in the plane. Moreover, by symmetry arguments, we know the relative orientations of C_1 and C_2 in all the other three quadrants.

□

Chapter 4

A'Campo deformations for real curve singularities

Chapter Overview

This Chapter consists of two different sections, Section 4.1 and Section 4.2. In Section 4.1 we recall A'Campo's algorithm of deformation of singularities, and some general results about deformations. We see in Section 4.1.1 that in the case of real curve singularities we obtain many different deformations. Moreover, we also see that if C and C' are real curve singularities such that they do not have the same combinatorial type, but their complexifications do, then the associated divides are not homotopic. In Section 4.1.2 we give some results about *marked points* (Definition 4.1.2). We see that in a certain sense, the marked points describe the topological type of the complexification of C (Corollary 4.1.8). In Section 4.1.3 we introduce the notion of *multi-loops* (Definition 4.1.10) and we give some general results about divides (Proposition 4.1.13).

In Section 4.2 we study an easier class of divides, the *canonical divides* (Definition 4.2.1 in Section 4.2.1), which are defined for *positive curve singularities*. Moreover, we consider the results obtained in Proposition 4.1.13 in the particular case of canonical divides (Proposition 4.2.4). We also see how to enrich the real lotus of a positive curve singularity to study its canonical divide. In Section 4.2.2 we restrict to study the relative position of multi-loops in the case of a *simple lotus* (Definition 1.4.27). We prove in the end Theorem 4.2.35, that gives a characterization of canonical divide of a positive real curve singularities, such that the associated lotus is a simple lotus. The general case of a positive real curve singularity is given in Section 4.2.3, Theorem 4.2.46.

4.1 Divides

4.1.1 A'Campo's algorithm

We want now to come back to A'Campo's deformation algorithm, which we have already described in Section 2.1. We recall that it is a method involving a sequence of translations and of contractions of the exceptional components having (complex) self-intersection -1. After each step of the deformation, we get a curve which intersects

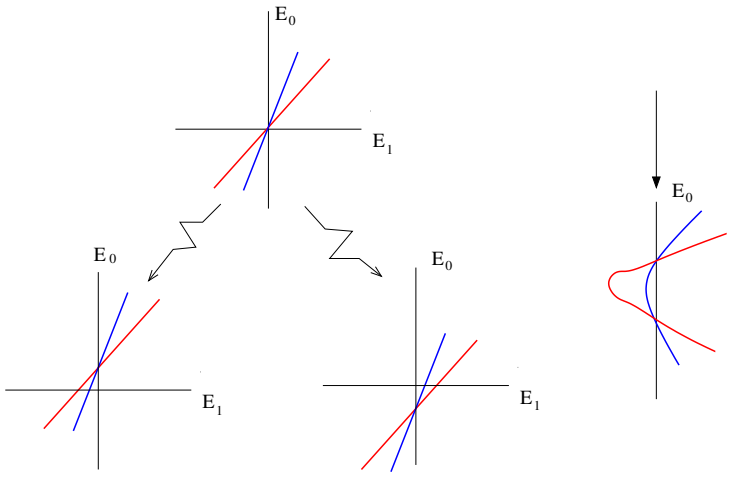

Figure 4.1 – Different deformations may give different divides. (1)

transversally all exceptional components having self-intersection -1. More precisely, it is a translation of the parametrized curve in the local charts along one of the two axis. An important difference is that now we want to consider real curve singularities. This case is combinatorially far richer than the complex case. In fact, we will have to consider the local order of the branches in $\mathbb{R}^2$. Moreover, while $\mathbb{C} - \{O\}$ is connected, $\mathbb{R} - \{O\}$ is not, so that the signs of the coefficients in the Puiseux series expansion of the singular curve are also important. In the following those signs will be hidden, because we will take a topological point of view.

Moreover, in the real case, at each step we have two ways of deforming the parametrized curve, one in the positive direction and one in the negative one. For a branch such that $E_0, \ldots, E_n$ are the exceptional components of its minimal embedded resolution space, we obtain at most 2^n different divides. This maximum is computed by considering that for every component E_i, $i = 0, \ldots, n-1$, there are 2 different possibilities for the translation, while the strict transform is not deformed on the component E_n.

In the case of branches which admit a Puiseux series having only characteristic monomials, endowed with positive coefficients, Schulze-Röbbecke described the topology of a special A'Campo divide (see [SR77]). We extend his result to arbitrary topological types of complex curve singularities, by defining *positive* representatives and associated *canonical* A'Campo divides. When we found this description, we did not know Schulze-Röbbecke's result, which we learned afterwards from Ebeling. We would like to mention that following Schulze-Röbbecke's work, there were not even formulations of conjectures about the description of A'Campo divides of *reducible* singularities.

Example 4.1.1. We consider the deformation of the singular real curve $(y^2-x^3)(y^2-2x^3) = 0$. We can see in Figure 4.1 and Figure 4.2 that we obtain two different divides.

Those are then all the deformations we can have for this singular curve. Let us see now what happens if we consider the curve $(y^2 - x^3)(y^2 + x^3) = 0$. We can obtain a different deformation from the previous one (see Figure 4.3), even if the two singular curves have the same combinatorial type when seen as complex germs.

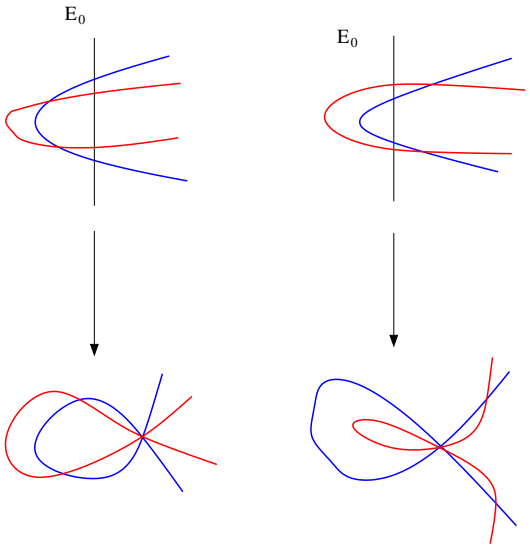

Figure 4.2 – Different deformations may give different divides. (2)

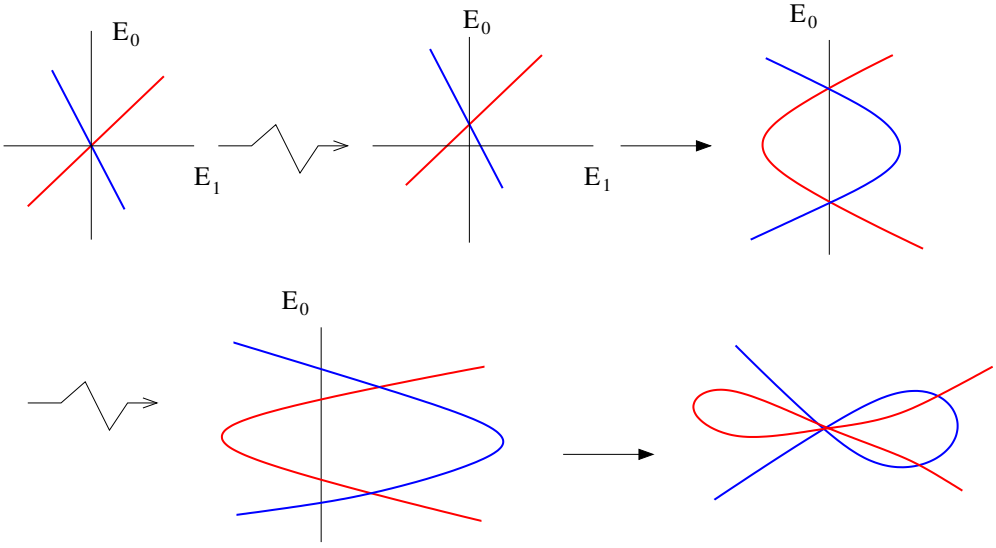

Figure 4.3 – Same complex topology with different real topology.

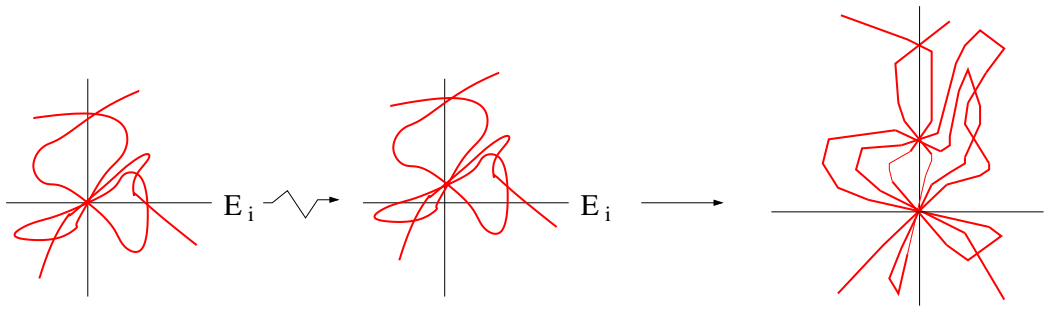

Figure 4.4 – An example of contraction.

4.1.2 Marked points

We will consider now the A'Campo process as defined in [A'C74] and [A'C75] and recalled in Section 4.1.1.

Definition 4.1.2. Let C be a real positive curve. The **marked point** $P_i(\underline{s})$ of a curve $C(\underline{s})$ is the point obtained by contraction of the exceptional component E_i.

Remark 4.1.3. By A'Campo algorithm we obtain at every step a family of curves $C^{(l)}(\underline{s}) := C^{(l)}(s_{l+1}, \ldots, s_n)$ where s_{l+1}, $\ldots$, s_n are real parameters. In the end, we obtain a family of curves $C(\underline{s}) = C(s_0, \ldots, s_n)$. We also obtain a family of points $P_i(\underline{s})$. In the following, we will drop the dependency on the parameter, and write just P_i for $P_i(\underline{s})$, and $C^{(l)}$ for $C^{(l)}_s$. With an abuse of notation, we will indicate by P_i also a point $O_i = P_i(0)$.

Lemma 4.1.4. *At a marked point P_i, the curve is locally the union of a finite number of pairwise transverse smooth branches.*

Proof. Let E_i be a (-1) component of the surface $\Sigma^{(l)}$. The translation of $C^{(l)}$ is such that $C^{(l)} \cup E_i$ has only normal crossings. Moreover, the two points $E_i \cap E_j$ and $E_i \cap E_k$ do not belong to $C^{(l)}$ (we remember our convention, $j = p_D(i)$ and $k = p_I(i)$).

The restriction of $C^{(l)}$ to a tubular neighbourhood of E_i is then the union of a finite number of smooth curves, intersecting E_i transversally in different points. Now we remember that E_i is the set of directions of lines in the tangent planes of $S^{(l-1)}$ at O_i.

Therefore the contraction of E_i gives a finite number of curves which are smooth and pairwise transversal (see Figure 4.4). □

Definition 4.1.5. Let P_i be a marked point. The number of smooth branches pairwise transversal at P_i is the **multiplicity** of the marked point P_i.

We want to compute the multiplicity of each marked point P_i. The marked point P_i is obtained as the contraction of the exceptional component E_i. In the complex case, the number of intersection points of the deformation of $C^{(l)}$ with E_i is exactly the multiplicity m_i. This happens to be the same for the real case, as we show in Lemma 4.1.6.

Lemma 4.1.6. *Let C be a singular curve, E_i an exceptional component and m_i the multiplicity of C at O_i. Then the marked point P_i is locally the intersection of m_i smooth pairwise transversal real branches.*

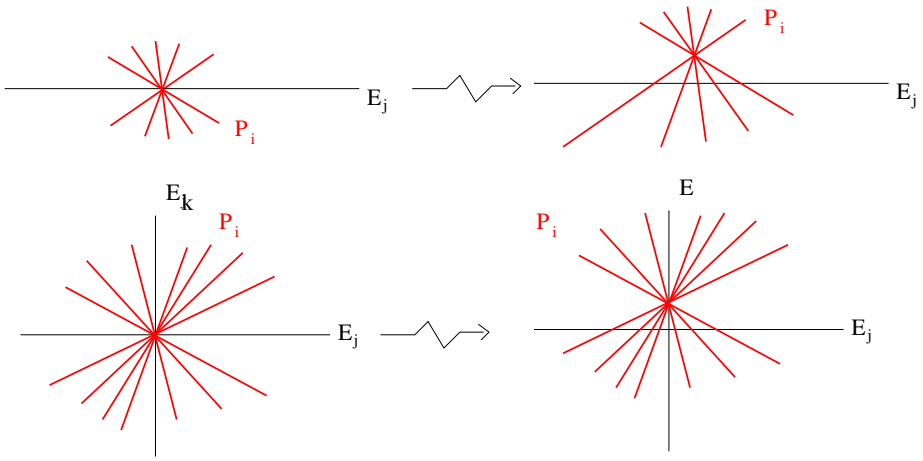

Figure 4.5 – Example of deformations at free and satellite points.

Proof. Let $C_r^{(l)}$ be a branch of $C^{(l)}$, $C_r^{(l)} \cup E$ has only normal crossings, and $C_r^{(l)}$ intersecting the exceptional component E_i. Clearly $C_r^{(l)}$ intersects E_i in a point. We proceed now by induction.

Let O_i be a free point, $j = p_D(i)$. After deformation, the point P_i belongs to the exceptional component E_j. Let us suppose that P_i has multiplicity $p_i \in \mathbb{N}$. A translation of $C^{(l)}$ is such that $P_i \notin E_j$. Moreover, by symmetry, we add p_i points of intersection between $C^{(l)}$ and E_j. After deformation the point P_i does not belong any more to the exceptional locus E. Then the point P_i is not involved any more in the process of deformation and contraction.

Let now O_i be a satellite point, $j = p_D(i)$, $k = p_I(k)$. Then $P_i \in E_j \cap E_k$. Let us suppose that the multiplicity of P_i is p_i We consider a first deformation of $C^{(l)}$, such that $P_i \in E_k$, $P_i \notin E_j$. Then, by symmetry reasons, the deformation of $C^{(l)}$ intersects E_j in p_i points. We can remark that, after deformation, P_i becomes a smooth point of E_k, so we can make the same considerations as for the free points. We get then also p_i intersection point of $C^{(l')}$ with E_k.

A point P_i is obtained by contraction of the exceptional component E_i. Its multiplicity p_i is then equal to the number of intersection points of the deformation of the strict transform of the curve $C^{(l)}$ with E_i. We have shown that this number is $\sum_{j':i=p_D(j')} p_{j'} + \sum_{k':i=p_I(k')} p_{k'} + c_i$, where c_i is the number of branches of C that are transversal at E_i. This formula is exactly the same formula used to compute the multiplicity m_i of E_i. Then $p_i = m_i$.

□

Remark 4.1.7. The marked points P_i are of two different types. Some points are singular points of the divide, and some are smooth points. The marked singular points are determined by the topology of the divide, in contrast to the smooth ones, which do not have a topological characterization.

Corollary 4.1.8. *Let $\tilde{C}$ be an A'Campo divide of a reducible curve $C = C_1 \cup \cdots \cup C_r$. Let $\mathcal{E}(C_l) = \{P_i \mid P_i \in C_l\}$ be the set of marked points P_i such that the branch C_l passes*

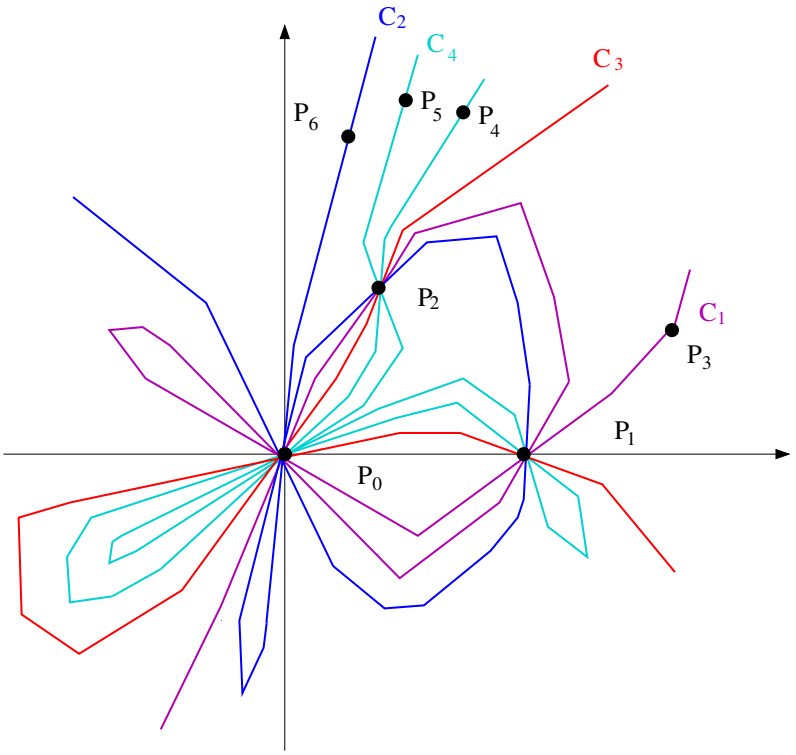

Figure 4.6 – An example of a deformation for the curve singularity of Example 4.1.9

through P_i. Then the data of the multiplicities m_i and of the sets $\{\mathcal{E}(C_l)\}_{l=1,\dots,r}$ determines the complex combinatorial type of C.

Proof. We have seen that the multiplicity of P_i is $m_i = mult_{O_i}(C)$. Moreover, $m_i = m_i^1 + m_i^2 + \cdots + m_i^r$, where $m_i^l = mult_{O_i}(C_l)$, the multiplicity of the branch C_l at O_i. For every branch C_l we can consider the associated lotus $\mathcal{L}_l$, where we consider a node E_i as corresponding to the exceptional component E_i, whose contraction gives P_i. The lotus of the curve C is then given as the union of the loti for all the branches, gluing the petals having the same labels. □

Example 4.1.9. Let us consider the A'Campo divide shown in Figure 4.6. The resolution space of the associated curve has 7 different exceptional components $E_0, E_1, \dots, E_6$. Moreover, $\mathcal{E}(C_3) = \{P_0, P_1, P_2\} \subset \mathcal{E}(C_l)$, for $l = 1, 2, 4$.

The multiplicities of the curve at the points $O_0, \dots, O_6$ are:

$$(m_0, m_1, m_2, m_3, m_4, m_5, m_6) = (12, 6, 5, 1, 1, 1, 1).$$

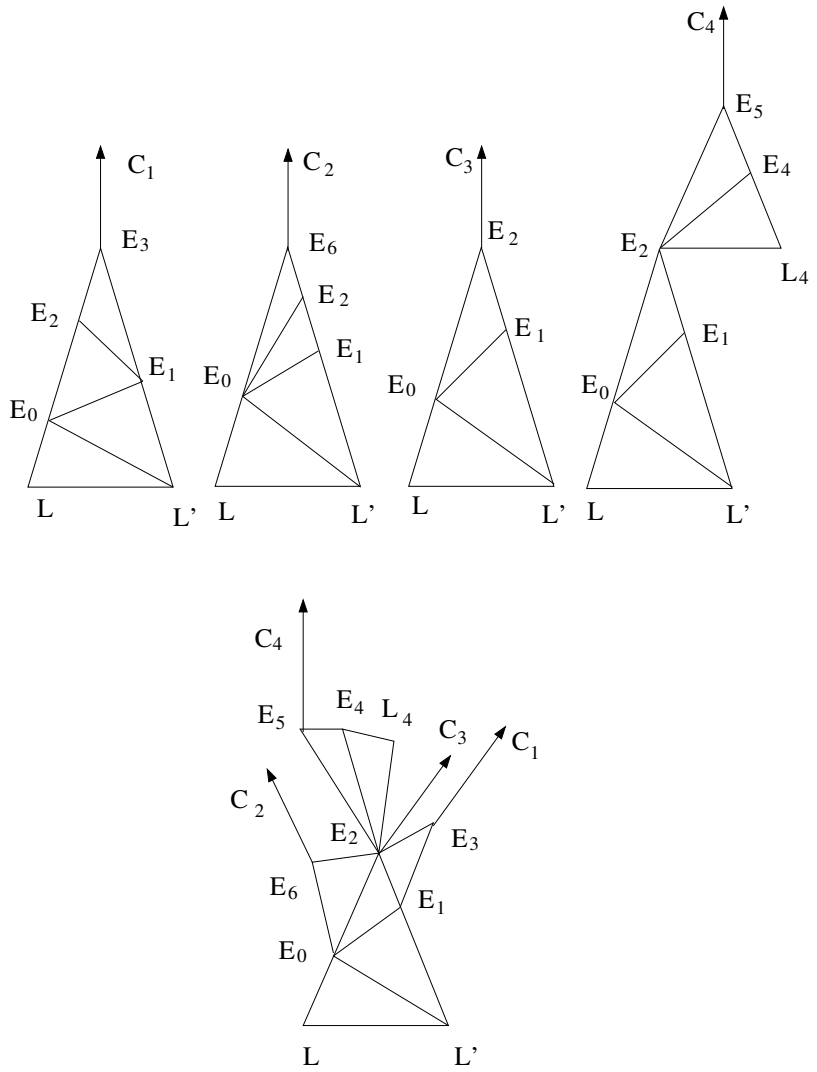

Figure 4.7 – The complex lotus of the curve singularity of Example 4.1.9

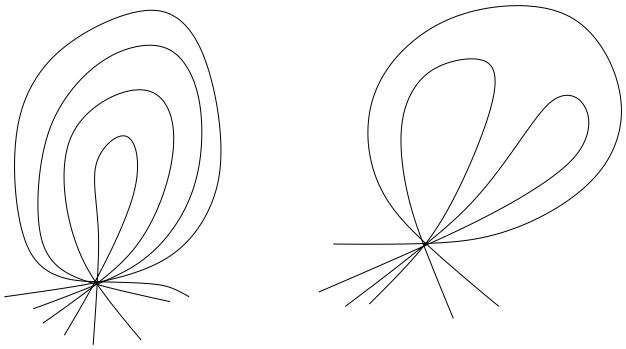

Figure 4.8 – On the left an example of multi-loop having multiplicity 5; on the right, 3 loops which do not form a multi-loop.

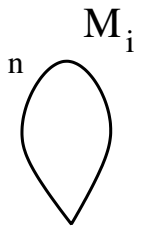

Figure 4.9 – A multi-loop with multiplicity n.

The multiplicities associated to each branch are:

$$\begin{cases} (3,2,1,1,0,0,0) & for\ C_1 \\ (3,1,1,0,0,0,1) & for\ C_2 \\ (2,1,1,0,0,0,0) & for\ C_3 \\ (4,2,2,0,1,1,0) & for\ C_4 \end{cases} \tag{4.1}$$

Necessarily $0 = p_D(1),\ 0 = p_D(6)$ and $0 = p_I(2)$. Moreover, $1 = p_D(2)$, $1 = p_I(3)$. At last, $2 = p_D(4) = p_I(5)$.

We can then consider for every branch the associated lotus, labelled in the same way as the marked points, and then glue petals if they are labelled in the same way (see Figure 4.7).

4.1.3 Multi-loops

Definition 4.1.10. Let P be a smooth point of a smooth real surface Σ. A **multi-loop** at P is the union of a finite number of loops embedded in Σ and based at P, which bound disks in Σ, pairwise included the ones into the others. If there are n such loops, then we say that the **multiplicity of the multi-loop** is n.

We will often indicate a multi-loop with multiplicity n as a simple loop with a number n attached to it (see Figure 4.9).

Let C be a real curve singularity and let $\tilde{C}$ be an associated divide. We know by Lemma 4.1.6 that there exist exactly n marked points of $\tilde{C}$, where n is the number of

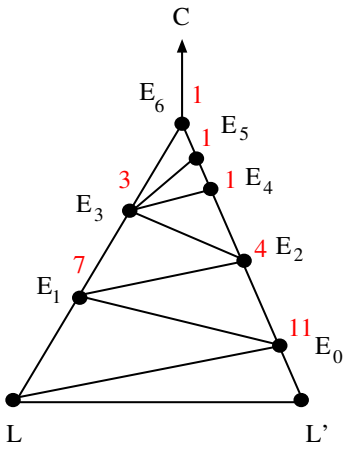

Figure 4.10 – A lotus for the curve singularity $y^{18} - x^{11} = 0$.

irreducible components of the exceptional locus E of the minimal embedded resolution of C. Moreover, the multiplicity at a point P_i is $m_i := mult_{O_i}(C)$.

Remark 4.1.11. If we do not consider the minimal embedded resolution surface, then we add a finite number of smooth marked points. Such points do not change the topology of the divide.

Definition 4.1.12. Let P_i be a marked point. The **localization** $D^{(l)} \mid_{P_i}$ of the divide $D^{(l)} \subset \Sigma^{(l)}$ at P_i is the restriction of $D^{(l)}$ to a neighbourhood of P_i.

Proposition 4.1.13. *Let C be a real curve singularity and let D be an associated divide. A node E_i has an associated multi-loop M_i if and only if E_i is a satellite node.*

Let E_i be a free node. Then there exists a point P_j, $j < i$, such that P_i and P_j are joined by m_i arcs.

Proof. Let E_i be a satellite node. Let $j = p_D(i)$ and $k = p_I(i)$. After translation, P_i belongs to the exceptional component E_k. The marked point P_j is obtained by the contraction of the exceptional component E_j. It is an easy remark that there are m_i arcs joining P_i to P_j. Let us consider a sequence of translations of marked points on the exceptional component E_k. Let P_h be the only marked point such that $P_h \in E_k$, $h < i$ and such that there are m_i arcs joining P_i to P_h. Those arcs are subdivided in two different sets by the exceptional component E_k. Let us suppose that one set contains l_i arcs, $0 \leq l_i \leq m_i$, and the second one contains $m_i - l_i$ arcs.

Let us now consider a translation of the point P_u, E_u the deviation point of E_i (that might coincide with the point P_h of the previous paragraph). Let us suppose that after translation the l_i arcs joining P_i to P_h do not intersect E_k, while each one of the $m_i - l_i$ arcs intersects E_k in two points. After contraction of the component E_k, those arcs give a multi-loop M_i, having multiplicity $m_i - l_i$.

Let E_i be a free node. Let P_h, $h < i$ be the point such that there are m_i arcs joining P_i to P_h. Such a point exists for the same reason as for a satellite node. Those points belong to a certain curvetta $L_{h'}$, so that the point P_i do not belong any more to the exceptional

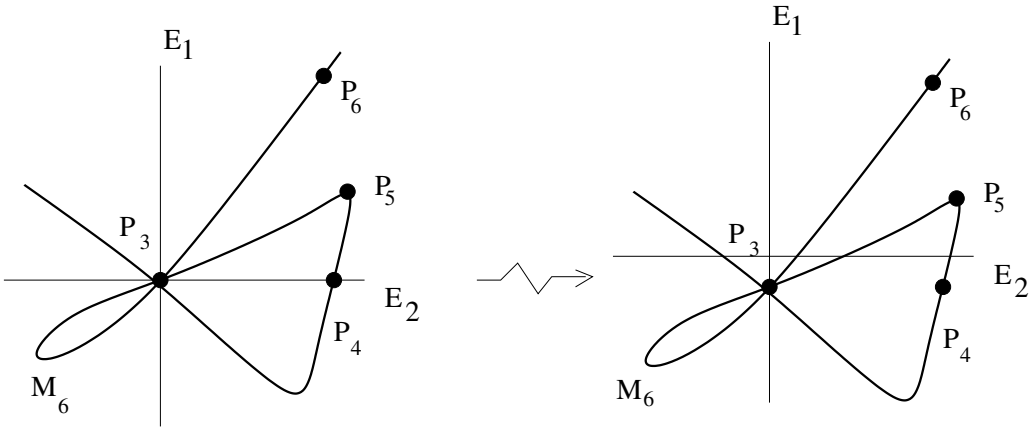

Figure 4.11 – Translation transversal to E_2.

locus E. Then there exists a point P_h such that P_i is joined to P_h by m_i arcs, and there are no associated multi-loops.

Let then E_i be a node, and M_i the associated multi-loop. Then necessarily E_i is a satellite node.

□

Corollary 4.1.14. *Let E_i be a satellite node. Then P_i is joined to at most two other points $P_{j'}$ and $P_{k'}$, $k' \leq j' < i$, (possibly with $j' = k'$), such that:*
— *P_i is joined to $P_{j'}$ by l_i arcs, $0 \leq l_i \leq m_i$;*
— *P_i is joined to $P_{k'}$ by m_i arcs.*

Proof. Let P_i be a marked point. Let E_h be the deviation node of E_i, i.e., the node such that $p_I(i) = p_D(h)$. Let P_h be marked points obtained by contraction of E_h. Before translation of P_h, P_i is joined to a point $P_{j'}$ by m_i arcs. The translation of P_h and the consequent contraction of the exceptional component E_k is such that P_i is joined to $P_{j'}$ by l_i arcs, and by m_i arcs to the marked point P_k.

The sequent translations and contractions are such that they can change the points to whom P_i is joined. It is an easy remark that there is a point $P_{k'}$ such that there are m_i arcs joining P_i to $P_{k'}$. It is also possible to find translations such that there is only one point $P_{k'}$ joined to P_i. In this case, we can still consider two different sets of arcs joining P_i to $P_{k'}$, one consisting of l_i arcs, and the second one of m_i arcs.

□

Example 4.1.15. Let C be a curve singularity having Puiseux pair $(11; 18)$. An associated lotus, enriched with the computation of the multiplicities, is shown in Figure 4.10.

Let us suppose that we have done the first steps of the translation and contraction process, and we have obtained the curve shown in Figure 4.11.

After contraction, we obtain the curve shown in Figure 4.12. We can remark that the point P_5 is joined only to the point P_2.

After contraction of the exceptional component E_1 we obtain the divide shown in Figure 4.13.

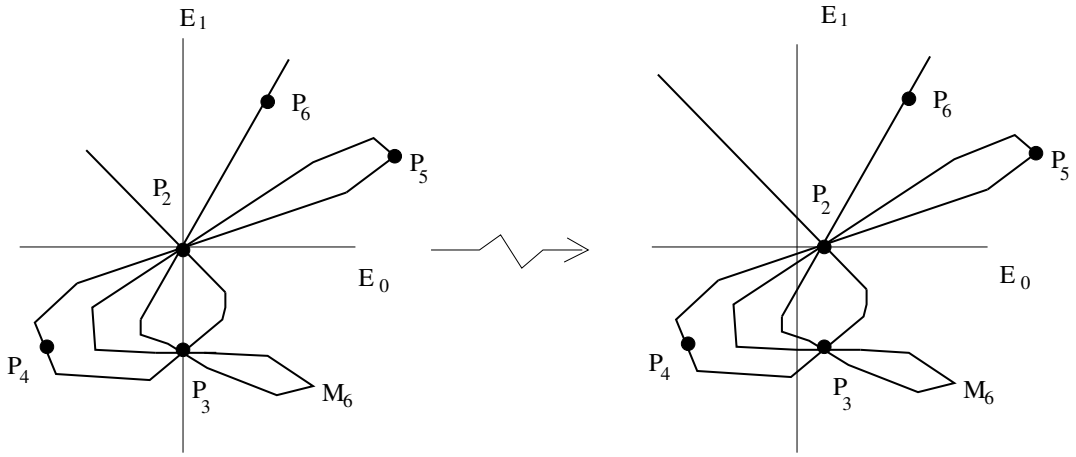

Figure 4.12 – Translation of $C^{(2)}$.

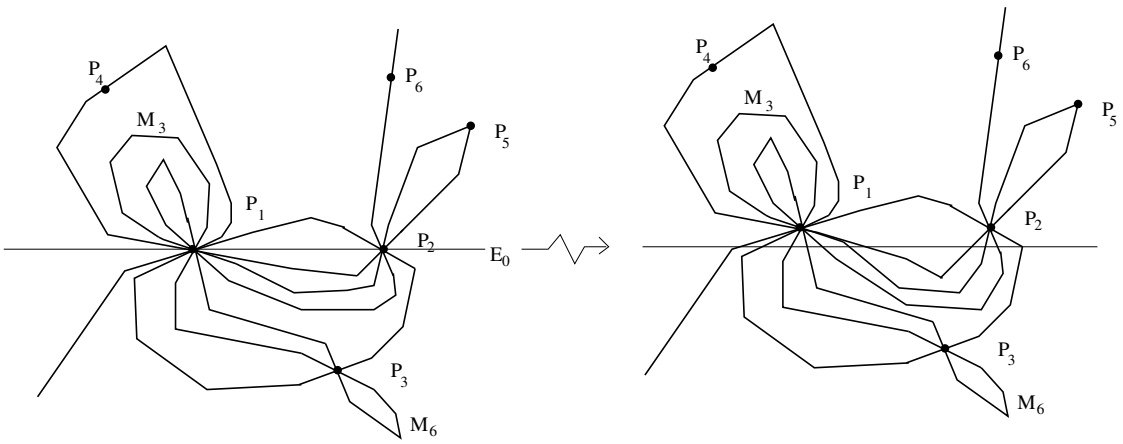

Figure 4.13 – Translation of $C^{(1)}$.

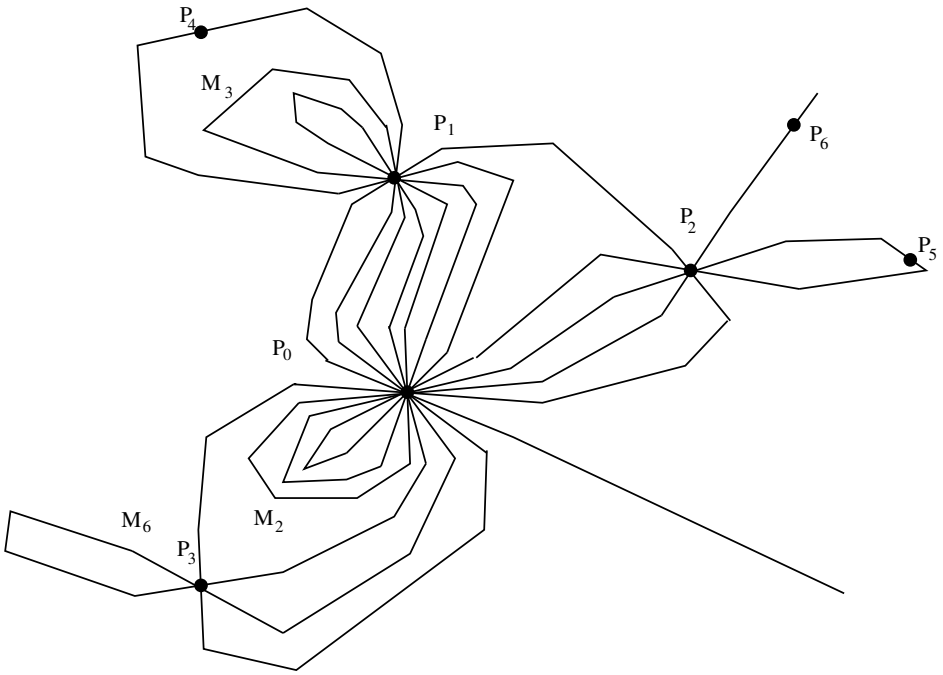

Figure 4.14 – The final divide.

In the end, we obtain the divide shown in Figure 4.14. We can notice that:
— P_1 is joined by $7 = m_1$ arcs to P_0;
— P_2 is joined by $1 = l_2$ arcs to P_1, and by $4 = m_2$ arcs to P_0;
— P_3 is joined by 4 arcs to the point P_0; moreover, this 4 arcs are divided in 2 different sets, one containing $1 = l_3$ arc, and the other $3 = m_3$ arcs;
— P_5 is joined to P_2 by two arcs, and we can consider $m_5 = 1$, $l_5 = 1$.

Remark 4.1.16. The combinatorics of the divide is complicated, because we are not choosing a canonical direction for the translation. We will see in the following section that it is possible to choose such canonical translations.

Moreover, in the general case there is no general formula for computing the number l_i. We will see that this computation is easier in the case of a canonical divide.

4.2 Canonical divides

4.2.1 Definition of a canonical divide

Definition 4.2.1. Let C be a positive real curve singularity. The **canonical divide** $\check{C}$ of C is the divide obtained by translating at every step of A'Campo's algorithm all marked points in the associated local first quadrant.

Proposition 4.2.2. *Let C be a real positive germ. Then the canonical divide of C is such that all marked points belong to the first quadrant.*

Proof. It follows from the fact that a real positive germ always has a half-branch contained

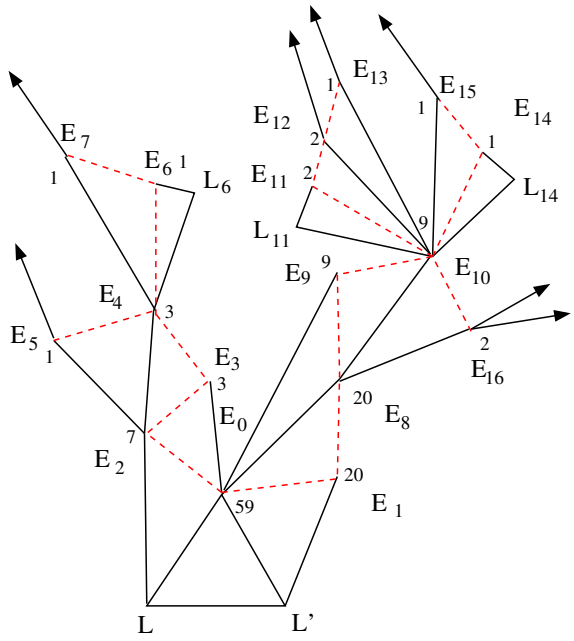

Figure 4.15 – A minimal lotus of a curve singularity.

in the local positive quadrant and that all translations are done in the local positive quadrant.

□

From now on, we will always consider real positive germs.

Proposition 4.2.3. *Let C be a real positive germ, and let $\check{C}$ be the associated canonical divide. Let P_i be a marked point of $\check{C}$. Then P_i is joined to at most two points P_h, $h < i$. If $\check{C}$ is the canonical divide of C, then P_i is joined to P_j and P_k, $j = p_D(i)$, $k = p_I(i)$.*

Proof. This is a consequence of Corollary 4.1.14, where we consider $j' = p_D(i)$ and $k' = p_I(i)$. In fact, if the translation is always done in the positive sense, then two marked points that are joined at a certain step are going to be joined at every further step. Then necessarily P_i is joined to P_j and P_k, $j = p_D(i)$, $k = p_I(i)$. □

Proposition 4.2.4. *Let C be a real positive germ and let $\check{C}$ be the associated canonical divide. We remember that $\mathcal{P}(E_i) = \{h > i \mid E_h, E_i \text{ are joined by an edge}\}$ and that $\mathcal{P}_D(E_i) = \{h > i \mid E_h, E_i = p_D(E_h)\}$.*

1. *Let P_i be a free point and let $j = p_D(i)$. Then:*
   - *a marked point P_h is joined to P_i if and only if $P_h \in \mathcal{P}(E_i)$ or $h = j$.*
   - *P_i is joined by $l_i := m_i$ arcs to P_j.*
2. *Let P_i be a satellite point. Let $j = p_D(i)$ and $k = p_I(i)$. Then:*
   - *a marked point P_h is joined to P_i if and only if $P_h \in \mathcal{P}(E_i)$, $h = j$ or $h = k$.*
   - *P_i is joined by m_i arcs to P_k.*

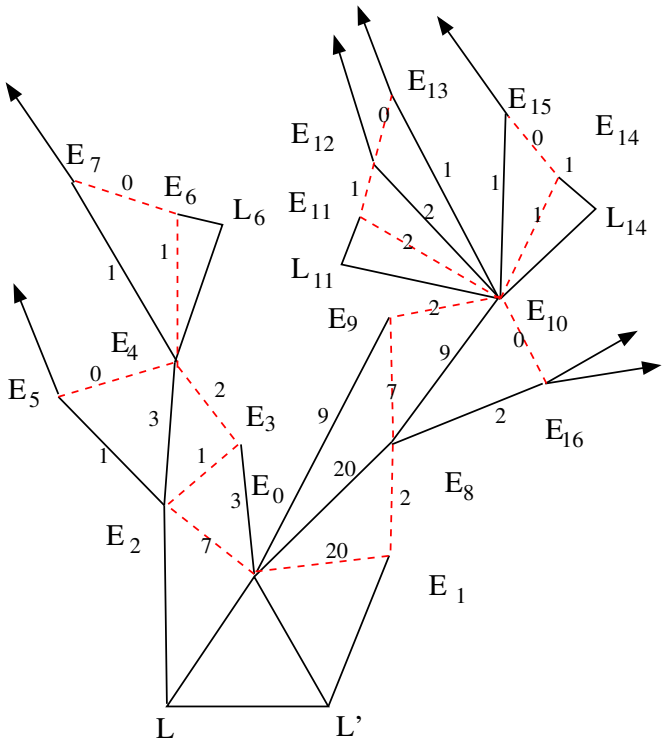

Figure 4.16 – The enriched lotus associated to the lotus in Figure 4.15.

— *P_i is joined by l_i arcs to P_j, where:*

$$l_i = \sum_{h|h\in\mathcal{P}_D(E_i)} (m_h - l_h).$$

Proof. Let P_i be a marked point. Let E_i be a (-1) node, and let m_i be its multiplicity. In a canonical divide, there are then m_i arcs joining P_i to the boundary of the disk, and by Corollary 4.1.14 there are m_i arcs joining it to P_k.

By Proposition 4.2.3, we know that a satellite point P_i is joined to the two points P_j and P_k, $j = p_D(i)$ and $k = p_I(i)$; if P_i is a free point node, P_i is joined by $l_i = m_i$ lines to P_j, $j = p_D(i)$.

For the previous assertions, a marked point P_i is joined to point P_h such that $h \in \mathcal{P}(E_i)$. Moreover, if $P_h \in \mathcal{P}_I(P_i)$, there exist m_h lines joining P_h to P_i; if $P_h \in \mathcal{P}_D(P_i)$, there exists l_h lines joining P_h to P_i. Because P_i has multiplicity m_i, there are $2m_i$ arcs incident to P_i. We know that:

$$m_i = c_i + \sum_{h:P_h\in\mathcal{P}_D(P_i)} m_h + \sum_{h:P_h\in\mathcal{P}_I(P_i)} m_h$$

We can then say that:

$$2m_i = l_i + m_i + c_i + \sum_{h:P_h\in\mathcal{P}_I(P_i)} m_h + \sum_{h:P_h\in P_D(P_i)} l_h;$$

$$m_i = l_i + c_i + \sum_{h:P_h\in\mathcal{P}_I(P_i)} m_h + \sum_{h:P_h\in P_D(P_i)} l_h;$$

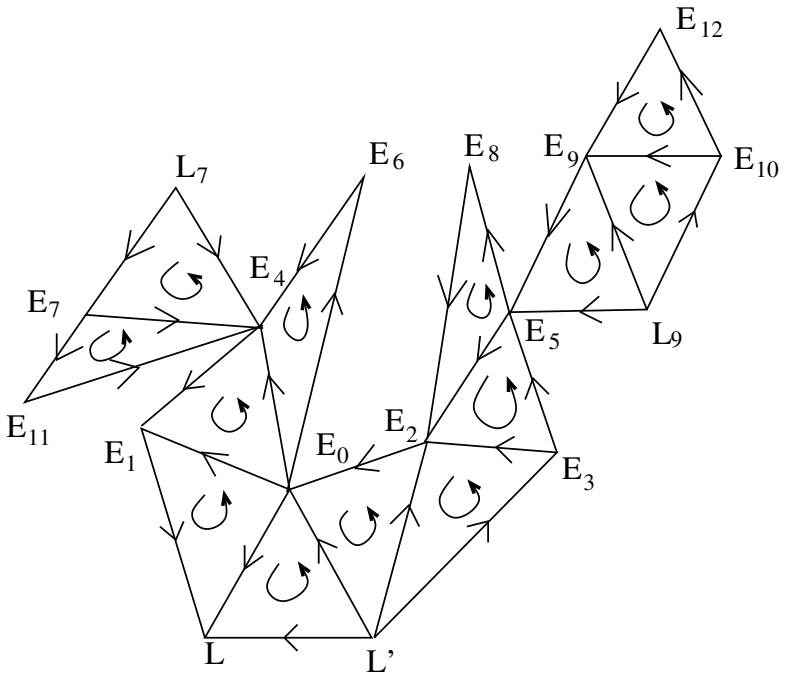

Figure 4.17 – A lotus, endowed with the orientations of its edges and petals.

By definition of m_i:

$$c_i + \sum_{h:P_h \in \mathcal{P}_D(P_i)} m_h + \sum_{h:P_h \in \mathcal{P}_I(P_i)} m_h = l_i + c_i + \sum_{h:P_h \in \mathcal{P}_I(P_i)} m_h + \sum_{h:P_h \in P_D(P_i)} l_h$$

that implies:

$$l_i = \sum_{h:P_h \in \mathcal{P}_D(P_i)} (m_h - l_h).$$

□

Corollary 4.2.5. *Let C be a positive real curve singularity, $\mathcal{L}$ the associated real lotus and let $\check{C}$ be the associated canonical divide. Then two marked points P_i and P_h are joined if and only if E_i and E_h are joined by an edge in the lotus $\mathcal{L}$.*

Proof. The proof is straightforward from the bijection from marked points P_i to nodes E_i. □

Definition 4.2.6. Let C be a real curve singularity. If $\mathcal{L}$ is an associated lotus, we enrich it with the following **edge weights**:

- if E_i is a satellite vertex and $j = p_D(i)$, $k = p_I(i)$, then we attach the number m_i to the edge $[E_iE_k]$ and the number l_i to the edge $[E_iE_j]$;
- if E_i is a free vertex, E_i joined neither to L or L', then we add the number $l_i = m_i$ to the edge $[E_iE_j]$, where $j = p_D(i)$;
- if E_i is a free vertex, E_i joined either to L or L', then we add the number l_i to the edge $[E_iE_j]$, $j = p_D(i)$.

Remark 4.2.7. The numbers l_i are attached to the sub-tree of direct edges, which is isomorphic to the Enriques tree (see Proposition 1.4.14).

Example 4.2.8. Let us consider the lotus in Figure 4.15, where we have attached at each node E_i the multiplicity m_i. Then it can be enriched according to Definition 4.2.6 by edge weights, as shown in Figure 4.16.

We end this subsection with the following Definition, which refines the notion of canonical embedding of a lotus from Definition 4.2.1:

Definition 4.2.9. Let $\mathcal{L}$ be a lotus, and let (L', L) be its basis. Let $\{L'_i\}$ be the associated system of curvettas. Moreover, we suppose that $\mathcal{L}$ is oriented, i.e., the basis (L', L) is oriented from the vertex L' to the vertex L, and we endowed each petal with the same orientation as the canonical orientation of $\mathbb{R}^2$ (as we have seen in Section 3.3.2).

The **canonical embedding of the lotus $\mathcal{L}$ in the first quadrant** is such that:
— to every node E_i we associate a point P_i in the first quadrant;
— if a node E_i is joined to the vertex L (resp. L'), then $P_i \in L$ (resp. L');
— if two nodes E_i and E_j are joined to a vertex L and to each other, then the arc $[P_i, P_j]$ belongs to the first quadrant:
— the embedding of the petals preserves their orientations.

4.2.2 The positions of the multi-loops in the plane

Proposition 4.2.10. *Let E_i be a satellite node. Then there is an associated multi-loop M_i, having multiplicity $m_i - l_i$.*

Proof. In the proof of Proposition 4.1.13 we have seen that, before the contraction of $E_{p_I(i)}$, there are m_i arcs joining P_i to $P_{p_D(i)}$. Moreover, those arcs are divided in two sets, one having l_i arcs, and the second one consisting of m_i arcs. The translation preceding the contraction of $E_{p_D(i)}$ is such that l_i arcs join directly P_i to $P_{p_D(i)}$, while the other $m_i - l_i$ arcs each intersect E_k in two distinct points. It is then those $m_i - l_i$ arcs that form the multi-loop M_i, which has then multiplicity $m_i - l_i$.

□

Let us consider the toric resolution of a singularity C such that the lotus of its complexification is a simple lotus. We can associate the vector $v_2 = (0, 1) \in \mathbb{F}_2^2$ to L' and the vector $v_1 = (1, 0) \in \mathbb{F}_2^2$ to L. Then the node E_0 has an associated vector $v_1 + v_2 = (1, 1)$. In general:

Definition 4.2.11. Let E_i be the vertex of the petal having basis $[\tilde{E}, \tilde{E}']$. Let us suppose that v and v', where v and $v' \in \mathbb{F}_2^2$, are the vectors associated to $[\tilde{E}, \tilde{E}']$. Then the **i-vector** $v_i \in \mathbb{F}_2^2$ associated to E_i is $v_i = v + v'$.

Remark 4.2.12. The vectors v_i are the reduction modulo 2 of the vectors used to obtain the toric minimal resolution of the curve C (see Definition 1.4.27).

Moreover, we can consider the function $sign(x) : \mathbb{R}^* \to \mathbb{F}_2$ such that:

$$\begin{cases} sign(x) = 0 & if\ x > 0 \\ sign(x) = 1 & if\ x < 0. \end{cases} \tag{4.2}$$

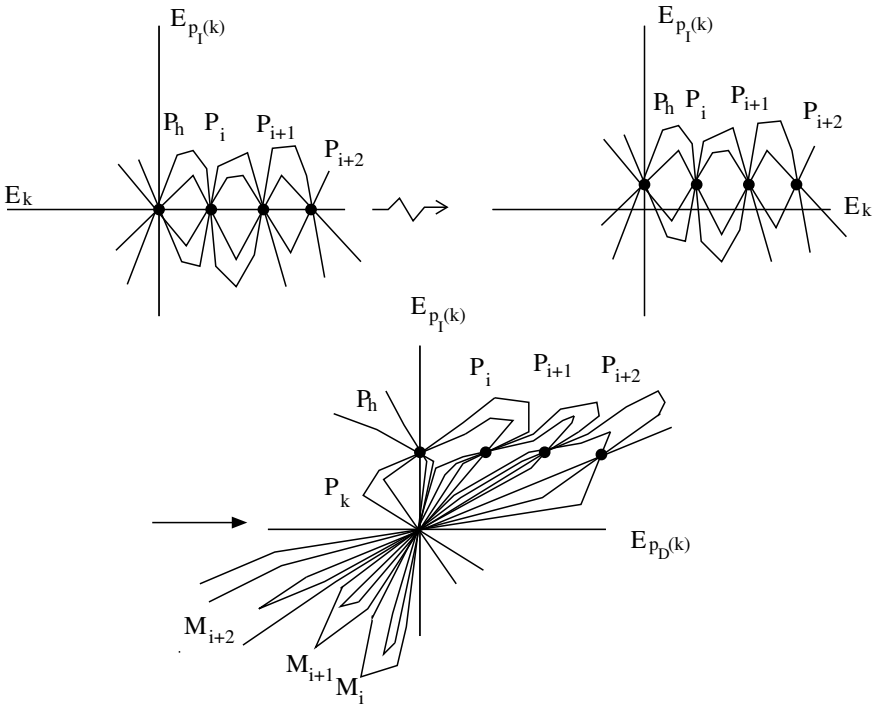

Figure 4.18 – Multi-loops belonging to the third quadrant.

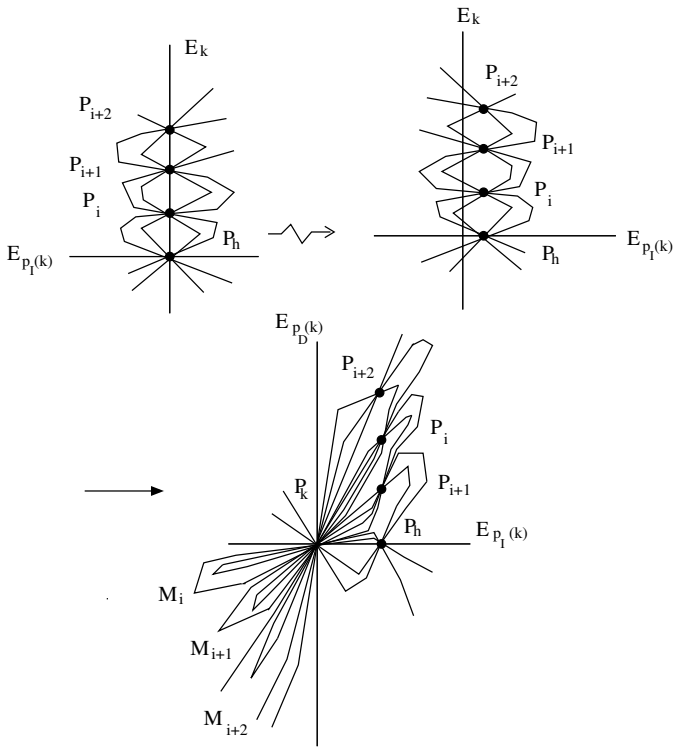

Figure 4.19 – Multi-loops belonging to the third quadrant.

We have seen in Section 1.3.2 that this function gives a morphism of groups between tori over the fields $\mathbb{R}$ and $\mathbb{F}_2$. We can then consider a point in the first quadrant as a point of type $(0,0)$, while points in the second, third, and fourth quadrant are respectively of type $(1,0)$, $(1,1)$ and $(0,1)$.

Remember that we can associate to every node E_i a vector $v_i \in \mathbb{N}^2$. Let us consider the reduction modulo 2 of those vectors. Moreover, we have seen that we can associate to each pair of vector (v_1, v_2) a matrix, such that the coefficients of the vectors v_1 and v_2 belong respectively to the first and second column. We obtain then the following 6 different matrices $\in M_2(\mathbb{F}_2)$:

$$A_1 = \begin{pmatrix} 1 & 0 \\ 0 & 1 \end{pmatrix} \qquad B_1 = \begin{pmatrix} 0 & 1 \\ 1 & 0 \end{pmatrix}$$

$$A_2 = \begin{pmatrix} 1 & 1 \\ 1 & 0 \end{pmatrix} \qquad B_2 = \begin{pmatrix} 1 & 1 \\ 0 & 1 \end{pmatrix}$$

$$A_3 = \begin{pmatrix} 0 & 1 \\ 1 & 1 \end{pmatrix} \qquad B_3 = \begin{pmatrix} 1 & 0 \\ 1 & 1 \end{pmatrix}$$

We can notice that the matrix B_i is obtained by permutation of the columns of the matrix A_i (and vice versa). Let v_1^i and v_2^i be the two vectors, whose coefficients are the columns of A_i and B_i. Let $v = (1,1)$. Then for every i:

$$A_i \cdot v^T = B_i \cdot v^T = v_1^i + v_2^i.$$

A matrix A_i is associated to the composition of the sequence of blow-ups. The base of i-petal is given by E_1^i and E_2^i, to whom we associate the two vectors v_1^i and v_2^i. The vector v_i represents the third quadrant in those coordinates. The vector $A_i \cdot v^T$ gives the position, in the local coordinates in $\mathbb{R}^2$, of the points of the third quadrant of the chart having coordinate axis of types v_1^i and v_2^i. Moreover, $A_i \cdot v^T = v_i$.

Proposition 4.2.13. *Let C be a positive curve and let $\check{C}$ be the associated canonical divide. Let us suppose that the lotus $\mathfrak{L}$ is a simple lotus.*

Let E_i be a satellite node and let E_k be the indirect node of E_i, $k = p_I(i)$. Then the multi-loop M_i belongs to the quadrant associated to the vector v_k.

Proof. At every step, the deformation is done in the positive sense. The multi-loop M_i is given by the contraction of the exceptional component E_k. Then necessarily it is in the third quadrant of the chart having as exceptional components $E_{p_D(k)}$ and $E_{p_I(k)}$. Those two cases are shown in Figure 4.18 and Figure 4.19: the first one is the case where E_k is the first coordinate axis in the local chart, while the second is the case where E_k is the second coordinate axis in the local chart.

Moreover, we have seen that the toric resolution has matrix A_k, such that the arcs are the vectors $v_{p_D(k)}$ and $v_{p_I(k)}$. The order is not important, because the image of the third quadrant is invariant by permutation of the columns of the matrix A_k. Then the position in $\mathbb{R}^2$ of the multi-loops in the local third quadrant are given by $A_k \cdot (1,1)^T = v_{p_D(k)} + v_{p_I(k)} = v_k$. □

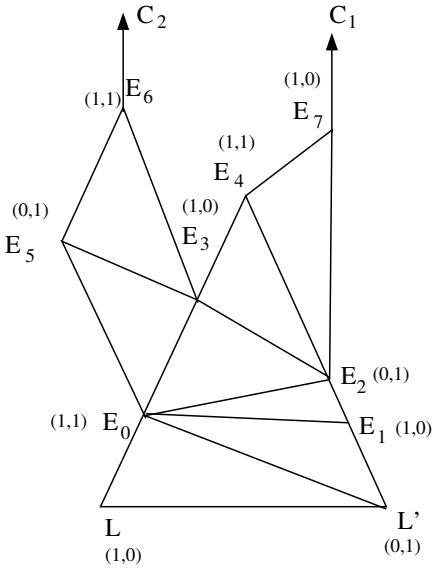

Figure 4.20 – The lotus for the curve singularity of Example 4.2.16.

Proposition 4.2.14. *Let C be a positive branch, which admits a simple lotus $\mathcal{L}$. Let E_i be the only node having self-intersection -1. Let C^A be the half-branch in the positive quadrant, and let C^B be the second one. Then the position of C^B is given by $A_i \cdot v = v_i$.*

Proof. If C is a positive branch which admits a simple lotus $\mathcal{L}$, then C is of the form $y^a = x^b$, where $(a, b) = 1$. Then necessarily only one half-branch belongs to the first quadrant.

Let us consider the curve $C^{(i)}$ and the blow up of the point O_i. By the hypothesis C is positive, then $C^{(i)}$ passes through the first and third local quadrant. The proposition then follows from this remark. □

Remark 4.2.15. In the following we will also denote by C_i the half-branch of C_i not belonging to the first quadrant.

Example 4.2.16. Let us consider the curve singularity having the lotus shown in Figure 4.20.

We can notice that $p_I(E_6) = E_3$, $p_I(E_5) = p_I(E_3) = p_I(E_2) = E_0$ and $p_I(E_7) = p_I(E_4) = E_2$. Moreover, $v_3 = (1, 0)$, $v_2 = (0, 1)$ and $v_0 = (1, 1)$. Then:

— M_6 belongs to the second quadrant;

— M_4 and M_7 belongs to the fourth quadrant;

— M_2, M_3 and M_5 belong to the third quadrant.

The canonical divide of C is shown in Figure 4.21.

Remark 4.2.17. We will explain in Proposition 4.2.33 and Proposition 4.2.34 the combinatorics of the mutual position of the multi-loops. Moreover, we haven't still clearly defined to which base-points they are attached (see Proposition 4.2.19).

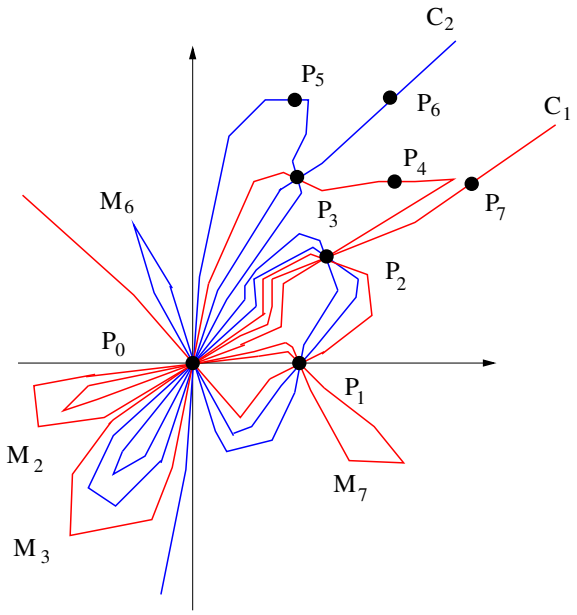

Figure 4.21 – The canonical divide for the curve singularity of Example 4.2.16.

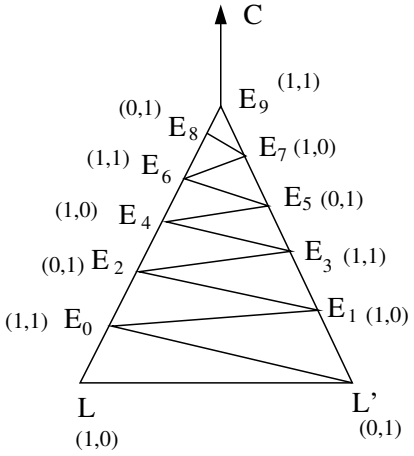

Figure 4.22 – A simple lotus for the curve singularity having Puiseux characteristic $(55; 89)$.

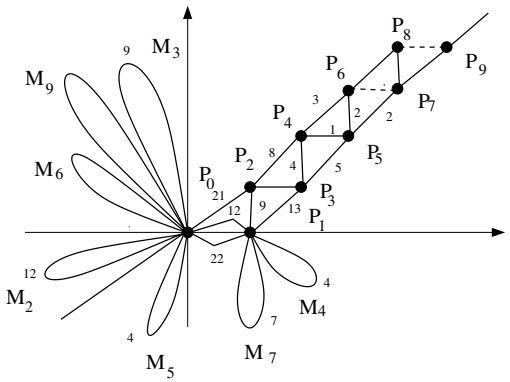

Figure 4.23 – The canonical divide for curve singularity of Example 4.2.18.

Example 4.2.18. Let us consider the curve singularity $y^{55} = x^{89}$, having Puiseux characteristic $(55; 89)$. An associated simple lotus is shown in Figure 4.22. The associated multiplicity sequence is:

$$(55, 34, 21, 13, 8, 5, 3, 2, 1, 1).$$

Moreover, it is an easy remark that, for all $i = 2, \ldots, 9$, E_{i-2} is the indirect node of E_i. Moreover:

— M_9, M_6 and M_3 belong to the second quadrant, and have multiplicities 1, 1 and 9;
— M_8, M_5 and M_2 belong to the third quadrant, and have multiplicities 0, 4 and 12;
— M_7 and M_4 belong to the third quadrant, and have multiplicities 2 and 4.

The canonical divide of the curve singularity $(55; 89)$ is shown in Figure 4.23.

Proposition 4.2.19. *Let C be a real positive germ and let $\check{C}$ be the canonical divide of C. Let M_i be a multi-loop.*

1. *if M_i belongs to the third quadrant, then P_0 is the base point of M_i;*
2. *if M_i belongs to the second quadrant, then $P_h = max\{l \mid l \preceq i, P_l \in L\}$ is the base point of M_i;*
3. *if M_i belongs to the fourth quadrant, then $P_h = max\{l \mid l \preceq i, P_l \in L'\}$ is the base point of M_i.*

Proof. If M_i belongs to the third quadrant, then the only marked point that has arcs in the third quadrant is P_0. Then necessarily P_0 is the base point of M_i.

Let us prove the two other assertions for a branch C. The generalisation to a reducible curve is clear. Let C be a branch. Let $\check{C}^l$ be the divide obtained after contraction of the exceptional component E_k, such that $k = min\{h \mid \exists n, h = p_I(n)\}$. Then $P_k \in E_{k_1} \cap E_{k_2}$. In this chart, we can suppose that there are multi-loops M_i on every quadrant. Let us suppose that the point P_k is translated on the L-axis. Then the multi-loops belonging to the local third and fourth quadrant intersect the exceptional component $E_{p_D(k)}$, while the multi-loops belonging to the second quadrant do not intersect any exceptional component. The statement follows from this remark, and from the fact that, being all translations positive on L, the multi-loops belonging to the second quadrant do not intersect any E_j, $0 \leq j \leq p_D(k)$.

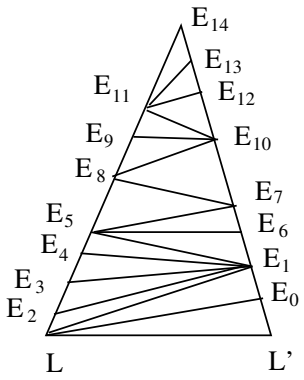

Figure 4.24 – A triangular lotus.

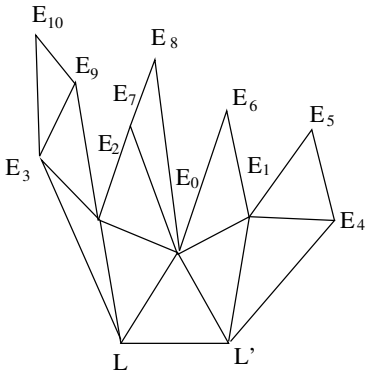

Figure 4.25 – A simple lotus.

The proof is exactly the same if we consider a branch and translations along L'. It is sufficient to exchange the second and the fourth quadrant.

□

Remark 4.2.20. If we analyze carefully Example 4.2.18 and the canonical divide shown in Figure 4.23, it is clear that the position of the multi-loop in a quadrant is not completely determined by the vectors v_i. In fact, we do not say anything about the local position of a multi-loop M_i relative to a multi-loop $M_{i'}$, such that both belong to the same quadrant.

Definition 4.2.21. Let $\mathcal{L}$ be a triangular lotus, E_i being its (-1)-node. We say that a node E_h, $h \neq 0$, is a **L-node** if $p_I(E_h)$ belongs to the edge $[L, E_i]$ and we say that a node E_h is a **L'-node** if $p_I(E_h)$ belongs to the edge $[L', E_i]$.

Example 4.2.22. Let us see which are the L-nodes and which nodes are the L'-nodes of the triangular lotus in Figure 4.24.

The nodes E_0, E_1, E_6, E_7, E_{10}, E_{12}, E_{13} belong to the edge $[L', E_{14}]$. This implies that E_1, E_2, E_7, E_8, E_{11}, E_{13} and E_{14} are the L'-nodes.

Then the nodes E_3, E_4, E_5, E_6, E_9, E_1 and E_{12} are the L-nodes.

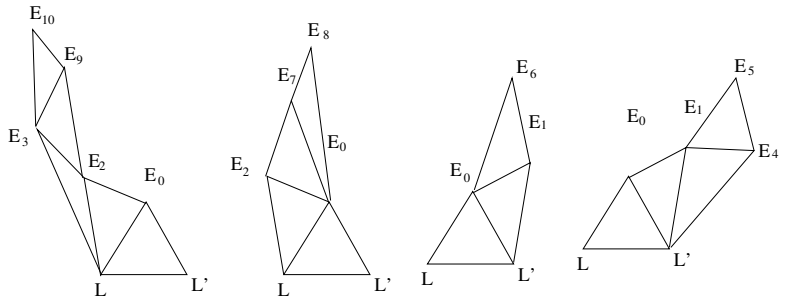

Figure 4.26 – The decomposition in triangular loti of the simple lotus in Figure 4.25

Definition 4.2.23. Let $\mathcal{L}$ be a simple lotus. Let E_i and E_j, $E_i \preceq E_j$. We say that they have the same **direct coordinate type** if there exists an irreducible component E'_k of $\check{E}$ and two charts such that E_i and E'_k determine the local cross of the first chart, while E_j and E'_k determine the local cross of the second chart.

In general, we say that E_i and E_j, $i = p_D^r(j)$ are of the same **coordinate type**, if there exists a sequence E_{i_1}, E_{i_2}, …, E_{i_n}, where $i = i_1$ and $j = i_n$, such that E_{i_k} and $E_{i_{k+1}}$ have the same direct coordinate type, for all $k = 1, \ldots, n-1$.

Definition 4.2.24. Let $\mathcal{L}$ be a simple lotus and let E_{i_1}, …, E_{i_n} be the (-1)-nodes. The **decomposition** of the simple lotus in triangular loti is the disjoint union $\coprod\{\mathcal{L}_{i_j}\}_{j=1\ldots,n}$ such that for every i_j we consider the sets of nodes $\{E_h \mid E_h \preceq E_{i_j}\}$ and the restriction $\mathcal{L}_{i_j}$ of the lotus $\mathcal{L}$ to those nodes.

Proposition 4.2.25. *Let $\mathcal{L}$ be a simple lotus and let $\mathcal{L}_{i_1}$ and $\mathcal{L}_{i_2}$ be two triangular loti of the decomposition of $\mathcal{L}$. Let $E_h \in \mathcal{L}_{i_1} \cap \mathcal{L}_{i_2}$, $h \neq 0$. Then if E_h is a L-**node** (respectively a L'-**node**) of $\mathcal{L}_{i_1}$, then E_h is a L-node (respectively a L'-node) of $\mathcal{L}_{i_2}$.*

Proof. The notion of being a L-node or a L'-node does not change by adding petals to a simple lotus. Then it is possible to consider the triangular sub-lotus having as (-1)-node the node E_h. □

Proposition 4.2.25 justifies the following Definition:

Definition 4.2.26. Let $\mathcal{L}$ be a simple lotus and let $E_h \in \mathcal{L}$ be a satellite node. Let us consider a triangular lotus $\mathcal{L}_{i_j}$ of its decomposition, such that $E_h \in \mathcal{L}_{i_j}$. Then E_h is a L-node (respectively L'-node) of $\mathcal{L}$ if E_h is a L-node (respectively, a L'-node) of $\mathcal{L}_{i_j}$.

Remark 4.2.27. The notion of L-node and L'-node is well defined also for (-1)-nodes.

Example 4.2.28. Let us consider the simple lotus shown in Figure 4.25.

The (-1)-nodes are E_5, E_6, E_8 and E_{10}. Its decomposition in triangular lotus is shown in Figure 4.26. Then:

— E_{10}, E_3 and E_2 are L-nodes, while E_9 is a L'-node;
— E_8 and E_7 are L'-nodes;
— E_6 is a L-node, while E_1 is a L'-node;
— E_5 is a L-node, while E_4 is a L'-node.

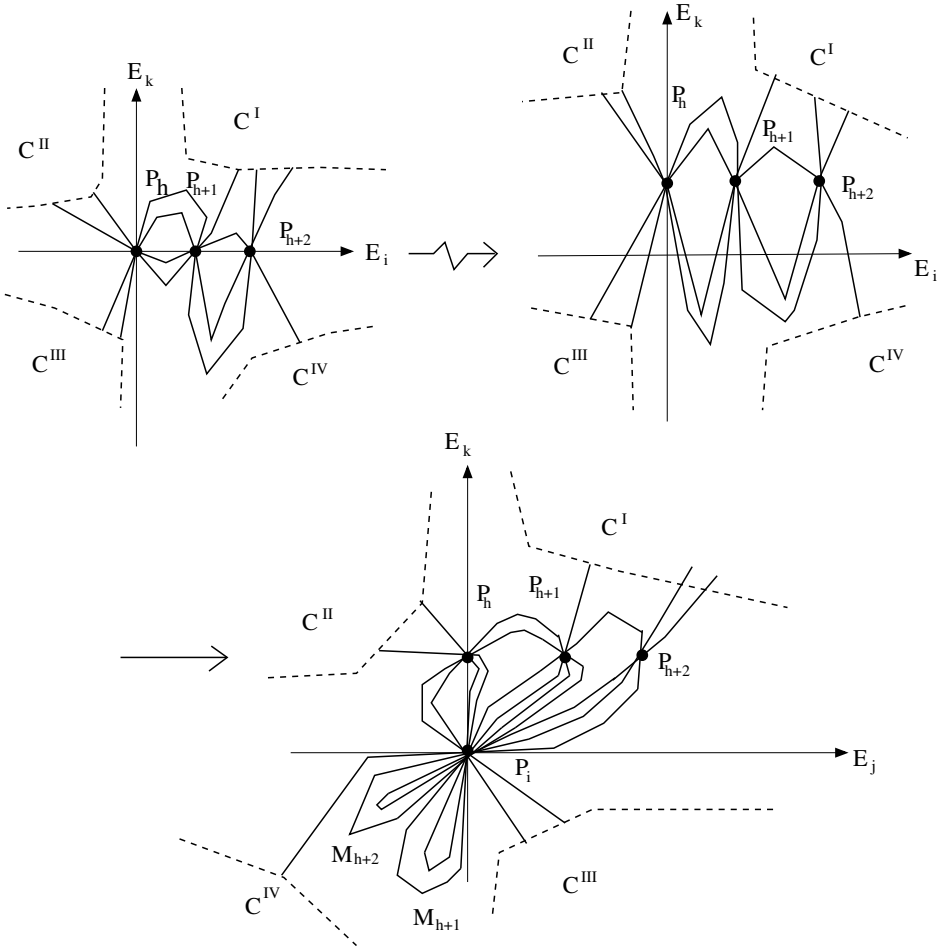

Figure 4.27 – The contraction of E_i.

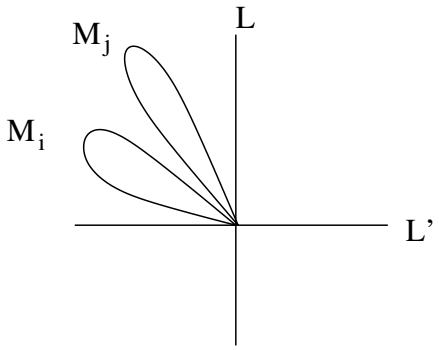

Figure 4.28 – The dihedral order $L'M_iM_jL$.

Lemma 4.2.29. *A node E_i is a L'-node if and only if E_i has the same coordinate type as L'.*

Proof. It is sufficient to prove the Lemma for a triangular lotus.

Let E_i be a L'-node. Let us consider a system of local coordinates, such that E_i is one of the axis. Then the second coordinate axis is a component E_j, such that the nodes E_i and E_j are the basis of a petal. Let us suppose that $j < i$. There are then two cases: either $j = p_D(i)$, either $j = p_I(i)$.

If $j = p_I(i)$, then the node $E_{j'}$, $j' = p_D(i)$ has the same direct coordinate type as E_i.

If $j = p_D(i)$, then E_i has the same direct coordinate type as E_k, $k = p_I(i)$.

Moreover, if E_i is a L'-node and it is a basis of a petal, then necessarily the second basis node is a L-node. Then, by recurrence, E_i has the same coordinate type as L'.

We can use the same argument to show that if E_i is a L-node, then E_i has the same coordinate type as L.

□

Definition 4.2.30. Let $M_{i_1}, \ldots, M_{i_n}$ be all the multi-loops of the canonical divide of a curve singularity C, such that the lotus of C is a simple lotus. It is possible to consider the **order** of the multi-loops in the plane.

Let M_i and M_j be two multi-loops, M_i and M_j belonging to the same quadrant of the cross (L', L) and based at the same point. We say that M_i is **closer** to L' than M_j if, restricting to the quadrant, they have a dihedral order $L'M_iM_jL$. In the same way, we also say that M_j is closer to L than M_i.

Remark 4.2.31. We can consider the notion of closeness relative to L' and L also for the half-branches of two different branches C_1 and C_2.

Lemma 4.2.32. *Let E_i be an exceptional component, and let M_j, M_k be in the chart $(E_i, E_{i'})$, $i' < i$, and such that M_j is closer to E_i than M_k. After the contraction of E_i, in the local chart there is an irreducible component E'_i of $\check{E}$. Then M_j is closer to E'_i than M_k.*

The notion of closeness is an invariant of the operation of contraction of an exceptional component.

Proof. The contraction of an exceptional component E_i determines the exchange of two quadrants par respect to a transversal axis to E_i (usually another exceptional component or a curvetta). Then if M_j is closer to E_i than M_k before contraction of E_i, so it is closer to E'_i after contraction of E_i.

□

Proposition 4.2.33. *Let C be a positive curve singularity, which has an associated simple lotus $\mathcal{L}$. Let $\check{C}$ be the canonical divide of C and let M_i and M_j be two multi-loops in the same quadrant. Then:*

- *if E_i is a L'-node, and $E_i \preceq E_j$, then M_i is closer to L than M_j;*
- *if E_i is a L-node, and $E_i \preceq E_j$, then M_i is closer to L' than M_j;*
- *let E_i and E_j be such that $E_i \not\preceq E_j$ and $E_i \not\succeq E_j$. Moreover let us suppose that $C_{i_1} \in \mathcal{B}(E_i)$, and $C_{j_1} \in \mathcal{B}(E_j)$, such that C_{i_1} is closer to L' than C_{j_1}. Then M_i is closer to L' than M_j.*

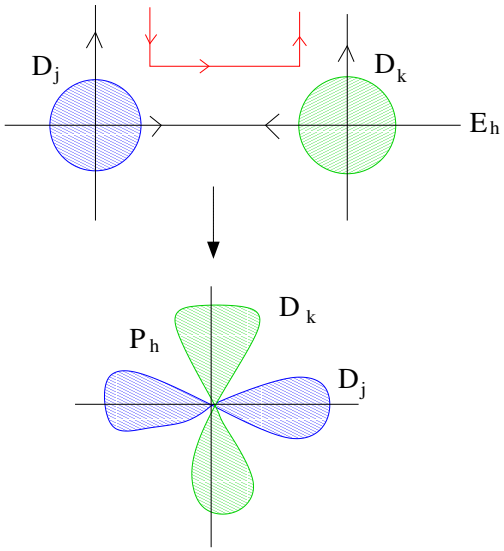

Figure 4.29

Proof. We have seen in Lemma 4.2.32 that the notion of closeness is invariant by further contractions. It is sufficient then to prove the Proposition after the contraction of the exceptional component E_k, $k = p_I(i)$.

Let E_i be a L'-node. Let us suppose that $E_i \preceq E_j$. Then either $p_I(j) \neq k$, or P_j and P_i both belong to the component E_k. The operation of translation of the curve and contraction of E_k is local, which implies that the new multi-loops are created closer to the irreducible component E'_k, which is either a curvetta or $E_{p_D(k)}$. Then if $p_I(j) \neq k$, M_i is closer to E'_k than M_j. In the second case, the arcs joining P_i to $P_{p_D(i)}$ are closer to E'_k than the arcs joining P_j to $P_{p_D(j)}$. Now, by the fact that the closeness is invariant for contraction and that E_i is a L'-node, we have that M_i is closer to L than M_j.

We can use the same argument in the case where E_i is a L-node. An example of this situation is shown in Figure 4.27.

Let us now suppose that E_i and E_j are such that $E_i \not\preceq E_j$ and $E_i \not\succeq E_j$. Moreover, let us consider two branches C_{i_1} and C_{j_1}, such that $C_{i_1} \in \mathcal{B}(E_i)$, and $C_{j_1} \in \mathcal{B}(E_j)$, and such that C_{i_1} is closer to L' than C_{j_1}. We can consider, for two not intersecting strict transforms $C^{(l)}_{i_1}$ and $C^{(l)}_{j_1}$, two disk $D^{(l)}_{i_1}$ and $D^{(l)}_{j_1}$. Let us suppose that $E_k \in \Sigma^{(l-1)}$ is the node such that $k = \max\{h \mid \{C_{i_1}, C_{j_1}\} \subset \mathcal{B}(E_h)\}$. The contraction of E_k gives a point P_k, and the two divides intersect at it. Moreover, it is their only point of intersection, and the image of a disk after contraction of E_k is the wedge sum of two disks, the intersection point being P_k. Then clearly all elements in $D^{(l-1)}_{i_1}$ are closer to the component L' than the elements of $D^{(l-1)}_{j_1}$. An example of this situation is shown in Figure 4.29.

□

Proposition 4.2.34. *Let M_i and C_j be a multi-loop and a half-branch, such that M_i and C_j belong to the same quadrant. Then:*

— *if E_i is a L'-node, and $C_j \in \mathcal{B}(E_i)$, then M_i is closer to L than C_j;*

— *if E_i is a L-node, and $C_j \in \mathcal{B}(E_i)$, then M_i is closer to L' than C_j;*

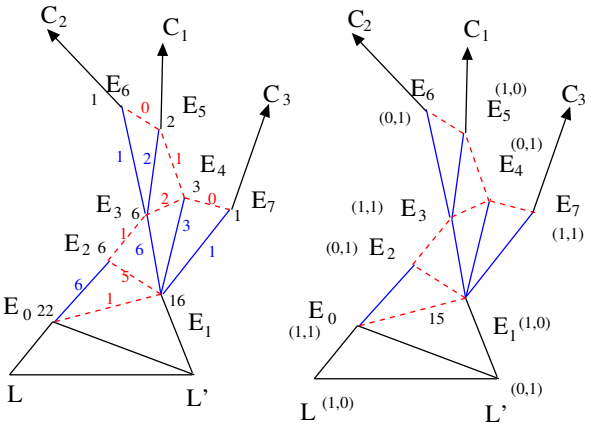

Figure 4.30 – The lotus of the curve in Example 4.2.36

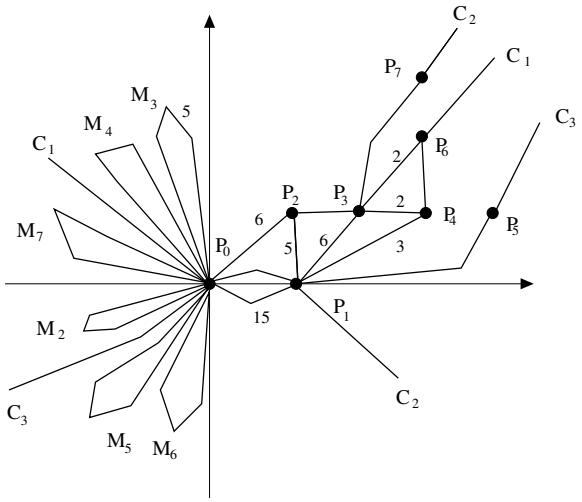

Figure 4.31 – The graph of the curve in Example 4.2.36

— *let $C_j \notin \mathcal{B}(E_i)$ and let $C_k \in \mathcal{B}(E_i)$. Moreover let us suppose that C_j is closer to L' (respectively L) than C_k. Then C_j is closer to L' (respectively L) than M_i.*

Proof. We can remark that a half-branch C_j appears in the method before every multi-loop. Then if $C_j \in \mathcal{B}(E_i)$ and E_i is a L'-node, necessarily M_i is closer to L than C_j. The same arguments works for L-nodes.

Let E_i be a node. Let us consider two branches C_j and C_k, such that $C_j \notin \mathcal{B}(E_i)$ and let $C_k \in \mathcal{B}(E_i)$. Let $E_h = max\{h' \mid \{C_j, C_k\} \subset \mathcal{B}(E_h)\}$. As before, we consider two disjoint disks D_j and D_k. After contraction of E_h, the two disks D_j and D_k have P_h as their only intersection point. Moreover, let E_n be an L'-node, E_n one of the two local coordinates. Then C_j is closer to E_n than M_i. By invariance of the closeness, C_j is closer to L' than M_i.

□

We have then proven the following Theorem:

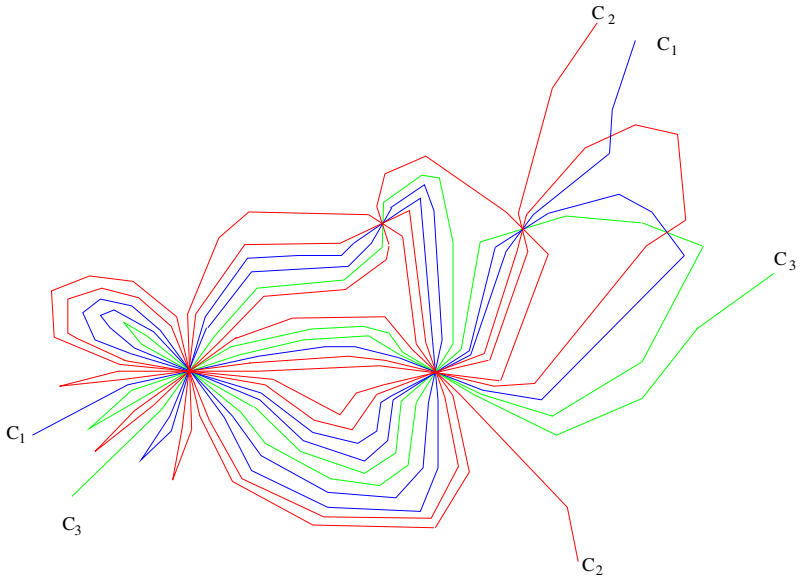

Figure 4.32 – The canonical divide of the curve in Example 4.2.36

Theorem 4.2.35. *Let C be a positive germ such that the associated lotus $\mathcal{L}$ is simple. Let E_i be a node and let v_i be the associated vector. Let $[E_i, E_{p_D(i)}]$ be the direct edge. Then we consider the weight $l_i = \sum_{h:i=p_D(h)}(m_i - l_i)$.*

Let E_i be a satellite vertex. We consider the weight m_i on the indirect vertex $[E_i, p_I(i)]$. For each satellite vertex E_i we consider a multi-loop M_i, having multiplicity $m_i - l_i$.

The graph of the canonical divide $\check{C}$ of C is then the embedding of the oriented simple lotus in the first quadrant, enriched by:

1. *if E_i and E_j are free points, joined by l_i arcs, we add $m_i - l_i$ arcs on the consequent quadrant;*
2. *for every satellite node E_i, a multi-loop M_i is situated in the quadrant given by the vector v_i, and attached to the point P_h in L or L' such that $E_h \preceq E_i$, and such that if $E_h \preceq E_l$, then E_l is a satellite node;*
3. *multi-loops and half-branches respect the relations of closeness.*

Example 4.2.36. Let us consider the curve singularity $(y^7 - x^{12})(y^{10} - x^{17})(y^5 - x^9) = 0$. Let C_1 be the branch $y^7 - x^{12} = 0$, C_2 be the branch $(y^{10} - x^{17}) = 0$, C_3 be the branch $y^5 - x^9 = 0$. We remark that $9/5 > 12/7 > 10/17$, which implies the order L', C_3, C_1, C_2, L.

The associated lotus is a simple lotus. In Figure 4.30 we can see the associated lotus. For an easier reading, we consider actually two different loti: in the first one we have computed the weight of all the edges, while in the second one we have computed the set of vectors v_i.

We start by noticing that $v_0 = (1, 1)$. Moreover, E_0 is the indirect predecessor of E_2, which is an L-node. Then we place the multi-loop M_2 in the third quadrant. Moreover, $m_2 = 6$, while $l_2 = 5$. Then the multiplicity $\tilde{m}_2$ of M_2 is $\tilde{m}_2 = m_2 - l_2 = 1$.

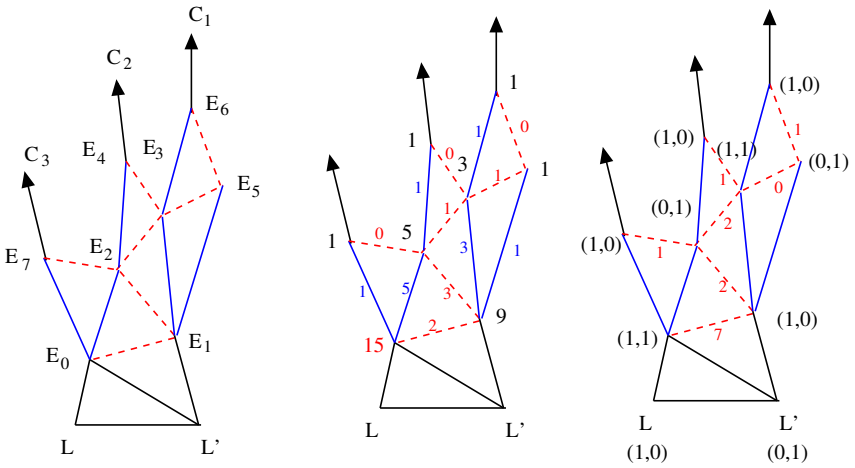

Figure 4.33 – The lotus of the curve in Example 4.2.37

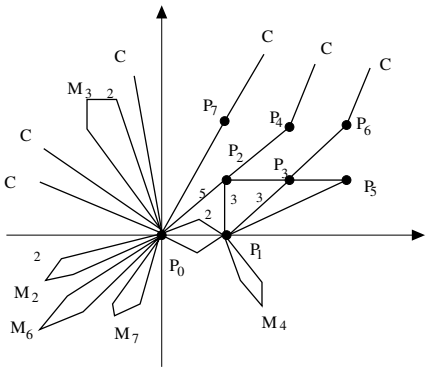

Figure 4.34 – The graph of the curve in Example 4.2.37

We continue then by noticing that $v_1 = (1, 0)$. The node E_1 is the indirect predecessor of E_3, E_4 and E_7, which are then L'-nodes. Then we have an order on the second quadrant L', M_7, M_4, M_3, L. Moreover, $\tilde{m}_7 = m_7 - l_7 = 1$, $\tilde{m}_4 = m_4 - l_4 = 1$, $\tilde{m}_3 = m_3 - l_3 = 5$.

There exists no node such that E_2 is its indirect predecessor. We consider then E_3, which is indirect predecessor of E_5 and E_6. $v_3 = (1, 1)$, which implies M_5 and M_6 belong to the third quadrant. Moreover, E_3 is a L-node. Then we have a dihedral order L', M_2, M_5, M_6, L.

In the end, we remark that $v_7 = (1, 1)$, $v_5 = (1, 0)$ and $v_6 = (0, 1)$. Then C_3 has a half- branch in the third quadrant, C_1 inn the second one and v_6 in the fourth. Moreover, $C_3 \notin \mathcal{B}(E_5) \supset \mathcal{B}(E_6)$, and we remember that E_2 is a L-node. Then we have an order L', M_2, C_3, M_5, M_6. In the same way, $C_5 \notin \mathcal{B}(E_7)$. Moreover, M_4 and M_5 are L' nodes. By adding the fact that we have a dihedral order L', C_3, C_1, L, then we have a dihedral order $L', M_7, C_1, M_4, M_5, L$. Then:

— C_1, M_3, M_4 and M_7 belong to the second quadrant, and there is a dihedral order $L', M_7, C_1, M_4, M_3, L$;

— M_2, C_3, M_5 and M_6 belong to the third quadrant, and there is a canonical order

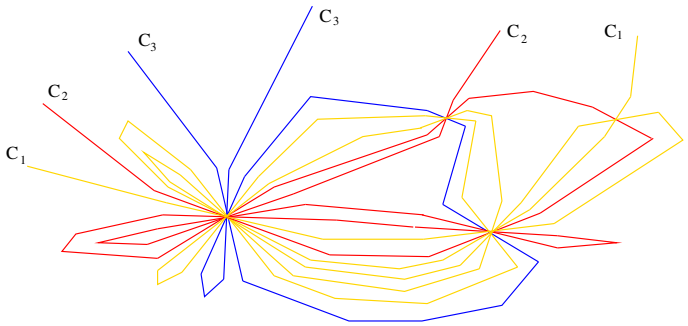

Figure 4.35 – The canonical divide of the curve in Example 4.2.37

$L', M_2, C_3, M_5, M_6, L$;

— C_2 belongs to the fourth quadrant.

The associated graph and the associated divide are shown respectively in Figure 4.31 and Figure 4.32.

Example 4.2.37. Let us consider the curve singularity $(y^7 - x^{12})(y^5 - x^8)(y^3 - x^4) = 0$. The associated lotus is again a simple lotus. In Figure 4.33 we can see the associated lotus. For an easier reading, we consider three different loti: the lotus is shown on the right, while in the centre and in the left one we have respectively computed the weight of all the edges and the set of vectors v_i.
We can then see that:

— M_3, C_1, C_2 and C_3 belong to the second quadrant, and there is a dihedral order $L', C_1, C_2, M_3, C_3, L$;

— M_2, M_6, M_7 belong to the third quadrant, and there is a canonical order L', M_2, M_6, M_7, L;

— M_4 belongs to the fourth quadrant.

The associated graph and the associated divide are shown respectively in Figure 4.34 and Figure 4.35.

Example 4.2.38. Let C be a branch. We say that C is a **Fibonacci singularity** if for every multiplicity m_i, $m_i = m_{i+1} + m_{i+2}$, and $m_{n-1} = m_n = 1$. Those singularities were characterized by an extremal property among all branches with the same blow-up complexity (see [PPP14]). Then:

1. if $i \cong 2 \ (mod\ 3)$, then M_i belong to the third quadrant;
2. if $i \cong 0 \ (mod\ 3)$, then M_i belong to the second quadrant;
3. if $i \cong 1 \ (mod\ 3)$, then M_i belong to the fourth quadrant.

Moreover:

if $i \cong 0 \ (mod\ 2)$, then E_i is a L-node;

if $i \cong 1 \ (mod\ 2)$, then E_i is a L'-node.

Moreover, for every i, $l_i = m_{i+1} - l_{i+1}$.

Let us consider the Fibonacci singularity having multiplicity sequence:

$$223 - 144 - 89 - 55 - 34 - 21 - 13 - 8 - 5 - 3 - 2 - 1 - 1$$

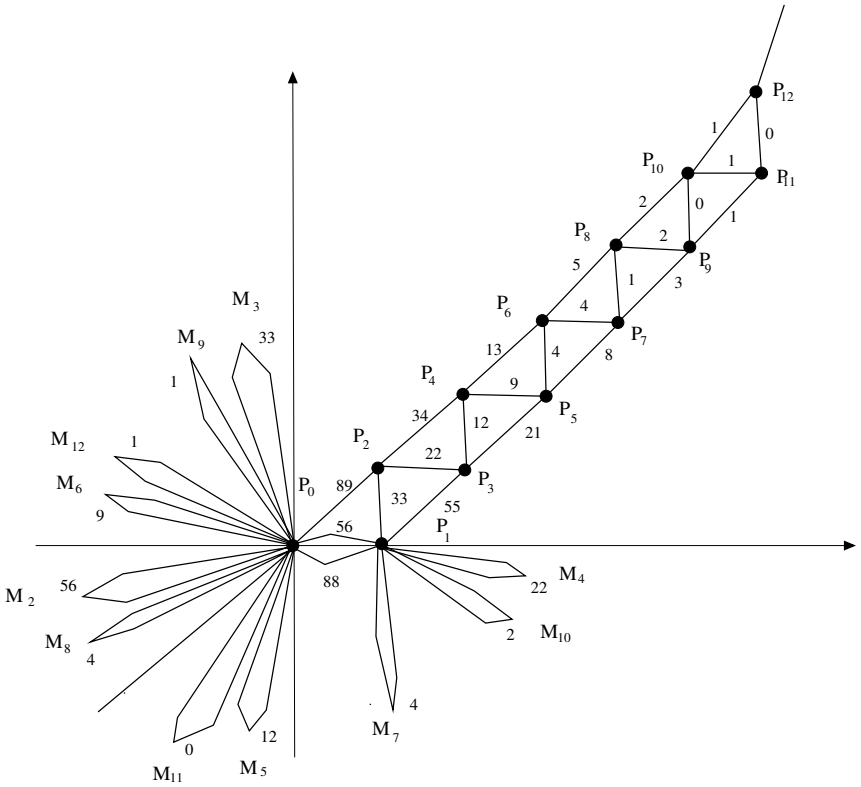

Figure 4.36 – The canonical divide of a Fibonacci singularity.

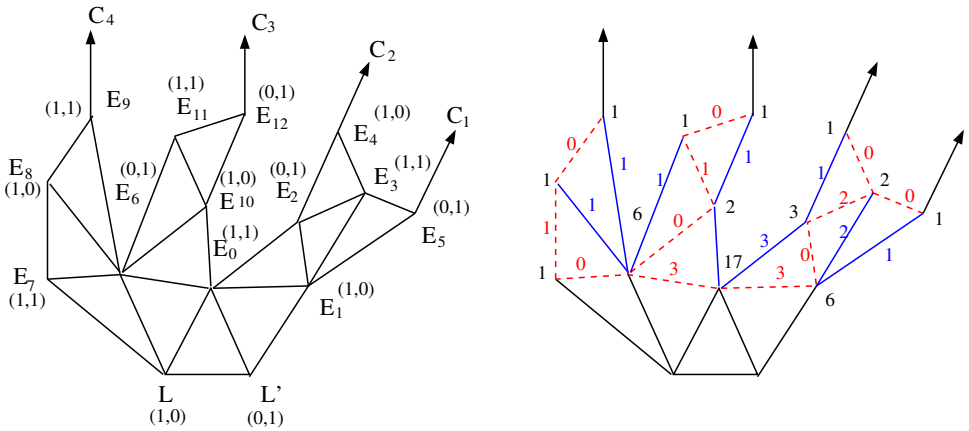

Figure 4.37 – The lotus of the curve singularity of Example 4.2.39.

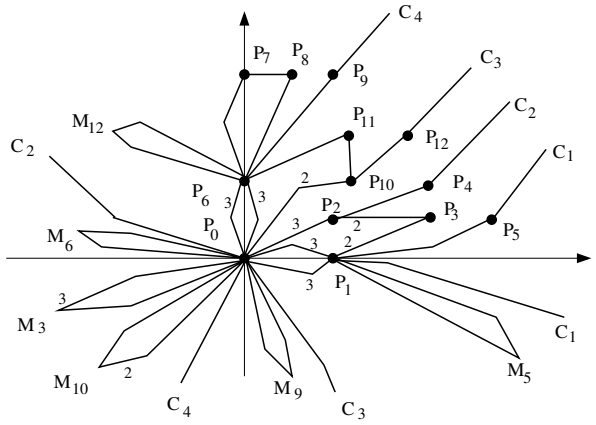

Figure 4.38 – The graph of the canonical divide of the curve singularity of Example 4.2.39.

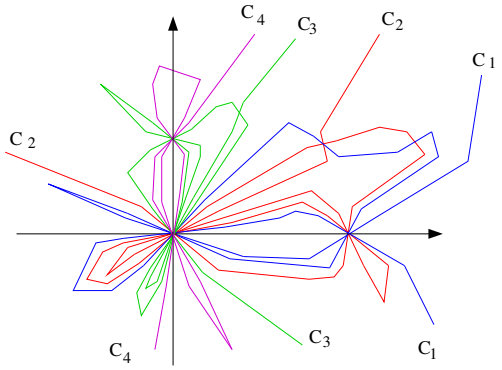

Figure 4.39 – The canonical divide of the curve singularity of Example 4.2.39.

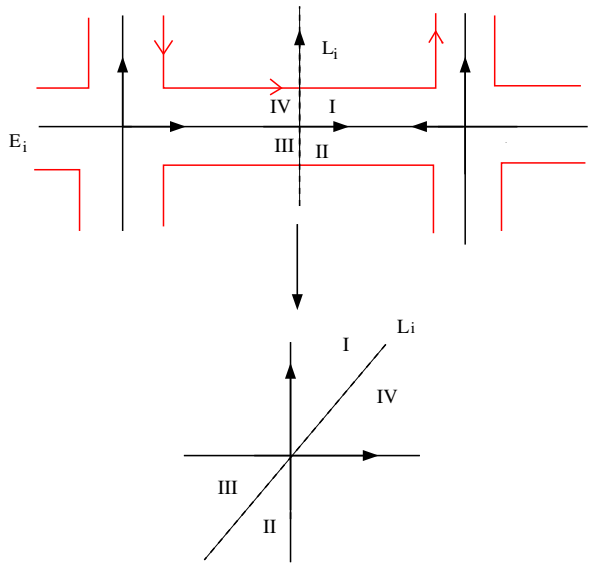

Figure 4.40 – The contraction of an exceptional component E_i such that O_{i+1} is a free point.

The associated canonical divide is shown in Figure 4.36.

Example 4.2.39. Let us consider the positive germ C shown in Figure 4.37. It has 4 different branches. In particular:

— the multiplicity sequence of C_1 is $4-3-1-1-1$;
— the multiplicity sequence of C_2 is $5-3-2-1-1$;
— the multiplicity sequence of C_3 is $5-3-2-1-1$;
— the multiplicity sequence of C_4 is $3-3-1-1-1$.

The graph of the canonical divide of C is shown in Figure 4.38. We can notice that marked points belong to both L and L', and then on both L and L' we can see that multi-loops are attached to different marked points. The multiplicities of multi-loops M_i are, as usually, $m_i - l_i$, and the closeness is computed by using Proposition 4.2.33 and Proposition 4.2.34.

We can remark that, from the fact that C_1 is closer to L' than M_5 because E_5 is a L' node. Always in the second quadrant, we can notice that M_9 is closer to L than C_3, because C_4 is closer to L than C_3. We can make the same remarks for all the other cases. The canonical divide is shown in Figure 4.2.39.

4.2.3 The general case

Let us now consider the case of a singularity C such that the associated lotus $\mathcal{L}$ is not a simple lotus.

Remark 4.2.40. Let C be a branch and let $(m; \beta_1, \ldots, \beta_n)$ be the associated Puiseux characteristic. Then there exists a lotus $\mathcal{L}$ relative to a complete system of curvettas $\mathcal{B}$ such that $\mathcal{L}$ is the lotus relative to the minimal resolution surface of C and $\mathcal{B}$ has $n+1$ elements.

Let us consider what happens in the case where E_i is a satellite node and E_{i+1} is a free node. Let $j = p_D(i)$, $k = p_I(i)$. In the chart E_j, E_k the divide intersects the exceptional component only in $P_i = E_j \cap E_k$. Moreover, we have a curvetta L'_i which is transverse to E_i. After contraction, the curvetta is smooth and passes through P_i.

Let C be a positive germ. Then the curvetta L'_i passes through the first quadrant and the local third quadrant. The divide is then contained in the same quadrants. Moreover, the curvetta L'_i subdivides each one of the two quadrants in two parts. We obtain then four different quadrants, that are actually the images of the local quadrants before contraction. This situation is shown in Figure 4.40.

Let us now analyse in detail what happens for the divide. We remember that the A'Campo's algorithm is local, i.e., it is applied to a neighbourhood of the exceptional locus E. The divide intersects E_j and E_k only at the point P_i. Moreover, the restriction of the divide to a neighbourhood of P_i is the union of m_i smooth branches, all intersecting the first quadrant. Then, we can consider this situation as if there are m_i positive branches transversal to the exceptional component E_i, or m_i arrowheads attached to the node E_i in the lotus.

Moreover, the translation and contraction algorithm can be restricted to a neighbourhood of E, and then all the marked points and multi-loops obtained before P_i are not any more involved in the algorithm.

Definition 4.2.41. Let $\mathcal{L}$ be a lotus. Let $\mathcal{B} = \{L', L, L'_{i_1}, \dots, L_{i_n}\}$. Let E_{i_h} be a node and let $j_h = p_D(i_j)$. Moreover, let $[E_{i_j}, L'_{i_j}]$ be the base of a petal. We attach to the node E_{i_h} c_{i_h} arrowheads, where:

$$c_{i_h} = \sum_{l: E_l \in \mathcal{P}(E_{j_h}), E_l \preceq E_{i_h}} m_l.$$

Moreover, we consider instead of the edge $[L_j, E_j]$ a new petal having oriented basis $[L'_j, L_j]$ and vertex E_j. We obtain then n different loti $\mathcal{L}_{i_1}, \dots, \mathcal{L}_{i_n}$ and a lotus $\mathcal{L}_0$ having basis L', L.

The **simplification** of $\mathcal{L}$ is the disjoint union of loti $\mathcal{L}_0, \mathcal{L}_{i_1}, \mathcal{L}_{i_2}, \dots, \mathcal{L}_{i_n}$.

An example of simplification is shown in Figure 4.41.

Remark 4.2.42. Let $\mathcal{L}$ be a lotus. Then $E_{i_h} = E_{i_{h'}}$ if and only if $h = h'$. It is possible that $i_h \neq i_{h'}$, but $p_D(i_h) = j_h = j_{h'} = p_D(i_{h'})$.

Remark 4.2.43. Let $\mathcal{L}$ be a lotus and let $\coprod_{j=1}^{n} \mathcal{L}_{i_j}$ be its simplification. Then for every j, $\mathcal{L}_{i_j}$ is a simple lotus. Moreover, for every j, we have two distinct nodes E_{i_j}, belonging to two different loti.

Proposition 4.2.44. *The multiplicity of a node is constant under the operation of simplification of a lotus.*

Proof. It is sufficient to prove it for a lotus having complete system of coordinates $\{L, L', L'_i\}$. For all h such that $h \not\prec i$, the multiplicity m_h is clearly invariant under simplification. The multiplicity of E_i is equal to m_i before and after simplification. Now, $m_{p_D(i)} = m_i$. Then all other nodes have the same multiplicity after simplification.

□

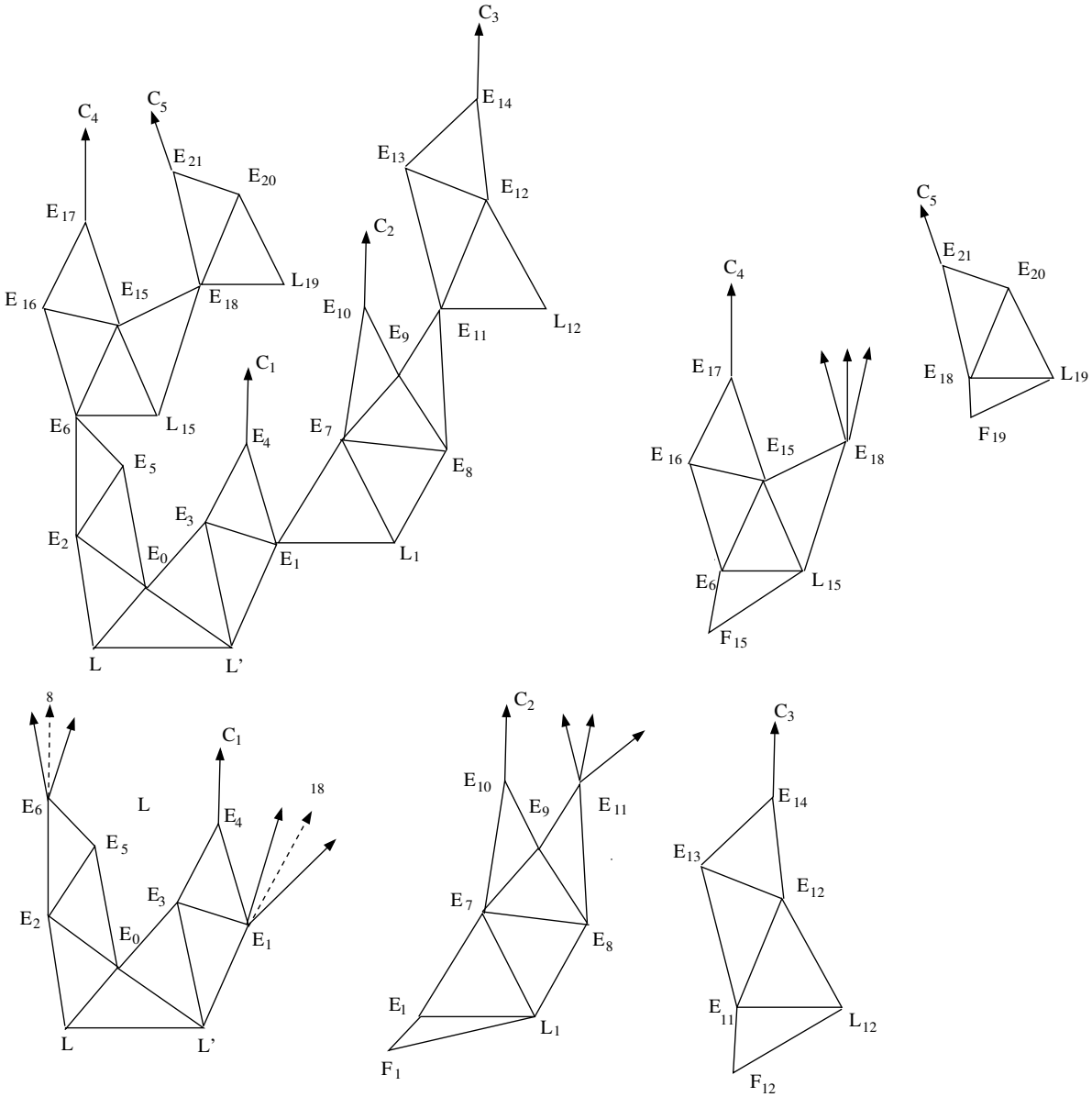

Figure 4.41 – An example of simplification.

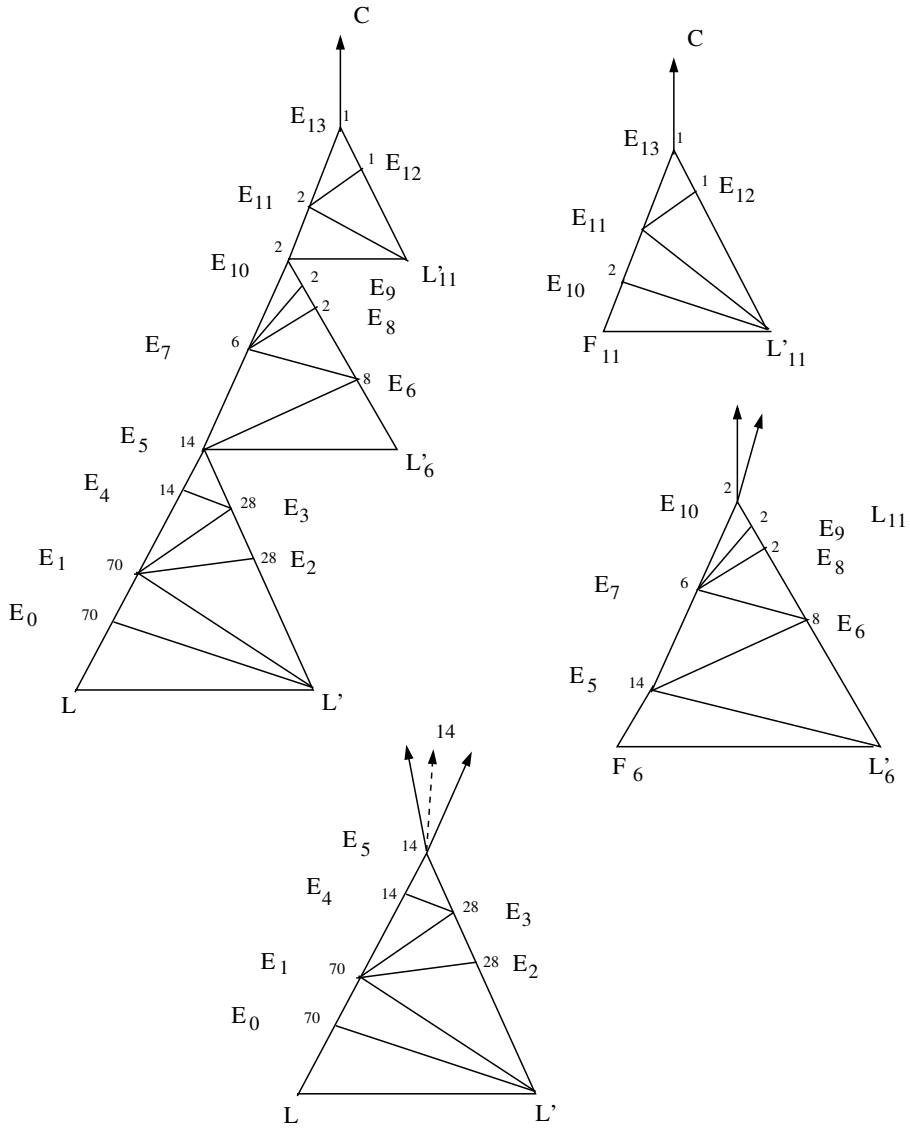

Figure 4.42 – The simplification of the curve singularity $(70; 158, 176, 179)$

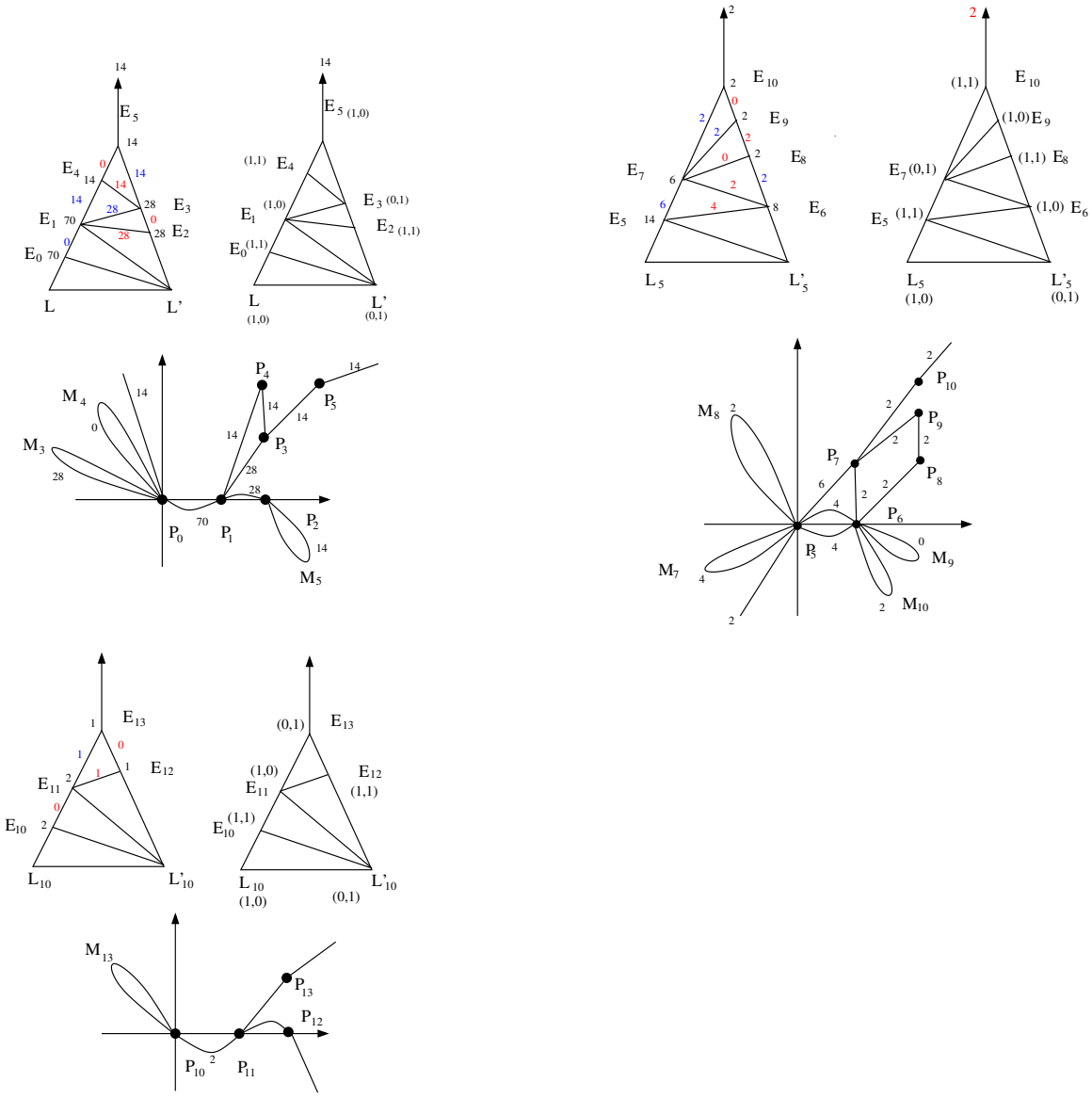

Figure 4.43 – The three simple loti of Example 4.2.48

.

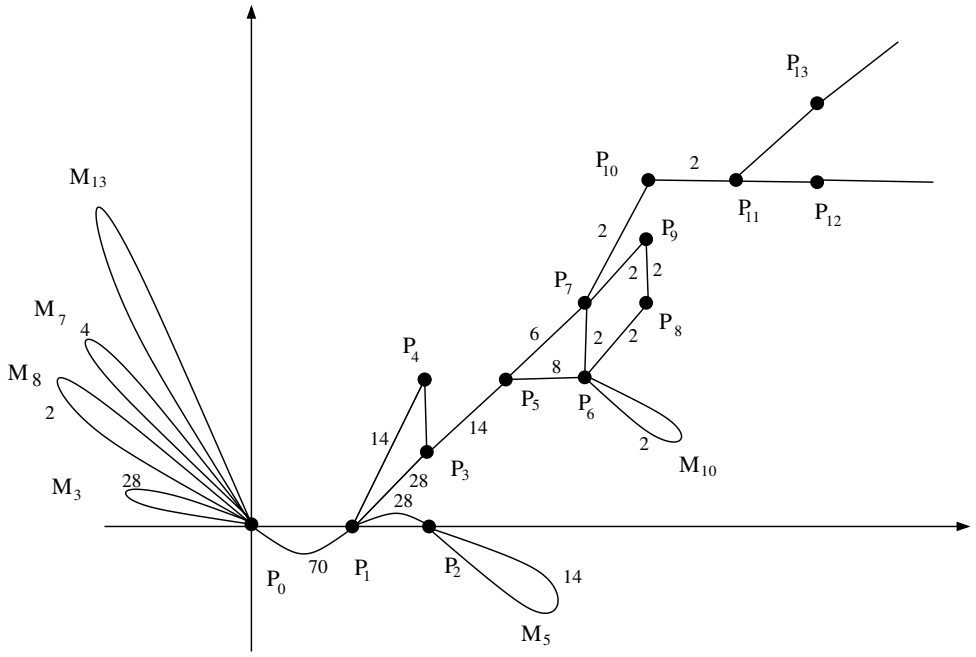

Figure 4.44 – The canonical divide of the curve singularity $(70; 158, 176, 179)$

Example 4.2.45. Let us consider the curve singularity C having Puiseux characteristic $(70; 158, 176, 179)$. Its simplification is shown in Figure 4.42.

We can remark that, because C is a branch and there are 3 distinct Puiseux exponents, then the simplification of $\mathcal{L}$ has three different lotus. Moreover, one lotus is the lotus of a branch having Puiseux characteristic $(2; 5)$. The second one is the lotus of a reducible curve such that its two branches has maximal order of contact and Puiseux characteristic $(7; 11)$. In the end, we have a lotus of a reducible curve such its 14 branches have maximal order of contact and Puiseux characteristic $(5; 12)$.

Let us now consider a lotus $\mathcal{L}$. Let us consider the simplification of $\mathcal{L}$, i.e., $n+1$ loti $\mathcal{L}_0, \mathcal{L}_{i_1}, \ldots, \mathcal{L}_{i_n}$. Let us consider a canonical divide $\check{C}_{i_j}$ for every lotus $\mathcal{L}_{i_j}$.

We start by considering the lotus $\check{C}_0$. Let E_{i_1} be a node in $\mathcal{L}$ such that $[E_{i_1}, L'_{i_1}]$ is a basis of a petal. Let us suppose that $E_{i_1} \in \mathcal{L}_0$. Then we have added m_{i_1} curvettas at E_{i_1}. Moreover, the vertex E_{i_1} is present in the two canonical divides $\check{C}_0$ and $\check{C}_{i_1}$. Let $\check{C}'_{i_1} = \check{C}_{i_1} - P_{i_1}$. We consider a **patching** $\check{C}_0 \wedge \check{C}_{i_1}$ of $\check{C}_0$ and $\check{C}_{i_1}$ as the divide such that:

- the first and fourth quadrant of $\check{C}'_{i_1}$ are embedded in the first quadrant of $\check{C}_{i_0}$, respecting the orientations;
- let us consider $v_{i_1} \in \mathcal{L}$. Then the half-branch of the arrowheads attached at E_{i_1} are in the quadrant associated to v_{i_1}. We consider then the second and the third quadrant of $\check{C}'_{i_1}$ in the quadrant associated to v_{i_1}, respecting the orientations and the dihedral order.

By iteration, we can patch all the loti $\mathcal{L}_{i_j}$, to obtain the divide $\check{C}$ of C. We have then proven the following Theorem:

Theorem 4.2.46. *Let C be a positive germ and let $\mathcal{L}$ be the lotus of C, associated to*

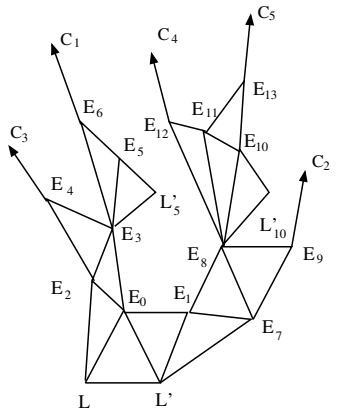

Figure 4.45 – The lotus of the positive curve singularity of Example 4.2.49.

a complete system of curvettas. Then the canonical divide $\check{C}$ is the divide obtained by patching the canonical divides of the multi-loti obtained by simplification of $\mathcal{L}$.

Remark 4.2.47. This theorem has been proven, for the special case of C an irreducible curve singularity, by Schulze-Robbecke in [SR77].

Example 4.2.48. Let us consider the curve singularity of Example 4.2.45. It is the positive germ having Puiseux characteristics $(70; 158, 176; 179)$. In Figure 4.43 we show the divide associated to the simple lotus of the decomposition of $\mathfrak{L}$, having basis (L', L).

We can do the same with the two simple loti of the decomposition, and having basis (L'_5, L_5) and (L'_{10}, L_{10}). The associated canonical divides are also shown in Figure 4.43.

The graph of the canonical divide obtained by patching is shown in Figure 4.44. We can remark that in the first quadrant we clearly see the fact that we have three different Puiseux characteristic numbers.

Example 4.2.49. Let C be the positive germ having lotus shown in Figure 4.45. The germ has 5 different branches C_1, C_2, C_3, C_4, C_5 of whom C_3 and C_2 have only one Puiseux characteristic number, while C_1, C_4 and C_5 have two Puiseux characteristic numbers. Moreover, C_4 and C_5 share the Puiseux characteristic number $\alpha_1 = \frac{5}{2}$, and have contact number $o_{4,5} > \alpha_1$.

It is clear that the lotus decomposition is given by 3 simple loti, such that the lotus having basis (L', L') and the lotus having basis (L'_{10}, L_{10}) are not triangular loti. The lotus having basis (L'_5, L_5), instead, is a triangular lotus. The three loti, and the associated canonical divides, are shown in Figure 4.46, in Figure 4.47 and in Figure 4.48.

Example 4.2.50. Now we consider the patching, shown in Figure 4.49. Then instead of the two curvettas L'_5 and L'_1 we consider the oriented embedding of the first and fourth quadrant, and of the second and third quadrant, in a way compatible with the definition of positive germ. From this graph we obtain the divide in Figure 4.50.

Let us consider another meaningful example. In this case, we consider 4 branches C_1, C_2, C_3 and C_4 such that:

1. the four curves have the same first Puiseux pair $\alpha_1 = \frac{3}{2}$;

2. $o_{ij} = \alpha_1$, $i, j = 1, \ldots, 3$, $i \neq j$;
3. $o_{3,4} > \alpha_1$.

The associated lotus is shown in Figure 4.51. From the hypothesis $o_{ij} = \alpha_1$ and α_1 is the first Puiseux pair of the three branches, we have then that the coefficients $a^i_{\alpha_1} \neq a^j_{\alpha_1}$, for $i, j = 1, \ldots, 3$, $i \neq j$. By the fact the branches are real, the coefficients are real, and the a_i can be ordered. In this case, $a^1_{3/2} < a^2_{3/2} < a^3_{3/2}$. Then in this case, we have a dihedral order L', C_1, C_2, C_3, L.

As in the previous examples, we consider the lotus decomposition of $\mathcal{L}$. We obtain 4 different loti, one having basis (L', L), another having basis (L'_3, L_3), the third one having basis (L'_5, L_5) and the last one having basis (L'_8, L_8). The four associated canonical divide are shown in Figure 4.52. We can remark that the arcs L'_i, $i = 3, 5, 8$, respect the orientations of the loti.

In Figure 4.53 we see the graph obtained by patching the four canonical divides. The final divide is shown in Figure 4.54.

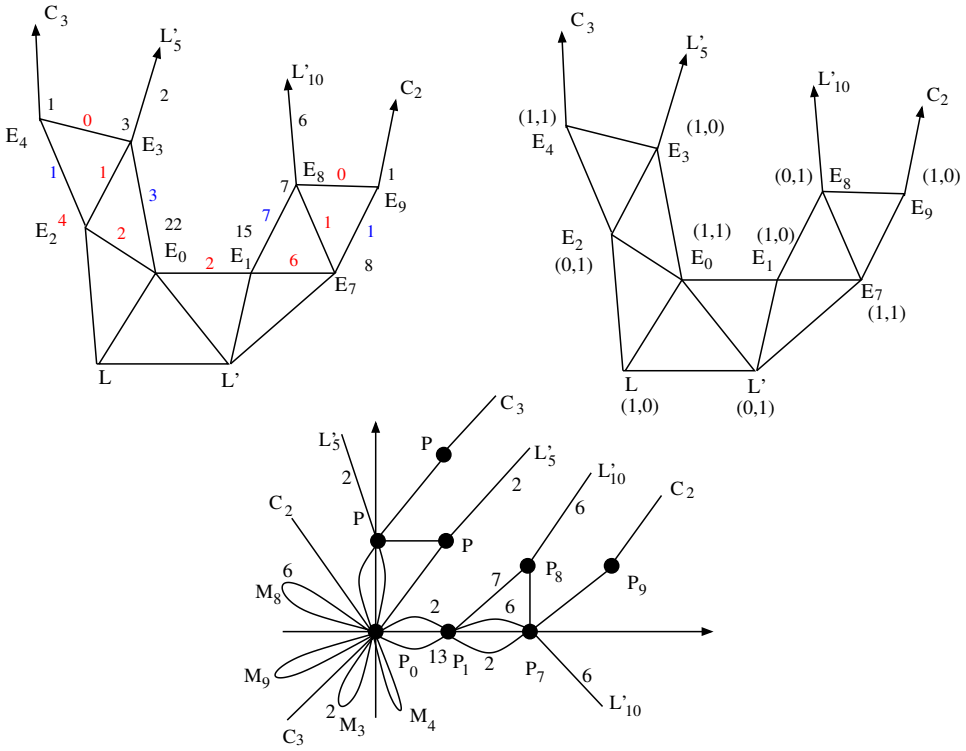

Figure 4.46 – The simple lotus having basis (L', L).

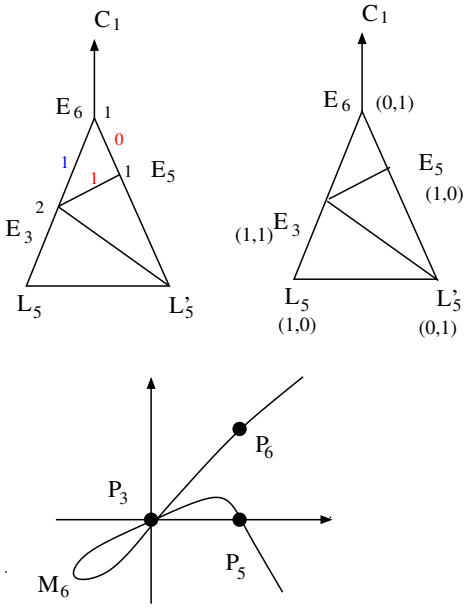

Figure 4.47 – The simple lotus having basis (L'_5, L_5).

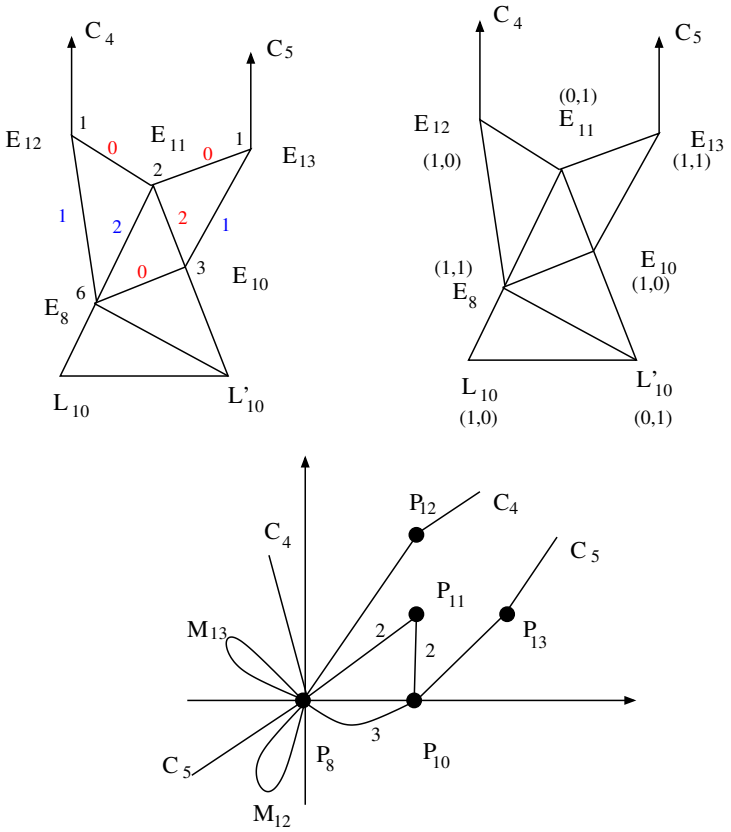

Figure 4.48 – The simple lotus having basis (L'_{10}, L_{10}).

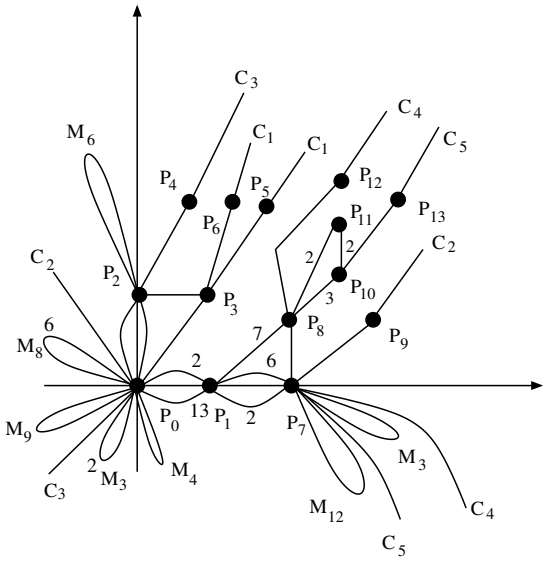

Figure 4.49 – The graph of the canonical divide of Example 4.2.49.

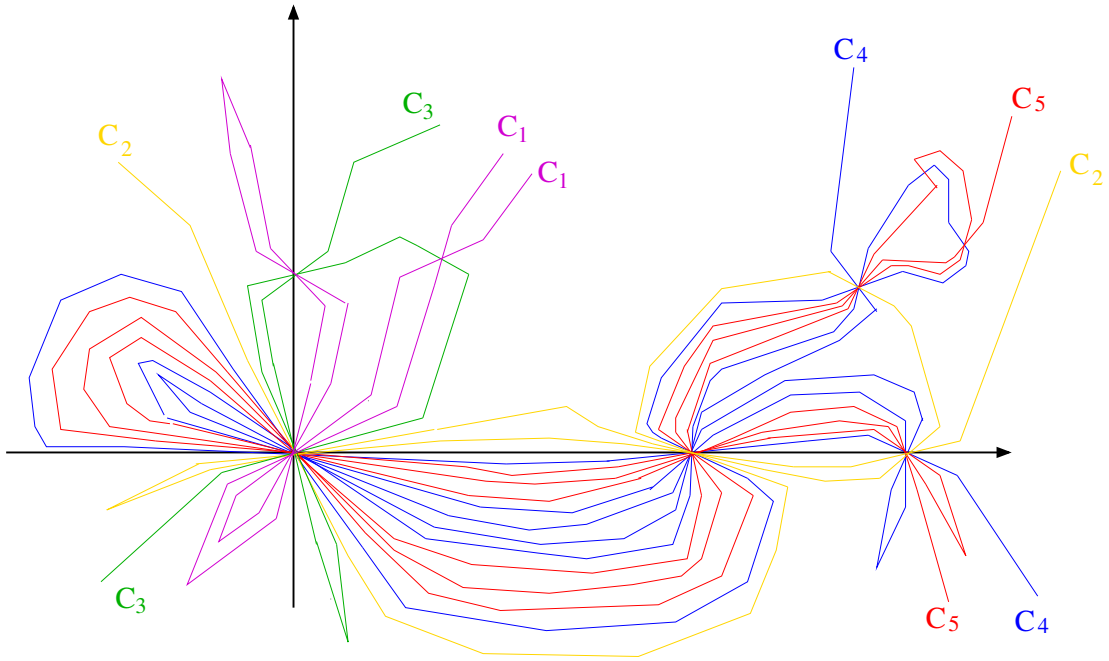

Figure 4.50 – The canonical divide of Example 4.2.49.

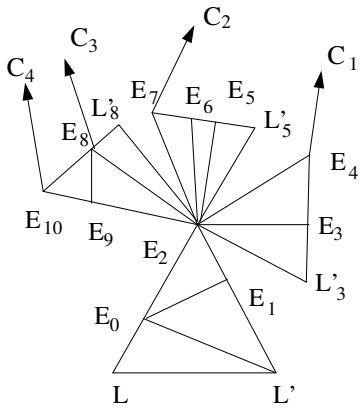

Figure 4.51 – The lotus of the curve singularity of Example 4.2.50

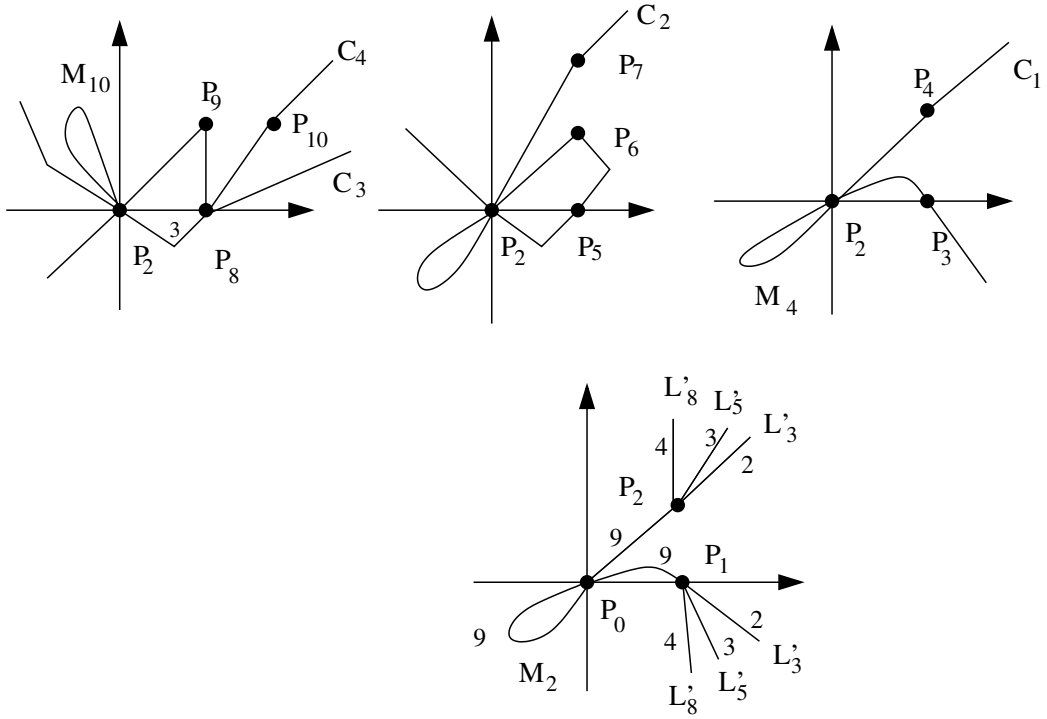

Figure 4.52 – The canonical divides of the simple loti of Example 4.2.50.

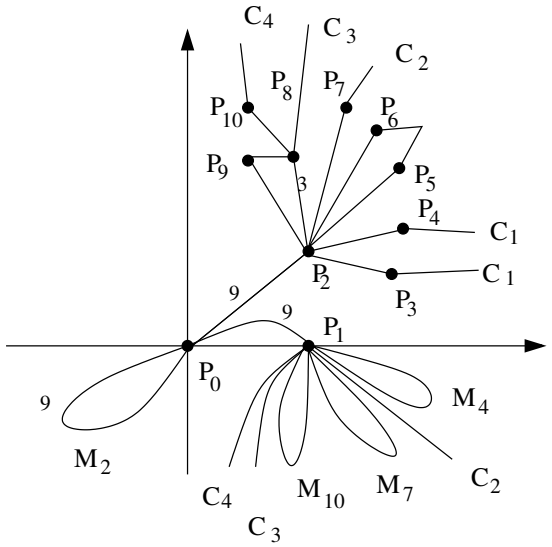

Figure 4.53 – The graph of the canonical divides of Example 4.2.50.

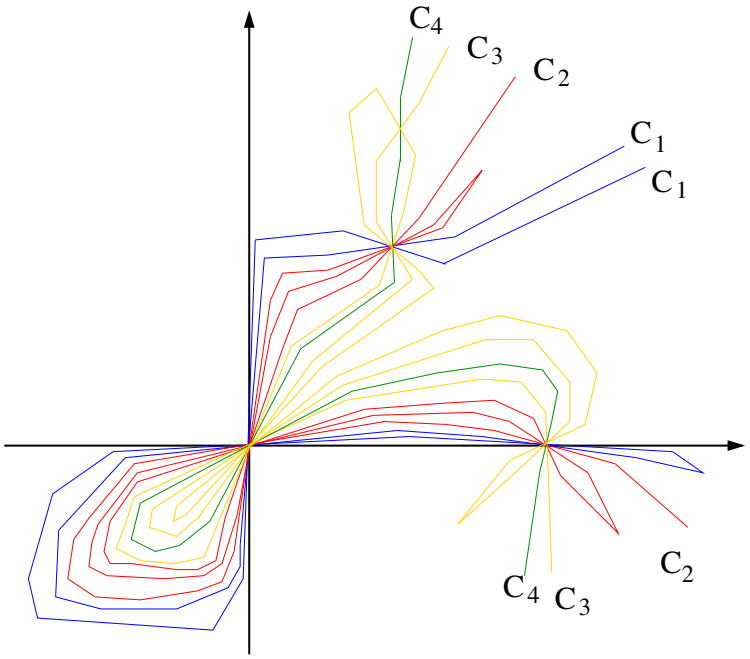

Figure 4.54 – The canonical divide of the positive germ of Example 4.2.50

References

[A'C74] N. A'Campo. Le groupe de monodromie du déploiement des singularités isolées de courbes planes II. In *Actes du Congrès International des Mathématiciens*, volume 1, pages 395–404, 1974.

[A'C75] N. A'Campo. Le groupe de monodromie du déploiement des singularités isolées de courbes planes I. *Mathematische Annalen*, 213(1):1–32, 1975.

[AS92] C. Angas Scott. On the higher singularities of plane curves. *American Journal of Mathematics*, 14:301–325, 1892.

[Bod07] A. Bodin. Jump of Milnor numbers. *Bulletin of the Brazilian Mathematical Society, New Series*, 38(3):389–396, 2007.

[BPPP14] E. García Barroso, P.González Pérez, and P. Popescu-Pampu. *Sails and lotuses of plane curve singularities.* Unfinished book, 2014.

[CA00] E. Casas-Alvero. *Singularities of plane curves.* Cambridge University Press, 2000.

[dJS98] T. de Jong and D. Van Straten. Deformation theory of sandwiched singularities. *Duke Math. J*, 95(3):451–522, 1998.

[EC15] F. Enriques and O. Chisini. *Lezioni sulla teoria geometrica delle equazioni e delle funzioni algebriche.* Zanichelli, 1915.

[Egg83] H. Eggers. *Polarinvarianten und die Topologie von Kurvensingularitäten*, volume 147. Bonner Math. Schriften, 1983.

[Ful93] W. Fulton. *Introduction to toric varieties.* Princeton University Press, 1993.

[Ghy13] É. Ghys. Intersecting Curves (Variation on an Observation of Maxim Kontsevich). *The American Mathematical Monthly*, 120(3):232–242, 2013.

[GZ74a] S.M. Gusein-Zade. Dynkin diagrams for singularities of functions of two variables. *Functional Analysis and its Applications*, 8(4):295–300, 1974.

[GZ74b] S.M. Gusein-Zade. Intersection matrices for certain singularities of functions of two variables. *Functional Analysis and its Applications*, 8(1):10–13, 1974.

[GZ87] S. M. Gusein-Zade. Singularities allowing small perturbations with a small number of critical values. *Functional Analysis and its Applications*, 21(1):66–68, 1987.

[GZ93] S.M. Gusein-Zade. On singularities from which an A_1 can be split off. *Functional Analysis and Its Applications*, 27(1):57–60, 1993.

[Kar13] O. Karpenkov. *Geometry of Continued Fractions.* Springer, 2013.

[KK99] M. Kobayashi and T.-C. Kuo. On Blow-analytic equivalence of embedded curve singularities. *Real analytic and algebraic singularities (Nagoya/Sapporo/Hachioji),* 30–37, Pitman Res. Notes Math. Ser., 381, Longman, Harlow, 1999.

[Kle96] F. Klein. Sur une représentation géométrique du développement en fraction continue ordinaire. In *Nouvelles annales de mathématiques*, volume 15, pages 327–331. Gauthier-Villars, 1896.

[KP10] S. Koike and A. Parusiński. Blow-analytic equivalence of two variable real analytic function germs. (3):439–472, 2010.

[Mil68] J. Milnor. *Singular points of complex hypersurfaces.* Annals of Mathematics Studies, No. 61. Princeton University Press, Princeton, N.J., 1968.

[Neu81] W. Neumann. A calculus for plumbing applied to the topology of complex surface singularities and degenerating complex curves. *Transactions of the American Mathematical Society*, 268(2):299–344, 1981.

[PP01] P. Popescu-Pampu. *Arbres de contact des singularités quasi-ordinaires et graphes d'adjacence pour les 3-variétés réelles.* PhD thesis, Université Paris-Diderot - Paris VII, 2001.

[PP07] P. Popescu-Pampu. The geometry of continued fractions and the topology of surface singularities. *Advanced Studies in Pure Mathematics*, 46:119–195, 2007.

[PP11] P. Popescu-Pampu. Le cerf-volant d'une constellation. *L'Enseignement Mathématique*, 57:303–347, 2011.

[PPP14] M. Pe Pereira and P. Popescu-Pampu. Fibonacci numbers and self-dual lattice structures for plane branches. *Bridging Algebra, Geometry and Topology, Springer Proceedings in Mathematics and Statistics*, 96:203–230, 2014.

[Ris74] J.J. Risler. Un théoreme des zéros en géométries algébrique et analytique réelles. In *Fonctions de Plusieurs Variables Complexes*, pages 522–531. Springer, 1974.

[SR77] T. Schulze-Röbbecke. *Algorithmen zur Auflösung und Deformation von Singularitäten ebener Kurven.* 1977. Diplomarbeit, Universität Bonn, Bonn, Bonner Mathematische Schriften, No. 96. 87 pages.

[Tei80] B. Teissier. Résolution simultanée, I et II. Séminaire sur les singularités des surfaces, Palaiseau 1976-77. *Lect. Notes in Maths. 777, Springer*, pages 71–146, 1980.

[Wal03] C.T.C. Wall. Chains on the Eggers tree and polar curves. *Revista Matemática Iberoamericana*, 19(2):745–754, 2003.

[Wal04] C.T.C Wall. *Singular points of plane curves.* Cambridge UP, 2004.

[Wal10] J. Walewska. The second jump of Milnor numbers. *Demonstratio Math*, 43(2):361–374, 2010.

Index